The effect of rock fragments on the water retention properties of New Zealand stony soils

---

A thesis

submitted in partial fulfilment

of the requirements for the Degree of

Doctor of Philosophy

at

Lincoln University

by

Balin Burns Robertson

Lincoln University

2020

Published research

Robertson B.B., Almond P.C., Carrick S.T., Penny V., Chau H.W. and Smith C.M.S., 2021. Variation in matric potential at field capacity in stony soils of fluvial and alluvial fans. Geoderma, 392. https://doi.org/10.1016/j.geoderma.2021.114978
(Chapter 3)

Robertson B.B., Almond P.C., Carrick S.T., Penny V., Eger A., Chau H.W. and Smith C.M.S., 2021. The influence of rock fragments on field capacity water content in stony soils from hard sandstone alluvium. Geoderma, 389. https://doi.org/10.1016/j.geoderma.2020.114912
(Chapter 4)

Robertson B.B., Carrick S.T., Almond P.C., McNeill S., Penny V., Chau H.W. and Smith C.M.S., 2021. Predicting field capacity in undisturbed stony soils. Geoderma, 401. https://doi.org/10.1016/j.geoderma.2021.115346
(Chapter 5)

Robertson B.B., Gillespie J.D., Carrick S.T., Almond P.C., Payne J., Chau H.W. and Smith C.M.S., 2021. Measuring the water retention curve of rock fragments: A novel repacked core methodology. European Journal of Soil Science, 1-7. https://doi.org/10.1111/ejss.13181
(Chapter 6)

Abstract of a thesis submitted in partial fulfilment of the requirements for the Degree of Doctor of Philosophy.

The effect of rock fragments on the water retention properties of New Zealand stony soils

by

Balin Burns Robertson

Globally there is increasing evidence of nutrient enrichment and water depletion in surface and groundwater systems due to agricultural practices. To mitigate nutrient enrichment, it is necessary to quantify nutrient discharge within catchments so that robust and effective land management practices and regulations can be developed. To provide this information, several countries and global projects have developed soil databases and information systems to supply maps of soil spatial variability and estimates of crucial soil water retention properties such as field capacity (FC) and available water holding capacity (AWC). These data are used with models to quantify nutrient losses so that nutrient discharge within catchments can be managed. However, when estimating soil water retention properties in stony soils, it is common practice to assume that rock fragments (RFs) have no effect and that FC is the water content (WC) at defined matric potential criteria such as -10 kPa. To test these assumptions and their impacts, I conducted four experiments as part of this PhD.

Experiment 1 involved characterising the depth variability of matric potential and WC (fines and RFs independently) at FC in 52 pits excavated to 60 cm depth in stony soils across the Canterbury Plains. For Experiment 2, matric potential after four to five days of drainage following a saturation event was measured to a depth of 1.5 m at five of the sites used in Experiment 1. Experiments 1 and 2 showed that matric potential was generally higher than the default -10 kPa typically assumed for New Zealand soils at FC. The matric potential-depth profile of the pits could be characterised into one of five modes. The most common mode was hydrostatic equilibrium, which generally develops when a shallow (~<2 m) water table establishes a zero matric potential boundary condition near the soil surface. The groundwater tables at all the sites studied (except one) were deep (>2 m), and instead, a coarse sandy gravel layer at ~1 m depth established a near-zero but finite matric potential boundary condition. Very slow unsaturated hydraulic conductivity in this layer allowed the near-zero matric potential to be maintained, above which hydrostatic equilibrium could evolve. This condition,

referred to as a capillary break, corresponded to either a layer of open framework gravels or fine earth with a specific surface area <15 m^2g^{-1}.

Experiment 1 WC results indicated that RFs could influence the fine earth bulk density, porosity, and soil chemistry within an *in situ* stony soil. RFs could also retain water: 2-20 mm RFs retained twice as much water (0.07 m^3 m^{-3}) as >20 mm RFs (0.03 m^3 m^{-3}). The water retention of the hard sandstone is low compared to other lithologies, but the volumetric abundance of RFs in the sampled stony soils meant that they accounted for ~10% of the water retained to a depth of 60 cm at FC. The results demonstrate that ~13 mm of water retained by RFs at FC is not currently considered in water budgets and nutrient leaching predictions, which may be relevant to best practice land management.

To understand the effect of including or excluding RF water storage on soil water retention predictive models, I developed two pedotransfer functions (PtFs) using data from Experiment 1. Results showed it was possible to accurately predict the WC at FC in stony soils using only explanatory variables that could be easily measured or estimated from a minimalistic field survey. An existing PtF calibrated on NZ soils (the logit PtF), which was constructed on the assumption that RFs had no effect on WC at FC other than reducing the fine earth volume, performed worse than the models developed in this study. By modifying the logit PtF, it was concluded that its poorer performance stems from its inability to account for deviations from 1) the matric potential it assumes for FC (-10 kPa), 2) water held by RFs, and 3) the effect of RFs on the water retention characteristics of the fine earth. The results demonstrate that even the low porosity RFs measured in this study can significantly affect model performance, but by including two variables (depth and volumetric proportion of RFs) that are routinely measured or estimated in most soil sampling projects, it is possible to improve prediction accuracy in established models such as the logit PtF.

Experiment 3 required developing a novel repacked soil core experiment to measure the water retention curve (WRC) of low porosity, greywacke RFs. The new method was necessary to account for the low water retention properties of greywacke RFs and the effect RFs have on fine earth porosity and bulk density (which is not considered in most repacked soil studies). A new measurement set up was developed to accomplish this, which allowed the use of large cores with repacked soils that incorporated RFs, glass fragments and fine earth. The method was accurate enough to measure the WRC of the greywacke RFs, which had an AWC of 0.03 ± 0.02 m^3 m^{-3} released between tensions of -10 kPa and -1500 kPa. In an average Canterbury stony soil to a depth of 60 cm, the AWC of just the RFs alone could release 6.4 ± 4.7 mm of water, a significant amount considering most New Zealand stony soils have low AWC.

Results from Experiment 1 and 3 were then used in OVERSEER® simulations to determine the effect of the RF plant available water on nutrient loss predictions for a simulated dairy farm in Canterbury.

Three soil types were tested (an average stony Brown soil, an average stony Recent soil and a very stony Brown soil) in simulations that included the WC of the RFs, compared to simulations that used only fine earth WC. The inclusion of RF WC had little to no effect on P and GHG losses but could reduce predicted N losses by 1-6 kg N ha^{-1} yr^{-1} depending on soil type. Variation in N losses was equivalent to a relative change of 4-19% for the simulated soils, which indicates that farmers on stony soils may be subject to N-leaching overestimates. A caveat to this conclusion is that the OVERSEER® model does not account for bypass flow, a common phenomenon in stony soils. Any N-leaching overestimates indicated by the present research should be treated as a desirable buffer for potential underestimates generated by N-loss processes unaccounted for in the current version of OVERSEER®.

Rock fragments are demonstrably able to affect not only the structural and chemical properties of stony soil but also the water retention properties. This project has indicated that the standard assumptions are prone to error when measuring stony soils, namely that:

1. De facto matric potential criteria can define FC in undisturbed stony soils
2. RFs do not retain water
3. RFs do not affect fine earth properties

This thesis has shown that current soil information systems and modelling practices regarding stony soils could be inaccurate if these assumptions are made. The work also justifies the need to 1) quantify the WC of RF lithologies at varying states of weathering; 2) explore the generality of findings to stony soils in other sedimentary facies or under differing land uses; 3) develop a method of efficiently identifying the depth of open framework gravels at the paddock and farm-scale and to fully characterise the capillary break, including what conditions and matric potentials it occurs.

Keywords: Undisturbed stony soil, alluvial fan soils, field capacity, hydrostatic equilibrium, capillary break, open framework gravels, rock fragment water content, available water content, rock fragment and fine earth interactions, pedotransfer functions, repacked cores, OVERSEER®.

Acknowledgements

Firstly, I would like to thank my supervisory team. To my main supervisor Peter Almond, your ability to put up with my antics is both commendable and inspiring. You have been pivotal to my success, and if I can remember just a sliver of the knowledge you have so kindly provided throughout my PhD, then I am already well equipped for the future; it has truly been a privilege. To my associate supervisor Sam Carrick, you have been a continual source of support, guidance (and money!) for the better part of five years. You have been a cornerstone in my studies and a huge positive influence in my life; I can't thank you enough for everything you have done for me. Henry Chau, I am still uncertain how you managed to trick me into studying soil physics; however, I am very grateful that you did! You have been a great source of humour and inspiration through my studies, always enticing me to do better and strive for better things; if one day I become a successful (and dear I say, respectable) researcher, then you will have played a large role in it. Carol Smith, thank you for your knowledge, support and most importantly, for pressuring me into soil judging! I have had a great time and learnt a lot.

A massive thanks to the Landcare Research crew: John Payne, Graeme Rogers, Stephen McNeill, Andre Eger, Nina Koele, Thomas Caspari, John Hunt and Anja Hess. You guys have been a non-stop source of help, guidance and support; I don't know where I would be without your help.

Veronica Penny, I can't thank you enough for everything you have done throughout my Honours and PhD. You have been a true friend and mentor, and the time you have spent helping (chiding) me could not be more appreciated.

A big thanks to Amal Torky for having the best laugh around and being the go-to person for any issues I may have, no matter how annoying I may be!

Neil Smith and Nigel Beale, thank you very much for your technical expertise.

A big thanks to my flatmates, friends and the rock climbing crew; you have been great at keeping me partially sane throughout this endeavour (no mean feat). Another big thanks to the other postgrads for your chat and support.

To my partner Olivia Bell, I can't thank you enough for all your support and time. You have shown endless love and had undying confidence in me throughout my PhD, and I am truly lucky to have you in my life.

Finally, my family, you have always been there for me and always know what to do to get me back on track. Your support is astounding, and I'm not sure what I would be without you.

Project Information

This research was funded by the Ministry of Business, Innovation and Employment's Endeavour Fund, through the Manaaki Whenua-led 'Next Generation S-map' research program, C09X1612, as well as the Ministry for Primary Industries Sustainable Farming Fund project 405305 'The Effect of Medium to Long-Term Irrigation on Soil Water Holding Properties', and support from Lincoln University. PhD supervision was provided by Dr. Peter Almond (Lincoln University), Dr. Sam Carrick (Manaaki Whenua – Landcare Research), Dr. Henry Chau (Lincoln University) and Dr. Carol Smith (Lincoln University). Publications resulting from this research:

Robertson B.B., Almond P.C., Carrick S.T., Penny V., Chau H.W. and Smith C.M.S., 2021. Variation in matric potential at field capacity in stony soils of fluvial and alluvial fans. Geoderma, 392. https://doi.org/10.1016/j.geoderma.2021.114978
(Chapter 3)

Robertson B.B., Almond P.C., Carrick S.T., Penny V., Eger A., Chau H.W. and Smith C.M.S., 2021. The influence of rock fragments on field capacity water content in stony soils from hard sandstone alluvium. Geoderma, 389. https://doi.org/10.1016/j.geoderma.2020.114912
(Chapter 4)

Robertson B.B., Carrick S.T., Almond P.C., McNeill S., Penny V., Chau H.W. and Smith C.M.S., 2021. Predicting field capacity in undisturbed stony soils. Geoderma, 401. https://doi.org/10.1016/j.geoderma.2021.115346
(Chapter 5)

Robertson B.B., Gillespie J.D., Carrick S.T., Almond P.C., Payne J., Chau H.W. and Smith C.M.S., 2021. Measuring the water retention curve of rock fragments: A novel repacked core methodology. European Journal of Soil Science, 1-7. https://doi.org/10.1111/ejss.13181
(Chapter 6)

Table of Contents

List of Tables

List of Figures

Acronyms and Abbreviations

Akaike information criterion value (AIC)

Available water holding capacity (AWC)

Field capacity (FC)

Fine earth (FE)

Fluvial and alluvial fan stony soils (FAFSS)

Glass fragment (GF)

Greenhouse gas (GHG)

Internal diameter (ID)

Mean absolute error (MAE)

Nitrogen (N)

Ordinary least squares regression (OLS)

Pedotransfer function (PtF)

Phosphorus (P)

Rock fragment (RF)

Root mean square error (RMSE)

Specific Surface Area (SSA)

Volumetric water content (VWC)

Water retention curve (WRC)

Water content (WC)

Wilting point (WP)

Chapter 1

Introduction

1.1 Background and significance of the study

Worldwide there are growing concerns over rising nutrient concentrations in surface and groundwater systems (Khatri and Tyagi, 2015; Olguin, 2003). A leading source of leached nutrients is agricultural land, which has expanded significantly with global food demand (Gregory et al., 2002; Wu et al., 2014). McDowell et al. (2020) predict that 31% of catchments globally may exhibit undesirable levels of periphyton growth, of which 76% was caused by phosphorus enrichment and mapped to catchments dominated by agricultural land. This arises as the use of mineral-based nutrients increases with the intensification of agricultural activity, which can have significant long-term impacts on the nutrient dynamics of rivers, river sediments and receiving water bodies (Jarvie et al., 2013; Wu et al., 2014). Even in lightly populated New Zealand, 70% of lakes with upstream catchments in pastoral land cover classes are in poor or very poor ecological health (Ministry for the Environment & Stats NZ, 2020). To mitigate nutrient losses, more effective land management practices operating within an appropriate regulatory environment are necessary. To monitor nutrient discharge within catchments, models have been developed to estimate nutrient losses under different farming practices, all of which require knowledge of soil water and nutrient retention properties (Cichota and Snow, 2009; Jomaa et al., 2016). To provide this information, several countries and global projects have developed soil databases and information systems to supply maps of soil spatial variability and estimates of crucial soil water retention properties such as field capacity (FC) (Arrouays et al., 2014; Johnston et al., 2003; Lilburne et al., 2012). However, these models (and the underpinning national soil databases) commonly rely on assumptions and lab measurement techniques that may not be appropriate for field soils (Evett et al., 2019; Iiyama, 2016). This is especially true for stony soils for which rock fragments (RFs) are assumed to not contribute to water storage, and for which FC is presumed to occur at a singular matric potential criterion such as -10 kPa (McNeill et al., 2018; Román Dobarco et al., 2019a; Román Dobarco et al., 2019b).

Stony soils are found worldwide, representing around 30% of the land area in Western Europe, 60% in the Mediterranean region and 18% in China (Ma and Shao, 2008; Poesen and Lavee, 1994). Even in New Zealand, there are 1.68 million hectares of land classified as stony soil that occurs on land with <15° slope, and therefore has the potential to be used for intensive land use (Carrick et al., 2013). With increasing populations, demand for agricultural products has resulted in stony soils, formerly seen as low productive land, being converted into progressively more intensive land uses such as

dairy (Carrick et al., 2013; Cichota et al., 2016). However, of the research done on stony soils, many of the studies do not consider the role of RFs (soil particles larger than 2 mm in diameter), even when their abundance cannot be neglected (Cousin et al., 2003).

International studies have shown that depending on the volumetric abundance, shape, size, degree of weathering and lithology, RFs are capable of retaining water (Poesen and Lavee, 1994; Tetegan et al., 2011), influencing fine earth porosity (Gargiulo et al., 2016; Poesen and Lavee, 1994; Stewart et al., 1970; Torri et al., 1994) and affecting the tortuosity of water flow pathways (Childs and Flint, 1990; Fiès et al., 2002). However, even with these significant RF influences, the management of stony soils is still commonly based on the hydraulic properties of the fine earth only. As a result, the de facto matric potential criteria used for determining FC in several countries, including New Zealand, are based solely on measurements in non-stony soils, even though soil physics theory indicates that soil layers with a high RF content may interact hydraulically and influence soil water release and retention (Clothier et al., 1977). Furthermore, the studies and models that have specifically addressed the relationship between RFs and soil hydro-physical properties (Cousin et al., 2014; Parajuli et al., 2017; Scheinost et al., 1997; Wang et al., 2013) generally rely upon measurement methods that may not be representative of field conditions: they used small sample sizes, relied upon repacked soil, or neglected to include the effect RFs may have on fine earth *in situ*. This indicates a significant gap in the international research regarding the characterisation of the water holding behaviour of stony soils *in situ* using soil volumes that adequately represent the soil.

1.2 Aims and objectives

This PhD aims to use a regional study of alluvial stony soils derived from indurated sandstone (greywacke) to:

- Study the soil properties affecting the water retention behaviour of undisturbed stony soils at FC;
- Investigate the validity of assumptions commonly adopted when measuring and modelling stony soil water holding behaviour.

To achieve these aims, four experiments were conducted.

1.2.1 Experiment 1

Experiment 1 involved the field measurement of the matric potential and soil water content (WC) in stony soils of Canterbury at FC using an operational definition of two days of drainage after a saturation event. The purpose was to identify the best method of defining FC in stony soils by:

1) determining the variability of matric potential of FC in stony soils; 2) determining how RFs influence soil properties and water retention.

Hypotheses:

- Because of the peculiar conductivity characteristics of stony soil horizons, a single matric potential of -10 kPa as adopted in NZ for defining FC is not appropriate.
- The water held at FC can be partitioned between fine earth and RFs at pedon scale.
- RFs have significant effects on soil hydraulic, physical and chemical properties.
- Statistical models used to predict soil WC at FC (pedotransfer functions) perform better when the characteristics of RFs are implicit.

To test the hypotheses, the experiment conducted had the following objectives:

- Measure how FC's matric potential varies with depth at the pedon scale and with different stony soil properties (such as variation in RF abundance, RF size, RF location, carbon, texture…).
- Determine the significance of RFs to the WC of undisturbed stony soils at FC.

1.2.2 Experiment 2

Experiment 2 involved field measurement of matric potential after four to five days of drainage following a saturation event to a depth of 1.5 m in stony soils of Canterbury. The purpose was to explore to a greater depth the controls on FC matric potential revealed by Experiment 1.

Hypothesis:

FC at shallow depths (<1 m) in stony soils is characterised by a state of hydrostatic equilibrium, which can establish because a shallow stony layer's drainage characteristics establish a finite but near-zero matric potential (0 to -4 kPa) close to the soil surface.

To test this hypothesis, an experiment with the following objectives was conducted:

- Characterise matric potential variation to a depth of 1.5 m in five stony soil profiles after four to five days' drainage.
- Characterise properties of soil layers to determine any conditions sufficient or necessary to establish a near-surface, near-zero matric potential.

1.2.3 Experiment 3

Experiment 3 involved developing a novel repacked soil core experiment to measure the plant available water of low porosity, greywacke RFs. Experiment 1 showed that RFs could account for an appreciable quantity of the WC at FC in stony soils. Though it was found RFs retained water, how much is available for plant growth was uncertain and required the water retention of the RFs to be characterised.

Hypothesis:

Greywacke RFs hold sufficient water and release it in a sufficiently systematic way that a water retention curve can be determined.

To test the hypothesis, an experiment with the following objectives was established.

- Develop a novel method for characterising the water retention at matric potentials >-100 kPa of greywacke RFs in a soil matrix repacked into a large core (4.9 cm in height with an inner diameter of 19.4 cm).
- Characterise the water retention of greywacke RFs at lower matric potentials by using a Meter WP4C dewpoint potentiometer.
- Develop models for the full water retention curve of greywacke RFs to allow water storage parameters (FC, available water holding capacity) to be estimated.

1.2.4 Experiment 4

Experiment 4 involved a simulation exercise using the OVERSEER® model and an irrigated, intensive dairy farm scenario, parameterised with results from Experiments 1 and 3 to determine the effect of RFs on water retention and nutrient loss predictions in stony soils.

Hypothesis:

Greywacke RFs substantially influence the accuracy of water retention and nutrient loss predictions in stony soils.

To test the hypothesis, the experiment adopted the following objectives:

- Parameterise model soil profiles representative of soils of different taxa, with and without the effect of water held by RFs.
- Compare predicted nutrient losses across the simulations and quantify the effects of RF water storage.

1.3 Thesis structure and chapter outline

My thesis is divided into eight chapters, including an introduction (Chapter 1), a literature review (Chapter 2), five sections dedicated to the main findings (Chapters 3-7), and a conclusion (Chapter 8).

Chapter 1 is a general introduction describing the significance of the research gap studied, then outlining the thesis aims, objectives, and the progression of experiments undertaken to achieve the study's aims.

Chapter 2 reviews the current research relating to stony soils, which demonstrates the effect of RFs on various soil properties and highlights the need for characterising the water holding behaviour of stony soils *in situ* using soil volumes that adequately represent the soil.

Chapter 3 is a manuscript that has been accepted by *Geoderma*, which analyses the depth profiles of the *in situ* FC matric potential of stony soils measured throughout Canterbury. This chapter uses results from Experiments 1 and 2 to determine the validity of the default FC matric potential criterion in Canterbury stony soils. It explores aspects of soil properties and processes that influence stony soil FC matric potential and WC.

Chapter 4 is a manuscript that has been accepted by *Geoderma*, which analyses the water retention of Canterbury stony soils at FC using results from Experiment 1. This chapter investigates the effects of RFs on soil properties and determines the significance of RFs on the WC of undisturbed stony soils at FC.

Chapter 5 is a manuscript that has been accepted by *Geoderma* that focuses on developing models (pedotransfer functions) and identifying variables that are important to predicting the WC at FC in *in situ* stony soils using data derived from Experiment 1. Model performance is compared against a published model, also calibrated on NZ soils, which does not account for water storage of RFs or the effects of RFs on fine earth water holding capacity.

Chapter 6 analyses the results of Experiment 3 and focuses on determining the water retention curve of greywacke RFs and discusses the efficacy of the novel measurement method developed within this section.

Chapter 7 analyses the results of Experiment 4 and determines the potential effects of plant available water sourced from greywacke RFs on the nutrient losses predicted by the OVERSEER® model for a stony soil dairy farm simulation in Canterbury.

Chapter 8 provides a synthesis of the main results described in Chapters 3 to 7 and conclusions based on the most important findings.

References

Arrouays, D., McBratney, A., Minasny, B., Hempel, J., Heuvelink, G., MacMillan, R., Hartemink, A., Lagacherie, P., McKenzie, N., 2014. The GlobalSoilMap project specifications. GlobalSoilMap: Basis of the Global Spatial Soil Information System, Release 2.4.

Carrick, S., Palmer, D., Webb, T., Scott, J., Lilburne, L., 2013. Stony soils are a major challenge for nutrient management under irrigation development. In: L.D. Currie, C.L. Christensen (Eds.), Accurate and Efficient Use of Nutrients on Farms, Occasional Report No. 26. Fertiliser and Lime Research Centre, Massey University, Palmerston North, New Zealand.

Childs, S.W., Flint, A.L., 1990. Physical properties of forest soils containing rock fragments. In: S.P. Gessel, D.S. Lacate, G.F. Weetman, R.F. Powers (Eds.), Sustained Productivity of Forest Soils. University of British Columbia, Faculty of forestry Publ., Vancouver, pp. 95-121.

Cichota, R., Kelliher, F.M., Thomas, S.M., Clemens, G., Fraser, P.M., Carrick, S., 2016. Effects of irrigation intensity on preferential solute transport in a stony soil. N. Z. J. Agric. Res. 59(2), 141-155. DOI:https://doi.org/10.1080/00288233.2016.1155631

Cichota, R., Snow, V.O., 2009. Estimating nutrient loss to waterways—an overview of models of relevance to New Zealand pastoral farms. N. Z. J. Agric. Res. 52(3), 239-260. DOI:https://doi.org/10.1080/00288230909510509

Clothier, B.E., Scotter, D.R., Kerr, J.P., 1977. Water retention in soil underlain by a coarse-textured layer: theory and a field application. Soil Sci. 123(6), 392-399.

Cousin, I., Nicoullaud, B., Coutadeur, C., 2003. Influence of rock fragments on the water retention and water percolation in a calcareous soil. Catena 53(2), 97-114. DOI:https://doi.org/10.1016/S0341-8162(03)00037-7

Cousin, I., Nicoullaud, B., Tetegan, M., de Forges, A.C.R., Arrouays, D., Bouthier, A., 2014. Estimating the available water content of highly heterogeneous soils including stony soils at the regional scale. Globalsoilmap: Basis of the Global Spatial Soil Information System. Taylor and Francis Group, London.

Evett, S.R., Stone, K.C., Schwartz, R.C., O'Shaughnessy, S.A., Colaizzi, P.D., Anderson, S.K., Anderson, D.J., 2019. Resolving discrepancies between laboratory-determined field capacity values and field water content observations: implications for irrigation management. Irrig. Sci. 37(6), 751-759. DOI:https://doi.org/10.1007/s00271-019-00644-4

Fiès, J.C., Louvigny, N.D.E., Chanzy, A., 2002. The role of stones in soil water retention. Eur. J. Soil Sci. 53(1), 95-104. DOI:https://doi.org/10.1046/j.1365-2389.2002.00431.x

Gargiulo, L., Mele, G., Terribile, F., 2016. Effect of rock fragments on soil porosity: a laboratory experiment with two physically degraded soils. Eur. J. Soil Sci. 67(5), 597-604. DOI:https://doi.org/10.1111/ejss.12370

Gregory, P.J., Ingram, J.S.I., Andersson, R., Betts, R.A., Brovkin, V., Chase, T.N., Grace, P.R., Gray, A.J., Hamilton, N., Hardy, T.B., Howden, S.M., Jenkins, A., Meybeck, M., Olsson, M., Ortiz-Monasterio, I., Palm, C.A., Payn, T.W., Rummukainen, M., Schulze, R.E., Thiem, M., Valentin, C., Wilkinson, M.J., 2002. Environmental consequences of alternative practices for intensifying crop production. Agric., Ecosyst. Environ. 88(3), 279-290. DOI:https://doi.org/10.1016/S0167-8809(01)00263-8

Iiyama, I., 2016. Differences between field-monitored and laboratory-measured soil moisture characteristics. Soil Sci. Plant Nutr. 62(5-6), 416-422. DOI:https://doi.org/10.1080/00380768.2016.1242367

Jarvie, H.P., Sharpley, A.N., Spears, B., Buda, A.R., May, L., Kleinman, P.J.A., 2013. Water quality remediation faces unprecedented challenges from "legacy phosphorus". Environ. Sci. Technol. 47(16), 8997-8998. DOI:https://doi.org/10.1021/es403160a

Johnston, R., Barry, S., Bleys, E., Bui, E.N., Moran, C., Simon, D., Carlile, P., McKenzie, N., Henderson, B., Chapman, G., 2003. ASRIS: the database. Soil Res. 41(6), 1021-1036. DOI:https://doi.org/10.1071/SR02033

Jomaa, S., Jiang, S., Thraen, D., Rode, M., 2016. Modelling the effect of different agricultural practices on stream nitrogen load in central Germany. Energy Sustainability Soc. 6(1), 11. DOI:https://doi.org/10.1186/s13705-016-0077-9

Khatri, N., Tyagi, S., 2015. Influences of natural and anthropogenic factors on surface and groundwater quality in rural and urban areas. Front. Life Sci. 8(1), 23-39. DOI:https://doi.org/10.1080/21553769.2014.933716

Lilburne, L.R., Hewitt, A.E., Webb, T.W., 2012. Soil and informatics science combine to develop S-map: a new generation soil information system for New Zealand. Geoderma 170, 232-238. DOI:https://doi.org/10.1016/j.geoderma.2011.11.012

Ma, D.H., Shao, M.G., 2008. Simulating infiltration into stony soils with a dual-porosity model. Eur. J. Soil Sci. 59(5), 950-959. DOI:https://doi.org/10.1111/j.1365-2389.2008.01055.x

McDowell, R.W., Noble, A., Pletnyakov, P., Haggard, B.E., Mosley, L.M., 2020. Global mapping of freshwater nutrient enrichment and periphyton growth potential. Sci. Rep. 10(1), 3568. DOI:https://doi.org/10.1038/s41598-020-60279-w

McNeill, S.J., Lilburne, L.R., Carrick, S., Webb, T.H., Cuthill, T., 2018. Pedotransfer functions for the soil water characteristics of New Zealand soils using S-map information. Geoderma 326, 96-110. DOI:https://doi.org/10.1016/j.geoderma.2018.04.011

Ministry for the Environment & Stats NZ, 2020. New Zealand's Environmental Reporting Series: Our Freshwater 2020 (ME 1490), Author, Wellington, New Zealand.

Olguin, E.J., 2003. Phycoremediation: key issues for cost-effective nutrient removal processes. Biotechnol. Adv. 22(1), 81-91. DOI:https://doi.org/10.1016/S0734-9750(03)00130-7

Parajuli, K., Sadeghi, M., Jones, S.B., 2017. A binary mixing model for characterizing stony-soil water retention. Agric. For. Meteorol. 244-245, 1-8. DOI:https://doi.org/10.1016/j.agrformet.2017.05.013

Poesen, J., Lavee, H., 1994. Rock fragments in top soils: significance and processes. Catena 23(1), 1-28. DOI:https://doi.org/10.1016/0341-8162(94)90050-7

Román Dobarco, M., Bourennane, H., Arrouays, D., Saby, N.P.A., Cousin, I., Martin, M.P., 2019a. Uncertainty assessment of GlobalSoilMap soil available water capacity products: a French case study. Geoderma 344, 14-30. DOI:https://doi.org/10.1016/j.geoderma.2019.02.036

Román Dobarco, M., Cousin, I., Le Bas, C., Martin, M.P., 2019b. Pedotransfer functions for predicting available water capacity in French soils, their applicability domain and associated uncertainty. Geoderma 336, 81-95. DOI:https://doi.org/10.1016/j.geoderma.2018.08.022

Scheinost, A.C., Sinowski, W., Auerswald, K., 1997. Regionalization of soil water retention curves in a highly variable soilscape, I. Developing a new pedotransfer function. Geoderma 78(3), 129-143. DOI:https://doi.org/10.1016/S0016-7061(97)00046-3

Stewart, V.I., Adams, W.A., Abdulla, H.H., 1970. Quantitative pedological studies on soils derived from silurian mudstones. J. Soil Sci. 21(2), 248-255. DOI:https://doi.org/10.1111/j.1365-2389.1970.tb01174.x

Tetegan, M., Nicoullaud, B., Baize, D., Bouthier, A., Cousin, I., 2011. The contribution of rock fragments to the available water content of stony soils: proposition of new pedotransfer functions. Geoderma 165(1), 40-49. DOI:https://doi.org/10.1016/j.geoderma.2011.07.001

Torri, D., Poesen, J., Monaci, F., Busoni, E., 1994. Rock fragment content and fine soil bulk density. Catena 23(1), 65-71. DOI:https://doi.org/10.1016/0341-8162(94)90053-1

Wang, H.F., Xiao, B., Wang, M.Y., Shao, M.A., 2013. Modeling the soil water retention curves of soil-gravel mixtures with regression method on the loess plateau of China. Plos One 8(3). DOI:https://doi.org/10.1371/journal.pone.0059475

Wu, W.-b., Yu, Q.-y., Peter, V.H., You, L.-z., Yang, P., Tang, H.-j., 2014. How could agricultural land systems contribute to raise food production under global change? J. Integr. Agric. 13(7), 1432-1442. DOI:https://doi.org/10.1016/S2095-3119(14)60819-4

Chapter 2

Literature review

In this review, I focus on six topics relating to the studies undertaken towards achieving my main aim: (1) field capacity; (2) stony soils and where to find them; (3) rock fragment water retention; (4) how rock fragments influence soil properties; (5) methods of measuring soil water attributes of stony soils and (6) modelling of soil hydraulic properties in stony soils.

2.1 Field capacity

Field capacity (FC) is a theoretical concept that may be considered as "the amount of water held in the soil after the excess water has drained away and the rate of downward movement of water has materially decreased" (Veihmeyer and Hendrickson, 1949). As such, FC represents the threshold water content (WC) beyond which soil begins to drain significantly (i.e., the upper drainable limit), which together with wilting point is used to determine soil available water holding capacity (AWC). Though simple in concept, defining FC remains challenging, as this soil hydraulic property can be affected by various soil attributes such as soil texture, presence of impeding or highly permeable layers, soil layering and depth to groundwater (Ottoni et al., 2014; Pirastru and Niedda, 2013; Twarakavi et al., 2009; Vogeler et al., 2019). As a consequence, a variety of criteria and proxies for FC have been developed, including the WC after an elapsed time after irrigation or rainfall, the attainment of a negligible internal drainage flux, reaching hydrostatic equilibrium, or a prescribed matric potential is attained. Despite its mercurial character, FC remains an essential parameter used extensively in research publications (de Jong van Lier, 2017; Ma et al., 2016), agronomic management decisions (Li et al., 2018), policy (Wheeler and Read, 2016), environmental reporting (Sparling et al., 2008) and in national (S-map in New Zealand, McNeill et al., 2018) and international (Global Soil Map, Arrouays et al., 2014) soil information systems.

In some coarse (sandy or stony) textured soils, negligible drainage rates (0.001, 0.005, 0.1, and 0.01 cm d^{-1}, Clothier et al., 1977; Cong et al., 2014; Twarakavi et al., 2009) can be reached in 1-2 days, while medium to fine-textured soils can drain for weeks (Assouline and Or, 2014). This demonstrates the inconsistency between elapsed time-based definitions that are applied universally to soils of any textural class and negligible drainage-based definitions of FC. However, in terms of a practical definition, two days of drainage can be quite robust (Twarakavi et al., 2009). It can also indicate the point beyond which the rate of drainage is sufficiently slow that plants have access to water for extended periods and hence that water should be considered as available. For soils with shallow water tables or underlain by a coarse-textured layer (Clothier et al., 1977), hydrostatic equilibrium

can be a proxy for FC. Hydrostatic equilibrium is a condition in the soil-water system when matric potential and gravitational potential are balanced. There is no vertical variation in total potential (if the osmotic potential is negligible) and consequently, water does not move. Accepting that FC prevails when drainage has materially ceased, then hydrostatic equilibrium (which is equivalent to 0.098 kPa cm^{-1} assuming the density of water is 1.00 g cm^{-3}) is a sufficient condition for FC. However, FC usually only approximates hydrostatic equilibrium in soils with shallow groundwater systems, i.e., ~<2 m from the soil surface to groundwater (Beldring et al., 1999; Dettmann and Bechtold, 2016; Pirastru and Niedda, 2013). The groundwater table produces a 0 kPa matric potential boundary condition close to the soil surface (Figure 1). Hydrostatic equilibrium can be established under this condition because matric potential towards the soil surface is not so low that the water can't move. For instance, if the soil surface were 1 m above the groundwater table, at hydrostatic equilibrium, matric potential would be -10 kPa at the surface, compared to -100 kPa if the soil surface was 10 m from the groundwater table. A change from -10 kPa to -100 kPa corresponds to a reduction in hydraulic conductivity of more than two orders of magnitude for a loam or coarser textured soil matrix (Doussan and Ruy, 2009). Hence, upper layers of a soil with a 10 m-deep groundwater table are so slowly conductive that hydrostatic equilibrium is not attained before other water transport processes become important (root water uptake, for example).

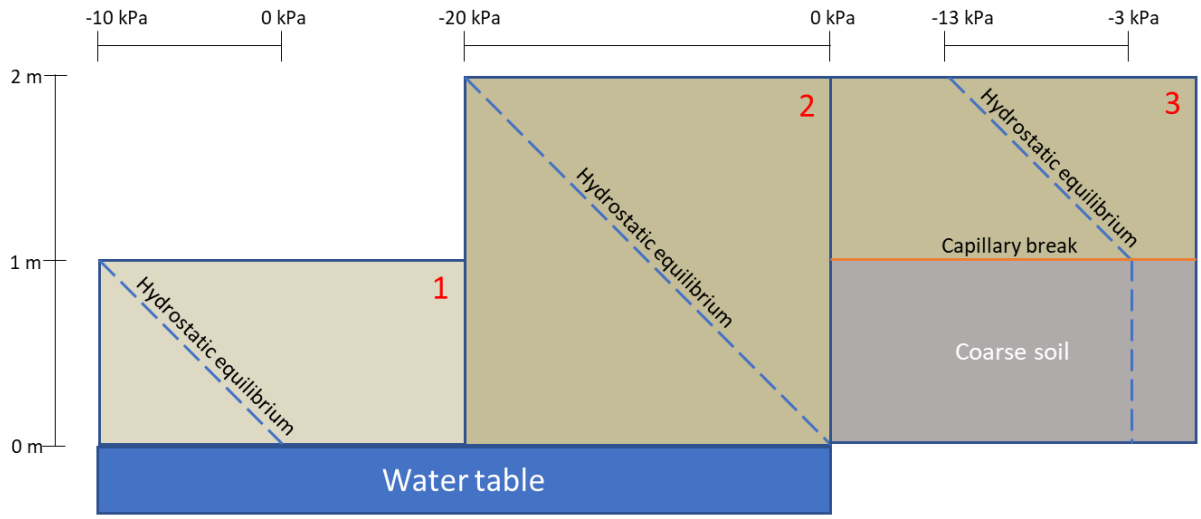

Figure 1 Schematic diagram of hydrostatic equilibrium established with the ground water table (1 and 2) and with an underlying coarse textured layer (3).

Hydrostatic equilibrium may also arise if the soil is underlain by a coarse-textured stratum at a depth of 1 to 2 m from the soil surface (Clothier et al., 1977). The coarse-textured soil produces a near-zero, but finite (negative) matric potential called a capillary break or barrier (Figure 1). The coarse soil will not drain effectively beyond a finite matric potential (discussed in more detail in Section 2.4.2) and so produces a boundary condition above which hydrostatic equilibrium (0.098 kPa cm^{-1}) can prevail.

As for the water table boundary condition, hydrostatic equilibrium will only establish if the capillary break is at a shallow depth (~<2 m).

In an attempt to standardise the definition of FC, an arbitrary matric potential is often adopted, under the assumption that drainage in all soils would become negligible at a threshold potential (Assouline and Or, 2014; Colman, 1947). Previous studies have demonstrated that no single matric potential can describe FC in soils, with proposed matric potentials for FC ranging from -33 to -5 kPa (Nemes et al., 2011; Richards and Weaver, 1944; Salter and Haworth, 1961). However, matric potential is still the de facto criterion for determining FC in several countries, including New Zealand, which currently uses a -10 kPa criterion for nutrient discharge regulations and irrigation management. Nonetheless, some New Zealand-based studies that used a two day-drainage criterion after rain/irrigation as a proxy for FC showed that matric potential could vary from -5 to -26 kPa (Gradwell, 1985; Gradwell, 1974; Rickard and Cossens, 1966). None of the soils in these studies was stony, nor are there other examples in the international literature where matric potential at FC in stony soils has been characterised. Considering rock fragments (RFs) are commonly associated with coarse-textured soils with low water retention (Carrick et al., 2013) and rapid drainage once wet above FC (Cichota et al., 2016), error in FC estimation could potentially propagate through to significant uncertainty in the AWC of these soils, or the quantity of drainage and nutrient leaching estimated from model simulations.

2.2 Stony soils and where to find them

Within soil taxonomy systems, stoniness (or skeletal/skeletic properties) is not used as a differentia at higher categories, being only recognised as one of the four criteria for defining the family level of the NZ Soil Classification (Webb and Lilburne, 2011), one of nine differentiae for defining the family level of the USDA (Soil Survey Staff, 2010) and only a qualifier for the second-level units of the WRB (IUSS Working Group WRB, 2015). In the NZSC, stony soils are classified as soils with ≥35% RFs by volume extending from a depth within 45 cm of the soil surface to a depth >100 cm (Webb and Lilburne, 2011). RFs are classified in soils by their size and shape, with various classification systems used worldwide (Table 1). As the term “stone” refers to a particular RF size class that can have different size definitions depending on the classification system used, the terms RF or clast have become a more appropriate nomenclature. Lithology and degree of weathering (or alteration status) are also key factors in most national soil classification systems (Jahn et al., 2006; Milne et al., 1995; Soil Science Division Staff, 2017; Webb and Lilburne, 2011).

Table 1 Rock fragment size classifications for various countries and institutions.

	Size (mm)	Classification
FAO	2-6	Fine gravel
	6-20	Medium gravel
	20-60	Coarse gravel
	60-200	Stones
	200-600	Boulders
(Jahn et al., 2006)	>600	Large boulders
New Zealand	2-6	Fine gravel
	6-20	Medium gravel
	20-60	Coarse gravel
	60-200	Very coarse gravel
(Milne et al., 1995)	>200	Boulders
U.K.	2-6	Very small stone
	6-20	Small stone
	20-60	Medium stone
	60-200	Large stone
	200-600	Very large stone
(Hodgeson, 1976)	>600	Boulder
USDA (non-flat fragments)	2-5	Fine gravel
	5-20	Medium gravel
	20-76	Coarse gravel
	76-250	Cobbles
	250-600	Stones
(Soil Science Division Staff, 2017)	>600	Boulders
USDA (flat fragments)	2-150	Channers
	150-380	Flagstones
	380-600	Stones
(Soil Science Division Staff, 2017)	>600	Boulders

An important class of stony soils occurs on alluvial and fluvial fans, which are present worldwide and represent the dominant sedimentary systems wherever streams and rivers leave regions of high relief to flow across lowlands. Upon reaching lowland areas, coarse alluvial sediment sourced from mountainous terrain is deposited where the fluvial transport capacity suddenly decreases with the decrease in gradient and lack of confinement, forming a fluvial or alluvial fan (Harvey, 2018). Fluvial fans and related megafans (radii > 30 km, Gohain and Parkash, 1990) occupy a vast area of alluvial lowlands at the foots of mountain chains such as the Andes (Casanova et al., 2013), the Himalaya (Ayaz et al., 2018; Kumar et al., 2007; Suresh et al., 2007), Alps-Pyrenees (Fontana et al., 2014; Jones, 2004), Sierra Nevada (Olmsted and Davis, 1961) and the Southern Alps (Weissmann et al., 2015). The characteristic properties of fluvial and alluvial fan stony soils include both the abundance of RFs and the tendency for depositional layering of materials of contrasting grain size and fabric. Streamflow on the fan surface tends to be wide, slow and demonstrates a braided river pattern with a tendency to switch position by avulsion (Harvey, 2018). This depositional process commonly results in cross-bedded units of sharply alternating grain sizes and RF-supported beds that are either open framework or loosely filled with a sand matrix (Dann et al., 2009; Fairbridge, 1997; Pierce and Scott, 1982).

A total of 1.68 million hectares of stony soil has been mapped across New Zealand on lowland surfaces with <15° slope and the potential for intensive land use (Carrick et al., 2013). Most stony soils occur in the Canterbury Region with 891,156 ha, followed by Otago with 197,937 ha, Southland with 159,561 ha, and the West Coast with 155,226 ha (Carrick et al., 2013). Much of this area is found on fluvial and alluvial plains (Dann et al., 2009; Gerrard, 1992; Rijkse, 1985). Though previously classified as unproductive land, considerable areas of these stony soils are now being used for agriculture (Figure 2), especially in Canterbury, where two-thirds of the irrigated land is on stony soils of fluvial origin.

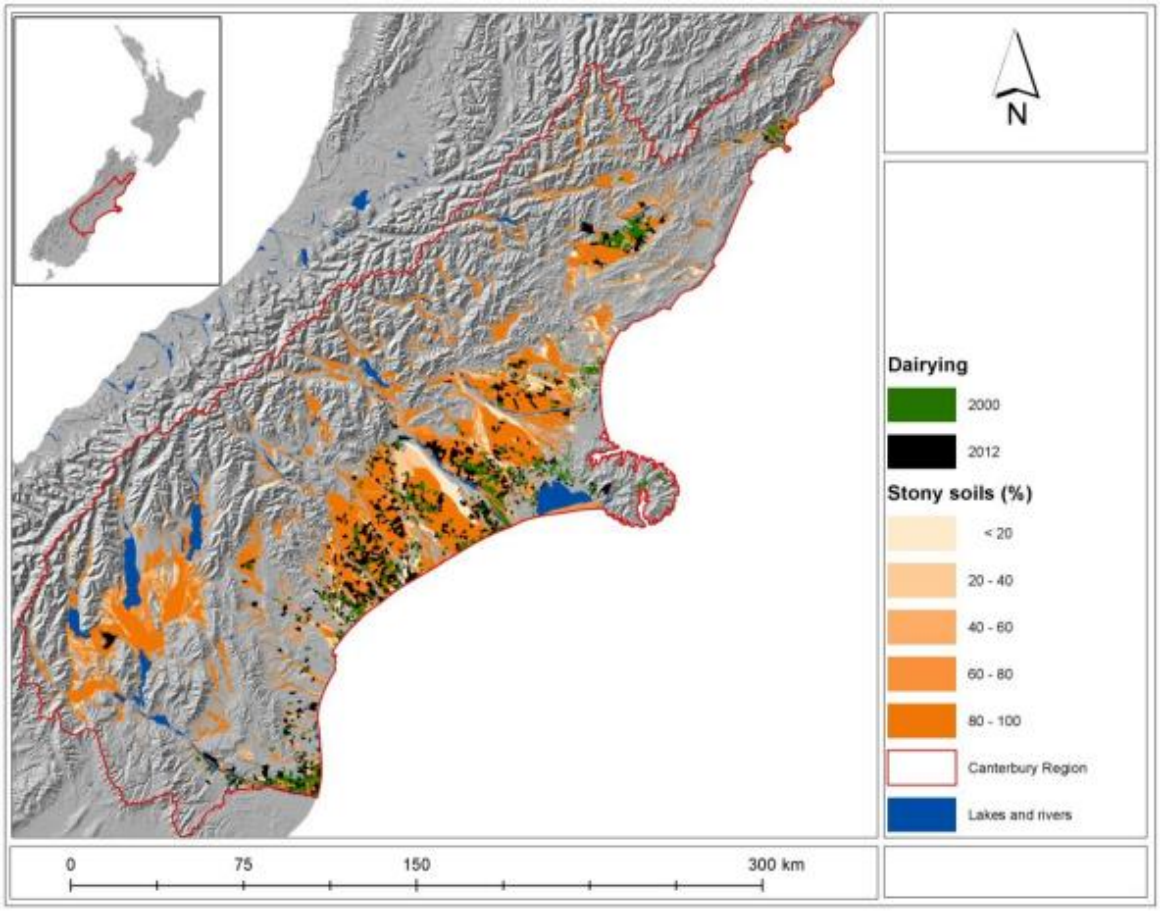

Figure 2 Increase in dairy land use on stony soils from 2000 to 2012 in the Canterbury Region. Retrieved from Carrick et al. (2013).

The Canterbury region is dominated by the Canterbury Plains, which are approximately 180 km long and 70 km at their widest and bordered by the Southern Alps to the west. The Southern Alps are an orogenic mountain belt associated with the obliquely convergent Pacific and Australian Plate boundary, which is marked by the Alpine Fault in the west. The Alpine Fault is a transform boundary that runs nearly the whole length of the South Island, with the crust on the west side moving north relative to the east side (Coates and Cox, 2002). The collision of the Australian and Pacific Plates has also compressed the New Zealand crust, pushing it up above sea level at rates of up to 11 mm per

year, forming the Southern Alps in an event dubbed the Kaikoura Orogeny (Ballance, 2017; Coates and Cox, 2002; Robertson et al., 2019). These mountains are mainly composed of indurated muddy fine sandstone known as "greywacke", of Late Paleozoic to (and including) Early Cretaceous age, with southern and western parts of the Alps formed of schist (Ballance, 2017; Robertson et al., 2019).

The Plains to the west of the Pacific coastal margin have been built by coalescing Pleistocene glacial outwash fans dominated by greywacke of the Rakaia terrane (Forsyth et al., 2008). Greywacke is characterised by a generally high bulk density (2.51-2.71 g cm^{-3}) and low porosity of 2-4% (Jones, 2016; McNamara et al., 2014; Tenzer et al., 2011). The fans are formed as alluvium carried by gravel-bed rivers sourced near the main divide of the Southern Alps is deposited upon reaching lowland areas. The surfaces of the fans are characterised by a relict braided channel pattern except where this is buried by loess. The large rivers sourced in the Southern Alps are now entrenched within the Pleistocene fans to form inset fans of Holocene age (Figure 3). Soils formed on both Pleistocene and Holocene surfaces are generally well to imperfectly drained with moderate to rapid permeability (Carrick et al., 2013).

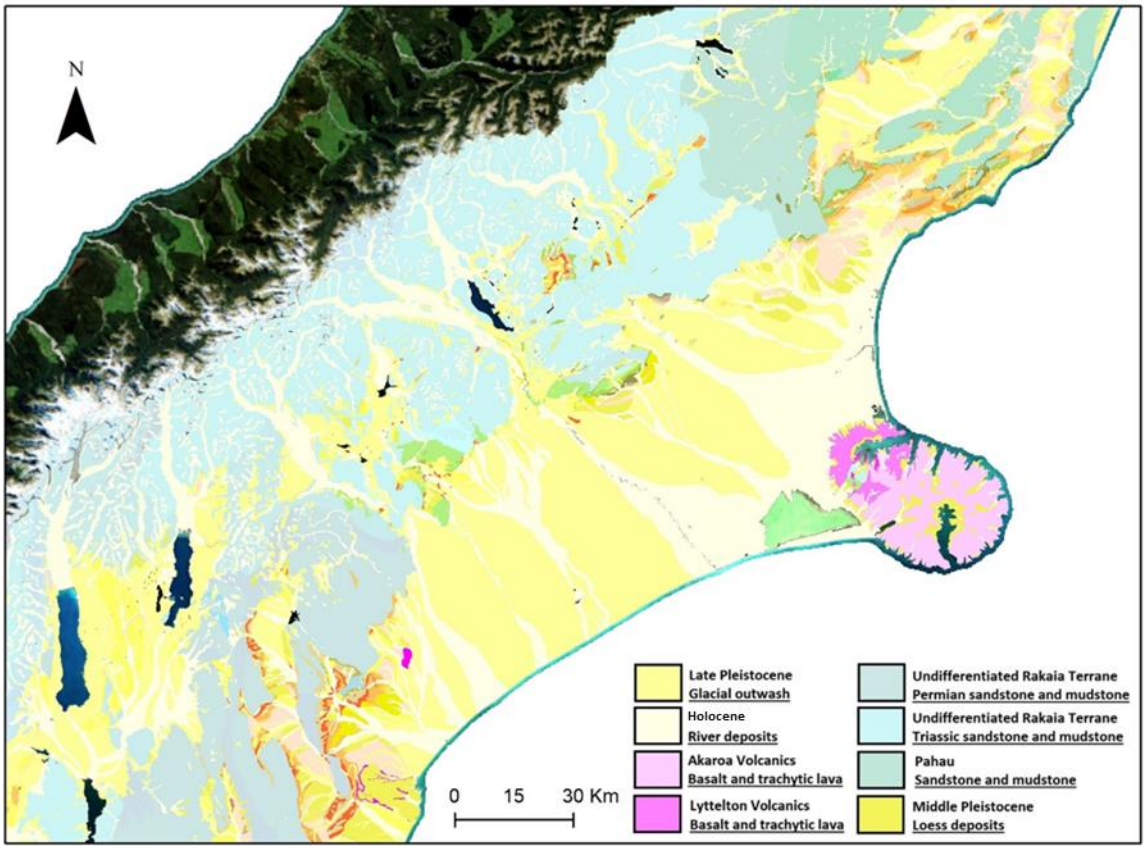

Figure 3 Geology of the Canterbury Plains. Contains data sourced from the LINZ Data Service licensed for reuse under CC BY 4.0.

2.3 Rock fragment water retention

RFs are commonly seen as inert. However, depending on the shape, size, degree of weathering and the geological origin, RFs are capable of significantly influencing soil hydro-physical properties (Hlavacikova et al., 2015).

Often, RFs are assumed to have little porosity for water intake or storage despite evidence to the contrary (Table 2). The magnitude of the effect of RFs on water storage can depend on the lithology of the rock; for example, saturated volumetric WC of pumice RFs can exceed 0.55 $m^3\ m^{-3}$, whereas the equivalent in fine sandstone fragments can be <0.025 $m^3\ m^{-3}$ (Table 2). Work by Deutschmann and Ludwig (2000) indicates this difference in water retention is due to variation in effective porosity. Measuring a range of rock types at various depths, they showed the effective porosity of RFs in different profiles ranged from 0.04 to 0.28 ($m^3\ m^{-3}$) and was largest for siltstones and diabase. However, considering the effective porosity of sandstone ranged from 0.04 to 0.23 ($m^3\ m^{-3}$), lithology is not the only factor determining porosity and water retention (Deutschmann and Ludwig, 2000). Ugolini et al. (1996) also found a range of porosities for sandstone fragments (0.18-0.31) from three profiles in Italy. These measurements were compared to unweathered sandstone, which had a total porosity of 0.05, demonstrating that weathering had a significant effect on the RF porosity (Ugolini et al., 1996).

Weathering of RFs involves a mixture of complex physical and chemical processes, which over time decreases the bulk density and increases porosity. Physical weathering can arise from rock deformation or unloading, freeze-thaw and crystallisation, or abrasion from colluvial and fluvial transport processes. Though significant in breaking down RFs, physical weathering's major impact is increasing the area of rock exposed to water. When exposed to water, RFs are broken down by hydrolysis. The H^+ ions present in water replace basic ions within the mineral structure of rocks causing the consequent collapse of the rock's structure. This process forms secondary minerals (such as clays) and increases the porosity of the RFs (Navarre-Sitchler et al., 2015). As a result, the water holding capacity and the mineral surface area of the RF increases, allowing more water to infiltrate into the rock, leading to more chemical weathering in a positive-feedback loop (Brantley et al., 2008). The rate and magnitude of this process is influenced by the solubility and proportion of primary minerals within the rock (White, 2008). For instance, actinolite and augite minerals solubilise much quicker than minerals like quartz (Navarre-Sitchler et al., 2015). Thus, rocks that are rich in augite such as basalt are likely to weather more rapidly and become more porous than rocks like granite, which are dominated by quartz and Na-rich or alkali feldspars (Navarre-Sitchler et al., 2015).

The effects of weathering have been characterised in numerous ways (Coulson et al., 2007; Jones and Graham, 1993; Ketcham and Iturrino, 2005; Tokunaga et al., 2003). Colour intensity, surface

roughness and shape are good indicators of weathering; however, the degree of weathering has also been found to correspond well with dimensional separation (Corti et al., 1998). The simplest criterion for weathering is size classification, whereby smaller rock fragments are more strongly weathered, have higher porosity and overall surface roughness per unit volume of soil (Corti et al., 1998; Ugolini et al., 1996). The robustness of this criterion has been demonstrated by numerous studies showing differences in the WC of RFs with the same lithology but different size class (Table 2). However, Tokunaga et al. (2003) highlighted that surface roughness is not the only factor affecting water retention in RFs, finding that for basalt, surface water was negligible in comparison to the water derived from intragranular pores at matric potentials less than -2 kPa.

Table 2 Water content at saturation (sat.), FC and wilting point (WP) for fragments of different rock type and size.

Rock type	Size	Bulk density	WC sat.	WC FC	WC WP	Source
	mm	g cm^{-3}	%	%	%	
Fine-grained sandstone	25	2.35	3.6v			(Parajuli et al., 2017)
	25	2.45	2.5v			(Parajuli et al., 2017)
Micaceous fine-grained sandstone	2-4	2.49	43.57v	16.48*v	3.13v	(Schoeman et al., 1997)
	4-10	2.49	17.65v	14.56*v	5.46v	(Schoeman et al., 1997)
	10-26	2.49	8.52v	7.01*v	3.93v	(Schoeman et al., 1997)
	26-75	2.49	9.28v	8.93*v	7.04v	(Schoeman et al., 1997)
Coarse-grained sandstone	2-4	2.40	35.74v	18.17*v	5.34v	(Schoeman et al., 1997)
	4-10	2.40	18.15v	13.17*v	7.07v	(Schoeman et al., 1997)
	10-26	2.40	17.64v	11.98*v	3.40v	(Schoeman et al., 1997)
	25	1.65	34.3v			(Parajuli et al., 2017)
	26-75	2.40	10.32v	9.94*v	6.55v	(Schoeman et al., 1997)
Micaceous shale	2-4	2.47	36.80v	24.17*v	9.12v	(Schoeman et al., 1997)
	4-10	2.47	16.89v	12.41*v	2.49v	(Schoeman et al., 1997)
	10-26	2.47	10.85v	9.84*v	5.74v	(Schoeman et al., 1997)
	26-75	2.47	7.13v	6.86*v	5.42v	(Schoeman et al., 1997)
Carbonaceous shale	2-4	2.08	34.16v	13.11*v	1.69v	(Schoeman et al., 1997)
	4-10	2.08	11.35v	7.32*v	0.08v	(Schoeman et al., 1997)
	10-26	2.08	7.21v	4.37*v	0.17v	(Schoeman et al., 1997)
	26-75	2.08	8.89v	8.43*v	7.27v	(Schoeman et al., 1997)
Dolostone	25	2.6	4.3v			(Parajuli et al., 2017)
Limestone	25	2.3	6.1v			(Parajuli et al., 2017)
	20-50	2.18		9^m		(Tetegan et al., 2011)
			7.9m	7.2m	1.4m	(Gras and Monnier, 1963)
Pumice	25	0.96	55v			(Parajuli et al., 2017)
Gaize	20-50	1.44		31^m		(Tetegan et al., 2011)
Chalk	20-50	1.76		21^m		(Tetegan et al., 2011)
			26.9m	25.7m	1.0	(Gras and Monnier, 1963)
Chert	20-50	2.07		13^m		(Tetegan et al., 2011)
Flint	20-50	2.22		6^m		(Tetegan et al., 2011)
			0.2m	0.1m	0.1m	(Gras and Monnier, 1963)
Shale	2-5	2.07	49.6m	26.7 ^{f}m	13.8m	(Hanson and Blevins, 1979)
	5-20	2.07	32.6m	18.4 ^{f}m	12.5m	(Hanson and Blevins, 1979)
	20-25	2.07	19.7m	17.3 ^{f}m	11.1m	(Hanson and Blevins, 1979)

v: Volumetric water content; m: Gravimetric water content

^: FC at -10 kPa; *: FC at -33 kPa; ^{f}: FC at field condition

2.4 How rock fragments influence soil properties

2.4.1 Effect on soil structure

RFs have been found to indirectly affect water movement by influencing soil structure and porosity (Naseri et al., 2019; Poesen et al., 1997; Ravina and Magier, 1984; Torri et al., 1994). For example, increasing RF content corresponds to a decrease in the bulk density of the fine earth (Gargiulo et al., 2016; Poesen and Lavee, 1994; Stewart et al., 1970; Torri et al., 1994). The reason for this negative relationship could be caused by one or several factors, such as:

1. Sedimentary processes can deposit RFs without sufficient fine earth to fill inter RF voids, resulting in lower bulk density in the fine earth (Lunt and Bridge, 2007; Poesen and Lavee, 1994; Stewart et al., 1970). Under specific flow regimes, this can ultimately culminate in the deposition of open framework gravels, a coarse layer where little to no fine earth is present (Dann et al., 2009).

2. In a mixture of two particle size grades, the presence of even a small proportion of large particles has a negative effect on the bulk density of the smaller particles because the smaller particles cannot pack as closely to the larger particles as they can with each other (Poesen and Lavee, 1994; Stewart et al., 1970). Also, fine earth and RFs react differently when expanding and contracting (e.g. during the process of wetting and drying or of freezing and thawing), which causes an increase in porosity for the size range larger than 250 µm (Gargiulo et al., 2016).

3. The presence of RFs in the soil changes the nature of the fine earth fraction. With increasing RF content, decaying OM, fertiliser inputs, rainwater etc. are concentrated in a decreasing mass of fine earth, affecting other soil properties such as soil structure (Poesen and Lavee, 1994).

Gargiulo et al. (2016) found significant reductions in fine earth bulk density could occur after only nine wetting and drying cycles, even in soils characterised by a massive structure in the field and a poor ability to self-structure. The study indicated that soil texture and RF content could influence results, with greater porosity changes occurring in soils with greater soil shrinkage potential (more clay), and a volumetric RF content of 25% or more. Fiès et al. (2002) documented similar reductions in fine earth bulk density with increasing clast content; however, clast contents were greater before any effect was registered. For fine earth bulk density to reduce, a clay content of 30% and a clast proportion of 0.50 kg kg^{-1} (~0.43 m^3 m^{-3}) was required in Fiès et al.'s (2002) experiments. The contrast in sensitivity to RF content between Gargiulo et al.'s (2016) experiment and the latter is

probably because Gargiulo et al.'s (2016) study included nine wetting and drying cycles before making measurements, facilitating the process of pore formation.

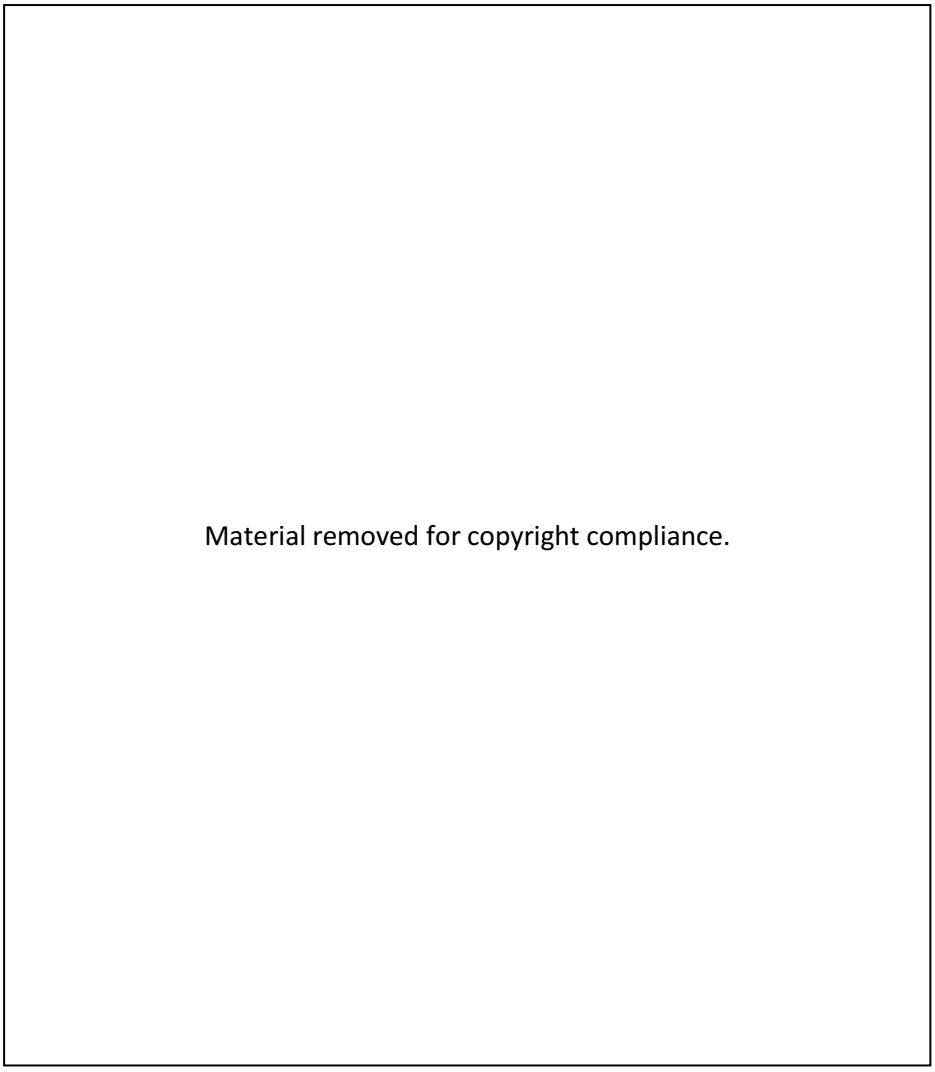

Figure 4 Cumulated pore size distributions for (a) Luvisol and (b) Regosol averaged from the three replicates for all the RF contents tested (Gargiulo et al., 2016).

Disagreement exists in the literature as to the pore fraction that is most strongly affected by increasing RF content. Multiple studies found the change in pore fraction caused by RFs involved only the creation of coarse lacunar pores around the surface of RFs (Baetens et al., 2009; Fiès et al., 2002; Shi et al., 2012; van Wesemael et al., 1995a). Other studies have shown effects across the whole range of pore sizes (Figure 4, Gargiulo et al., 2016), leading to an increase in water holding capacity (Ingelmo et al., 1994). Gargiulo et al. (2016) proposed that differential shrinkage between RFs and fine earth is the leading mechanism for generating pores, which may explain the greater sensitivity of porosity changes to RF abundance and shrinkage potential (Ingelmo et al., 1994). However, most experiments investigating these effects use repacked cores and a single wetting and drying event, making results prone to packing artefacts.

In a field trial, Chow et al. (2007) measured the porosity of RF-amended soil over three years. They found the macroporosity significantly increased with RF content in the first year but reverted to control conditions over the second and third. Although land management over that time may have been the cause, the results demonstrate that repacked soil without multiple wetting and drying cycles may not be representative of field conditions. Sauer and Logsdon (2002) hypothesised from a field tension infiltrometer study that the provenance of RFs (weathering in place, colluvial and alluvial origin) and contact with the surrounding fine earth fraction might influence the effect of the RFs in the soil. As these conditions are unlikely to be replicated in repacked cores, field trials may have different results; for example, Meng et al. (2018) found macroporosity decreased with increasing RFs in undisturbed forest stony soils. The contradictory results described above demonstrate a gap in the literature, justifying more field and undisturbed-soil research on stony soils.

2.4.2 Hydrodynamics

RFs are commonly perceived to reduce the whole soil porosity and water storage capacity of the soil, causing stony soils to be classified as a particular risk to nutrient leaching (Carrick et al., 2013). These assumptions are currently utilised in the New Zealand nutrient budgeting model OVERSEER®, in which an increase in the volume of RFs results in a decrease in water holding capacity and increase in infiltration rate. This is considered a blanket rule for all stony soils in New Zealand despite McLeod et al. (2014) showing drainage characteristics of soils appear to be strongly related to a threshold RF abundance (Khetdan et al., 2017). Zhou et al. (2009) found saturated conductivity and infiltration initially decreased with increasing RF abundance until a gravimetric RF content of 40%, beyond which, rates increased. Similar results were observed by Chow et al. (2007) but at a threshold volumetric RF content between 20-30%. These threshold RF contents align approximately with the RF content marking the transition from a matrix-supported to a clast-supported fabric (Milne et al., 1995). Below these threshold RF contents, RFs restrict the movement of water by reducing the cross-sectional area available for water to be conducted. When the threshold is reached or exceeded, RFs are in contact and lacunar pores are interconnected, causing saturated hydraulic conductivity to increase significantly. However, due to the size of these interconnected macropores, when matric potential decreases from near-saturated conditions, the pores effectively cease draining, causing the unsaturated conductivity of stony soils to rapidly decrease as they dry (Arias et al., 2019; Baetens et al., 2009). Though conductive, with rapid drainage and leaching, these high RF and high macroporosity layers can be advantageous and even desired, for example, in practices such as mine rehabilitation, toxic waste management and civil engineering operations (Gee et al., 2002; Larochelle et al., 2019; Parent and Cabral, 2006; Zornberg et al., 2010). Artificially created high RF concentration layers increase water retention of overlying soil. This arises because the underlying coarse layer's (unsaturated) hydraulic conductivity is very low and its drainage is the rate-limiting step in the

drainage of the overlying fine textured layer (Clothier et al., 1977; Park and Fleming, 2006). Slow hydraulic conductivity occurs as a capillary break is formed at the interface between the fine-grained and coarse-grained materials (Figure 5). The coarse-grained material has large pores, which only drain at matric potentials close to saturation. As a result, even though the fine-grained material remains conductive, the drainage through the profile will only occur when the interface reaches these near-saturated conditions.

Drainage characteristics of soils can also be influenced by the position, alignment, size and shape of RFs; however, the nature of those effects appear to be inconsistent, and some inferences rely on modelling (Beckers et al., 2016; Hlaváčiková et al., 2016; Ma and Shao, 2008; Yang et al., 2013).

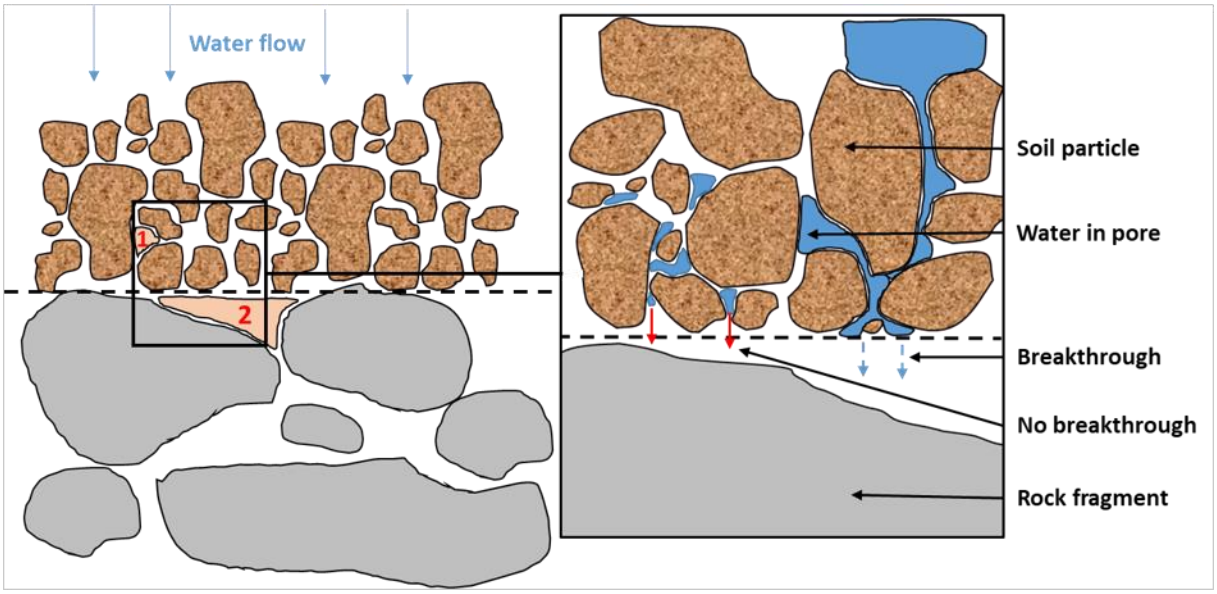

Figure 5 Capillary break effect on soil-rock fragment interface. Area 1 and 2 emphasise the difference in pore size between the two contrasting layers. Adapted from the schematic in Zornberg et al. (2010).

2.4.3 Productivity in stony soils

Up until recently, the prevailing assumption was that RFs decrease the total volume of fine earth and in so doing make stony soils unproductive land. However, the growing use of stony soils in agriculture has demonstrated that although fine earth volume may be low, RFs can be beneficial to production. Jones and Graham (1993) measured the AWC of shallow (~0.3 m), coarse-textured soils and the underlying weathered granitic rock within a forestry system. They found that not only could the underlying weathered RFs retain plant available water, they often held more water than the overlying fine earth. More recently, Tetegan et al. (2011) found the AWC of a loamy clay horizon with 30% chalk pebbles would be underestimated by 33% if the RFs were considered inert. How water is released from RFs, however, may be different from the release of water from fine earth. Tetegan et al. (2015) found during an evaporation experiment that the fine earth WC decreased as soon as

desiccation started, whereas the RFs released water after several days. The findings demonstrated that RFs can be a water reservoir for plants from which plants could extract water directly, or after water migrated into the surrounding fine earth. Unexpectedly, RFs can imbue soils with a drought resistance, which is compounded by their effects on water conservation, as described below. Danalatos et al. (1995) found under conditions of moderate water stress, water conservation was generally greater in stony soils, with cobbles on the surface increasing the biomass of wheat by 20%. Kosmas et al. (1993), Kosmas et al. (1994) and Nyssen et al. (2001) found similar positive effects on biomass production under dry climatic conditions. RFs promote water conservation by two interacting effects: by reducing evaporation (Groenevelt et al., 1989; Kemper et al., 1994; Ma and Li, 2011) and by increasing the penetration depth of rainwater (van Wesemael et al., 1995a). Kosmas et al. (1994) found that surface mulching with RFs may have reduced evaporation by 20-30% under dry weather conditions, with similar results found by van Wesemael et al. (1995b) when the soil surface was wet. The presence of RFs also increases the percolation depth of water because of the decrease in total porosity and increase in macroporosity that can occur with increasing RF content (van Wesemael et al., 1995a). Hence, percolating water is stored at greater depth in stony soils compared to non-stony soils, and thus is less susceptible to evaporation (Kosmas et al., 1993; van Wesemael et al., 1995a). However, under exceptionally wet conditions or pronounced drought, RFs negatively affect water conservation and biomass production (Danalatos et al., 1995; Kosmas et al., 1994).

RFs can also affect plant growth by promoting numerous beneficial growth conditions. As mentioned previously, RFs may decrease the fine earth bulk density, but have also been found to increase the resistance of the soil to compaction (Gargiulo et al., 2016; Rücknagel et al., 2013), erosion (Poesen et al., 1994; Rieke-Zapp et al., 2007) and mechanical degradation from cultivation (van Wesemael et al., 1995a). Several international studies have also identified an increase in carbon in the topsoil of stony soils (Bornemann et al., 2011; Poesen and Lavee, 1994; van Wesemael et al., 1995a). The cause for this is commonly attributed to a disproportionate input of organic matter in a progressively lower volume of fine earth as RF volume increases. RFs have also been found to contribute to soil fertility and plant nutrition (Korboulewsky et al., 2010b; Ramos et al., 2014; Uhlig and von Blanckenburg, 2019). Korboulewsky et al. (2010a) found the exchangeable Ca, Mg and K released from limestone could account for about 50%, 20% and 10%, respectively, of those released from the surrounding fine earth. However, the overall effect of RFs on productivity can be quite complex, with opposing results occurring with different conditions and plant species (Poesen and Lavee, 1994). For instance, Korboulewsky et al. (2010b) found RFs supplied nutrients, but when RFs reached relatively high proportions (40%), root development was limited, masking the nutrition effect on biomass.

2.5 Methods of measuring soil water attributes of stony soils

The presence of RFs in soil poses problems when measuring water flow, retention and physical properties because inserting probes in soils without altering soil structure is problematic (Ma et al., 2010). Stony soils are also inherently complex, potentially being composed of several fractions including fine earth (<2 mm), fine gravel (2-6 mm), medium gravel (6-20 mm), coarse gravel (20-60 mm), very coarse gravel (60-200 mm) and boulders (>200 mm) (Standards Association of New Zealand, 1986). As a result, several methodologies have been used to characterise stony soils.

The most common method of characterising stony soil is the use of repacked soils (Beckers et al., 2016; Ma et al., 2010; Parajuli et al., 2017). Considering the inherently complex nature of stony soils, the ability to construct a soil with specific RF content, size and shape can be a very powerful simplification. However, several studies have demonstrated that the soil structure and porosity of the fine earth can be altered with additions of RFs (Baetens et al., 2009; Fiès et al., 2002; Poesen and Lavee, 1994; Shi et al., 2012; Torri et al., 1994). As a result, repacking a stony soil is unlikely to represent neither the pore network nor the hydraulic dynamics of undisturbed stony soil (Ma et al., 2010).

Another measurement technique is the use of small undisturbed soil cores. These cores are ~50 x 100 mm in size, and aim to maintain the 'natural' structure of field soil, while still being relatively quick to collect and analyse (Khetdan et al., 2017; Reeve et al., 1973). Although a potential improvement on repacked soils, the volume of soil disturbed by the core collection process is a relatively large proportion. Hence, artefacts of sampling are likely to be dramatic in small cores (Baetens et al., 2009). Moreover, a small sampling volume is unlikely to be representative of the soil being measured, especially in stony soils, which require large representative elementary volumes (Buchter et al., 1994; Vincent and Chadwick, 1994).

Field trial and undisturbed lysimeter methods offer an alternative to small cores. Though they are the most accurate in representing field conditions, these methods require considerable labour and extended times for equilibrium. The process of collecting lysimeters can cause soil compaction due to friction between the soil and the walls of the lysimeter (Klocke et al., 1993). Developments in lysimeter extraction, with a focus on supporting soil pedestals, has meant monolith lysimeters can be collected without alteration of physical properties (Bowman et al., 1994). Furthermore, liquefied petrolatum injected into the gap between the monolith and lysimeter casing has been shown to prevent preferential edge flow (Cameron et al., 1992). However, stony soils remain difficult to encase as the presence of RFs makes it difficult to carve the soil to the shape of the lysimeter without disturbing the soil. Additionally, the labour and equipment required to not only excavate and carve the lysimeters but to transport, house and instrument them, means the use of lysimeters to cover

multiple sites, let alone a whole region, is financially prohibitive. Furthermore, concerns remain regarding the hydrodynamics within free drainage lysimeters (Weihermuller et al., 2007). The lower boundary of lysimeters are exposed to atmospheric pressure and as a result, the bottom of the lysimeter must be saturated before drainage will occur. These temporary anaerobic conditions may influence degradation, solute transport, capillary rise and the matric potential depth gradient at FC (Bergström, 1990; Giesler et al., 1996). As a result, few studies have used these methods, and a significant research gap exists concerning the hydraulic properties of undisturbed stony soils.

Field trials by Al-Yahyai et al. (2006) and Thoma et al. (2014) have demonstrated it is possible to measure water retention properties in stony soils in the field. However, the experimental requirements, including equipment and site-specific probe calibration, often confine experiments to one site. By reducing field trials to spot measurements, measuring becomes cheap and easy and allows many more sites to be measured (Buitenwerf et al., 2014). By utilising this method, the effect of RFs for numerous soil properties can be determined across large areas or many sites, a scale that has only previously been achieved in stony soil studies utilising tension infiltrometer measurements (Baetens et al., 2009), the results from which were restricted to the soil surface only.

2.6 Modelling of soil hydraulic properties in stony soils

Measurement methods have become steadily more sophisticated and diverse with time as the needs for soil science research has expanded into fields of precision agriculture, climate change, soil mapping and policy. A number of these fields require soil information over scales that can vary from the paddock and farm-scale to the national and global scale. However, parameters such as WC at FC, are frequently difficult or impossible to obtain at a broad scale directly from detailed field measurement, without excess cost or time. To satisfy these demands, research has focussed on the development of pedotransfer functions (PtFs) that can provide spatially distributed estimates of soil retention properties like FC using more readily available field or lab data (Vereecken et al., 1990). The variables used in models commonly depends on how predictions will be utilised, but, PtFs for predicting soil WC typically use input variables such as carbon, bulk density (whole soil or fine earth) and continuous measures of texture (i.e. proportion sand, silt or clay) (Mohamed and Ali, 2006; Ostovari et al., 2015; Pollacco, 2008; Román Dobarco et al., 2019b; Santra et al., 2018). However, a significant limitation is often these PtF models use variables that are too costly, time-consuming and labour-intensive to measure (McNeill et al., 2018).

S-map, the national soil information system of New Zealand (Lilburne et al., 2012), uses PtF's combining soil taxonomic information such as soil order and drainage class, with soil physical and morphological data, to predict the soil water characteristics of soils across New Zealand (McNeill et al., 2018). One potentially significant source of error for the S-map PtFs is that RFs in the soil are

considered as inert, such that all retention properties are based on the fine earth only. However, despite this assumption being common-place for the majority of PtFs (Arias et al., 2019; Hlaváčiková et al., 2016; Khaleel and Relyea, 1997; Novák and Kňava, 2012), it results in underestimates of stony soil water retention. Though this issue has been raised as a high priority in several publications (Pineda et al., 2018; Román Dobarco et al., 2019a; Román Dobarco et al., 2019b), only a few PtFs can be found that have attempted to include the water retention of RFs (Cousin et al., 2014; Parajuli et al., 2017; Scheinost et al., 1997; Wang et al., 2013).

Wang et al. (2013) measured the water retention curve (WRC) of soil-gravel mixtures in a small core (5 cm high x 5 cm inner diameter) lab experiment, utilising RFs with different degrees of weathering from two locations in Shaanxi province, China. The relationships between the effective degree of saturation and the gravel contents were then combined with the model of Brooks and Corey (Brooks and Corey, 1964) and the van Genuchten equation (van Genuchten, 1980). Results demonstrated that the WRC was significantly affected by the type and volume of RFs in the core. However, artefacts (as discussed in Section 2.4.1 and 2.5) associated with repacked cores limit the applicability of results to the field.

Tetegan et al. (2011) sampled soils developed over sedimentary rocks, at different locations, but mainly in the central part of France. RFs included gaize, chalk, chert, flint, and limestone lithologies, some of which were divided into subclasses, depending on their degree of weathering. The gravimetric WC at FC and wilting point, which were defined as the WC at -10 kPa and -1584 kPa, respectively, were determined with the use of a pressure plate apparatus. A simple model using the RF density and two fitting parameters to determine the AWC of the RFs was generated, requiring another prediction of the fine earth WC to determine whole soil WC. The simplicity of the PtF of this study (which requires only the dry bulk density of RFs and volumetric proportion of RFs) means it could be applicable for regional/national scale soil characterisation. However, results were not validated against field measurement of whole soil WC (fine earth and RF WC), so the accuracy of predictions in the field is uncertain. A potential source of error arises from using PtFs that predict the WC of RFs and the fine earth separately, as it likely removes the complex relationships (Section 2.4.1 and 2.4.2) between these soil fractions that could affect results.

Finally, Scheinost et al. (1997) developed a Van Genuchten-type function where the parameters were substituted by linear equations. The linear equations incorporated the bulk density, organic C, clay, silt, sand, and RF abundance (<63 mm). Model parameters were calibrated using water retention data from 396 small (365 cm^3) undisturbed soil cores measured with pressure chambers and ceramic plates. The study found RFs had a significant effect on the WRC of a stony soil. The WRC of the undisturbed cores was also estimated using the PtF of Vereecken et al. (1989). Based on the root

mean square difference between measured and predicted WRCs, it was found that Scheinost et al.'s (1997) model predicted the WRC 60% better than Vereecken et al.'s (1989) model, but only within the study area. This improvement was mainly caused by accounting for RFs in skeletal soils and soils with low density and high organic matter content. The use of undisturbed soil allows the results of this study to be immediately applicable to soil conditions in the field, demonstrating an improvement on other PtFs. The results also indicate it is possible to predict the water retention of soils with RFs accurately. However, model parameterisation requires lab work that is both costly and laborious, which restricts its use in large-scale studies. Additionally, though RFs were included, the small size of the cores may not account for the full variability in the field (as discussed in Section 2.5) especially in areas where the diameter of RFs is >64 mm. The PtF was also not explicitly validated on stony soils, with an average of ~10% gravimetric RF content in the model training dataset and validation dataset. As a result, the full influence of RFs may not be accounted for, while the validity of the PtF in soils with appreciable quantities of RFs (>30% by volume) is uncertain.

2.7 Gaps in research

Owing to the difficulties of studying stony soils, especially intact soil at a field scale, and the ambiguities related to the effects of RFs on soil hydraulic properties, the following simplifying assumptions are often applied in numerical simulation models and PtFs:

1. A singular matric potential can define FC in stony soils;
2. RFs do not retain water;
3. RFs do not affect fine earth properties.

In the current research paradigm, in which modelling is a dominant tool used in managing and regulating soil land uses, these assumptions may result in errors that have important environmental, production and economic implications. That these assumptions are wrong is certain; however, it remains to be determined, at the field scale wherever possible, the magnitude of the errors propagating from them. The priority is to characterise the water holding behaviour of stony soils *in situ* and to determine the important correlated independent variables. The characterisation must use soil volumes that adequately represent soils with abundances of RFs greater than 30% and where RFs range from 2 mm to 60 mm or greater. From such a dataset, predictive models can be developed, optimised for parsimony and generality, validated, and their performance tested against existing models that use the assumptions above.

References

Al-Yahyai, R., Schaffer, B., Davies, F.S., Munoz-Carpena, R., 2006. Characterization of soil-water retention of a very gravelly loam soil varied with determination method. Soil Sci. 171(2), 85-93. https://doi.org/10.1097/01.ss.0000187372.53896.9d.

Arias, N., Virto, I., Enrique, A., Bescansa, P., Walton, R., Wendroth, O., 2019. Effect of stoniness on the hydraulic properties of a soil from an evaporation experiment using the wind and inverse estimation methods. Water 11(3), 440. https://doi.org/10.3390/w11030440.

Arrouays, D., McBratney, A., Minasny, B., Hempel, J., Heuvelink, G., MacMillan, R., Hartemink, A., Lagacherie, P., McKenzie, N., 2014. The GlobalSoilMap project specifications. GlobalSoilMap: Basis of the Global Spatial Soil Information System, Release 2.4.

Assouline, S., Or, D., 2014. The concept of field capacity revisited: defining intrinsic static and dynamic criteria for soil internal drainage dynamics. Water Resour. Res. 50(6), 4787-4802. https://doi.org/10.1002/2014wr015475.

Baetens, J.M., Verbist, K., Cornelis, W.M., Gabriels, D., Soto, G., 2009. On the influence of coarse fragments on soil water retention. Water Resour. Res. 45. https://doi.org/10.1029/2008wr007402.

Ballance, P.F., 2017. New Zealand Geology: An Illustrated Guide. Miscellaneous Publication No. 148. Geoscience Society of New Zealand.

Beckers, E., Pichault, M., Pansak, W., Degré, A., Garré, S., 2016. Characterization of stony soils' hydraulic conductivity using laboratory and numerical experiments. SOIL 2(3), 421-431. https://doi.org/10.5194/soil-2-421-2016.

Beldring, S., Gottschalk, L., Seibert, J., Tallaksen, L., 1999. Distribution of soil moisture and groundwater levels at patch and catchment scales. Agric. For. Meteorol. 98, 305-324. https://doi.org/10.1016/S0168-1923(99)00103-3.

Bergström, L., 1990. Use of lysimeters to estimate leaching of pesticides in agricultural soils. Environ. Pollut. 67(4), 325-347. https://doi.org/10.1016/0269-7491(90)90070-S.

Bornemann, L., Herbst, M., Welp, G., Vereecken, H., Amelung, W., 2011. Rock fragments control size and saturation of organic carbon pools in agricultural topsoil. Soil Sci. Soc. Am. J. 75(5), 1898-1907. https://doi.org/10.2136/sssaj2010.0454.

Bowman, B.T., Brunke, R.R., Reynolds, W.D., Wall, G.J., 1994. Rainfall simulator grid lysimeter system for solute transport studies using large, intact soil blocks. J. Environ. Qual. 23(4), 815-822. https://doi.org/10.2134/jeq1994.00472425002300040029x.

Brantley, S.L., Bandstra, J., Moore, J., White, A.F., 2008. Modelling chemical depletion profiles in regolith. Geoderma 145(3), 494-504. https://doi.org/10.1016/j.geoderma.2008.02.010.

Brooks, R.H., Corey, A.T., 1964. Hydrology Paper No. 3. Colorado State University.

Buchter, B., Hinz, C., Flühler, H., 1994. Sample size for determination of coarse fragment content in a stony soil. Geoderma 63(3), 265-275. https://doi.org/10.1016/0016-7061(94)90068-X.

Buitenwerf, R., Kulmatiski, A., Higgins, S.I., 2014. Soil water retention curves for the major soil types of the Kruger National Park. Koedoe 56(1), 1-9. https://doi.org/10.4102/koedoe.v56i1.1228.

Cameron, K.C., Smith, N.P., McLay, C., Fraser, P.M., McPherson, R., Harrison, D., Harbottle, P., 1992. Lysimeters without edge flow: an improved design and sampling procedure. Soil Sci. Soc. Am. J. 56(5), 1625-1628. https://doi.org/10.2136/sssaj1992.03615995005600050048x.

Carrick, S., Palmer, D., Webb, T., Scott, J., Lilburne, L., 2013. Stony soils are a major challenge for nutrient management under irrigation development. In: L.D. Currie, C.L. Christensen (Eds.), Accurate and Efficient Use of Nutrients on Farms., Occasional Report No. 26. Fertiliser and Lime Research Centre, Massey University, Palmerston North, New Zealand.

Chow, T., Rees, H., Monteith, J., Toner, P., Lavoie, J., 2007. Effects of coarse fragment content on soil physical properties, soil erosion and potato production. Can. J. Soil Sci. 87, 565-577. https://doi.org/10.4141/CJSS07006.

Cichota, R., Kelliher, F.M., Thomas, S.M., Clemens, G., Fraser, P.M., Carrick, S., 2016. Effects of irrigation intensity on preferential solute transport in a stony soil. N. Z. J. Agric. Res. 59(2), 141-155. https://doi.org/10.1080/00288233.2016.1155631.

Clothier, B.E., Scotter, D.R., Kerr, J.P., 1977. Water retention in soil underlain by a coarse-textured layer: theory and a field application. Soil Sci. 123(6), 392-399.

Coates, G., Cox, G.J., 2002. The Rise and Fall of the Southern Alps. Canterbury University Press Christchurch.

Colman, E.A., 1947. A laboratory procedure for determining the field capacity of soils. Soil Sci. 63(4), 277-284.

Cong, Z.-t., Lü, H.-f., Ni, G.-h., 2014. A simplified dynamic method for field capacity estimation and its parameter analysis. Water Sci. Eng. 7(4), 351-362. https://doi.org/10.3882/j.issn.1674-2370.2014.04.001.

Corti, G., Ugolini, F., Agnelli, A., 1998. Classing the soil skeleton (greater than two millimeters): proposed approach and procedure. Soil Sci. Soc. Am. J. 62(6), 1620-1629. https://doi.org/10.2136/sssaj1998.03615995006200060020x.

Coulson, I., Beech, M., Nie, W., 2007. Physical properties of Martian meteorites: porosity and density measurements. Meteorit. Planet. Sci. 42, 2043-2054. https://doi.org/10.1111/j.1945-5100.2007.tb01006.x.

Cousin, I., Nicoullaud, B., Tetegan, M., de Forges, A.C.R., Arrouays, D., Bouthier, A., 2014. Estimating the available water content of highly heterogeneous soils including stony soils at the regional scale. Globalsoilmap: Basis of the Global Spatial Soil Information System. Taylor and Francis Group, London.

Danalatos, N.G., Kosmas, C.S., Moustakas, N.C., Yassoglou, N., 1995. Rock fragments II. Their impact on soil physical properties and biomass production under Mediterranean conditions. Soil Use Manag. 11(3), 121-126. https://doi.org/10.1111/j.1475-2743.1995.tb00509.x.

Dann, R., Close, M., Flintoft, M., Hector, R., Barlow, H., Thomas, S., Francis, G., 2009. Characterization and estimation of hydraulic properties in an alluvial gravel vadose zone. Vadose Zone J. 8(3), 651-663. https://doi.org/10.2136/vzj2008.0174.

de Jong van Lier, Q., 2017. Field capacity, a valid upper limit of crop available water? Agri. Water Manage. 193, 214-220. https://doi.org/10.1016/j.agwat.2017.08.017.

Dettmann, U., Bechtold, M., 2016. Deriving effective soil water retention characteristics from shallow water table fluctuations in peatlands. Vadose Zone J. 15(10). https://doi.org/10.2136/vzj2016.04.0029.

Deutschmann, G., Ludwig, B., 2000. Exchangeable cations in rock fractions and fine earth in soil profiles of different genesis. J. Plant Nutr. Soil Sci. 163(2), 183-189. https://doi.org/10.1002/(sici)1522-2624(200004)163:2<183::aid-jpln183>3.0.co;2-d.

Doussan, C., Ruy, S., 2009. Prediction of unsaturated soil hydraulic conductivity with electrical conductivity. Water Resour. Res., 45, W10408. https://doi.org/10.1029/2008wr007309.

Fiès, J.C., Louvigny, N.D.E., Chanzy, A., 2002. The role of stones in soil water retention. Eur. J. Soil Sci. 53(1), 95-104. https://doi.org/10.1046/j.1365-2389.2002.00431.x.

Forsyth, P.J., Jongens, R., Barrell (Compilers), D.J.A., 2008. Geology of the Christchurch Area. Institute of Geological & Nuclear Sciences 1:250 000 geologial map 16. GNS Science, Lower Hutt, New Zealand.

Gargiulo, L., Mele, G., Terribile, F., 2016. Effect of rock fragments on soil porosity: a laboratory experiment with two physically degraded soils. Eur. J. Soil Sci. 67(5), 597-604. https://doi.org/10.1111/ejss.12370.

Gee, G.W., Ward, A.L., Wittreich, C.D., 2002. The Hanford Site 1000-year cap design test, (No. PNNL-14143). Pacific Northwest National Lab., Richland, WA (US).

Gerrard, A.J., 1992. Soil Geomorphology: An Integration of Pedology and Geomorphology. Chapman & Hall, London.

Giesler, R., Lundström, U.S., Grip, H., 1996. Comparison of soil solution chemistry assessment using zero-tension lysimeters or centrifugation. Eur. J. Soil Sci. 47(3), 395-405. https://doi.org/10.1111/j.1365-2389.1996.tb01413.x.

Gradwell, M., 1985. Verifying estimates of field capacity for some New Zealand soils. N. Z. J. Agric. Res. 28(3), 381-385. https://doi.org/10.1080/00288233.1985.10430442.

Gradwell, M.W., 1974. The available-water capacities of some southern and central zonal soils of New Zealand. N. Z. J. Agric. Res. 17(4), 465-478. https://doi.org/10.1080/00288233.1974.10421034.

Gras, R., Monnier, G., 1963. Contribution de certains elements grossiers du sol a l'alimentation en eau des vegetaux. Science du sol (1), 1-8.

Groenevelt, P.H., van Straaten, P., Rasiah, V., Simpson, J., 1989. Modifications in evaporation parameters by rock mulches. Soil Technol. 2(3), 279-285. https://doi.org/10.1016/0933-3630(89)90012-3.

Hanson, C.T., Blevins, R.L., 1979. Soil water in coarse fragments. Soil Sci. Soc. Am. J. 43(4), 819-820. https://doi.org/10.2136/sssaj1979.03615995004300040044x.

Hlavacikova, H., Novak, V., Holko, L., 2015. On the role of rock fragments and initial soil water content in the potential subsurface runoff formation. J. Hydrol. Hydromech. 63(1), 71-81. https://doi.org/10.1515/johh-2015-0002.

Hlaváčiková, H., Novák, V., Šimůnek, J., 2016. The effects of rock fragment shapes and positions on modeled hydraulic conductivities of stony soils. Geoderma 281, 39-48. https://doi.org/10.1016/j.geoderma.2016.06.034.

Hodgeson, J., 1976. Soil Survey Handbook. Soil Survey Technical Monograph 5, Rothamsted Experimental Station, Harpenden, England.

Ingelmo, F., Cuadrado, S., Iban˜ez, A., Hernandez, J., 1994. Hydric properties of some Spanish soils in relation to their rock fragment content: implications for runoff and vegetation. Catena 23(1), 73-85. https://doi.org/10.1016/0341-8162(94)90054-X.

IUSS Working Group WRB, 2015. World Reference Base for Soil Resources 2014: International Soil Classification System for Naming Soils and Creating Legends for Soil Maps. Update 2015. World soil resources report 106. FAO Rome.

Jahn, R., Blume, H., Asio, V., Spaargaren, O., Schad, P., 2006. Guidelines for Soil Description. FAO.

Jones, D.P., Graham, R.C., 1993. Water-holding characteristics of weathered granitic rock in chaparral and forest ecosystems. Soil Sci. Soc. Am. J. 57(1), 256-261. https://doi.org/10.2136/sssaj1993.03615995005700010044x.

Jones, T.P.C., 2016. Physical and mechanical controls of matrix permeability on rocks from Rotokawa Geothermal Field, Taupo Volcanic Zone, New Zealand, University of Canterbury.

Kemper, W., Nicks, A., Corey, A., 1994. Accumulation of water in soils under gravel and sand mulches. Soil Sci. Soc. Am. J. 58(1), 56-63. https://doi.org/10.2136/sssaj1994.03615995005800010008x.

Ketcham, R.A., Iturrino, G.J., 2005. Nondestructive high-resolution visualization and measurement of anisotropic effective porosity in complex lithologies using high-resolution X-ray computed tomography. J. Hydrol. 302(1), 92-106. https://doi.org/10.1016/j.jhydrol.2004.06.037.

Khaleel, R., Relyea, J.F., 1997. Correcting laboratory-measured moisture retention data for gravels. Water Resour. Res. 33(8), 1875-1878. https://doi.org/10.1029/97wr01068.

Khetdan, C., Chittamart, N., Tawornpruek, S., Kongkaew, T., Onsamrarn, W., Garré, S., 2017. Influence of rock fragments on hydraulic properties of Ultisols in Ratchaburi Province, Thailand. Geoderma Reg. 10, 21-28. https://doi.org/10.1016/j.geodrs.2017.04.001.

Klocke, N.L., Todd, R.W., Hergert, G.W., Watts, D.G., Parkhurst, A.M., 1993. Design, installation, and performance of percolation lysimeters for water-quality sampling. Transactions of the ASAE 36(2), 429-435. https://doi.org/10.13031/2013.28355.

Korboulewsky, N., Besnault, A., Tétégan, M., Cousin, I., 2010a. Contribution of rock fragments to soil fertility, EGU General Assembly Conference Abstracts, pp. 6558.

Korboulewsky, N., Tétégan, M., Besnault, A., Cousin, I., 2010b. Do rock fragments participate to plant water and mineral nutrition?, EGU General Assembly Conference Abstracts, pp. 6537.

Kosmas, C., Moustakas, N., Danalatos, N.G., Yassoglou, N., 1994. The effect of rock fragments on wheat biomass production under highly variable moisture conditions in Mediterranean environments. Catena 23(1), 191-198. https://doi.org/10.1016/0341-8162(94)90060-4.

Kosmas, C.S., Danalatos, N.G., Moustakas, N., Tsatiris, B., Kallianou, C., Yassoglou, N., 1993. The impacts of parent material and landscape position on drought and biomass production of wheat under semi-arid conditions. Soil Technol. 6(4), 337-349. https://doi.org/10.1016/0933-3630(93)90024-9.

Larochelle, C.G., Bussière, B., Pabst, T., 2019. Acid-generating waste rocks as capillary break layers in covers with capillary barrier effects for mine site reclamation. Water Air Soil Pollut. 230(3), 57. https://doi.org/10.1007/s11270-019-4114-0.

Li, H., Li, J., Shen, Y., Zhang, X., Lei, Y., 2018. Web-based irrigation decision support system with limited inputs for farmers. Agri. Water Manage. 210, 279-285. https://doi.org/10.1016/j.agwat.2018.08.025.

Lilburne, L.R., Hewitt, A.E., Webb, T.W., 2012. Soil and informatics science combine to develop S-map: a new generation soil information system for New Zealand. Geoderma 170, 232-238. https://doi.org/10.1016/j.geoderma.2011.11.012.

Lunt, I.A., Bridge, J.S., 2007. Formation and preservation of open-framework gravel strata in unidirectional flows. Sedimentology 54(1), 71-87. https://doi.org/10.1111/j.1365-3091.2006.00829.x.

Ma, D., Shao, M., Zhang, J., Wang, Q., 2010. Validation of an analytical method for determining soil hydraulic properties of stony soils using experimental data. Geoderma 159(3), 262-269. https://doi.org/10.1016/j.geoderma.2010.08.001.

Ma, D.H., Shao, M.G., 2008. Simulating infiltration into stony soils with a dual-porosity model. Eur. J. Soil Sci. 59(5), 950-959. https://doi.org/10.1111/j.1365-2389.2008.01055.x.

Ma, L., Ahuja, L.R., Trout, T.J., Nolan, B.T., Malone, R.W., 2016. Simulating maize yield and biomass with spatial variability of soil field capacity. Agron. J. 108(1), 171-184. https://doi.org/10.2134/agronj2015.0206.

Ma, Y.J., Li, X.Y., 2011. Water accumulation in soil by gravel and sand mulches: influence of textural composition and thickness of mulch layers. J. Arid. Environ. 75(5), 432-437. https://doi.org/10.1016/j.jaridenv.2010.12.017.

McLeod, M., Aislabie, J., McGill, A., Rhodes, P., Carrick, S., 2014. Leaching of Escherichia coli from stony soils after effluent application. J. Environ. Qual. 43(2), 528-538. https://doi.org/10.2134/jeq2013.06.0256.

McNamara, D., Faulkner, D., McCarney, E., 2014. Rock properties of greywacke basement hosting geothermal reservoirs, New Zealand: preliminary results, Thirty-Ninth Workshop on Geothermal Reservoir Engineering, Stanford University, Stanford, California.

McNeill, S.J., Lilburne, L.R., Carrick, S., Webb, T.H., Cuthill, T., 2018. Pedotransfer functions for the soil water characteristics of New Zealand soils using S-map information. Geoderma 326, 96-110. https://doi.org/10.1016/j.geoderma.2018.04.011.

Meng, C., Niu, J.-z., Yin, Z.-c., Luo, Z.-t., Lin, X.-n., Jia, J.-w., 2018. Characteristics of rock fragments in different forest stony soil and its relationship with macropore characteristics in mountain area, northern China. J. Mt. Sci. 15(3), 519-531. https://doi.org/10.1007/s11629-017-4638-y.

Milne, J., Clayden, B., L., S.P., Wilson, A.D., 1995. Soil Description Handbook. Manaaki Whenua Press, Lincoln, New Zealand.

Mohamed, J., Ali, S., 2006. Development and comparative analysis of pedotransfer functions for predicting soil water characteristic content for Tunisian soils. Proceedings of the 7th Edition of TJASSST, 170-178.

Naseri, M., Iden, S., Richter, N., Durner, W., 2019. Influence of stone content on soil hydraulic properties: experimental investigation and test of existing model concepts. Vadose Zone J. 18. https://doi.org/10.2136/vzj2018.08.0163.

Navarre-Sitchler, A., Brantley, S.L., Rother, G., 2015. How porosity increases during incipient weathering of crystalline silicate rocks. In: C.I. Steefel, S. Emmanuel, L.M. Anovitz (Eds.), Pore-Scale Geochemical Processes. Reviews in Mineralogy & Geochemistry, pp. 331-354.

Nemes, A., Pachepsky, Y.A., Timlin, D.J., 2011. Toward improving global estimates of field soil water capacity. Soil Sci. Soc. Am. J. 75(3), 807-812. https://doi.org/10.2136/sssaj2010.0251.

Novák, V., Kňava, K., 2012. The influence of stoniness and canopy properties on soil water content distribution: simulation of water movement in forest stony soil. Eur. J. For. Res. 131(6), 1727-1735. https://doi.org/10.1007/s10342-011-0589-y.

Nyssen, J., Haile, M., Poesen, J., Deckers, J., Moeyersons, J., 2001. Removal of rock fragments and its effect on soil loss and crop yield, Tigray, Ethiopia. Soil Use Manag. 17(3), 179-187. https://doi.org/10.1111/j.1475-2743.2001.tb00025.x.

Ostovari, Y., Asgari, K., Cornelis, W., 2015. Performance evaluation of pedotransfer functions to predict field capacity and permanent wilting point using UNSODA and HYPRES datasets. Arid Land Res. Manag. 29(4), 383-398. https://doi.org/10.1080/15324982.2015.1029649.

Ottoni, T.B., Ottoni, M.V., de Oliveira, M.B., de Macedo, J.R., Reichardt, K., 2014. Revisiting field capacity (FC): variation of definition of FC and its estimation from pedotransfer functions. Rev. Bras. Ciênc. Solo 38(6), 1750-1764. https://doi.org/10.1590/s0100-06832014000600010.

Parajuli, K., Sadeghi, M., Jones, S.B., 2017. A binary mixing model for characterizing stony-soil water retention. Agric. For. Meteorol. 244-245, 1-8. https://doi.org/10.1016/j.agrformet.2017.05.013.

Parent, S.-É., Cabral, A., 2006. Design of inclined covers with capillary barrier effect. Geotech. Geol. Eng. 24(3), 689-710. https://doi.org/10.1007/s10706-005-3229-9.

Park, K.D., Fleming, I.R., 2006. Evaluation of a geosynthetic capillary barrier. Geotext. Geomembr. 24(1), 64-71. https://doi.org/10.1016/j.geotexmem.2005.06.001.

Pineda, M.C., Viloria, J., Martínez-Casasnovas, J.A., Valera, A., Lobo, D., Timm, L.C., Pires, L.F., Gabriels, D., 2018. Predicting soil water content at −33 kPa by pedotransfer functions in stoniness 1 soils in northeast Venezuela. Environ. Monit. Assess. 190(3), 161. https://doi.org/10.1007/s10661-018-6528-3.

Pirastru, M., Niedda, M., 2013. Evaluation of the soil water balance in an alluvial flood plain with a shallow groundwater table. Hydrol. Sci. J. 58(4), 898-911. https://doi.org/10.1080/02626667.2013.783216.

Poesen, J., Lavee, H., 1994. Rock fragments in top soils: significance and processes. Catena 23(1), 1-28. https://doi.org/10.1016/0341-8162(94)90050-7.

Poesen, J., Wesemael, B.v., Govers, G., Martinez-Fernandez, J., Desmet, P., Vandaele, K., Quine, T., Degraer, G., 1997. Patterns of rock fragment cover generated by tillage erosion. Geomorphol. 18(3), 183-197. https://doi.org/10.1016/S0169-555X(96)00025-6.

Poesen, J.W., Torri, D., Bunte, K., 1994. Effects of rock fragments on soil erosion by water at different spatial scales: a review. Catena 23(1), 141-166. https://doi.org/10.1016/0341-8162(94)90058-2.

Pollacco, J.A.P., 2008. A generally applicable pedotransfer function that estimates field capacity and permanent wilting point from soil texture and bulk density. Can. J. Soil Sci. 88(5), 761-774. https://doi.org/10.4141/CJSS07120.

Ramos, C.G., de Mello, A.G., Kautzmann, R.M., 2014. A preliminary study of acid volcanic rocks for stonemeal application. Environ. Nanotechnol. Monit. Manage. 1-2, 30-35. https://doi.org/10.1016/j.enmm.2014.03.002.

Ravina, I., Magier, J., 1984. Hydraulic conductivity and water retention of clay soils containing coarse fragments. Soil Sci. Soc. Am. J. 48(4), 736-740. https://doi.org/10.2136/sssaj1984.03615995004800040008x.

Reeve, M., Smith, P., Thomasson, J., 1973. The effect of density on water retention properties of field soils. Eur. J. Soil Sci. 24(3), 355-367. https://doi.org/10.1111/j.1365-2389.1973.tb00771.x.

Richards, L., Weaver, L., 1944. Moisture retention by some irrigated soils as related to soil moisture tension. J. Agric. Res. 69(6), 215-235.

Rickard, D., Cossens, G., 1966. Irrigation investigations in Otago, New Zealand: I. Description and physical properties of irrigated soils of the Ida Valley. N. Z. J. Agric. Res. 9(2), 197-217.

Rieke-Zapp, D., Poesen, J., Nearing, M., 2007. Effects of rock fragments incorporated in the soil matrix on concentrated flow hydraulics and erosion. Earth Surf. Process. Landforms 32(7), 1063-1076. https://doi.org/10.1002/esp.1469.

Rijkse, W.C. (Ed.), 1985. Soil Groups of New Zealand. Part 8, Recent soils. New Zealand Society of Soil Science, Lower Hutt, New Zealand.

Robertson, A.H.F., Campbell, H.J., Johnston, M.R., Mortimer, N., 2019. Chapter 1 Introduction to Paleozoic–Mesozoic geology of South Island, New Zealand: subduction-related processes adjacent to SE Gondwana. In: A.H.F. Robertson (Ed.), Paleozoic–Mesozoic Geology of South Island, New Zealand: Subduction-Related Processes Adjacent to SE Gondwana. Geological Society Memoirs No. 49, Geological Society, London, pp. 1-14.

Román Dobarco, M., Bourennane, H., Arrouays, D., Saby, N.P.A., Cousin, I., Martin, M.P., 2019a. Uncertainty assessment of GlobalSoilMap soil available water capacity products: a French case study. Geoderma 344, 14-30. https://doi.org/10.1016/j.geoderma.2019.02.036.

Román Dobarco, M., Cousin, I., Le Bas, C., Martin, M.P., 2019b. Pedotransfer functions for predicting available water capacity in French soils, their applicability domain and associated uncertainty. Geoderma 336, 81-95. https://doi.org/10.1016/j.geoderma.2018.08.022.

Rücknagel, J., Götze, P., Hofmann, B., Christen, O., Marschall, K., 2013. The influence of soil gravel content on compaction behaviour and pre-compression stress. Geoderma 209-210, 226-232. https://doi.org/10.1016/j.geoderma.2013.05.030.

Salter, P.J., Haworth, F., 1961. The available-water capacity of a sandy loam soil. J. Soil Sci. 12(2), 326-334. https://doi.org/10.1111/j.1365-2389.1961.tb00922.x.

Santra, P., Kumar, M., Kumawat, R., Painuli, D., Hati, K., Heuvelink, G., Batjes, N., 2018. Pedotransfer functions to estimate soil water content at field capacity and permanent wilting point in hot Arid Western India. J. Earth Syst. Sci. 127. https://doi.org/10.1007/s12040-018-0937-0.

Sauer, T.J., Logsdon, S.D., 2002. Hydraulic and physical properties of stony soils in a small watershed. Soil Sci. Soc. Am. J. 66(6), 1947-1956. https://doi.org/10.2136/sssaj2002.1947.

Scheinost, A.C., Sinowski, W., Auerswald, K., 1997. Regionalization of soil water retention curves in a highly variable soilscape, I. Developing a new pedotransfer function. Geoderma 78(3), 129-143. https://doi.org/10.1016/S0016-7061(97)00046-3.

Schoeman, J.L., Kruger, M.M., Loock, A.H., 1997. Water-holding capacity of rock fragments in rehabilitated opencast mine soils. S. Afr. J. Plant Soil 14(3), 98-102. https://doi.org/10.1080/02571862.1997.10635089.

Shi, Z.J., Xu, L.H., Wang, Y.H., Yang, X., Jia, Z., Guo, H., Xiong, W., Yu, P., 2012. Effect of rock fragments on macropores and water effluent in a forest soil in the stony mountains of the Loess Plateau, China. Afr. J. Biotechnol. 11(39), 9350-9361. https://doi.org/10.5897/AJB12.145.

Soil Science Division Staff, 2017. Soil Survey Manual. USDA Handbook 18. Government Printing Office, Washington, D.C.

Soil Survey Staff, 2010. Keys to Soil Taxonomy. Eleventh Edition ed. Department of Agriculture: Natural Resources Conservation Service.

Sparling, G., Lilburne, L., Vojvodic-Vukovic, M., 2008. Provisional targets for soil quality indicators in New Zealand. Landcare Research Science Series No. 34. Manaaki Whenua Press: Lincoln, New Zealand.

Standards Association of New Zealand, 1986. Methods of testing soils for civil engineering purposes - Part 1: Preliminary and general. Author, Wellington.

Stewart, V.I., Adams, W.A., Abdulla, H.H., 1970. Quantitative pedological studies on soils derived from silurian mudstones. J. Soil Sci. 21(2), 248-255. https://doi.org/10.1111/j.1365-2389.1970.tb01174.x.

Tenzer, R., Sirguey, P., Rattenbury, M., Nicolson, J., 2011. A digital rock density map of New Zealand. Comput. Geosci. 37(8), 1181-1191. https://doi.org/10.1016/j.cageo.2010.07.010.

Tetegan, M., Korboulewsky, N., Bouthier, A., Samouëlian, A., Cousin, I., 2015. The role of pebbles in the water dynamics of a stony soil cultivated with young poplars. Plant and Soil 391(1), 307-320. https://doi.org/10.1007/s11104-015-2429-1.

Tetegan, M., Nicoullaud, B., Baize, D., Bouthier, A., Cousin, I., 2011. The contribution of rock fragments to the available water content of stony soils: proposition of new pedotransfer functions. Geoderma 165(1), 40-49. https://doi.org/10.1016/j.geoderma.2011.07.001.

Thoma, M.J., Barrash, W., Cardiff, M., Bradford, J., Mead, J., 2014. Estimating unsaturated hydraulic functions for coarse sediment from a field-scale infiltration experiment. Vadose Zone J. 13(3). https://doi.org/10.2136/vzj2013.05.0096.

Tokunaga, T.K., Olson, K.R., Wan, J., 2003. Moisture characteristics of Hanford gravels. Vadose Zone J. 2(3), 322-329. https://doi.org/10.2136/vzj2003.0322.

Torri, D., Poesen, J., Monaci, F., Busoni, E., 1994. Rock fragment content and fine soil bulk density. Catena 23(1), 65-71. https://doi.org/10.1016/0341-8162(94)90053-1.

Twarakavi, N.K.C., Sakai, M., Simunek, J., 2009. An objective analysis of the dynamic nature of field capacity. Water Resour. Res. 45. https://doi.org/10.1029/2009wr007944.

Ugolini, F.C., Corti, G., Agnelli, A., Piccardi, F., 1996. Mineralogical, physical, and chemical properties of rock fragments in soil. Soil Sci. 161(8), 521-542. https://doi.org/10.1097/00010694-199608000-00007.

Uhlig, D., von Blanckenburg, F., 2019. How slow rock weathering balances nutrient loss during fast forest floor turnover in montane, temperate forest ecosystems. Front. Earth Sci. 7, 159. https://doi.org/10.3389/feart.2019.00159.

van Genuchten, M.T., 1980. A closed-form equation for predicting the hydraulic conductivity of unsaturated soils. Soil Sci. Soc. Am. J. 44(5), 892-898. https://doi.org/10.2136/sssaj1980.03615995004400050002x.

van Wesemael, B., Poesen, J., de Figueiredo, T., 1995a. Effects of rock fragments on physical degradation of cultivated soils by rainfall. Soil Tillage Res. 33(3), 229-250. https://doi.org/10.1016/0167-1987(94)00439-L.

van Wesemael, B., Poesen, J., Kosmas, C.S., Danalatos, N.G., 1995b. The role of rock fragments in evaporation from cultivated soils under mediterranean climatic conditions. Phys. Chem. Earth. 20(3), 293-299. https://doi.org/10.1016/0079-1946(95)00040-2.

Veihmeyer, F.J., Hendrickson, A.H., 1949. Methods of measuring field capacity and permanent wilting percentage of soils. Soil Sci. 68, 75-94. https://doi.org/10.1097/00010694-194907000-00007.

Vereecken, H., Maes, J., Feyen, J., 1990. Estimating unsaturated hydraulic conductivity from easily measured soil properties. Soil Sci. 149(1), 1-12. https://doi.org/10.1016/0016-7061(95)92543-X.

Vereecken, H., Maes, J., Feyen, J., Darius, P., 1989. Estimating the soil-moisture retention characteristic from texture, bulk-density, and carbon content. Soil Sci. 148(6), 389-403. https://doi.org/10.1097/00010694-198912000-00001.

Vincent, K.R., Chadwick, O.A., 1994. Synthesizing bulk density for soils with abundant rock fragments. Soil Sci. Soc. Am. J. 58(2), 455-464. https://doi.org/10.2136/sssaj1994.03615995005800020030x.

Vogeler, I., Carrick, S., Cichota, R., Lilburne, L., 2019. Estimation of soil subsurface hydraulic conductivity based on inverse modelling and soil morphology. J. Hydrol. 574, 373-382. https://doi.org/10.1016/j.jhydrol.2019.04.002.

Wang, H.F., Xiao, B., Wang, M.Y., Shao, M.A., 2013. Modeling the soil water retention curves of soil-gravel mixtures with regression method on the loess plateau of China. Plos One 8(3). https://doi.org/10.1371/journal.pone.0059475.

Webb, T.H., Lilburne, L.R., 2011. Criteria for Defining the Soil Family and Soil Sibling: the Fourth and Fifth Categories of the New Zealand Soil Classification. Landcare Research Science Series No. 3. Manaaki Whenua Press, Lincoln, New Zealand.

Weihermuller, L., Siemens, J., Deurer, M., Knoblauch, S., Rupp, H., Gottlein, A., Putz, I., 2007. In situ soil water extraction: a review. J. Environ. Qual. 36(6), 1735-1748. https://doi.org/10.2134/jeq2007.0218.

Wheeler, D., Read, C., 2016. Spotlight on OVERSEER: perspectives and approaches to addressing nutrient management challenges using an integrated farm systems model, International Nitrogen Initiative Conference, Melbourne, Australia.

White, A.F., 2008. Quantitative approaches to characterizing natural chemical weathering rates. In: S.L. Brantley, J.D. Kubicki, A.F. White (Eds.), Kinetics of Water-Rock Interaction. Springer New York, New York, NY, pp. 469-543.

Yang, Y.-f., Wang, Q.-j., Zhuang, J., 2013. Estimating hydraulic parameters of stony soils on the basis of one-dimensional water absorption properties. Acta Agric. Scand. 63. https://doi.org/10.1080/09064710.2012.762424.

Zhou, B.B., Shao, M.A., Shao, H.B., 2009. Effects of rock fragments on water movement and solute transport in a Loess Plateau soil. C. R. Geosci. 341(6), 462-472. https://doi.org/10.1016/j.crte.2009.03.009.

Zornberg, J., Bouazza, A., McCartney, J., 2010. Geosynthetic capillary barriers: current state of knowledge. Geosynth. Int. 17(5), 273-300. https://doi.org/10.1680/gein.2010.17.5.273.

Chapter 3

Variation in matric potential at field capacity in stony soils of fluvial and alluvial fans

The manuscript has been accepted by *Geoderma*:

Robertson B.B., Almond P.C., Carrick S.T., Penny V., Chau H.W. and Smith C.M.S., 2021. Variation in matric potential at field capacity in stony soils of fluvial and alluvial fans. *Geoderma*. https://doi.org/10.1016/j.geoderma.2021.114978

Abstract

Field capacity is fundamental for many agronomic management decisions, as well as hydrological and environmental models. Around the world, field capacity is assumed to occur at defined matric potentials, -10 kPa and -33 kPa being common criteria. However, these criteria have not been tested in fluvial and alluvial fan stony soils (FAFSS). In this project, 57 pits on FAFSS located on the Canterbury Plains were watered to saturation. After two days of drainage (a proxy for field capacity), a 30 x 30 cm pit was excavated in 10 cm increments to a depth of 60 cm for 52 of the pits. At each increment, matric potential was measured. For the remaining five pits, matric potential was measured after 4-5 days to a depth of 1.5 m. Matric potential was generally higher than -10 kPa and the matric potential-depth profile of the pits could be characterised into one of five modes. The most common mode was hydrostatic equilibrium, which is typically associated with soils that have a shallow water table (~<2 m). Our results indicate that a capillary break due to a coarse sandy gravel layer at ~1 m depth causes a near-zero matric potential boundary condition that allows hydrostatic equilibrium to occur regardless of the depth to groundwater. This capillary break was linked to two soil conditions: a layer of open framework gravels or fine earth (<2 mm fraction) with specific surface area <15 $m^2 g^{-1}$. Our results provide a basis for better approximations of the matric potential at field capacity and improved modelling of soil water behaviour in FAFSS.

3.1 Introduction

Field capacity (FC) was first defined by Veihmeyer and Hendrickson (1931) as “the amount of water held in the soil after excess gravitational water has drained away and after the rate of downward movement of water has materially decreased”. As such, FC represents the upper drainable limit of soil, and together with wilting point is used to determine the available water holding capacity (AWC) of different soils. Amongst soil physicists, there is significant debate on how to define FC and hence how to measure and predict it (Assouline and Or, 2014; Nachabe, 1998). Even so, FC remains an

essential parameter that is used extensively in research publications (de Jong van Lier, 2017; Ma et al., 2016), agronomic management decisions (Li et al., 2018), policy (Wheeler and Read, 2016), environmental reporting (Sparling et al., 2008), environmental modelling (Keating et al., 2003; Wheeler and Read, 2016) and for national (S-map in New Zealand, McNeill et al., 2018) and international soil information systems (Global Soil Map, Arrouays et al., 2014). To estimate it accurately, it is necessary to identify factors that can influence the way FC is attained, such as soil texture, presence of impeding or highly permeable layers, soil layering and depth to groundwater (Ottoni et al., 2014). However, current literature focuses on FC in non-stony soils, with no papers that have discussed what affects FC in stony soils of fluvial origin.

Webb and Lilburne (2011) have defined stony soils as soils with ≥35% rock fragments (RFs) by volume extending from a depth within 45 cm of the soil surface to a depth >100 cm. This classification applies to the family level of the NZ Soil Classification (Hewitt, 2010). Similarly, stony soils may be considered to be soil families of the USDA soil taxonomy system (Soil Survey Staff, 2014) with skeletal or fragmental particle size classes, or taxa having the skeletic soil qualifier for the second-level units of the WRB (IUSS Working Group WRB, 2015). An important group of stony soils occurs on alluvial and fluvial fans, which are present worldwide and represent the dominant sedimentary systems wherever streams and rivers leave regions of high relief to flow across lowlands. Criteria discriminating fluvial and alluvial fans refer to both scale and diversity of depositional systems, but here it is sufficient to say the former are larger (multi-kilometre scale radii) and include a broader range of depositional environments and sedimentary facies (Ventra and Clarke, 2018). Upon reaching lowland areas, coarse alluvial sediment sourced from mountainous terrain is deposited as the fluvial transport capacity suddenly decreases with the decrease in gradient and lack of confinement, forming a fluvial or alluvial fan (Harvey, 2018). Fluvial fans and related megafans (radii > 30 km, Gohain and Parkash, 1990) occupy a vast area of alluvial lowlands at the foots of mountain chains such as the Andes (Casanova et al., 2013), the Himalaya (Ayaz et al., 2018; Kumar et al., 2007; Suresh et al., 2007), Alps-Pyrenees (Fontana et al., 2014; Jones, 2004), Sierra Nevada (Olmsted and Davis, 1961) and the Southern Alps (Weissmann et al., 2015). Characteristic properties of fluvial and alluvial fan stony soils (FAFSS) include both the abundance of RFs and the tendency for depositional layering of materials of contrasting grain size and fabric. Streamflow on the fan surface tends to be wide, slow and demonstrate a braided river pattern with a tendency to switch position by avulsion (Harvey, 2018). This depositional process commonly results in cross-bedded units of sharply alternating grain sizes and RF-supported beds that are either open framework or loosely filled with a sand matrix (Dann et al., 2009; Fairbridge, 1997; Pierce and Scott, 1982). Considering the effect of layering on water movement (Li et al., 2013; Miller and Gardner, 1962; Zhao et al., 2010), these conditions are likely to cause FAFSS to have distinct properties with regard to water retention (Poesen and Lavee,

1994; Schoeman et al., 1997; Tokunaga et al., 2003), hydraulic conductivity (Sauer and Logsdon, 2002; Verbist et al., 2009) and fine earth bulk density (Gargiulo et al., 2016; Poesen and Lavee, 1994; Torri et al., 1994). Though formerly considered as unproductive land, large areas of FAFSS are now being used for agriculture, including two-thirds of the irrigated land in Canterbury, New Zealand (Carrick et al., 2013b). Despite how extensive these soils can be, FAFSS are commonly understudied, despite contaminant leaching and irrigation scheduling shown to be particularly difficult on this type of soil (Cichota et al., 2016; Gray et al., 2016; McLeod et al., 2014; Pollaco et al., 2014). FC is a crucial parameter for nutrient management of FAFSS, because they have been shown to have often rapid drainage once wet above FC (Cichota et al., 2016). Because FAFSS typically have low water holding capacity (Carrick et al., 2013b), accurate characterisation of FC can significantly influence water use efficiency of irrigation systems. However, in New Zealand, as in Australia and Sweden, FC has been defined on a matric potential criterion of -10 kPa, and this criterion has undergone no testing of its appropriateness for FAFSS. We hypothesise that the abrupt changes in hydraulic conductivity characteristic of layered sediments within FAFSS cause interactions between layers that influence matric potential at FC. A corollary of this hypothesis is that a default FC tension of -10 kPa is not appropriate to use in FAFSS type soils. To test this hypothesis, several FAFSS across Canterbury, New Zealand, were sampled to cover a range of RF abundance, RF size, soil carbon content and texture, to account for as much of the variability that can occur in these soils as possible. The purpose is to provide a better understanding of how and under what conditions FAFSS attain FC so that this parameter remains meaningful for soil and environmental management in the context of these soils.

3.2 Materials and methods

3.2.1 Regional setting

Fifty-two sampling locations were selected on the Canterbury Plains, on the South Island of New Zealand (Figure 6). The Canterbury Plains are approximately 180 km long and 70 km at their widest and are bordered by the >3500-m-high Southern Alps to the west. The Plains away from the Pacific coastal margin have been built by coalescing Pleistocene glacial outwash megafans (ca 50 km in length) (Davidson et al., 2013) comprising alluvium carried by gravel-bed rivers sourced near the main divide of the Southern Alps. The alluvium is dominated by an indurated muddy fine sandstone (greywacke) of the Rakaia terrane (Forsyth et al., 2008). The surfaces of the mid fan and fan head areas are characterised by a relict braided channel pattern except where this is buried by loess, and the large rivers are incised through these reaches. The incised channels have formed inset fans of Holocene age, which grade to the fan toes. The fan toes are influenced more strongly by overbank, aeolian and coastal sedimentation amongst swamps (Figure 6).

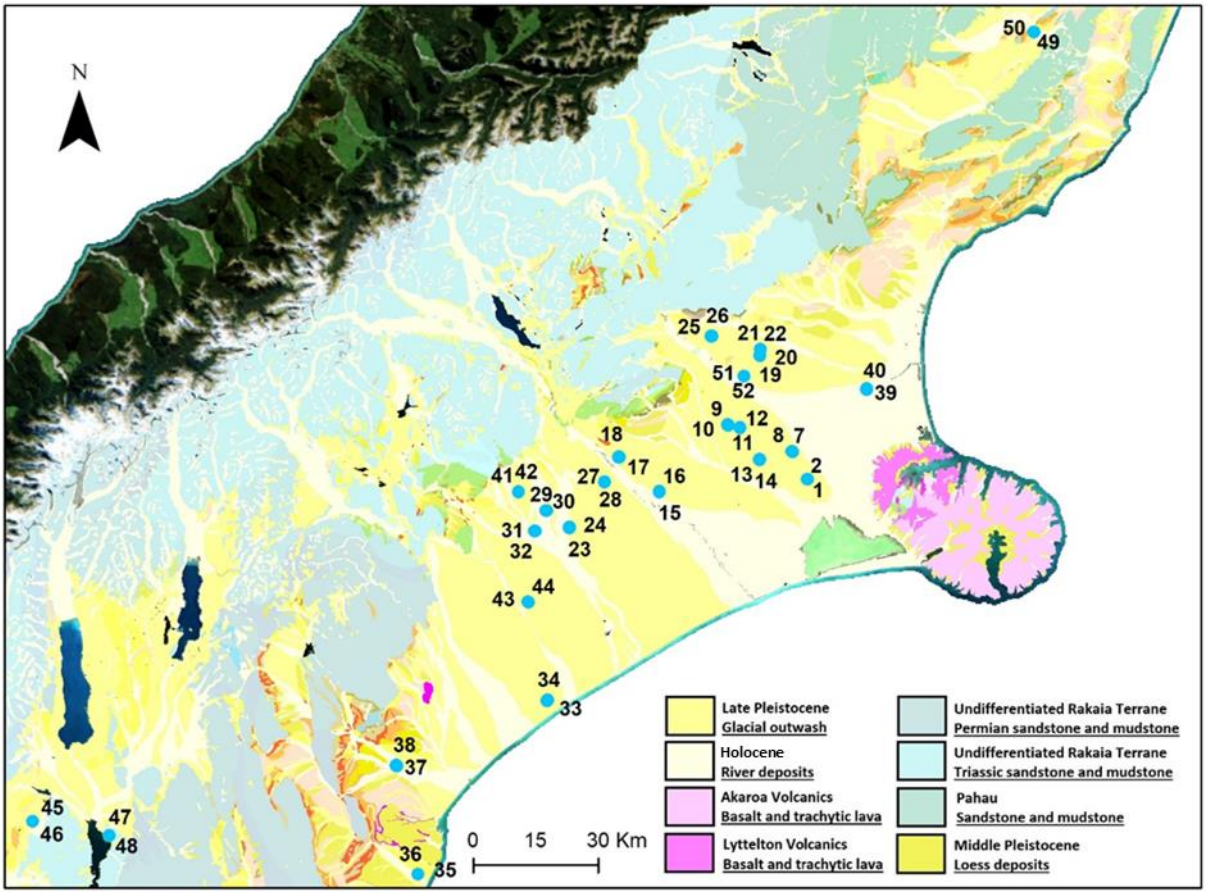

Figure 6 Geology of the Canterbury Plains and the location of pits. Contains data sourced from the LINZ Data Service licensed for reuse under CC BY 4.0.

The climate in Canterbury is influenced by north-westerly winds, which create a rainfall gradient spanning about 1000 mm yr^{-1} along the western edge of the Plains, to about 600 mm yr^{-1} along the coast (Dann et al., 2009). The average potential evapotranspiration rates can vary from 745-919 mm yr^{-1}, which generally exceeds annual rainfall (Macara, 2016). On the late Pleistocene surfaces, Pallic and Brown soils dominate, while Holocene surfaces are dominated by Recent soils of the New Zealand Soil Classification (Hewitt, 2010). The stony soils of the Canterbury Plains include Firm Brown Soils (Dystrudepts and Dystrustepts) and Fluvial Recent Soils (Fluvents and Ustepts).

3.2.2 Experimental setup

Field sampling was carried out over the winter to early spring months of 2017 and 2018 (May to September). At each sampling site, two locations were selected for pit sampling. The soil was first wet-up and allowed to drain for two days as a proxy for FC. This proxy was used because Twarakavi et al. (2009) identified time-based approaches to be more robust than matric potential based approximations of FC, while coarse stony soils also tend to drain and cease draining within short periods of time (Carrick et al., 2017; Graham et al., 2018). The soil was then excavated in increments to measure matric potential, and sample for RF abundance and properties of the fine earth (<2 mm fraction) down the profile. During the periods of autumn, winter and early spring, antecedent soil

moisture remained close to FC, hence pre-wetting via ponded infiltration was enough to wet the soil profile thoroughly. In late spring, soils became progressively drier. To ensure the profile was wetted properly, additional irrigation was applied after the infiltration measurement. Soils were described according to the terminology of Milne et al. (1995) and classified to the subgroup level of the New Zealand Soil Classification, according to Hewitt (2010).

3.2.3 Wetting-up

At each sampling location, a level area was found and cleaned of above-ground vegetation. An infiltration ring (50 cm diameter) was then driven ~1 cm into the soil by hitting a length of wood laid across the ring with a rubber mallet. A spirit level was used to ensure the ring was driven in evenly. Two-litre volumes of water were applied in consecutive increments until infiltration times became constant (after ~100 mm of water), which meant the saturated hydraulic conductivity rate had been reached. As 58% of Canterbury FAFSS have low AWC (30-90 mm to 1 m depth, Carrick et al., 2013b), the infiltration volume we used would be sufficient to thoroughly wet the soil profile considering the antecedent soil moisture remained close to FC. In the drier periods, soils had an additional 111 mm of water applied at 9 mm hr^{-1} by an irrigation system to increase matrix flow and ensure the soil profile was wetted thoroughly. The irrigation was gravity supplied from a 60 L drum held at the height of 1 m (Appendix A) and distributed through 6 lines of Aqua-TraXX 1.14 L h^{-1} drip tape, spaced at 10 cm intervals. The drip tape had emitters every 10 cm and covered an area of 60 x 50 cm, an area greater than the area to be sampled to ensure no boundary effect. To control the irrigation rate, a Jobmate Dial Water Timer was used so that soil was irrigated for 15 minutes every hour. Irrigation lasted 12 hours. The soil was then covered to prevent evapotranspiration losses or additional rainfall input for 48 hours before further measurement.

3.2.4 Soil sampling and measurement

At each sampling site, a 30 x 30 cm metal frame was inserted at the centre of the wetted area of the infiltration ring (Appendix B). The soil was excavated within the frame in 10-cm increments to a depth of 60 cm. Based on the method described in Hedley et al. (2012), after each increment was excavated, the pit was backfilled with plastic beads (with a bulk density of 0.562 g cm^{-3}) and the beads (diameter 0.6 cm; height 0.3 cm) were weighed to determine the volume of the pit and the volume of each increment (V_T). The 'dead volume' between the soil surface and the top of the frame was also measured, to allow accurate determination of the pit volume to the 'datum' of the soil surface.

Excavated material for each depth increment was passed through a 20 mm sieve in the field. All the >20 mm RFs were collected and weighed (M_{RF}) to prevent misrepresentation through sub-sampling.

The <20 mm fraction, called the coarse fines, was weighed (M_{CF}) before being thoroughly mixed, spread out in a large sampling tray and quartered. One quarter was collected and weighed (M_b) to estimate the whole soil bulk density, the fine earth bulk density and the 2 – 20 mm RF size distribution. One scoopful (with a trowel) was collected for estimating specific surface area (SSA) of the fine earth (for methods see Section 3.2.5 Specific surface area sample), while a second quarter of the coarse fines was used for particle size analysis.

Matric potential measurements were made immediately after the excavation of each 10 cm depth increment, by inserting UMS T5 pressure transducer tensiometers horizontally into the pit wall, with readings taken with an infield 7C handheld read-out device (UMS, 2009). To ensure accurate measurements, a soil corer with a diameter slightly smaller than the tensiometer was used to form a pilot hole in which the tensiometer was inserted. The probe was nestled in a sandbag after it was inserted into the pit wall, which served to hold the probe in place and reduce pressure variations caused by the weight or movement of the probe and cable. Lastly, a cover was placed over the pit to further reduce any interference by the wind or sun. A matric potential measurement for an increment was an average of three readings on different sides of the soil pit. Each reading was taken after the tensiometer had equilibrated with the soil, which took ~10 minutes on average but could vary from 2 to >30 minutes.

3.2.5 Laboratory analysis

Bulk density sample and >20 mm sample

The bulk density subsample and the >20 mm sample were oven-dried at 105°C before being weighed (M_{b-d} and M_{RF-d}) respectively). The samples were then wet sieved into rock size classes defined by Milne et al. (1995): 2-6 mm and 6-20 mm for the bulk density sample; 20-60 mm and >60 mm for the >20 mm sample. RFs were collected and the fine material was washed away, with RFs being thoroughly cleaned by hand or by agitating them with a gold panning-like action. Clean RFs were oven-dried at 105°C and weighed according to their size classes. The total volume of 2-20 mm RFs in an increment ($V_{T[2-20]}$) was estimated by multiplying the weight of the oven-dried cleaned RFs from the bulk density sample ($M_{b[2-6]}$ plus $M_{b[6-20]}$) by a scaling ratio (R) before dividing by a rock density of 2.65 g cm^{-3} (Manger, 1963), such that

$$V_{T[2.20]} = \frac{R\left(M_{b[2-6]}+M_{b[6-20]}\right)}{2.65} \quad (1)$$

where

$$R = \frac{M_{CF}}{M_b} \quad (2)$$

The scaling ratio is a means of extrapolating measures from the bulk density subsample (such as $M_{b[2-6]}$ or M_{b-d}) to the whole depth increment. The total volume of >20 mm RFs in an increment ($V_{T[>20]}$) was estimated by dividing the weight of the oven-dried cleaned RFs from the >20 mm sample ($M_{RF[20-60]}$ plus $M_{RF[>60]}$) by the rock density.

$$V_{T[>20]} = \frac{M_{RF[20-60]} + M_{RF[>60]}}{2.65} \quad (3)$$

A cross-check of volumes calculated in this manner against the water displacement method showed discrepancies of 2% for any of the RF size classes. The volume of the fines ($V_{T<2}$) was back-calculated using the volume of the RFs and the total volume of the increment (V_T) estimated from the bead volume.

$$V_{T<2} = V_T - V_{T[>20]} - V_{T[2-20]} \quad (4)$$

Bulk density (ρ_b) was then estimated by dividing the sum of the oven-dried weights of the scaled bulk density sample and >20 mm sample by the total volume of the depth increment.

$$\rho_b = \frac{M_{b-d}.R + M_{RF-d}}{V_T} \quad (5)$$

Finally, the fines bulk density ($\rho_{<2}$) was estimated by firstly scaling the mass of the fines in the bulk density sample by R (Equation 2), then adding on the mass of the fines attached to the >20 mm RFs, before dividing this sum by the volume of fines in the whole increment ($V_{T<2}$).

$$\rho_{<2} = \frac{R\left(M_{b-d} - M_{b[2-6]} - M_{b[6-20]}\right) + \left(M_{RF-d} - M_{RF[20-60]} - M_{RF[>60]}\right)}{V_{T<2}} \quad (6)$$

Specific surface area sample

The SSA sample was sieved in a field moist state through a 2 mm sieve. The <2 mm material was collected and weighed after being dried in a Weiss Gallenkamp fitotron (hgc 1514) set at 30°C and 30% relative humidity ($M_{<2-a}$), and after being dried at 105°C in an oven ($M_{<2-d}$). The SSA was then estimated following the equation of Parfitt et al. (2001):

$$SSA = \frac{2000(M_{<2-a} - M_{<2-d})}{M_{<2-d}} \quad (7)$$

Particle size analysis sample

The sample was analysed for particle size distribution of the <2 mm soil fraction. Particle distribution was measured using the pipette method following Claydon (1989).

3.2.6 Deep matric potential profile experiment

In July 2019, five of the sites measured using the methods above were revisited (Figure 7). At each of the revisited sites, the soil was wet up as before except the wetted area was increased to 70 x 50 cm. The soil was irrigated with ~115 mm of water at a rate of ~10 mm hr^{-1} before being covered and left to drain. Three days after irrigation had ceased, an excavator was used to excavate a 1.5 m-deep trench bordering the wetted area of soil. Tarpaulin sheets were used to cover the wetted area, the trench face and the trench as a whole to reduce evaporation. On the fourth- or fifth-day following irrigation, an alcove was dug incrementally down the profile. The back wall of the alcove was ~30 cm into the wetted area of soil, the soil moisture of which should not have been influenced by the open trench. The first measurement of matric potential was taken at a depth of 10 cm after the alcove had been excavated to 15 cm using the same equipment and methods as above, except for the inclusion of a hessian sack which was draped over the exposed pit to reduce wind disturbance on the tensiometer. The alcove was then excavated and matric potential measured incrementally in 10-20 cm intervals. Depth of matric potential readings varied to include horizons that may otherwise go unmeasured if a set increment depth was used.

Figure 7 Photoplate of deep matric potential profile experiment. Top left: prewetting stage, top right: trench excavation with a tarpaulin covering the wetted area of soil, bottom left: covering wetted area and trench, bottom right: matric potential measurement set-up.

3.3 Results

3.3.1 Soil physical characteristics

The fine earth particle size distribution for samples varied from <10% to >90% for sand and silt; 1% through to 45% for clay. The proportion of RFs to an increment's volume varied from 0% to 89%. In general, the texture of the fine earth became coarser with depth: the fine earth exceeded 50% silt at the 0-10 cm increment compared to >70% sand at the 50-60 cm increment (Table 3). The SSA correlated well with soil texture, decreasing with increasing depth and with increasing sand content (Table 3). Bulk density and the proportion of RFs increased with depth but became relatively constant on average below 40 cm (Table 3). Average fine earth bulk density was lowest in the 0-10 cm increment and relatively constant through 10-60 cm depths, with the highest fine earth bulk density in the 30-40 cm increment (Table 3). Brown Soils were the dominant soil order encountered (58%), followed by Recent Soils (34%), and finally Gley and Pallic Soils (4% each). The sampled pits were distributed over three geomorphic surfaces: 82% were on Late Pleistocene glacial outwash, 22% were on Holocene alluvial deposits and 4% were on Late Pleistocene to Holocene alluvial deposits.

Table 3 Soil physical characteristics of measured pits. Values in parentheses are standard errors.

Depth	Sand	Silt	Clay	Volumetric proportion RFs	Bulk density	Fine earth bulk density	SSA
cm	%	%	%	%	g cm^{-3}	g cm^{-3}	m^2 g^{-1}
0-10	26 (2)	53 (1)	21 (1)	11 (2)	1.32 (0.03)	1.16 (0.02)	44.56 (2)
10-20	28 (2)	51 (2)	21 (1)	17 (3)	1.58 (0.04)	1.36 (0.02)	40.24 (2)
20-30	33 (3)	47 (2)	20 (1)	36 (4)	1.85 (0.05)	1.39 (0.04)	36.22 (2)
30-40	45 (4)	37 (2)	18 (1)	51 (4)	2.06 (0.05)	1.48 (0.05)	34.93 (2)
40-50	65 (3)	22 (2)	12 (1)	62 (3)	2.17 (0.03)	1.37 (0.04)	32.62 (2)
50-60	78 (3)	14 (2)	9 (1)	62 (3)	2.15 (0.04)	1.32(0.07)	27.83 (2)

3.3.2 Matric potential depth profiles

Aggregated data

The matric potential at FC was generally higher than -10 kPa, but there was significant variability for any one depth (Figure 8A). Below 10 cm there was a relatively linear increase in the average matric potential with increasing depth. The slope of a linear regression through the bottom five increments (red line) was 0.06 kPa cm^{-1}, which for comparison is shown with the gradient of matric potential at hydrostatic equilibrium (0.098 kPa cm^{-1}; black line) (Figure 8A).

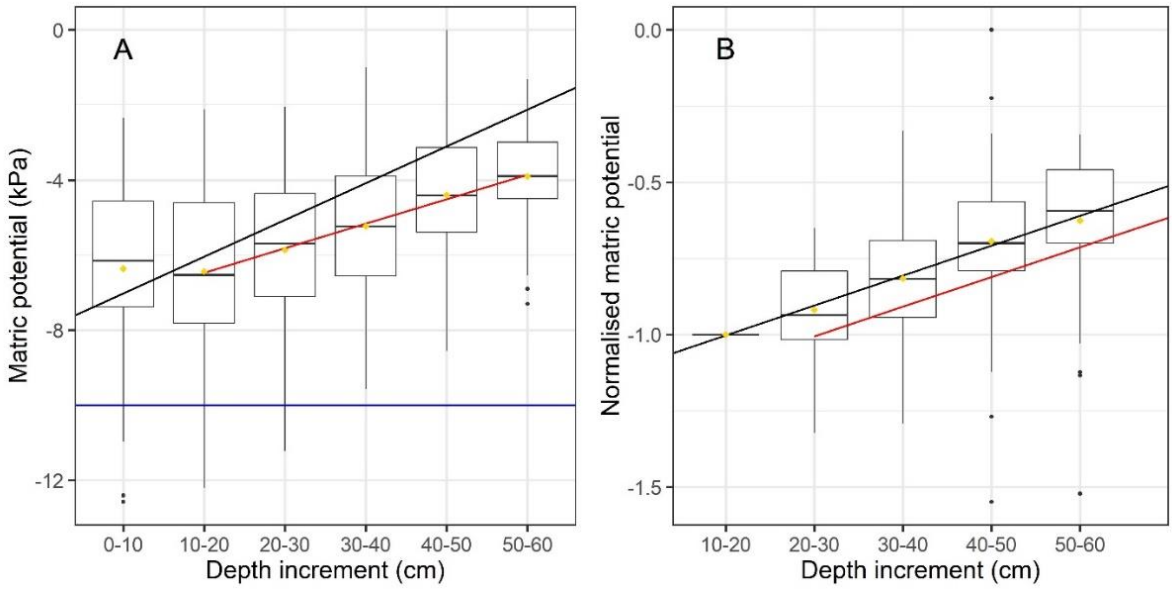

Figure 8 Plot A: Variation in matric potential with depth. Plot B: Variation in normalised matric potential with depth. Yellow dots: Mean value, blue line: -10 kPa, red line: regression line for 10-60 cm, black line: hydrostatic equilibrium.

Hydrostatic equilibrium corresponds to the gradient of matric potential when changes in matric potential are balanced by changes in gravitational potential such that there is no change in total potential (ignoring any osmotic potential gradient). This condition should exist when drainage materially ceases. Because hydrostatic equilibrium can be established across a range of matric potentials in individual soil pits, we normalised matric potential from each pit using the 10-20 cm depth increment matric potential (Figure 8B). We did not use the 0-10 cm increment data because this increment appeared to have anomalously high potentials. The matric potential gradient after the normalisation was 0.097 kPa cm^{-1} with a 95% confidence interval of ±0.017 kPa cm^{-1}; making the normalised matric potential gradient indistinguishable from hydrostatic equilibrium.

Individual pit data

When each pit was considered individually, the variation of matric potential with depth followed one of five broad modes of behaviour, which we present exemplars of in Figure 9 (see Appendix C, Appendix D and Appendix E for all other matric potential with depth profiles).

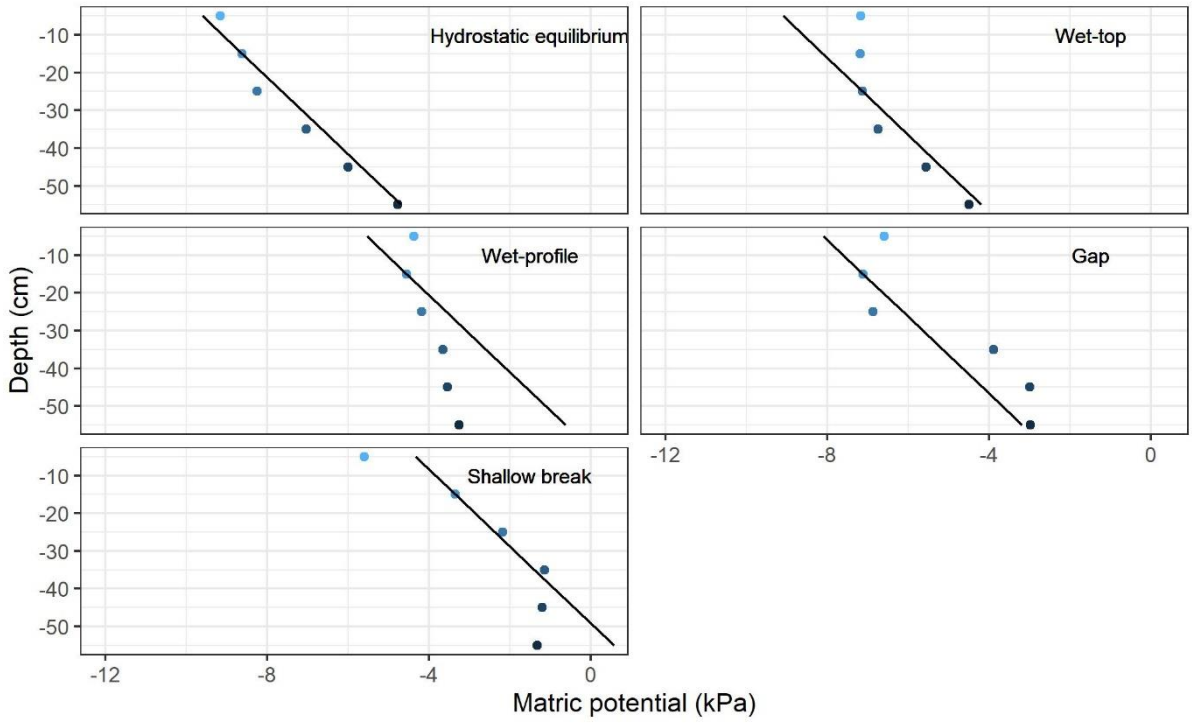

Figure 9 Examples of observed modes of matric potential with depth. Black line represents hydrostatic equilibrium (0.098 kPa cm^{-1}).

Hydrostatic equilibrium mode

The matric potential increased linearly with increasing depth at a rate commensurate with hydrostatic equilibrium (0.098 kPa cm^{-1}) and was observed in 17 (33%) pits. Soil profiles with this mode were often characterised by a deviation from the hydrostatic equilibrium trend in the uppermost increment, such that the 0 – 10 cm increment was usually at a higher matric potential than expected. There was no systematic pattern of soil properties associated with this mode, with this near hydrostatic equilibrium behaviour being observed in soils with a range of profile forms and texture and -RF abundance depth-profiles.

Wet-top mode

The lower depths of the profile (30-40 cm and deeper) had a matric potential depth gradient similar to hydrostatic equilibrium. However, an inflection occurred at 20 – 40 cm depth above which the matric potential remains relatively constant. Soil profiles with this mode remained wetter in the upper part of the profile than those with the hydrostatic equilibrium mode. The mode was observed in 12 pits (23%), 10 of which the inflection was located at a boundary between an upper silt loam horizon and a lower horizon where sand increased >25%.

Wet-profile mode

The whole profile diverged from hydrostatic equilibrium, with matric potential changing little with depth. This mode was seen in 15% of measured pits (8 pits). Four of the pits had coarse fine earth at

the lower depths with >70% sand, while the remaining pits had >40% silt (for 3 pits) or >40% clay (1 pit) at the 50-60 cm increment.

Gap mode

In 10% of the pits (5 pits), a disjunction occurred in the matric potential depth profile, such that matric potential increased in a stepwise fashion down-profile over a 10 cm increment. This disjunction could occur between the 20-30 cm, 30-40 cm or 40-50 cm depth increments. Like the wet-top mode, the matric potential at the top of the profile did not change with depth; however, unlike the wet-top mode, the lower depths of the profile did not have a linear increase with depth. In four of the five pits, the disjunction in matric potential occurred at horizon boundaries where sand increased by >30% and fines bulk density decreased by >0.45 g cm^{-3} downwards across the boundary. For the remaining pit, the gap in matric potential occurred at a horizon boundary without any significant changes in measured properties.

Shallow break mode

The matric potential gradient with depth at the top of the profile approximated hydrostatic equilibrium, but an inflection occurred in the lower part of the profile. Over the upper region at hydrostatic equilibrium, matric potentials were relatively low compared to profiles showing the hydrostatic equilibrium mode. Below the inflection, they remained constant at ~-4 kPa or higher. This mode occurred in 8% (4) of the pits. In these profiles, increments below 30 cm had >80% sand in the fine earth and SSA was <15 m^2 g^{-1}.

Though most of the modes could be associated with characteristic profile discontinuities or changes in morphological soil boundaries (such as >25% change in sand for wet-top), all those characteristics could be found in soils that displayed hydrostatic equilibrium. Thus, the presence of the profile discontinuities that might be necessary for the other modes to occur are not sufficient to guarantee that those particular modes will be observed. The single necessary and sufficient condition appears to be taxonomic; i.e. the shallow break mode only occurred in Typic Fluvial Recent Soils (found on Holocene surfaces), which in turn only demonstrated the shallow break mode. Pits demonstrating the wet-top mode were also affected by soil taxonomy, with 67% of the wet-top mode pits occurring in Typic Firm Brown Soils. Geomorphic surface was also important to the gap mode, which only occurred in soils on late Pleistocene surfaces. Soil taxa and geomorphic surface had no clear effect on other modes, while RF volume and bulk density had no clear effect on any of the modes.

3.3.3 Deep matric potential profile data

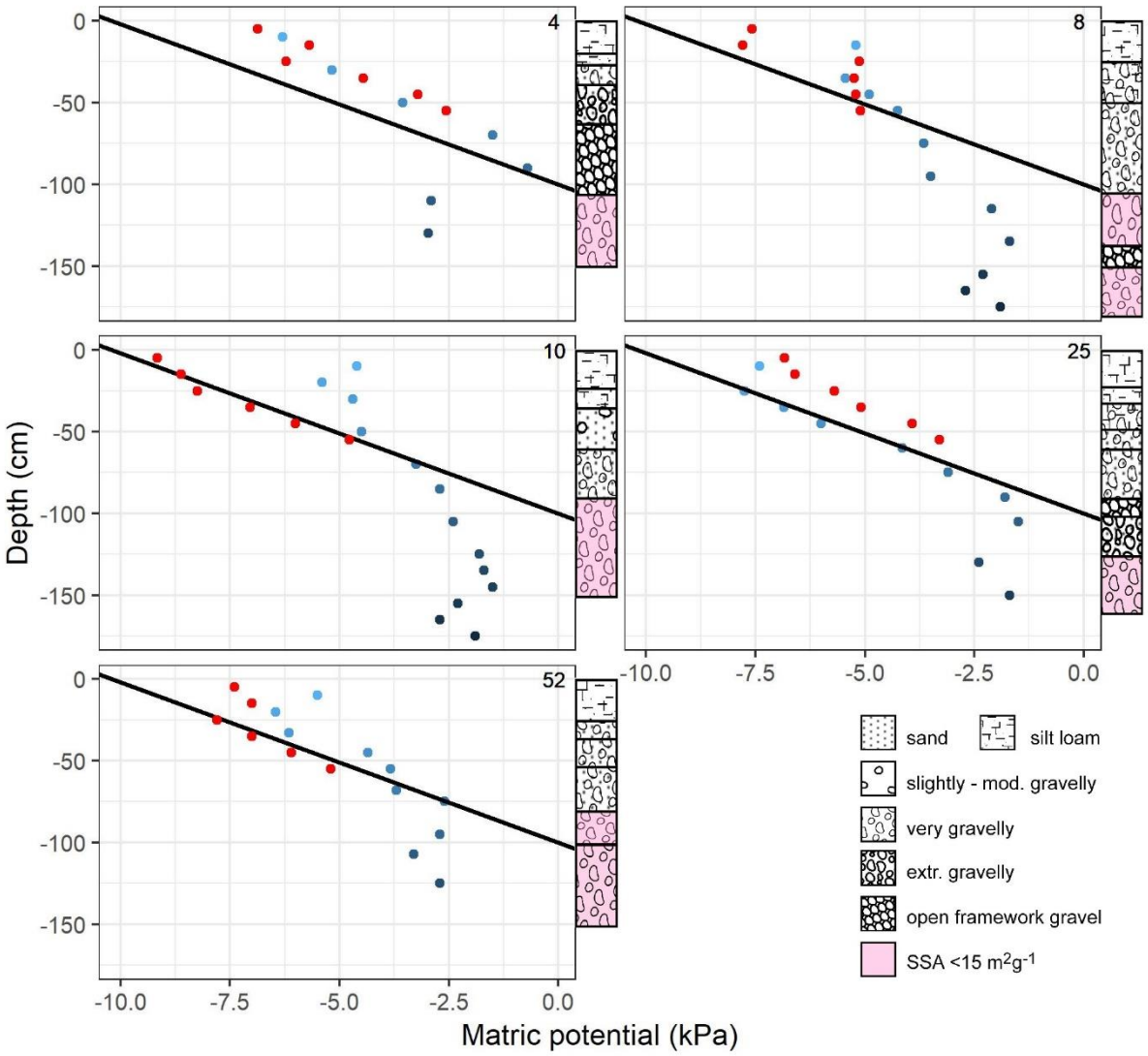

Figure 10 Matric potential depth profiles and soil profile layering. Numbers in the right-hand top corner of each plot is the pit number. Red symbols represent data from the shallow pits (60 cm), whereas blue points represent data from the deep (150 cm) pits. The black line represents hydrostatic equilibrium (0.098 kPa cm^{-1}).

Apart from Pit 10, matric potential depth-profiles were similar between the shallow pit and deep pit experiments even though deep pits had an additional 2-3 days of drainage (Figure 10). For Pits 4, 25 and 52 an inflection occurred at the lower part of the profile, below which matric potential remained in the 2-3 kPa range. This inflection coincided with a layer of open framework gravels in Pits 4 and 25, with few to no fines present, at a depth of 63 cm and 90 cm, respectively. Matric potential at a depth of 30 cm varied between the two pits, with matric potential 2.1 kPa higher in Pit 4 than in Pit 25. Pit 52 lacked a layer of open framework gravels; however, matric potential stabilised upon reaching fine earth with SSA <15 m^2 g^{-1} at 80 cm depth, similar conditions to the shallow pits demonstrating shallow break mode.

Pits 8 and 10 had a similar near-constant matric potential below 0.8 – 1 m, but did not have such a noticeable inflection in the profile (Figure 10). Pit 8 contained a layer of open framework gravels at ~140 cm while Pit 10 had SSA <15 m^2 g^{-1}at depths >90 cm.

3.4 Discussion

Hydrostatic equilibrium is a condition in the soil-water system when matric potential and gravitational potential are balanced. Gravitational water potential varies by -98 J kg^{-1} m^{-1} or -9.8 kPa m^{-1} (or- 0.098 kPa cm^{-1}) assuming the density of water is 1000 kg m^{-3}. Consequently, the matric potential gradient should be the same magnitude but opposite sign (9.8 kPa cm^{-1}). Under this condition, there is no vertical variation in total potential (if osmotic potential is negligible), and consequently, water does not move. Thus, accepting that FC prevails when drainage has materially ceased, then hydrostatic equilibrium is a sufficient condition for FC. Hydrostatic equilibrium at FC is the dominant mode in our dataset. FC normally only approximates hydrostatic equilibrium in soils with shallow groundwater systems, i.e. ~<2 m from soil surface to groundwater (Beldring et al., 1999; Dettmann and Bechtold, 2016; Pirastru and Niedda, 2013). The groundwater table establishes a 0 kPa matric potential boundary condition close to the soil surface. Hydrostatic equilibrium can be attained under this condition because the lowest matric potentials (near the soil surface) dictated by this gradient are not so low that low hydraulic conductivity prevents water from moving. For instance, if the soil surface were 1 m above the groundwater table, at hydrostatic equilibrium, matric potential would be -10 kPa at the surface, compared to -100 kPa if the soil surface was 10 m from the groundwater table. Considering a change of -10 kPa to -100 kPa corresponds to a reduction in hydraulic conductivity of more than two orders of magnitude for a loam or coarser soil matrix (Doussan and Ruy, 2009), water movement is likely to cease near the soil surface in the case of the deeper water table before hydrostatic equilibrium occurs. Thus, for a deep-water table, hydrostatic equilibrium will exist only in the increment above the water table over which the declining matric potential does not cause drainage to be so low that the soil cannot drain. Considering the water tables for the pits measured in this study were anywhere from <1 m to >60 m from the soil surface (Canterbury Maps, 2018) and the occurrence of the hydrostatic equilibrium mode was not correlated to water table depth, some property in these soils must be allowing hydrostatic equilibrium to occur regardless of groundwater depth.

An explanation for the existence of hydrostatic equilibrium in the FAFSS we sampled, despite often deep groundwater, appears to be the existence of a near-zero but finite (negative) matric potential near the soil surface. Hillel (1998) and Miller and Gardner (1962), show that sublayers of sand or aggregates can impede water movement at high matric potentials. This phenomenon (known as a capillary break) occurs because coarser materials (sand and sand-RF mixtures) show a highly

nonlinear water release behaviour, with a marked decrease in water content as matric potential drops below zero (Zornberg et al., 2010). As a result, these coarse-textured materials can have very low hydraulic conductivities and very slow drainage at matric potentials drier than -6 kPa (Obreza et al., 1997; Zornberg et al., 2010).

We see evidence in our deep pits and in the shallow break mode observed in the shallow pits of such a capillary break. Deep Pits 4 and 25 show an inflection from hydrostatic equilibrium upon reaching a layer of open framework gravels. These open framework gravels have minimal fine earth (<10% g g^{-1}), fitting the "coarse" conditions required of a capillary break. The open framework gravels are a characteristic depositional product in alluvial fans (Burbery et al., 2018; Hooke, 1967; Nichols, 2009) that are formed by the flow separation of sand and gravel at the crest of bedforms (Lunt and Bridge, 2007). The shallow pits of the shallow break mode showed unchanging matric potential in the base of the profile corresponding to sediment with fine earth fraction sand >80% and SSA <15 m^2 g^{-1} in the 30-60 cm increments. These conditions are similar to those seen in deep Pits 52 and 8, which after reaching fine earth with SSA <15 m^2 g^{-1}, matric potential became constant with depth.

We posit that the coarse-textured, stony and low SSA layers in which matric potential became constant provide the necessary conditions for slow hydraulic conductivity at high matric potentials (i.e. matric potentials close to zero). This is supported by Carrick et al. (2013a), who found the drainage of a lysimeter containing a Canterbury FAFSS remained the same whether it was under a free drainage lower boundary or when an artificial suction of 6 kPa was applied to the bottom. Carrick et al.'s experiment demonstrated that the lower layer of the FAFSS, which was sandy gravel, was effectively not conductive at a matric potential of -6 kPa. Consequently, this matric potential could not be imposed on the horizons above, and hence there was no drainage response in the overlying horizons. Of the profiles we examined that exhibited hydrostatic equilibrium, similar sediment at the base establishes a low matric potential boundary condition, above which hydrostatic equilibrium can be established. Where this condition appears at shallow depths in the soil (i.e. shallow break mode) soils are Typic Fluvial Recent Soils found on the youngest geomorphic surface. This finding suggests that post-depositional processes acting over time lead to a contrast in pore size distribution above and below the capillary break. Above the break, pedogenesis (e.g. C accumulation, silt and clay formation and translocation) and possibly aeolian accessions act to create a pore network capable of draining at lower matric potentials than the material below the break.

We speculate that the FAFSS that deviate from hydrostatic equilibrium are characterised by a pore discontinuity, where finer horizons at the top of the profile are not in connection with horizons below at relatively high matric potentials, causing the soil above to be wetter. Due to the impaired drainage, two days is insufficient for them to reach hydrostatic equilibrium. However, Pits 8, 10 and

52 from Experiment 2 did not reach hydrostatic equilibrium after 4-5 days of drainage following irrigation. This may indicate that soils have effectively stopped draining (i.e. reached FC) and are not likely to attain hydrostatic equilibrium in the short term. The soil properties we measured provided little or no explanation of why some horizons/profiles were slower draining than others. Divergence from the hydrostatic equilibrium matric potential gradient occurred at horizon boundaries for all modes (except the wet-profile mode and the divergent 0-10 cm increments in hydrostatic equilibrium mode), across which we observed no stepwise change in soil properties. However, our sampling strategy for the shallow pits was even-increment based not horizon based, and hence some discrete changes may not have been resolved. The propensity of Typic Firm Brown Soils or soils on late Pleistocene surfaces to demonstrate wet-top and gap modes may indicate that low conductivity may have been due to characteristics of the pore network (size, continuity and tortuosity, Alaoui et al., 2011; Seguel et al., 2013; Shinomiya et al., 2001). Either the older age of these soils and/or enrichment of the B-horizon with sesquioxides may increase the individual development of horizons within a profile (Saunders, 1965), increasing the likelihood of pore discontinuities across horizon boundaries. Alternatively, for the hydrostatic equilibrium soils with wetter 0-10 cm increments, surface compaction could be the cause of pore discontinuities. Soils under intensive dairy land use are particularly prone to soil compaction, which can significantly alter the pore network of a soil (Houlbrooke and Laurenson, 2013; Mesman, 2014) and in this case, may cause pore discontinuities. However, as characteristics of the pore network could not be examined from the soil properties we measured, we can only speculate.

Though a number of the soils we sampled may still have been draining after 2-days (e.g. pits displaying wet-profile), the primary mode seen in pits was near hydrostatic equilibrium, which suggests FC prevailed. We have hypothesised that this drainage behaviour is controlled by a lower boundary condition (non-conductive sandy gravels) that dictates that FC is reached in the topsoil at relatively high matric potentials (>-10 kPa). In free-draining non-stony soil lacking a shallow capillary break, and where a groundwater table is not close to the surface (> ~2 m), FC is not characterised by a condition of hydrostatic equilibrium. Instead, drainage lowers matric potential to the point that hydraulic continuity within the horizons of the internally draining soil profile is disrupted before equilibrium is reached (Assouline and Or, 2014). As a result, FC matric potential is usually controlled by the size distribution of the hydraulically connected pores, resulting in the matric potential of FC varying from -3 kPa to -188 kPa depending on the texture and horizon contrasts within the soil profile (Assouline and Or, 2014). In soils that are not free draining, such as soils with a dense slowly draining subsoil horizon, a different mode of FC can occur. In these soils the low saturated conductivity of the impeding layer causes soil water to ‘perch’ above, effectively creating an ephemeral water table in the subsoil (Vogeler et al., 2019), above which FC will likely follow hydrostatic equilibrium. Thus we

propose three distinct mechanisms determining FC in soils: 1) the presence of a shallow zero or near-zero matric potential boundary condition, due to either a shallow water table or a coarse-textured sandy gravel layer, allows hydrostatic equilibrium to be attained, 2) soil drains until the low matric potentials within the soil profile cause very low unsaturated conductivities amongst texturally variable layers resulting in the internal drainage of the soil profile to be disrupted, 3) soils with impeding layer with very low saturated conductivities at a shallow depth produce an ephemeral water table in the subsoil, with a capillary fringe above at hydrostatic equilibrium.

3.4.1 Implications to soil management

We have found that FAFSS have a higher FC matric potential than the often-assumed arbitrary value of -10 kPa, which could have significant implications for soil management, considering a change of only 2 kPa can equate to a 15% change in AWC in some coarse-textured soils (Obreza et al., 1997). This could have implications for irrigation scheduling, which is reliant on using FC to determine when and how much to irrigate the soil to ensure stress-free plant growth while avoiding excessive drainage losses. Furthermore, management of FAFSS to avoid nutrient leaching may also be affected. In New Zealand, nutrient discharge limits are determined by estimates of leaching losses using models, which are sensitive to the AWC and thus FC parameters. Considering FAFSS on the Canterbury Plains are intensively irrigated, have low AWC and a free-draining nature, accurate knowledge of FC is crucial for knowing the water storage and when and how much leaching occurs under rainfall events throughout the year (Cichota et al., 2016; Lilburne et al., 2010). For accurate estimation of FC, it may be necessary to identify the depth to sandy gravel capillary break layers in the profile. The depth to this layer sets the range of matric potential established at hydrostatic equilibrium. The deeper the capillary break, the lower the matric potential near the soil surface. Comparing the matric potential of deep Pits 4 and 25 at an arbitrary depth of 30 cm, Pit 4 was 2.1 kPa higher than Pit 25 in accord with a 27 cm decrease in depth to the capillary break. The drainage limitation below the capillary break could be used to limit losses of irrigation water and nutrients. If the depth of the capillary break is known (h, cm), as is the matric potential at which the material effectively becomes conductive (ψ_T, kPa), then irrigation applications should be limited so that the matric potential in the soil immediately above the capillary break remains below the threshold value. Adopting this strategy, the depth of water the soil can hold at FC (FC_{mm}) is estimated by integrating the moisture retention curve ($\theta(\psi)$) between ψ_T and the matric potential at the soil surface (ψ_0) such that

$$FC_{mm} = \frac{1}{\frac{d\psi}{dz}_{hydro}} \int_{\psi_0}^{\psi_T} \theta(\psi) d\psi \quad (8)$$

where

$$\psi_0 = \psi_T - h\frac{d\psi}{dz}_{hydro} \quad (9)$$

and

$\frac{d\psi}{dz}_{hydro}$ is the vertical matric potential gradient at hydrostatic equilibrium (0.098 kPa cm^{-1}).

How much water is applied in an irrigation event then depends on the deficit from this water depth. We note that this approach would be conservative with regard to a refill point: the soils we studied were always wetter at FC than hydrostatic equilibrium would dictate when hydrostatic equilibrium was not achieved. This strategy, of course, does not obviate water losses by macropore flow, related to application rate and soil pore size distribution. Still, it is a more informed approach than assuming a constant matric potential with depth at FC.

3.5 Conclusions

Following two days of drainage in FAFSS on Pleistocene and Holocene age surfaces, matric potential-depth profiles were variable but generally exhibited matric potentials higher than the often-assumed FC value of -10 kPa, which is adopted for the purposes of environmental modelling and land management. Matric potential depth-profiles could be assigned into five modes of drainage behaviour (hydrostatic equilibrium, wet-top, gap, wet-profile and shallow break), with hydrostatic equilibrium being the most common mode. The four other modes tend towards hydrostatic equilibrium, but some form of drainage impediment meant that hydrostatic equilibrium was not reached after only two days of drainage. Our results support our hypothesis, as we have shown that a near-surface layer with low conductivity at negative but near-zero matric potentials is an alternative condition to a shallow water table to allow hydrostatic equilibrium to be established at FC. The low unsaturated hydraulic conductivity at near-zero matric potential causes a capillary break at a shallow depth, allowing FC to be reached in the upper soil at relatively high matric potentials (>-10 kPa). The capillary break may correspond to either: 1) a layer of open framework gravels or 2) fine earth with <15 m^2 g^{-1} SSA. Our finding could have significant implications for management practices, such as irrigation scheduling, which should aim to not wet the material causing the capillary break to the point it is conductive. If kept at non-conductive matric potentials, the capillary break should allow the water (and nutrients) in the soil above to be retained for longer periods.

3.6 Appendix

Appendix A Irrigation system and cover.

Appendix B Pit and bead method (from left to right). Metal frame fitted flush to the soil surface; soil material is excavated in depth increments and volume of the excavated hole is estimated with plastic beads.

Appendix C The matric potential gradient with depth for pits 1-18. Black line is hydrostatic equilibrium gradient (0.098 kPa cm^{-1}) and the number in top right is the pit number.

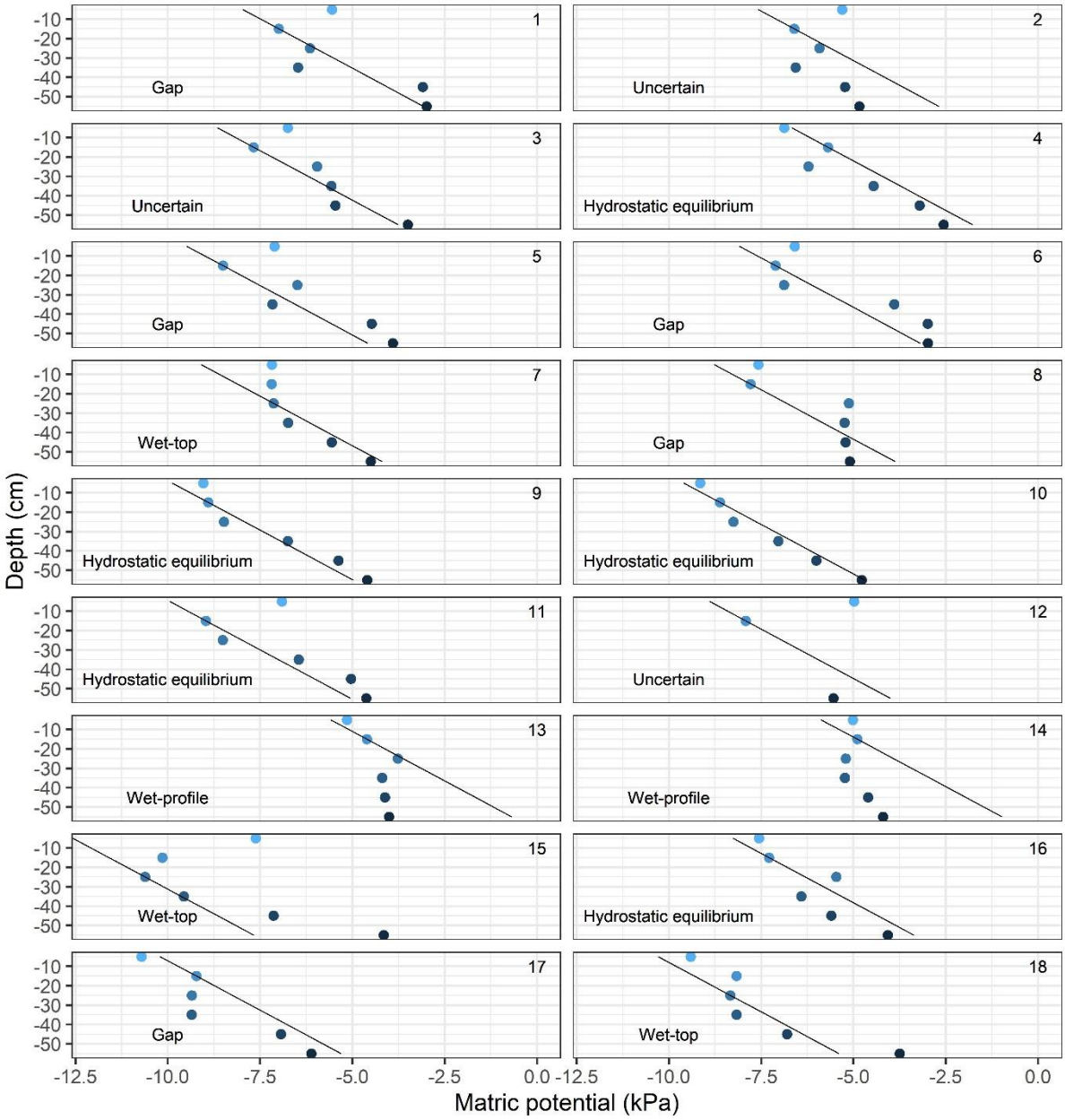

Appendix D The matric potential gradient with depth for pits 19-36. Black line is hydrostatic equilibrium gradient (0.098 kPa cm^{-1}) and the number in top right is the pit number.

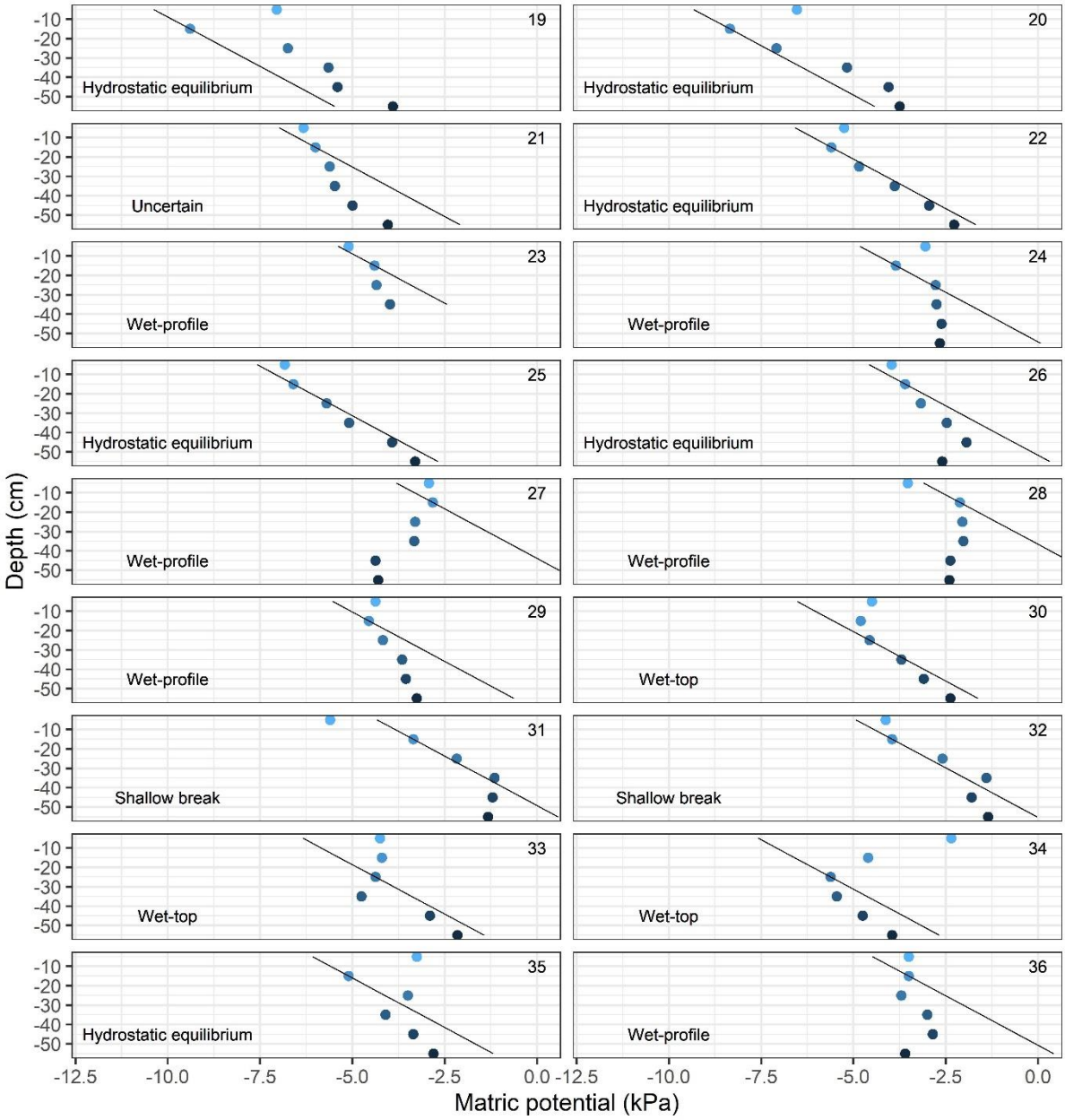

Appendix E The matric potential gradient with depth for pits 37-52. Black line is hydrostatic equilibrium gradient (0.098 kPa cm^{-1}) and the number in top right is the pit number.

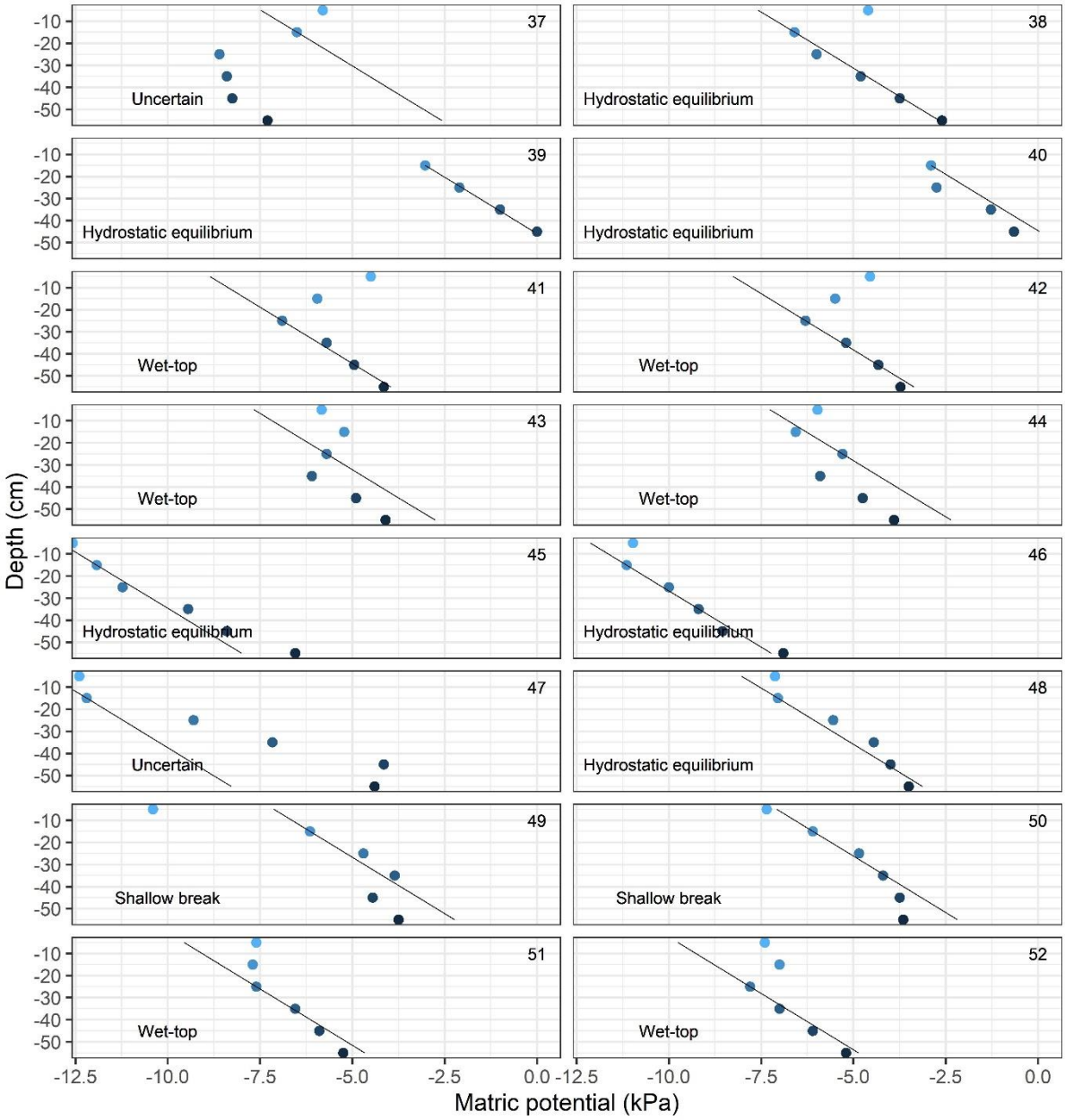

References

Alaoui, A., Lipiec, J., Gerke, H.H., 2011. A review of the changes in the soil pore system due to soil deformation: a hydrodynamic perspective. Soil Tillage Res. 115, 1-15, https://doi.org/10.1016/j.still.2011.06.002.

Arrouays, D., McBratney, A., Minasny, B., Hempel, J., Heuvelink, G., MacMillan, R., Hartemink, A., Lagacherie, P., McKenzie, N., 2014. The GlobalSoilMap project specifications. GlobalSoilMap: Basis of the Global Spatial Soil Information System, Release 2.4.

Assouline, S., Or, D., 2014. The concept of field capacity revisited: defining intrinsic static and dynamic criteria for soil internal drainage dynamics. Water Resour. Res. 50(6), 4787-4802, https://doi.org/10.1002/2014wr015475.

Ayaz, S., Biswas, M., Dhali, M.K., 2018. Morphotectonic analysis of alluvial fan dynamics: comparative study in spatio-temporal scale of Himalayan foothill, India. Arabian J. Geosci. 11(2), 41, https://doi.org/10.1007/s12517-017-3308-2.

Beldring, S., Gottschalk, L., Seibert, J., Tallaksen, L., 1999. Distribution of soil moisture and groundwater levels at patch and catchment scales. Agric. For. Meteorol. 98, 305-324, https://doi.org/10.1016/S0168-1923(99)00103-3.

Burbery, L.F., Moore, C.R., Jones, M.A., Abraham, P.M., Humphries, B.L., Close, M.E., Ventra, D., Clarke, L.E., 2018. Study of connectivity of open framework gravel facies in the Canterbury Plains aquifer using smoke as a tracer. In: D. Ventra, L.E. Clarke (Eds.), Geology and Geomorphology of Alluvial and Fluvial Fans: Terrestrial and Planetary Perspectives. Geological Society, London, Special Publications, 440, pp. 327-344.

Canterbury Maps, 2018. Depth To Groundwater. Canterbury Maps.

Carrick, S., Fraser, P., Dennis, S., Knight, T., Tabley, F., 2013a. Challenges for leachate monitoring from alluvial sedimentary soils. In: L.D. Currie, C.L. Christensen (Eds.), Accurate and Efficient Use of Nutrients on Farms., Occasional Report No. 26. Fertiliser and Lime Research Centre, Massey University, Palmerston North, New Zealand.

Carrick, S., Palmer, D., Webb, T., Scott, J., Lilburne, L., 2013b. Stony soils are a major challenge for nutrient management under irrigation development. In: L.D. Currie, C.L. Christensen (Eds.), Accurate and Efficient Use of Nutrients on Farms., Occasional Report No. 26. Fertiliser and Lime Research Centre, Massey University, Palmerston North, New Zealand.

Carrick, S., Rogers, G., Cameron, K., Malcolm, B., Payne, J., 2017. Testing large area lysimeter designs to measure leaching under multiple urine patches. N. Z. J. Agric. Res. 60(2), 205-215, https://doi.org/10.1080/00288233.2017.1291527.

Casanova, M., Osvaldo, S., Oscar, S., Walter, L., 2013. The Soils of Chile. World Soils Book Series. Springer, New York.

Cichota, R., Kelliher, F.M., Thomas, S.M., Clemens, G., Fraser, P.M., Carrick, S., 2016. Effects of irrigation intensity on preferential solute transport in a stony soil. N. Z. J. Agric. Res. 59(2), 141-155, https://doi.org/10.1080/00288233.2016.1155631.

Claydon, J.J., 1989. Determination of particle size in fine grained soils – pipette method. Division of Land and Soil Sciences Technical Record (LH5), DSIR Division of Land & Soil Sciences.

Dann, R., Close, M., Flintoft, M., Hector, R., Barlow, H., Thomas, S., Francis, G., 2009. Characterization and estimation of hydraulic properties in an alluvial gravel vadose zone. Vadose Zone J. 8(3), 651-663, https://doi.org/10.2136/vzj2008.0174.

Davidson, S.K., Hartley, A.J., Weissmann, G.S., Nichols, G.J., Scuderi, L.A., 2013. Geomorphic elements on modern distributive fluvial systems. Geomorphol. 180, 82-95, https://doi.org/10.1016/j.geomorph.2012.09.008.

de Jong van Lier, Q., 2017. Field capacity, a valid upper limit of crop available water? Agri. Water Manage. 193, 214-220, https://doi.org/10.1016/j.agwat.2017.08.017.

Dettmann, U., Bechtold, M., 2016. Deriving effective soil water retention characteristics from shallow water table fluctuations in peatlands. Vadose Zone J. 15(10), https://doi.org/10.2136/vzj2016.04.0029.

Doussan, C., Ruy, S., 2009. Prediction of unsaturated soil hydraulic conductivity with electrical conductivity. Water Resour. Res., 45, W10408., https://doi.org/10.1029/2008wr007309.

Fairbridge, R.W., 1997. Outwash plain, fan, terrace, sandur, Geomorphology. Springer Berlin Heidelberg, Berlin, Heidelberg, pp. 796-798.

Fontana, A., Mozzi, P., Marchetti, M., 2014. Alluvial fans and megafans along the southern side of the Alps. Sediment. Geol. 301, 150-171, https://doi.org/10.1016/j.sedgeo.2013.09.003.

Forsyth, P.J., Jongens, R., Barrell (Compilers), D.J.A., 2008. Geology of the Christchurch Area. Institute of Geological & Nuclear Sciences 1:250 000 geologial map 16. GNS Science, Lower Hutt, New Zealand.

Gargiulo, L., Mele, G., Terribile, F., 2016. Effect of rock fragments on soil porosity: a laboratory experiment with two physically degraded soils. Eur. J. Soil Sci. 67(5), 597-604, https://doi.org/10.1111/ejss.12370.

Gohain, K., Parkash, B., 1990. Morphology of the Kosi Megafan. In: A.H. Rachocki, M. Church (Eds.), Alluvial Fans: A Field Approach. Wiley, Chichester, pp. 151-178.

Graham, S., Srinivasan, M.S., Faulkner, N., Carrick, S., 2018. Soil hydraulic modeling outcomes with four parameterization methods: comparing soil description and inverse estimation approaches. Vadose Zone J. 17, https://doi.org/10.2136/vzj2017.01.0002.

Gray, C.W., McDowell, R.W., Carrick, S., Thomas, S., 2016. The effect of irrigation and urine application on phosphorus losses to subsurface flow from a stony soil. Agric. Ecosyst. Environ. 233, 425-431, https://doi.org/10.1016/j.agee.2016.09.040.

Harvey, A., 2018. Alluvial Fans. Reference Module in Earth Systems and Environmental Sciences, Elsevier, https://doi.org/10.1016/B978-0-12-409548-9.11066-8.

Hedley, C.B., Payton, I.J., Lynn, I.H., Carrick, S.T., Webb, T.H., McNeill, S., 2012. Random sampling of stony and non-stony soils for testing a national soil carbon monitoring system. Soil Res. 50(1), 18-29, https://doi.org/10.1071/SR11171.

Hewitt, A.E., 2010. New Zealand Soil Classification. Landcare Research science series no. 1. 3rd ed. Manaaki Whenua Press, Lincoln, New Zealand.

Hillel, D., 1998. Environmental Soil Physics: Fundamentals, Applications, and Environmental Considerations. Academic Press, Cambridge, MA.

Hooke, R.L., 1967. Processes on arid-region alluvial fans. J. Geol. 75(4), 438-460.

Houlbrooke, D.J., Laurenson, S., 2013. Effect of sheep and cattle treading damage on soil microporosity and soil water holding capacity. Agric. Water Manage. 121, 81-84, https://doi.org/10.1016/j.agwat.2013.01.010.

IUSS Working Group WRB, 2015. World Reference Base for Soil Resources 2014: International Soil Classification System for Naming Soils and Creating Legends for Soil Maps. Update 2015. World soil resources report 106. FAO Rome.

Jones, S., 2004. Tectonic controls on drainage evolution and development of terminal alluvial fans, southern Pyrenees, Spain. Terra Nova 16, https://doi.org/10.1111/j.1365-3121.2004.00539.x.

Keating, B.A., Carberry, P.S., Hammer, G.L., Probert, M.E., Robertson, M.J., Holzworth, D., Huth, N.I., Hargreaves, J.N.G., Meinke, H., Hochman, Z., McLean, G., Verburg, K., Snow, V., Dimes, J.P., Silburn, M., Wang, E., Brown, S., Bristow, K.L., Asseng, S., Chapman, S., McCown, R.L., Freebairn, D.M., Smith, C.J., 2003. An overview of APSIM, a model designed for farming systems simulation. Eur. J. Agron. 18(3), 267-288, https://doi.org/10.1016/S1161-0301(02)00108-9.

Kumar, R., Suresh, N., Sangode, S.J., Kumaravel, V., 2007. Evolution of the Quaternary alluvial fan system in the Himalayan foreland basin: implications for tectonic and climatic decoupling. Quat. Int. 159(1), 6-20, https://doi.org/10.1016/j.quaint.2006.08.010.

Li, H., Li, J., Shen, Y., Zhang, X., Lei, Y., 2018. Web-based irrigation decision support system with limited inputs for farmers. Agri. Water Manage. 210, 279-285, https://doi.org/10.1016/j.agwat.2018.08.025.

Li, X., Chang, S.X., Salifu, K.F., 2013. Soil texture and layering effects on water and salt dynamics in the presence of a water table: a review. Environ. Rev. 22(1), 41-50, https://doi.org/10.1139/er-2013-0035.

Lilburne, L., Webb, T., Ford, R., Bidwell, V.J., 2010. Estimating nitrate-nitrogen leaching rates under rural land uses in Canterbury. Environment Canterbury Report no. R10/127., Environment Canterbury.

Lunt, I.A., Bridge, J.S., 2007. Formation and preservation of open-framework gravel strata in unidirectional flows. Sedimentology 54(1), 71-87, https://doi.org/10.1111/j.1365-3091.2006.00829.x.

Ma, L., Ahuja, L.R., Trout, T.J., Nolan, B.T., Malone, R.W., 2016. Simulating maize yield and biomass with spatial variability of soil field capacity. Agron. J. 108(1), 171-184, https://doi.org/10.2134/agronj2015.0206.

Macara, G.R., 2016. The Climate and Weather of Canterbury. 2nd ed. NIWA.

Manger, G.E., 1963. Porosity and bulk density of sedimentary rocks. U.S. Geological Survey Bulletin 1144-E.

McLeod, M., Aislabie, J., McGill, A., Rhodes, P., Carrick, S., 2014. Leaching of Escherichia coli from stony soils after effluent application. J. Environ. Qual. 43(2), 528-538, https://doi.org/10.2134/jeq2013.06.0256.

McNeill, S.J., Lilburne, L.R., Carrick, S., Webb, T.H., Cuthill, T., 2018. Pedotransfer functions for the soil water characteristics of New Zealand soils using S-map information. Geoderma 326, 96-110, https://doi.org/10.1016/j.geoderma.2018.04.011.

Mesman, N.L., 2014. The effect of increased land use intensification on the physical properties of a silt loam topsoil, Lincoln University, Lincoln, 70 p pp.

Miller, D.E., Gardner, W.H., 1962. Water infiltration into stratified soil. Soil Sci. Soc. Am. J. 26(2), 115-119,

Milne, J., Clayden, B., L., S.P., Wilson, A.D., 1995. Soil Description Handbook. Manaaki Whenua Press, Lincoln, New Zealand.

Nachabe, M.H., 1998. Refining the definition of field capacity in the literature. J. Irr. Drain. Eng. 124(4), 230-232, https://doi.org/10.1061/(asce)0733-9437(1998)124:4(230).

Nichols, G., 2009. Sedimentology and Stratigraphy. 2nd ed. John Wiley & Sons, West Sussex.

Obreza, T., Pitts, D., Parsons, L., Wheaton, T., Morgan, K., 1997. Soil water-holding characteristic affects citrus irrigation scheduling strategy. Proc. Fla. State Hort. Soc. 110, 36-39.

Olmsted, F.H., Davis, G.H., 1961. Geologic Features and Ground-Water Storage Capacity of the Sacramento Valley, California. Geological survey water-supply paper 1497. US Government Printing Office, D.C.

Ottoni, T.B., Ottoni, M.V., de Oliveira, M.B., de Macedo, J.R., Reichardt, K., 2014. Revisiting field capacity (FC): variation of definition of FC and its estimation from pedotransfer functions. Rev. Bras. Ciênc. Solo 38(6), 1750-1764, https://doi.org/10.1590/s0100-06832014000600010.

Parfitt, R., Whitton, J., Theng, B., 2001. Surface reactivity of A horizons towards polar compounds estimated from water adsorption and water content. Aust. J. Soil Res. 39, 1105-1110, https://doi.org/10.1071/SR00059.

Pierce, K.L., Scott, W.E., 1982. Pleistocene episodes of alluvial-gravel deposition, southeastern Idaho. In: B. Bill, B. R. M. (Eds.), Cenozoic Geology of Idaho. Idaho Bureau of Miners and Geology Bulletin 26, pp. 685-702.

Pirastru, M., Niedda, M., 2013. Evaluation of the soil water balance in an alluvial flood plain with a shallow groundwater table. Hydrol. Sci. J. 58(4), 898-911, https://doi.org/10.1080/02626667.2013.783216.

Poesen, J., Lavee, H., 1994. Rock fragments in top soils: significance and processes. Catena 23(1), 1-28, https://doi.org/10.1016/0341-8162(94)90050-7.

Pollaco, A.P., Lilburne, L.R., Webb, T.H., Wheeler, D.M., 2014. Preliminary assessment and review of soil parameters in Overseer® 6.1. Landcare Research Contract Report LC2002. Landcare Research, Lincoln, New Zealand.

Sauer, T.J., Logsdon, S.D., 2002. Hydraulic and physical properties of stony soils in a small watershed. Soil Sci. Soc. Am. J. 66(6), 1947-1956, https://doi.org/10.2136/sssaj2002.1947.

Saunders, W.M.H., 1965. Phosphate retention by New Zealand soils and its relationship to free sesquioxides, organic matter, and other soil properties. N. Z. J. Agric. Res. 8(1), 30-57, https://doi.org/10.1080/00288233.1965.10420021.

Schoeman, J.L., Kruger, M.M., Loock, A.H., 1997. Water-holding capacity of rock fragments in rehabilitated opencast mine soils. S. Afr. J. Plant Soil 14(3), 98-102, https://doi.org/10.1080/02571862.1997.10635089.

Seguel, O., Baginsky, C., Contreras, A., Covarrubias, J.I., Gonzalez, C., Poblete, L., 2013. Physical properties of a fine textured haplocambid after three years of organic matter amendments management. J. Soil Sci. Plant Nutr. 13(3), 690-705, https://doi.org/10.4067/s0718-95162013005000046.

Shinomiya, Y., Takahashi, K., Kobiyama, M., Kubota, J., 2001. Evaluation of the tortuosity parameter for forest soils to predict unsaturated hydraulic conductivity. J. For. Res. 6(3), 221-225.

Soil Survey Staff, 2014. Keys to Soil Taxonomy. 12th ed. U.S.D.A. & N.R.C. Service, Washington, DC.

Sparling, G., Lilburne, L., Vojvodic-Vukovic, M., 2008. Provisional targets for soil quality indicators in New Zealand. Landcare Research Science Series No. 34. Manaaki Whenua Press: Lincoln, New Zealand.

Suresh, N., Bagati, T.N., Kumar, R., Thakur, V.C., 2007. Evolution of Quaternary alluvial fans and terraces in the intramontane Pinjaur Dun, Sub-Himalaya, NW India: interaction between tectonics and climate change. Sedimentology 54(4), 809-833, https://doi.org/10.1111/j.1365-3091.2007.00861.x.

Tokunaga, T.K., Olson, K.R., Wan, J., 2003. Moisture characteristics of Hanford gravels. Vadose Zone J. 2(3), 322-329, https://doi.org/10.2136/vzj2003.0322.

Torri, D., Poesen, J., Monaci, F., Busoni, E., 1994. Rock fragment content and fine soil bulk density. Catena 23(1), 65-71, https://doi.org/10.1016/0341-8162(94)90053-1.

Twarakavi, N.K.C., Sakai, M., Simunek, J., 2009. An objective analysis of the dynamic nature of field capacity. Water Resour. Res. 45, https://doi.org/10.1029/2009wr007944.

UMS, 2009. User Manual: T5/T5x Pressure Transducer Tensiometer. UMS GmbH München.

Veihmeyer, F., Hendrickson, A., 1931. The moisture equivalent as a measure of the field capacity of soils. Soil Sci. 32(3), 181-194.

Ventra, D., Clarke, L.E., 2018. Geology and geomorphology of alluvial and fluvial fans: current progress and research perspectives. Geological Society, London, Special Publications 440(1), 1-21, https://doi.org/10.1144/sp440.16.

Verbist, K., Baetens, J., Cornelis, W.M., Gabriels, D., Torres, C., Soto, G., 2009. Hydraulic conductivity as influenced by stoniness in degraded drylands of Chile. Soil Sci. Soc. Am. J. 73, 471-484, https://doi.org/10.2136/sssaj2008.0066.

Vogeler, I., Carrick, S., Cichota, R., Lilburne, L., 2019. Estimation of soil subsurface hydraulic conductivity based on inverse modelling and soil morphology. J. Hydrol. 574, 373-382, https://doi.org/10.1016/j.jhydrol.2019.04.002.

Webb, T.H., Lilburne, L.R., 2011. Criteria for defining the soil family and soil sibling: The fourth and fifth categories of the New Zealand Soil Classification. Landcare Research Science Series No. 3. Manaaki Whenua Press, Lincoln, New Zealand.

Weissmann, G.S., Hartley, A.J., Scuderi, L.A., Nichols, G.J., Owen, A., Wright, S., Felicia, A.L., Holland, F., Anaya, F.M.L., 2015. Fluvial geomorphic elements in modern sedimentary basins and their potential preservation in the rock record: a review. Geomorphology 250, 187-219, https://doi.org/10.1016/j.geomorph.2015.09.005.

Wheeler, D., Read, C., 2016. Spotlight on OVERSEER: perspectives and approaches to addressing nutrient management challenges using an integrated farm systems model, International Nitrogen Initiative Conference, Melbourne, Australia.

Zhao, P., Shao, M.-a., Melegy, A., 2010. Soil water distribution and movement in layered soils of a dam farmland. Water Resour. Manage. 24, 3871-3883, https://doi.org/10.1007/s11269-010-9638-4.

Zornberg, J., Bouazza, A., McCartney, J., 2010. Geosynthetic capillary barriers: current state of knowledge. Geosynth. Int. 17(5), 273-300, https://doi.org/10.1680/gein.2010.17.5.273.

Chapter 4

The influence of rock fragments on field capacity water content in stony soils from hard sandstone alluvium

The manuscript has been accepted by *Geoderma*:

Robertson B.B., Almond P.C., Carrick S.T., Penny V., Eger A., Chau H.W. and Smith C.M.S., 2021. The influence of rock fragments on field capacity water content in stony soils from hard sandstone alluvium. *Geoderma*. https://doi.org/10.1016/j.geoderma.2020.114912

Abstract

Worldwide, rock fragments (RFs) are generally considered inert with respect to bulk soil hydraulic properties, such that all soil water retention properties predicted by national pedotransfer functions (such as S-map) are based on the volumetric fraction of the fine earth (<2 mm fraction) only. Research findings contradict those assumptions, but studies commonly focus on porous RFs, and rely on repacked cores and lab studies, leaving uncertainty as to how low porosity RFs characteristic of common strongly indurated lithologies affect the soil in the field. We address this question by examining soil water storage in 52 pits excavated into stony soils on the Canterbury Plains, New Zealand, which are formed in sediment derived from a indurated sandstone. The soils at each site were watered to saturation, and then after two days of drainage (a proxy for field capacity), a 30 x 30 cm pit was excavated in 10 cm increments to a depth of 60 cm. From each increment, soil samples were collected and analysed to determine the volumetric size distribution of RFs, the water content of the fine earth and the water content of the RFs themselves. Our results indicated that RFs could influence the fine earth bulk density, porosity, and soil chemistry. RFs could also retain water: 2-20 mm RFs (0.07 $m^3\ m^{-3}$) retained twice as much water as >20 mm RFs (0.03 $m^3\ m^{-3}$). The water retention of the hard sandstone was low compared to other lithologies, but the volumetric abundance of RFs in the stony soils we sampled meant that they accounted for ~10% of the water retained to a depth of 60 cm at field capacity. Our results demonstrate that ~13 mm of water retained by RFs at field capacity is not currently considered in water budgets and nutrient leaching predictions, which may be relevant to best practice land management.

4.2 Introduction

Worldwide, there are concerns about rising nutrient concentrations in surface and groundwater systems. A leading source of leached nutrients is agricultural land, which has expanded in area and is being used more intensively on account of increasing global food demand. To mitigate nutrient

leaching, more effective land management practices and nutrient discharge regulations are necessary, making knowledge of soil water and nutrient retention properties indispensable. To provide the data needed, several countries are developing national datasets of these key soil water properties (Hallett et al., 2017; McNeill et al., 2018), while other organisations are developing datasets at the international and global scale (Baruck et al., 2016; Batjes, 2009; Dai et al., 2019; Shangguan et al., 2014). These datasets commonly rely on pedotransfer functions to estimate properties such as the water content at field capacity (FC). But, the accuracy of any model depends on the representativeness of the data used for model development and validation. Currently, soils containing rock fragments (RFs) are frequently understudied, with most soil information systems and models relying on the assumption that RFs retain no water (Pineda et al., 2018; Román Dobarco et al., 2019). However, international studies have shown that depending on the shape, size, degree of weathering and lithology, RFs are capable of significantly influencing soil hydro-physical properties (Hlavacikova et al., 2015). For instance, Korboulewsky et al. (2020) found that ignoring the water retained in limestone pebbles could equate to a 30% underestimation of soil available water content, while pumice RFs at saturation have been measured with volumetric water content (VWC) of 0.55 (Parajuli et al., 2017). Even RFs with higher densities, such as fine-grained sandstone, can have VWCs between 0.03-0.4 when at saturation depending on RF size and weathering (Parajuli et al., 2017; Schoeman et al., 1997). This could have significant impacts to the management of stony soils (soils with >35% RFs by volume within 45 cm of the soil surface to a depth >100 cm; Webb and Lilburne, 2011), which are being increasingly used for intensive irrigated agriculture (Carrick et al., 2013b). However, the research that has been conducted on stony soil hydraulic properties, especially regarding water retention, utilise repacked soils or lab-based measurements. The few field-based studies in the literature demonstrate that RFs can significantly affect the water retention and drainage properties of stony soils but do not detail how RFs can affect the water-holding properties of the fine earth fraction, or quantify the actual volumetric/gravimetric water content of the RFs themselves at FC (Al-Yahyai et al., 2006; Scheinost et al., 1997). Considering repacked soil is unlikely to represent the pore network and hence the proper hydraulic dynamics of an undisturbed stony soil (da Silva et al., 2016), a potentially significant research gap remains internationally in how RFs influence the water storage of stony soils *in situ*.

Our paper aims to determine the effect of RFs and irrigation on water storage in undisturbed stony soils formed from fine-grained hard sandstone. To do this, 24 stony soil sites across Canterbury, New Zealand, were sampled to cover a range of RF abundance, RF size, soil carbon content and texture, to encompass as much of the variability that occurs in these soils as possible. The purpose is to provide a better understanding of the water retention at FC in stony soils so that this parameter remains meaningful for soil and environmental management in the context of these soils.

4.3 Materials and methods

4.3.1 Site information and fieldwork

Sampling sites were located on the Canterbury Plains, on the South Island of New Zealand (Figure 11). The sampling locations were distributed over two geomorphic surfaces of Pleistocene and Holocene age. Landforms on the Plains are dominated by coalescing Pleistocene glacial outwash fans derived from indurated muddy fine sandstone (greywacke) of the Rakaia terrane sourced from the Southern Alps (Forsyth et al., 2008). The fans are characterised by a relict braided channel pattern except where this is buried by loess or at the fan toes where other depositional environments (floodplain, coastal, swamp) exist. Most of the soils on the Canterbury Plains are shallow stony soils (Carrick et al., 2013a). Significant soil orders (Hewitt, 2010) on the late Pleistocene surfaces include Brown Soils (Dystrudepts and Dystrustepts in Soil Taxonomy), and Recent Soils (Fluvents and Ustepts) on the Holocene age surfaces (Hewitt, 2010; Manaaki Whenua - Landcare Research, 2019).

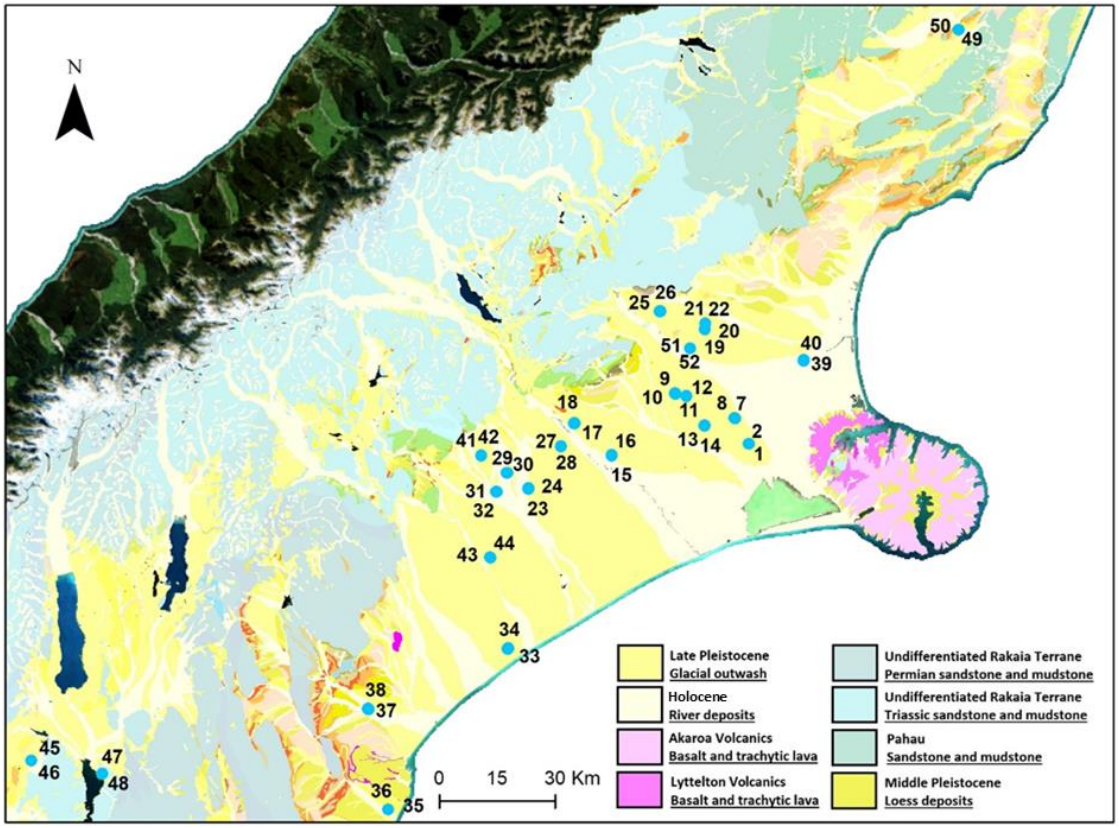

Figure 11 Geology of the Canterbury Plains and the location of pits. Contains data sourced from the LINZ Data Service licensed for reuse under CC BY 4.0.

Fifty-two sampling locations were selected, spanning 24 sites on land under pasture for a minimum of three years and which were predominantly grazed by dairy cattle. At each site, a minimum of two locations were selected for pit sampling, with one site under a sprinkler irrigator for a minimum of 2 years, and the other in the same paddock but in soil that had never been irrigated (e.g. in the corner of the paddock outside the arc of a centre pivot irrigator). The time-consuming nature of the

sampling and the sample size made it necessary for fieldwork to be extended over the Austral winter to early spring months of 2017 and 2018 (May to September). Sampling occurred during this period because rainfall is greater, with low evapotranspiration, resulting in consistently high antecedent soil moisture which ensures there are no 'dry spots' or hydrophobicity in the soil. The season in which sampling occurred was included in the regression analysis to account for any temporal influences (refer to Section 4.3.3). For each sampling location, the soil was first wet-up through ponded infiltration. Infiltration was conducted by first clearing the sampling location of above-ground vegetation. Using a 50 cm diameter infiltration ring, two-litre volumes of water (equivalent to 1 cm application depth) were applied consecutively until infiltration times became constant (after ~100 mm of water). For soils sampled in spring, the potentially greater evapotranspiration may see greater drying of the soil matrix, with a risk of not being fully rewetted if the water is applied by ponded water alone. To minimise this risk, an irrigation system was used to add a further circa 110 mm of water to ensure saturation was achieved. The irrigation system covered an area of 60 x 50 cm, greater than the area to be sampled to ensure no boundary effect. The system comprised six lines of Aqua-TraXX 1.14 L h^{-1} drip tape, spaced at 10 cm intervals and emitters every 10 cm. Water was gravity supplied from a tank using a garden water timer to apply irrigation for 15 min every hour at a rate of 9 mm hr^{-1} over 12 hours. Following the wetting of soil profiles (whether by ponded water alone or by ponded and irrigated water), the soil was then covered to prevent evapotranspiration losses or additional rainfall input for 48 hours as a proxy for FC. We chose a time-based criterion for FC on the strength of Twarakavi et al.'s (2009) work, which showed a time basis to be more robust than matric potential based approximations of FC, and a duration of two days because of the rapid drainage of coarse stony soils (Carrick et al., 2017; Graham et al., 2018).

After the 48 hour drainage period, the soil was excavated in 10 cm increments to a depth of 60 cm, within a 30 x 30 cm metal frame centred at the middle of the wetted area of the infiltration ring (Figure 12). At each increment, the matric potential was measured by inserting a UMS T5 pressure transducer tensiometer horizontally into the pit wall, with readings taken with an Infield 7C handheld read-out device (UMS, 2009).

The volume of the individual increments and the pit as a whole were estimated by the pit and bead method (Figure 12), which is the standard method for measuring volume in stony soils in New Zealand (Hedley et al., 2012). This method can accommodate inconsistencies in pit dimensions caused by the roughness RFs create in the pit walls, either by protruding into the pit or leaving holes in the side of the pit when removed. Before any excavation had occurred, a plastic bag was placed inside the frame and filled with plastic beads, which were levelled off flush with the lip of the frame. Beads were then weighed and recorded as the 'dead weight', which represented the volume between the soil surface and the top of the frame. After each increment was excavated, the pit was

lined with a plastic bag, backfilled with plastic beads and made flush with the lip of the metal frame, making sure to fill in cavities between protruding RFs and the edges of the pit. The beads (0.6 cm diameter; 0.3 cm height) were then weighed and converted to a volume using the bulk density of the beads (0.562 g cm^{-3}). As this method calculates the volume of the whole pit, the volume of any one depth increment (V_T) required the volume of the previously dug, shallower increments to be subtracted. For instance, the volume of the 40-50 cm increment would equal the pit volume to 50 cm minus the pit volume to 40 cm, while the 0-10 cm increment volume would equal the pit volume to 10 cm minus the dead volume.

Figure 12 Pit and bead method (from left to right). The metal frame fitted flush to the soil surface, soil material is excavated in depth increments, and volume of the excavated hole is estimated with plastic beads.

Excavated material for each depth increment was passed through a 20 mm sieve in the field. All the largest (>20 mm) RFs were collected and weighed (M_{RF}) to avoid any biases introduced by sub-sampling. The <20 mm fraction, called the coarse fines, was weighed (M_{CF}) before being thoroughly mixed, spread out in a large sampling tray and quartered. One quarter was collected and weighed (M_b) to estimate the whole soil bulk density, the fine earth bulk density and the 2 – 20 mm RF size distribution and the water content (WC) of the 2-20 mm RF fraction. One scoopful (with a trowel) was collected and weighed (M_θ) for estimating the WC of the fine earth, as well as the specific surface area (SSA) of the fine earth (for methods see below). A second quarter of the coarse fines was sieved at 10 mm; the <10 mm material was used for soil carbon, particle size analysis and WC of the fine earth at -1500 kPa. Soils were then described according to the terminology of Milne et al. (1995) and classified to the subgroup level of the New Zealand Soil Classification, according to Hewitt (2010).

4.3.2 Laboratory analysis

The progression of measurements throughout field and lab work is shown in Figure 13. The <20 mm bulk density subsample and the >20 mm sample were weighed at field moisture (M_b and M_{RF}

respectively) and after being oven dried at 105°C ($M_{b,od}$ and $M_{RF,od}$, respectively). The samples were then wet sieved into rock size classes defined by Milne et al. (1995) (2-6 mm, 6-20 mm, 20-60 mm and >60 mm). RFs were then thoroughly cleaned by hand or by agitating them with a gold panning-like action. Clean RFs were oven-dried at 105°C and weighed according to their size classes ($M_{b,[2.6],\mathrm{cod}}$, $M_{b,[6.20],\mathrm{cod}}$, $M_{RF,[20.60],\mathrm{cod}}$ and $M_{RF,[>60],\mathrm{cod}}$). The volumes of the RFs were then estimated by assuming a rock density of 2.65 g cm^{-3}, which is a density for this rock type that is commonly used in studies (Lee, 2019).To determine the accuracy of this rock density value, RF volume estimations were compared to results measured using the volume displacement method. Trial measurements had a variation of <2% between estimated and measured RF volumes, which was deemed negligible.

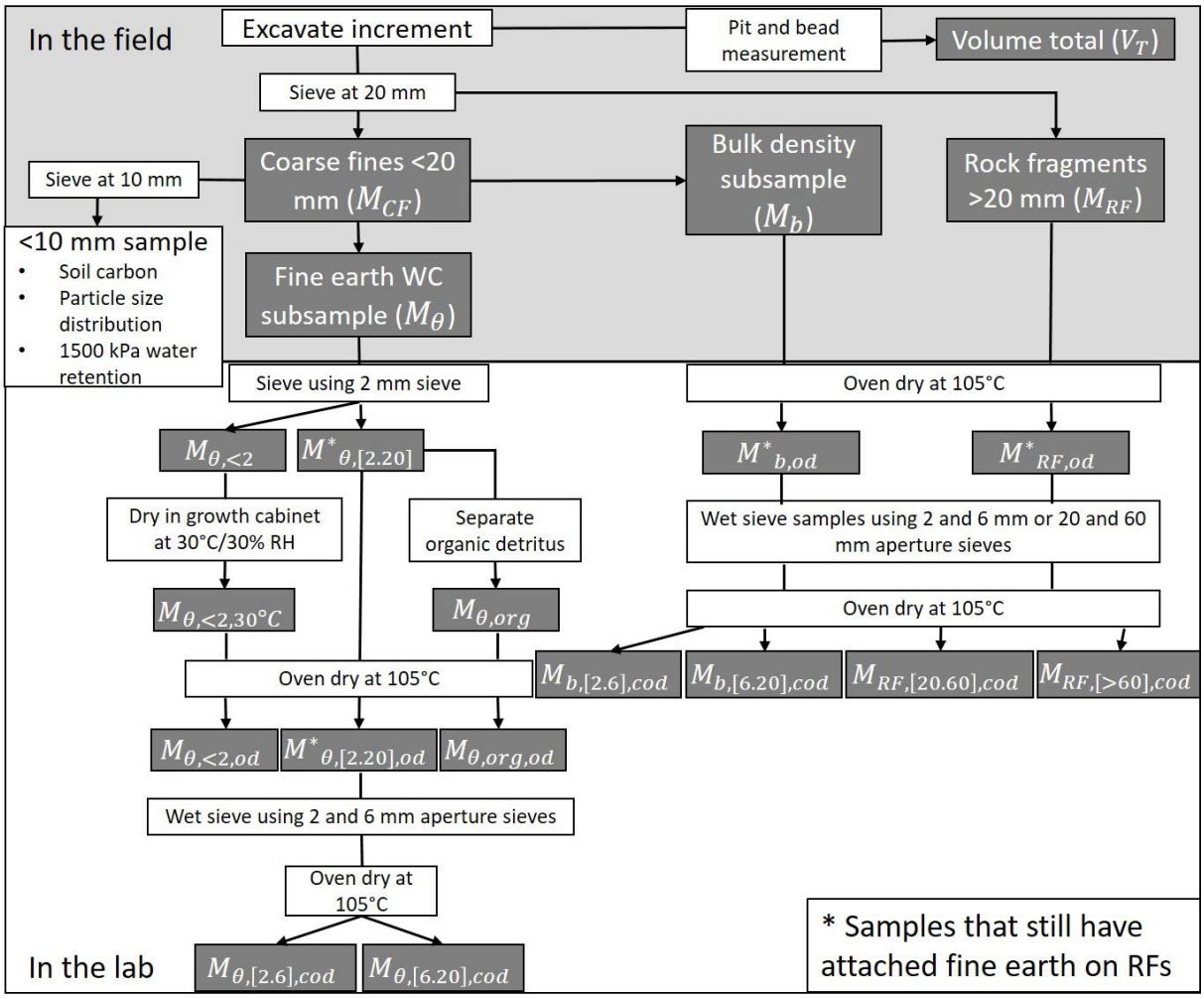

Figure 13 Flow chart of measurements taken throughout the field- and labwork.

The volumes of two size fractions of RFs were calculated:

$$V_{T[>20]} = \frac{M_{RF,[20.60],cod} + M_{RF,[>60],cod}}{2.65} \quad (10)$$

$$V_{T[2.20]} = \frac{R\left(M_{b,[2.6],cod} + M_{b,[6.20],cod}\right)}{2.65} \quad (11)$$

A scaling ratio (R) was also calculated as a means of extrapolating measures from the bulk density subsample (such as $M_{b[2-6]}$ or M_{b-d}) to the whole depth increment.

$$R = \frac{M_{CF}}{M_b} \quad (12)$$

The volume of the fine earth ($V_{T<2}$) was back-calculated using the volume of the RFs and the total volume of the increment (V_T) measured using the pit and bead method.

$$V_{T<2} = V_T - V_{T[>20]} - V_{T[2.20]} \quad (13)$$

The whole soil bulk density (ρ_b) was estimated by,

$$\rho_b = \frac{M_{b,od}.R+M_{RF,od}}{V_T} \quad (14)$$

while the fine bulk density ($\rho_{<2}$) was estimated by

$$\rho_{<2} = \frac{R\left(M_{b,od}-M_{b,[2.6],cod}-M_{b,[6.20],cod}\right)+\left(M_{RF,od}-M_{RF,[20.60],cod}-M_{RF,[>60],cod}\right)}{V_{T<2}} \quad (15)$$

The second term in the numerator of Equation 15 ensures any fine earth attached to coarse RFs is included. The fine earth WC subsample was sieved at field moisture through a 2 mm sieve, separating the sample into the <2 mm fine earth and the >2 mm material, which included the >2 mm RFs, attached fine earth (the fine earth adhered to RFs) and organic detritus (roots and other plant material). The <2 mm fine earth was weighed at field moisture ($M_{\theta,<2}$), again after being dried in a Weiss Gallenkamp fitotron (hgc 1514) set at 30°C and 30% relative humidity ($M_{\theta,<2,30°C}$), and finally, after being dried at 105°C in an oven ($M_{\theta,<2,od}$). The differences in mass were used to estimate SSA, see Equation 28 below. The >2 mm material had the organic detritus separated by hand. The organic detritus and remaining >2 mm material were then weighed at field moisture ($M_{\theta,org}$ and $M_{\theta,[2.20]}$ respectively) and after being dried at 105°C in an oven ($M_{\theta,org,od}$ and $M_{\theta,[2.20],od}$ respectively). The oven-dried >2 mm material was then wet sieved as for the bulk density and >20 mm samples, with clean RFs oven-dried and weighed according to their size classes ($M_{\theta,[2.6],cod}$ and $M_{\theta,[6.20],cod}$).

The gravimetric WC (w) of the fine earth ($w_{<2}$) and the fine earth with organic detritus ($w_{<2+org}$) were estimated by,

$$w_{<2} = \frac{M_{\theta,<2}-M_{\theta,<2,od}}{M_{\theta,<2,od}} \quad (16)$$

$$w_{<2+org} = \frac{M_{\theta,<2}+M_{\theta,org}-M_{\theta,<2,od}-M_{\theta,org,od}}{M_{\theta,<2,od}+M_{\theta,org,od}} \quad (17)$$

By assuming these WCs are equal to the WC of the attached fine earth, the WC of the RFs could be back-calculated by accounting for the water derived from the attached fine earth, whether it be mineral or mineral plus organics, in a sample. The gravimetric WC of the 2-20 mm RFs was estimated by,

$$w_{2.20} = \frac{M_b - M_{b,od} - w_{<2+org}(M_{b,od} - M_{b,[2.6],cod} - M_{b,[6.20],cod})}{M_{b,[2.6],cod} + M_{b,[6.20],cod}} \quad (18)$$

Because the bulk sample contained fine earth mixed with organic detritus (such as fine roots), $w_{<2+Org}$ was used for calculating $w_{2.20}$. Finally, the w of the >20 mm RFs could be derived as,

$$w_{RF,[>20]} = \frac{M_{RF} - M_{RF,od} - w_{<2}(M_{RF,od} - M_{RF,[20.60],cod} - M_{RF,[>60],cod})}{M_{RF,[20.60],cod} + M_{RF,[>60],cod}} \quad (19)$$

As the fine earth attached to the >20 mm RFs did not contain organic detritus, $w_{<2}$ was the appropriate WC to use.

The depth of water (h, mm) derived from each soil constituent was estimated by,

$$h_{<2} = \frac{R.M_{b,<2,od}.w_{\theta<2+org} + w_{\theta<2}(M_{RF,od} - M_{RF,[20.60],cod} - M_{RF,[>60],cod})}{\rho_w A} \quad (20)$$

where $M_{b,<2,od}$ is equal to $M_{b,od}$-($M_{b,[2.6],cod} + M_{b,[6.20],cod}$),

$$h_{[2.20]} = \frac{R(M_{b,[2.6],cod} + M_{b,[6.20],cod}).w_{2.20}}{\rho_w A} \quad (21)$$

$$h_{[>20]} = \frac{w_{RF[>20]}(M_{RF,[20.60],cod} + M_{RF,[>60],cod})}{\rho_w A} \quad (22)$$

where ρ_w is the density of water, which was assumed to be 1 g cm^{-3} and A is the area of the pit (30x 30 cm = 900 cm^2). By dividing the volume of water by the volume of the soil constituent, VWC, θ, could be estimated,

$$\theta_{<2} = \frac{A.h_{<2}}{V_{T<2}} \quad (23)$$

$$\theta_{[2.20]} = \frac{A.h_{[2.20]}}{V_{T[2.20]}} \quad (24)$$

$$\theta_{[>20]} = \frac{A.h_{[>20]}}{V_{T[>20]}} \quad (25)$$

$$\theta_T = \frac{A(h_{<2} + h_{[2.20]} + h_{[>20]})}{V_T} \quad (26)$$

The total porosity (ε) could also be estimated by using the fine earth bulk density and the particle density (ρ_p),

$$\varepsilon = 1 - \frac{\rho_{<2}}{\rho_p}, \quad (27)$$

where the particle density measurement method is described below.

Using the different dry weights of the fine earth, the apparent SSA was then estimated following the equation of Parfitt et al. (2001),

$$SSA = \frac{2000(M_{\theta,<2,30℃} - M_{\theta,<2,od})}{M_{\theta,<2,od}} \quad (28)$$

Finally, the <10 mm sample was sieved to remove the 2-10 mm RFs, then analysed for soil carbon, total nitrogen, particle size distribution, permanent wilting point and phosphate retention (P-retention). Soil carbon and total nitrogen were analysed using the Dumas dry combustion principle according to the methods described by Leco (2003). Particle size distribution was derived from the pipette method following Claydon (1989). The proportions of sand (p_{sand}), silt (p_{silt}), and clay (p_{clay}) in the range 0–1, were used to classify the texture of the fine earth (Milne et al., 1995). As these fractions are part of a ternary simplex, a structural correlation exists (McNeill et al., 2018). For computational convenience, texture proportions were transformed to a Cartesian system as this generally reduces the apparent correlation between texture fractions by removing the structural correlation component. As per the method used by McNeill et al. (2018) and Cornell (1981), the texture proportions were transformed to a Cartesian system by generating two auxiliary variables as follows,

$$\omega_1 = 2p_{sand} - p_{silt} - p_{clay} \quad (29)$$

$$\omega_2 = p_{silt} - p_{clay} \quad (30)$$

The water retention of the fine earth at permanent wilting point (15 bar) was measured using small repacked cores within a pressure chamber (Gradwell and Birrell, 1972). Particle density was measured following the method of Gradwell and Birrell (1972). Ground soil was placed in a bottle, covered with water and then placed in a vacuum desiccator. The bottle was brought to a constant temperature before the water level was then raised to a standard mark in the bottle. The weight of the bottle + soil + water and the oven-dried soil was measured before calculating the ratio of the weight of soil to the weight of water displaced by the soil. Phosphate retention was evaluated by centrifuging a soil sample with a 32 mol m^{-3} P solution before measuring the remaining P in solution (Saunders, 1965). The concentration of P left in solution gives a high degree of differentiation

between soils of high and low anion retention and was measured using a QuickChem 87500 flow injection analyser (Lachat Instruments, 1998g).

4.3.3 Statistical analysis

Before any statistical analyses were performed, the data set was censored according to relative errors in data values. Many of the variables used in the analyses are derived from calculations on primary variables, with inherent uncertainty. Those uncertainties compound and grow in relative magnitude, especially where subtractions and divisions are involved. We quantified the magnitude of errors, both absolute and relative, by applying Gaussian error propagation (refer to Appendix F). Increments were removed if the relative error for an increment's fine earth VWC, fine earth bulk density or total porosity was >25%. When RF VWC was the response variable, an additional filter was used, which removed increments in which the relative error for 2-20 mm and >20 mm RF VWC was >25%. As the NZSC Order was used as an explanatory variable, increments from soils belonging to rare soil orders (Pallic (2 pits) and Gley (2 pits)) were also excluded.

To determine if a significant difference in WC exists between the 2-20 mm and >20 mm RF fractions, a rank based fixed effect regression was used. The effect of RFs and irrigation treatment on soil properties were analysed using multiple linear regression. To determine effects, regression models were generated that included all possible explanatory variables (Table 4) with treatment or RF volume at the end, so that the effect of these variables could be determined after taking account of all other explanatory variables. If explanatory variables were derived from the response variable then they were not included, for instance, the fine earth bulk density would not be included as an explanatory variable if the whole soil bulk density was the response variable. When all increments were used in the analysis, depth was included as an explanatory variable; however, depth specific relationships were also determined by using data from particular depth increments only. To ensure sampling over two different seasons did not introduce any error in results, 'season' was included as an explanatory variable in the analysis (Table 4) but was found to have no significant effect on the total VWC.

Table 4 List of explanatory variables used in multiple linear regression analysis.

Surface age	C:N
NZSC Order	Fine earth bulk density
Season	15 bar WC
FC matric potential	Texture
Particle density	SSA
Organic carbon	ω_1
Total porosity	ω_2
Whole soil bulk density	Treatment
Nitrogen	Volumetric proportion RFs
Phosphate retention	

4.4 Results

4.4.1 Variation in soil attributes

Brown soils were the dominant soil order encountered (61%) followed by Recent soils (39%). Soil pits were distributed over two geomorphic surfaces: 80% were on Late Pleistocene glacial outwash, 16% were on Holocene alluvial deposits and 4% were on Late Pleistocene to Holocene alluvial deposits. The soil attributes averaged across the measured pits tended to change with depth (Table 5). The fine earth VWC decreased from 40% in the 0-10 cm increment to 16% by the 50-60 cm increment. This decrease in WC with depth was characterised by notable reductions every 20 cm, which may be consistent with major horizon boundaries (e.g. A horizon: 0-20 cm, B horizon: 20-40 cm and C horizon: 40-60 cm). Both carbon and nitrogen decreased considerably with depth in the top three increments (~1% and ~0.1% per 10 cm, respectively), followed by relatively small decreases with depth in the bottom three increments (~0.2% and ~0.02% per 10 cm, respectively). In contrast, P-retention was lowest in the 0-10 cm increment (22%) and increased with depth until it stabilised at ~36% in the bottom three increments (30-60 cm depths). Particle density increased from 2.58 g cm^{-3} in the 0-10 cm increment to a constant density of 2.68 g cm^{-3} in the 40-50 cm and 50-60 cm increments. Average fine earth bulk density was lowest in the 0-10 cm and 50-60 cm increments and relatively constant through the 10-50 cm depths. Whole soil bulk density had the lowest average value in the 0-10 cm increment (1.34 g cm^{-3}) below which it increased to a relatively constant density of ~2.05 g cm^{-3} in the 30-60 cm depths.

Table 5 Changes in average soil attributes of measured pits with depth. P is the P-retention, values in parentheses are standard error to one significant figure.

Depth	Fine earth VWC	Carbon	P	Nitrogen	Particle density	Fine earth bulk density	Whole soil bulk density
cm	%	%	%	%	g cm^{-3}	g cm^{-3}	g cm^{-3}
0-10	40 (0.9)	3.7 (0.2)	22 (1)	0.34 (0.01)	2.58 (0.01)	1.16 (0.02)	1.34 (0.03)
10-20	38 (0.8)	2.7 (0.1)	25 (1)	0.25 (0.01)	2.62 (0.01)	1.35 (0.02)	1.56 (0.03)
20-30	33 (1)	1.8 (0.1)	30 (2)	0.16 (0.01)	2.65 (0.01)	1.31 (0.02)	1.77 (0.05)
30-40	31 (1)	1.4 (0.1)	35 (3)	0.13 (0.01)	2.67 (0.005)	1.36 (0.04)	1.98 (0.05)
40-50	23 (1)	1.2 (0.1)	37 (3)	0.11 (0.01)	2.68 (0.004)	1.29 (0.04)	2.11 (0.04)
50-60	16 (2)	1.1 (0.1)	35 (3)	0.09 (0.01)	2.68 (0.004)	1.12 (0.06)	2.05 (0.05)

4.4.2 Particle size and RF distribution

Within and across the sites there was a good representation of different particle sizes, ranging from 5 to 96% sand, 0 to 67% silt, and 1 to 45% clay (Figure 14). The proportion of RFs to an increment's volume varied from 0% to 83%. In general, the texture of the fine earth became coarser with depth; the fine earth typically exceeded 50% silt in the 0-10 cm increment compared to >70% sand in the 50-60 cm increment. The volume of RFs also increased with depth: RFs typically made up <13% of the total soil volume in the 0-10 cm increment, but >55% for 40-50 cm and 50-60 cm increments (Figure 4). The volumetric proportions of 2-6 mm and >60 mm RFs were similar in individual increments, respectively increasing from 1 and 2% in the 0-10 cm increment to 8 and 6% in the 50-60 cm increment. The volumetric proportions of 6-20 mm and 20-60 mm RFs were also similar in any one increment, but increased with depth from 3 and 6%, respectively, in the 0-10 cm increment, to 25 and 21%, in the 50-60 cm increment.

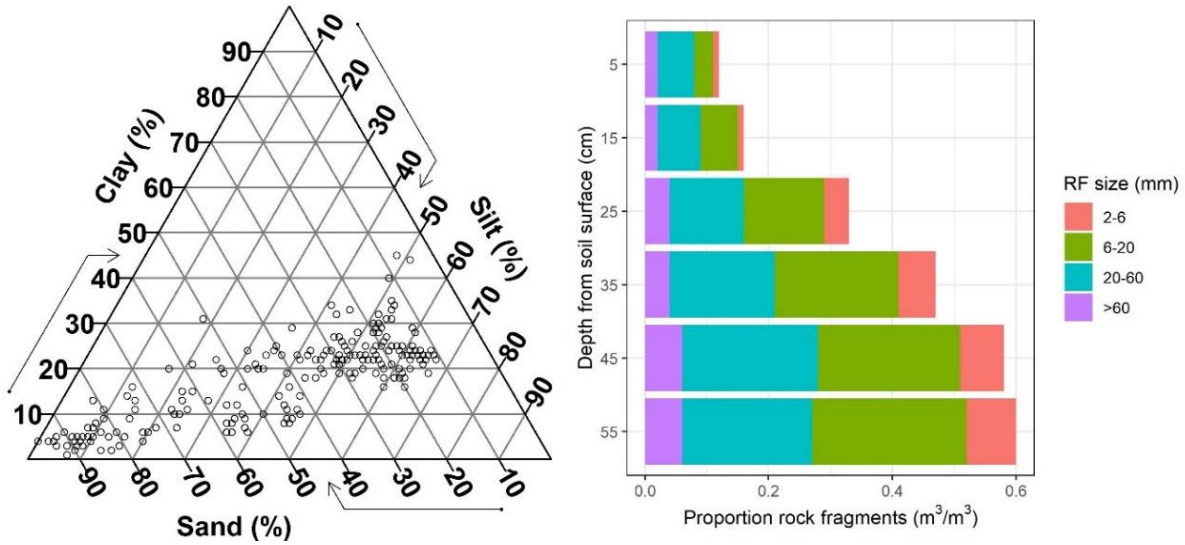

Figure 14 Left: Soil texture diagram displaying textures for each increment. Right: The proportion of an increment's volume made up of RFs.

4.4.3 Water content in rock fragments

The average whole-soil volume of water at FC to 60 cm depth was 142 mm. Averaged across all pits classified as stony soils (soils with >35% RFs by volume within 45 cm of the soil surface), RFs in the 0-60 cm increments accounted for ~10% of the retained water, which was equivalent to ~13 mm. The proportion of soil-water retained in RFs increased with depth, exceeding 35% on average in the 50-60 cm increment (Figure 15). The total WC of an increment decreased with depth from an average of 36 mm in the 0-10 cm increment to 10 mm in the 50-60 cm increment. RFs accounted for <1% of the water in pits with few to no RFs, to >20% in pits where RFs account for >55% of the volume (Appendix G). For every pit and every depth increment, the 2-20 mm RFs retained at least twice as much water as the >20 mm RFs. The mean VWC for the two size fractions in the 0-60 cm increments were 0.07 and 0.03 for the 2-20 mm and >20 mm RFs, respectively. The VWC for the 2-20 mm RFs and the >20 mm RFs were significantly (P<0.0001) different at all depths below 30 cm (Figure 16). As a result of few degrees of freedom and a non-normal distribution, the difference in VWC of RFs of different size could not be determined for the 0-10 cm and 10-20 cm increments.

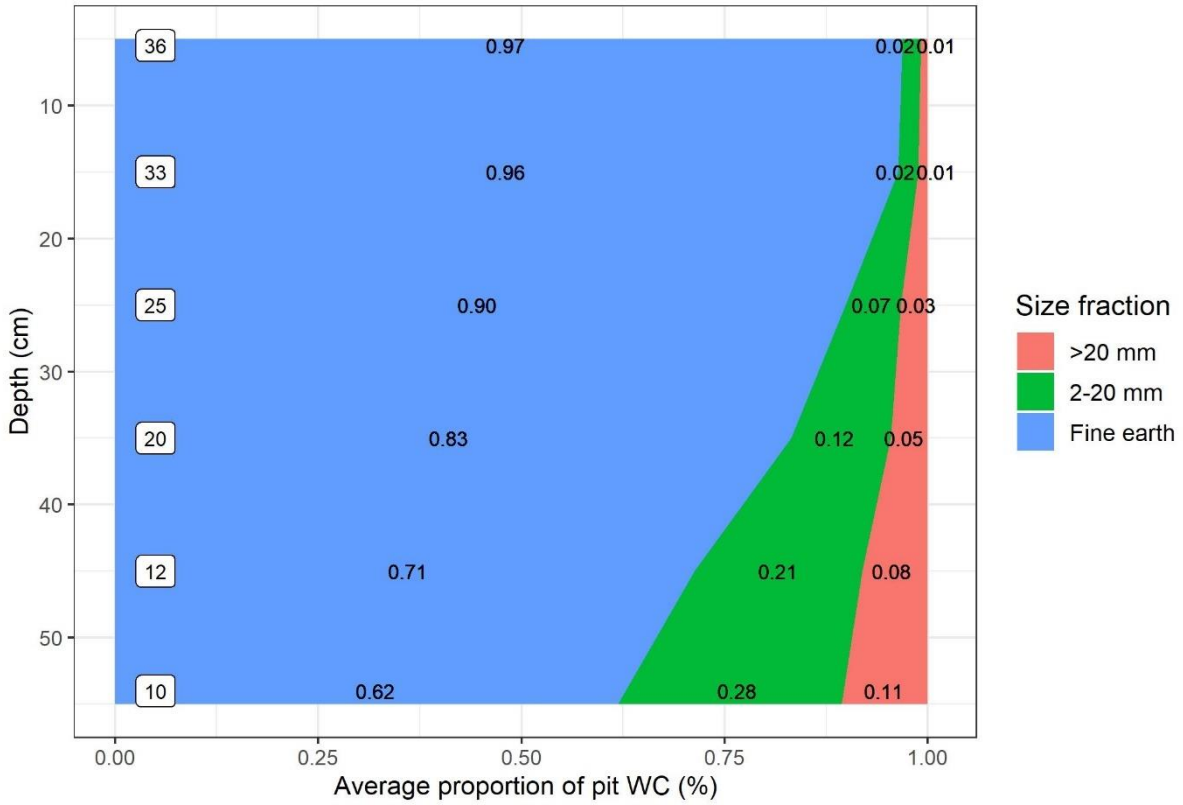

Figure 15 The average contribution of different size fractions to the total volume of water at different depth increments averaged across all pits. Values in boxes depict the average whole-soil WC in mm for each increment.

Multiple linear regression analysis was used to determine the effects of other variables on the RF VWC (output data can be found in Appendix H). When whole soil profiles were analysed, as the total volume of RFs increased, their VWC decreased. Furthermore, the WC of the 2-20 mm fraction

decreased as the coarser part of the fraction (6-20 mm) increased in abundance. Similarly, for the >20 mm fraction, the VWC decreased as the proportion of the >60 mm RFs increased. We also found that the VWC of particular size fractions were affected by RFs outside that size fraction: 1) in the 40-50 cm increment, the VWC of the 2-20 mm fraction increased with the proportion of 20-60 mm RFs; 2) the VWC of the >20 mm fraction increased as the proportion of 2-20 mm RFs increased (on a whole soil profile basis). Due to few degrees of freedom and the large number of explanatory variables used in the regression analysis, statistical tests could not be refined to individual depth increments for the 0-30 cm depths.

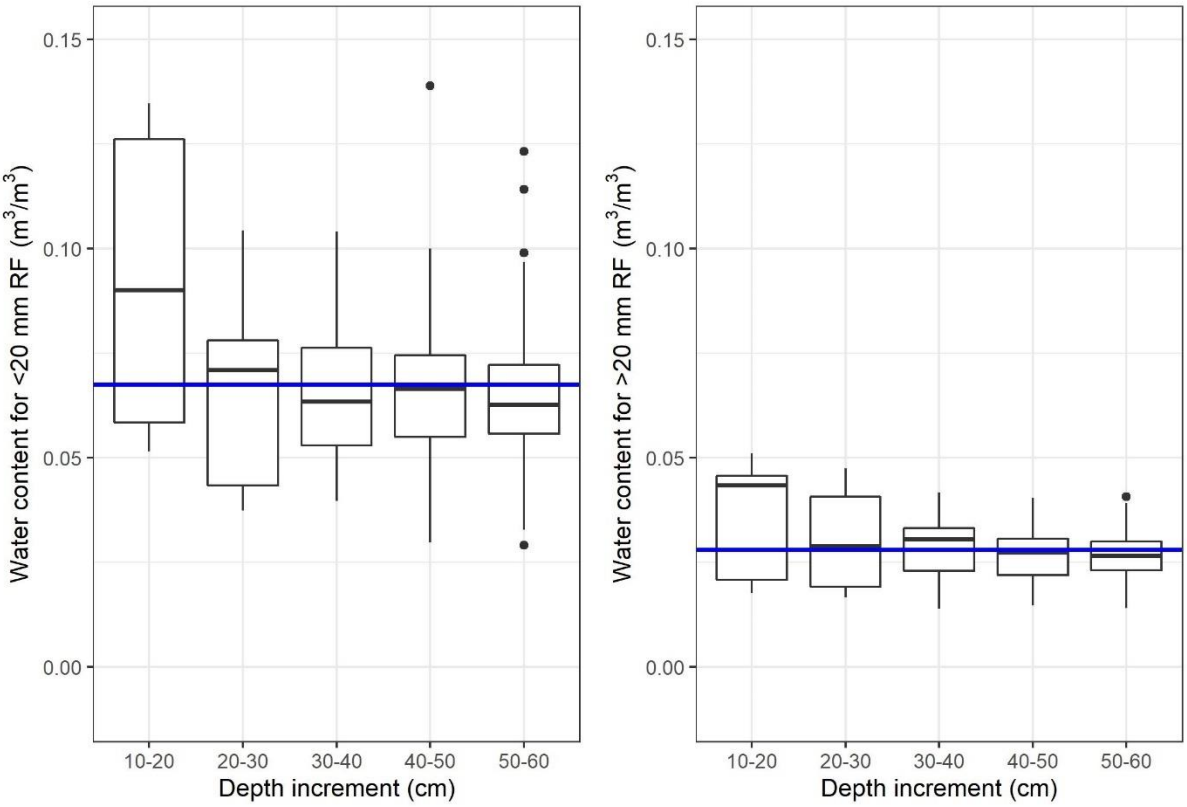

Figure 16 Comparing the VWC of <20 mm RFs to >20 mm RFs for the 10-60 cm increments. Blue line: Average VWC for the 10-60 cm depths.

4.4.4 RF effect on fine earth

Using multiple linear regression, we found several interactions between RFs and fine earth properties (output data found in Appendix I). For instance, the whole soil VWC decreased with increasing RF volume, which is consistent with RFs holding less water than fine earth. Total porosity was positively affected by the volume proportion of 2-20 mm RFs when the whole profile was analysed and at the 20-30 cm and 30-40 cm depths. Total porosity was also positively affected by the 20-60 mm RFs in the 20-30 cm increment. Correspondingly, fine earth bulk density was negatively affected by the volume proportion of 2-20 mm RFs when the whole soil profile was considered, while both the 2-20 mm and 20-60 mm RFs had negative effects to fine earth bulk density in the 20-30 cm increment. The

fine earth VWC decreased with increasing RF volume at each depth increment and when whole soil profiles were considered. However, the relationship is not consistently detected when the analysis is refined to individual depth increments and RF size fractions. This is illustrated by the 2-20 mm RFs having a negative effect on fine earth WC when the whole soil profile is considered and at the 30-40 cm depth, whereas the 20-60 mm RFs had a significant negative effect but only when whole soil profiles were considered in the analysis. The >60 mm RFs also had a significant negative effect on fine earth WC, but only in the 0-20 cm increments.

There were also multiple correlations between the volume of RFs and the properties of the fine earth fraction outlined in Table 5 (output data found in Appendix J). Carbon was positively affected by the volume of the 2-20 mm RFs in the 0-10 cm increment but negatively affected by the volume of 6-20 mm RFs in the 40-60 cm increments. P-retention had a positive relationship with the total volume of RFs when whole soil profiles were considered in the analysis. Nitrogen was negatively affected by the volume of 2-6 mm RFs when whole soil profiles were considered and in the 0-10 cm and 20-30 cm increments.

4.4.5 Treatment effect on fine earth

A history of irrigation had an overall positive effect on the WC of the fine earth when the whole profile was analysed, and when refined to the 10-20 cm increment (regression output data found in Appendix K). No significant relationship was identified between irrigation treatment and total porosity, indicating the effect may be related to the pore size distribution rather than pore concentration. Irrigation treatment had a positive effect on the P-retention in the 10-20 cm increment and a negative effect on soil carbon when the whole profile was analysed.

4.5 Discussion

4.5.1 Hard sandstone RFs hold water but not much compared to other lithologies

Our results demonstrate that RFs retain appreciable quantities of water within 60 cm of the soil surface (~13 mm). However, we show that the dominant lithology of RFs on the Canterbury Plains, greywacke – a hard, muddy fine sandstone, holds relatively little water and that the significant contribution they make to water retention arises from their volumetric abundance. Tetegan et al. (2011) found the gravimetric WC of 20-50 mm RFs at FC varied from 0.31 in gaize, 0.21 in chert, and 0.09 in flint, all exceeding the 0.01 (0.03 m^3 m^{-3}) value measured in the >20 mm greywacke sandstone RFs in this study. The generally high bulk density and low porosity for greywacke sandstone (2.51-2.71 g cm^{-3} and 2-4%, respectively), is likely to be responsible (Jones, 2016; McNamara et al., 2014). Other studies of fine sandstone material report average bulk densities of 2.4 g cm^{-3} (Schoeman et al., 1997) and 2.35 g cm^{-3} (Hanson and Blevins, 1979), associated with VWC at FC

of >0.07 and >0.14 respectively, both of which are still greater than the 2-20 mm VWC of 0.07 measured in this study. Thus, even amongst fine sandstones, the greywacke sandstone of our study has a higher bulk density and thus lower porosity and water retention.

4.5.2 Size and weathering matter

Our results also show that RF size can affect RF VWC. The significantly higher VWC in the 2-20 mm RF fraction compared to the >20 mm RF fraction we observed is consistent with several studies (Poesen and Lavee, 1994; Schoeman et al., 1997), which commonly relate the difference to greater weathering and hence porosity in smaller RFs. Although the thickness of the weathering rind between RF sizes may not vary (as they are exposed to the same weathering conditions), the greater SSA of smaller RFs results in a greater proportion of the clast's volume having undergone weathering, resulting in greater water retention. The same finding was also evident within the VWC of the 2-20 mm and >20 mm RFs: the 2-20 mm VWC decreased with an increasing proportion of 6-20 mm RFs; whereas the >20 mm RF VWC was negatively affected by the proportion of >60 mm RFs. The negative effect of the total volume of RFs on the VWC of both the 2-20 mm and >20 mm RFs may also be an expression of how soil age affects the water retention of the RFs. On the Canterbury Plains, older soils have a larger contribution of loess (Ives, 1973), which dilutes the coarse fraction (RFs). Older soils are more likely also to have more weathered RFs, which have higher porosity and store more water (Cuniglio et al., 2009; Tetegan et al., 2011).

Unexpectedly, the 2-20 mm RF VWC was positively affected by the 20-60 mm RFs, whilst the >20 mm RF VWC was positively affected by the 2-20 mm RFs. This may reflect an increase in RF contact points, as some studies have found RFs may store significant quantities of water at contact points between neighbouring RFs or as puddles on the rock surface for larger RFs (Poesen and Lavee, 1994; Schoeman et al., 1997).

4.5.3 RF-fine earth interactions

Fines VWC

Besides their ability to retain water, RFs appear to indirectly affect the chemistry, structure and water retention properties of the fine earth. We speculate that the influences of RF abundance on the fine earth VWC are indirect and that the direct causes are changes in matrix grain size that are correlated to RF abundance. For instance, the negative relationship between the total volume of RFs and the fine earth WC is likely due to the strong correlation between RF volume and coarse sand (2-0.6 mm), as coarse sand has low water retention and would negatively affect fine earth WC. The 20-60 mm and >60 mm RFs did not have strong correlations with coarse sand. We expect that these larger RFs may allow water to run freely on the surface of the RFs with little interaction with the

adjacent fine earth (Pollacco, 2017; Zhou et al., 2011). We observed this phenomenon where percolating water was diverted around large RFs (>150 mm in diameter) leaving the underlying soil noticeably drier than the surrounding soil. The >20 mm RFs could have a similar effect (albeit not as visible) causing a negative relationship with fine earth WC.

Porosity and fine earth bulk density

The decrease in fine earth bulk density and increase in the total porosity with RF volume is consistent with international literature (Baetens et al., 2009; Shi et al., 2012). Poesen and Lavee (1994) attribute RF-induced porosity changes (or changes in fine earth bulk density) to the following:

a) Sedimentary processes can deposit RFs without sufficient fine earth to fill inter RF voids (Lunt and Bridge, 2007), resulting in lower bulk density in the fine earth. Under specific flow regimes, this can ultimately culminate in open framework gravels, a clast-supported coarse layer where little to no fine earth is present (Dann et al., 2009).

b) In a mixture of two particle size grades, the presence of even small numbers of large particles has a negative effect on the bulk density of the smaller particles because the smaller particles cannot pack as closely to the larger particles as they can with each other. Also, fine earth and RFs react differently when expanding and contracting (e.g. during the process of wetting and drying or freezing and thawing), which causes an increase in porosity for the size range larger than 250 µm (Gargiulo et al., 2016).

c) The presence of RFs in the soil changes the nature of the fine earth fraction. With increasing RF content, decaying organic matter, fertiliser inputs, rainwater etc. are concentrated in a decreasing mass of fine earth, which facilitates the formation of pores and the reduction of fine earth bulk density.

Though the reduction in fine earth bulk density (or increase in total porosity) with increasing RFs is not an uncommon finding, very little of the current literature represents field conditions, with the majority of the research sourced from repacked soil experiments that may be prone to artefacts (da Silva et al., 2016; Gargiulo et al., 2016). Even the studies that measure undisturbed field soils are open to criticism, as they commonly utilise small sample volumes or only sample to a limited depth (Du et al., 2017). Our results not only demonstrate that the RF-fine earth bulk density and RF-total porosity trends occur in the field over a whole region, but that these trends are mostly linked to the 2-20 mm RFs in the 20-40 cm depth increments. The strong correlation with the smaller 2-20 mm RFs is consistent with the results of van Wesemael et al. (1995), who found 17-27 mm RFs negatively affected fine earth bulk density at RF contents of >0.30 kg kg^{-1}, compared to the >50 kg kg^{-1} RF content required by 77 mm RFs for a similar negative effect to fine earth bulk density to be observed.

Between 20 and 40 cm, the soil is generally characterised by a fine-textured matrix (silt loam) and a high RF volume (33-46 m^3 m^{-3} on average for the 20-30 cm and 30-40 cm depths, respectively). We propose that the average clay content in the 20-30 cm and 30-40 cm depth increments (20% and 21%, respectively), imbues sufficient contrast between matrix and RFs in their propensity to shrink and swell on drying and wetting, that lacunar pores develop in the matrix, resulting in a lower fine earth bulk density (Point b. above). When compared to other studies, our *in situ* measurements may identify potential issues in using results based on repacked soil experiments. For instance, Fiès et al. (2002) found the volume of lacunar pores increased with the proportion of clasts in the soil but only when clay content exceeded 30%, a value much higher than the 20% observed in this study. Alternatively, Gargiulo et al. (2016) observed an increase in porosity occurring in repacked soils with 18-19% clay content, but only after the soil had been exposed to nine wetting and drying cycles to facilitate the formation of soil structure. These comparisons indicate that for repacked soils to be comparable to undisturbed stony soils, repacked soil must undergo numerous wetting and drying cycles.

Soil chemistry

The significant positive relationship between 2-20 mm RFs and carbon concentration in the 0-10 cm increment is reproduced in several international studies (Meersmans et al., 2012; Schiedung et al., 2017). This effect is attributed to a concentration of carbon inputs into a smaller volume of fines as the proportion of RFs increases in the topsoil. Alternatively, in the subsoil (40-60 cm depth) the proportion of 6-20 mm RFs had a negative relationship with carbon. This may be due to limitations to plant growth caused by RF proportion (such as reduced water holding capacity or reduced nutrient supply), which could result in reduced carbon inputs at depth if conditions persist for years (Schiedung et al., 2017).

Total nitrogen had a negative relationship with the proportion of 2-6 mm RFs in the 0-10 and 20-30 cm increments while P-retention was positively affected by the volume of RFs when whole soil profiles were considered. We could speculate about the causes of these correlations, but we do not have the data required to support robust inferences.

4.5.4 Irrigation effects

Irrigation was found to have a significant positive effect on the fine earth WC when the whole profile was analysed and when refined to the 10-20 cm increment, but no clear effect on the RF WC. Other than a positive effect on P-retention in the 10-20 cm increment, and a negative effect on carbon, no other measured soil property was significantly affected by irrigation. Houlbrooke et al. (2008) and Houlbrooke and Laurenson (2013) found irrigation caused a shift in pore size distribution towards greater microporosity because of compaction from grazing on moist irrigated soils. This positive

effect on micropores (water storage pores) could explain the increase in fine earth WC at FC observed in this study; however, as pore size distribution was not determined, we can only speculate. Artigao et al. (2002) and Presley et al. (2004) found after 25 and 30 years of spray irrigation respectively, there was evidence of increased mineral weathering in the soil, which may explain the positive effect of irrigation on P-retention. The negative effect of irrigation on carbon is similar to the results in Mudge et al. (2017) who proposed that irrigation may reduce soil carbon by decreasing root biomass, increasing microbial activity (respiration and decomposition) or by increasing the leaching of existing soil carbon.

4.5.5 Management effect

Results of this study demonstrate that assuming RFs are inert with respect to soil water retention can lead to non-negligible underestimates of soil water storage. On average, ignoring RFs would lead to a ~10% under-estimate of FC in Canterbury stony soils. These soils have low water storage capacity (Carrick et al., 2013a), and are sensitive to irrigation management. Ignoring ~10% of water storage capacity in soils like this could be significant and raises questions about current management and measurement practices worldwide. The fact that international datasets and national environmental models consider RFs that have a greater porosity (and thus water retention) to those measured in this study as inert, demonstrates a potentially significant source of error with numerous undesirable effects. For example, in New Zealand, environmental protection legislation prescribes nutrient leaching limits for the protection of surface waters and shallow groundwater. Nutrient leaching is estimated with a numerical model, which itself is sensitive to the available WC parameter, and hence FC (McNeill et al., 2018). The sensitivity of nutrient leaching simulations to the water holding capacity of RFs needs to be considered. However, although we have confirmed greywacke RFs in stony soils hold a non-trivial amount of water at FC, it remains to be determined how much of that water is plant available. This question must be the focus of future research.

4.6 Conclusions

Results of this study demonstrate that hard sandstone RFs in Canterbury stony soils are not inert and can in fact retain water and affect the properties of the fine earth. For instance, RFs had positive relationships with carbon, total porosity and P-retention, and negative relationships with the fine earth bulk density, total nitrogen and fine earth WC. In addition, we found irrigation had a negative effect on soil carbon but a positive relationship with fine earth VWC and P-retention. In terms of water retention, even though hard sandstone has relatively low water storage in comparison to other lithologies, the volumetric abundance of RFs in stony soils means RFs still account for a substantial quantity of the water retained at FC. The water retention of the RFs was found to be strongly influenced by size, whereby the VWC of 2-20 mm RFs was found to be twice that of >20 mm

RFs. The proportion of RFs may have positive or negative relationships with RF VWC. Our findings could have significant implications for management practices, such as irrigation scheduling, as the effect of RFs (even those with much greater porosity than those measured in this study) are not currently accounted for in most parts of the world. For New Zealand, this means the ~13 mm of water stored in the RFs of Canterbury stony soils is not being included in water budgets or nutrient discharge predictions, leading potentially to apparent breaches of regulations where there are none, or unnecessarily strict limits on land management practices. However, we urge caution in factoring RF water holding capacity into decision-making until we determine the proportion of the water stored in RFs of greywacke lithology that is available to plants. This is the focus of our future work.

4.7 Appendix

Appendix F Error Analysis.

Errors in derivative variables such as porosity, bulk density and WC were estimated by simplified rules of Gaussian error propagation (Kirchner, 2001). This method requires the assumption that uncertainties in variables involved in calculations are uncorrelated. Errors in sums and differences were estimated as the standard deviations of the assumed error distributions added in quadrature, whereas the relative errors in products and quotients were estimated as error standard deviations divided by estimated values added in quadrature. That is

for $z = x \pm y \pm t$, the standard deviation of the joint error distribution is given by

$$s_z = \sqrt{(s_x)^2 + (s_y)^2 + (s_t)^2}, \quad (31)$$

or, for $z = x \cdot or / y \cdot or / t$, the standard deviation of the joint error distributions is given by

$$s_z = \sqrt{(\frac{s_x}{x})^2 + (\frac{s_y}{y})^2 + (\frac{s_t}{t})^2}, \quad (32)$$

All error distributions were assumed to be normal, although the error analysis approach does not require this assumption. The standard deviations of error distributions for mass measurements came from the manufacturer's specifications. The error distribution in the increment volume estimate was quantified by a test of the pit-and-bead method against a water volume estimate. This test involved excavating pits in 10 cm increments and calculating volume increments by weighing the required volume of beads or water to fill the volume when lined with a flexible impermeable membrane. We considered the water method to be optimal because the water pressure ensures better filling of cavernous under-hanging voids in the pit wall left by excavating RFs. We expected the error distribution to be skewed towards underestimates by the pit-and-bead method but, surprisingly, the errors were normally distributed, probably because variations in bead packing overwhelmed other errors. Volume estimates had the highest relative error of all variables. Error standard deviation of the RF density (0.15) was assigned based on the findings of McNamara et al. (2014) and Tenzer et al. (2011), while the error of the water density (0.002) was based on estimates of temperature variability and the temperature sensitivity of water density. The error standard deviation of particle density was equated to the standard deviation of particle density (0.05) as a worst-case estimate. For the fine earth gravimetric WC, we observed a difference between samples of different volume of the same increment (i.e. the bulk density sample and the SSA sample) that were larger than those attributable to instrument precision. This error was normally distributed when rare samples with high clay content were excluded. The standard deviation of the normally distributed error was used as the fine earth gravimetric WC error.

We used multiple ordinary least squares regression (OLS) to investigate relationships among predictor (independent) and response (dependent) variables. Those relationships are quantified by coefficients (slopes) associated with independent variables in the multiple linear regression equations. Both kinds of variables included secondary derivative variables – variables calculated from derived variables – which tended to accumulate error the greater the number of calculations involved, particularly when volume was included. An assumption of OLS is that independent variables are error-free. When this is not true, a phenomenon known as attenuation occurs, whereby the slope of the true (error-free relationship) between dependent and independent variables is reduced. In the case of single independent variable OLS, attenuation is quantified by $\frac{p}{1-p}$ where $= \frac{\sigma_{\delta_x}}{\sigma_x}$, the ratio of the measurement error variance to the variance in the independent variable (McArdle, 2003). Despite the assumptions of OLS being violated, we retained this analytical method because the relationships we intended to investigate were asymmetric; i.e. one set of variables *causes* another (Smith, 2009), and the analytical alternatives are complex.

Examining the relative error distributions in the independent secondary derived variables most prone to error, namely, fine earth bulk density and total porosity, we found at least 90% of estimates had relative errors less than 25%, while the remaining <10% had relative errors much larger (Figure A.1). The relative error distributions indicate two distinct populations of estimates; a larger population of relatively low error, and a smaller population with large error. Samples (variable estimates) from the inferred low relative error population produced *p* values of no less than 0.8, which establishes the worst-case amount attenuation relative to the OLS estimate; i.e. the OLS slope is no less than 0.8 times the true slope.

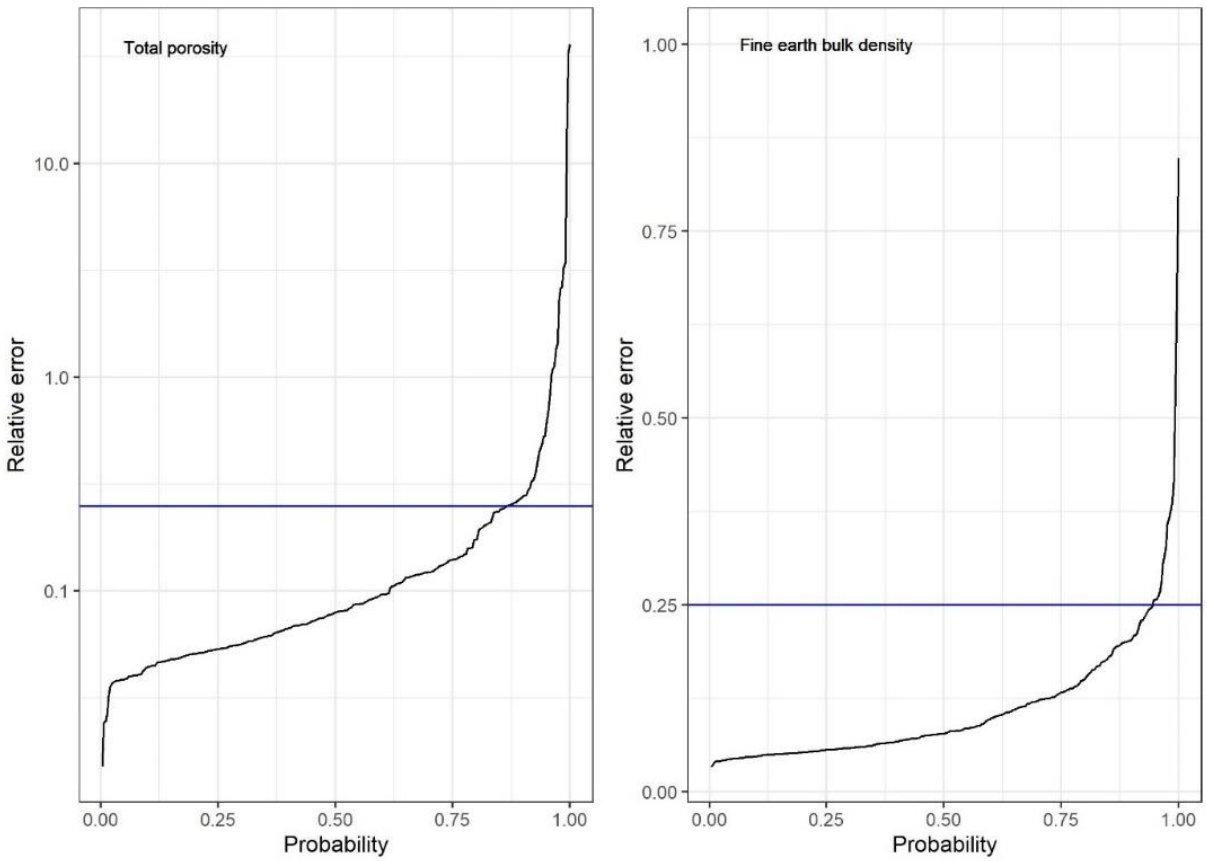

Figure A.1 Cumulative probability distribution of relative errors in total porosity and fine earth bulk density. The blue horizontal line corresponds to a relative error of 0.25.

A similar pattern of relative error distribution occurred in dependent variables prone to error, which include fine earth VWC, and VWC of 2-20 mm RFs and >20 mm RFs (Figure A.2). We chose to censor data in these data sets according to the same criterion (relative error <25%). Our intent was to avoid biases in derived relationships created by conflating two distinct populations of estimates within the dependent variable, one with potentially very large error.

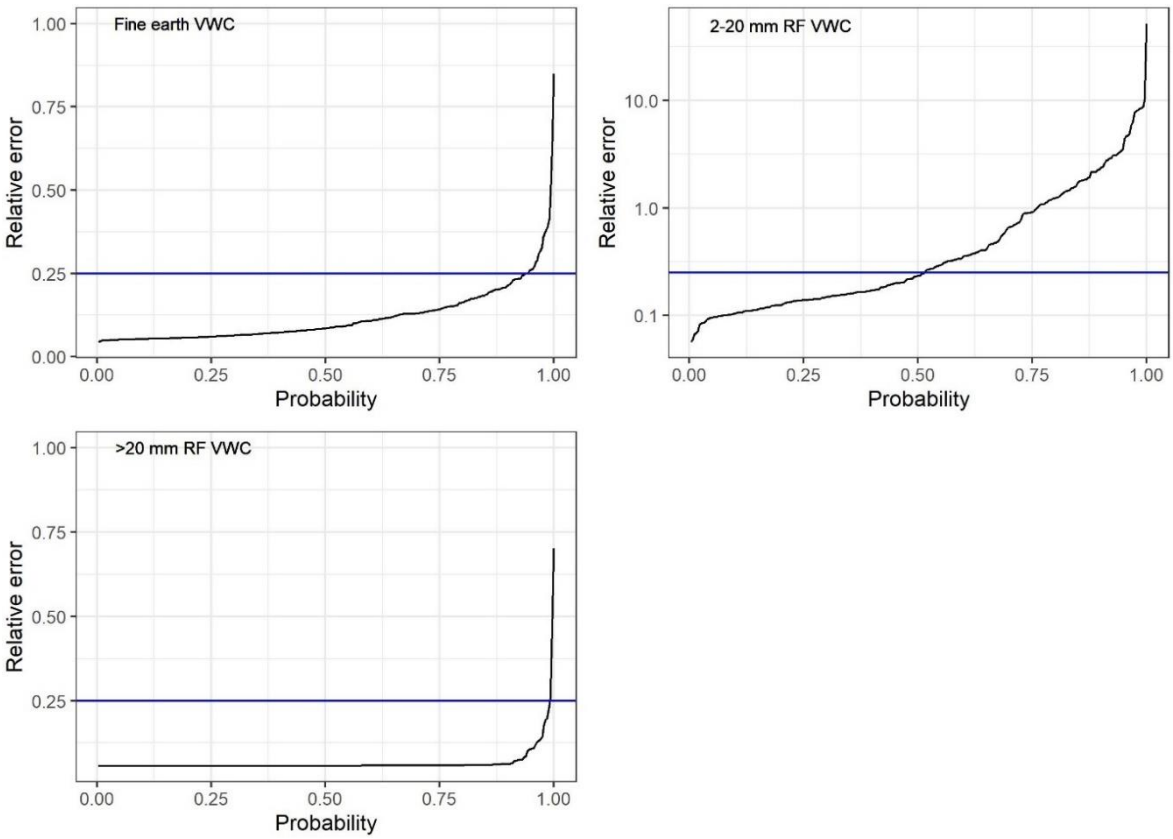

Figure A.2 Cumulative probability distributions of relative error in volumetric water contents of fine earth, 2-20 and >20 mm RFs. The horizontal blue line marks 25% relative error.

References

Kirchner, J.W., 2001. Data analysis toolkit #5: Uncertainty analysis and error propagation. Retrieved October 17, 2020 from http://seismo.berkeley.edu/~kirchner/eps_120/Toolkits/Toolkit_05.pdf

McArdle, B.H., 2003. Lines, models, and errors: Regression in the field. Limnol. Oceanogr. 48(3), 1363-1366.

McNamara, D., Faulkner, D., McCarney, E., 2014. Rock properties of greywacke basement hosting geothermal reservoirs, New Zealand: Preliminary results, Thirty-Ninth Workshop on Geothermal Reservoir Engineering, Stanford University, Stanford, California.

Smith, R.J., 2009. Use and misuse of the reduced major axis for line-fitting. Am. J. Phys. Anthropol. 140(3), 476-486. https://doi.org/10.1002/ajpa.21090.

Tenzer, R., Sirguey, P., Rattenbury, M., Nicolson, J., 2011. A digital rock density map of New Zealand. Comput. Geosci. 37(8), 1181-1191. https://doi.org/10.1016/j.cageo.2010.07.010.

Appendix G The average contribution of different size fractions to the total volume of water measured in each pit. Blue: fine earth fraction, green: 2-20 mm RFs and red: >20 mm RFs.

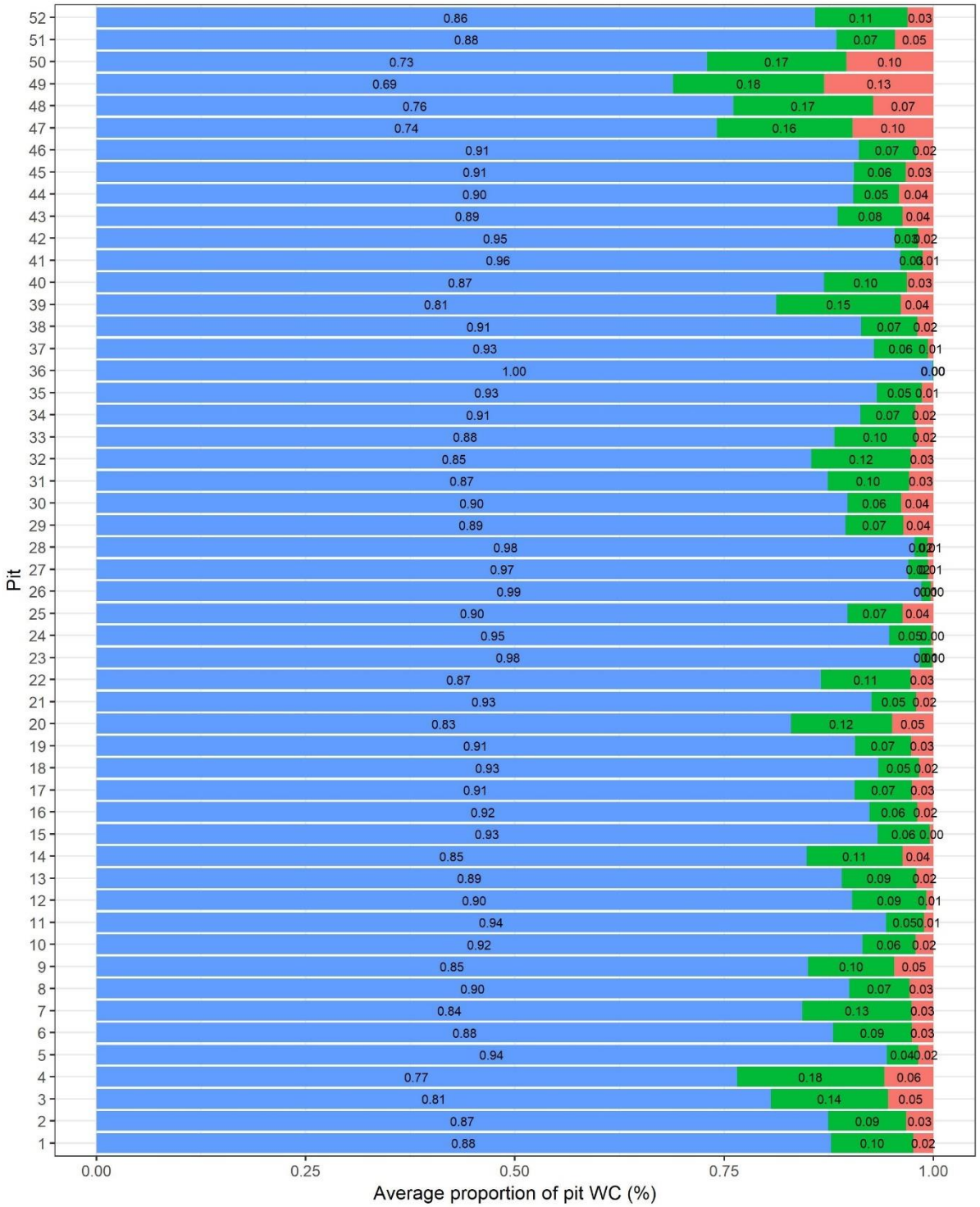

Appendix H Output data for the RF VWC regression analyses with significant effects.

Response variable	Principal explanatory variable*	Volume	Relationship^	P-value	R^2
VWC 2-20 mm RFs	Proportion of RFs	Whole profile	Negative	3.24E-06	0.55
VWC >20 mm RFs	Proportion of RFs	Whole profile	Negative	6.01E-03	0.60
VWC 2-20 mm RFs	Proportion 20-60 mm RFs	40-50 cm	Positive	0.016	0.73
VWC >20 mm RFs	Proportion 20-60 mm RFs	40-50 cm	Positive	0.034	0.71
VWC 2-20 mm RFs	Proportion 6-20 mm RFs	Whole profile	Negative	0.022	0.48
VWC >20 mm RFs	Proportion 2-20 mm RFs	Whole profile	Positive	0.020	0.59
VWC >20 mm RFs	Proportion >60 mm RFs	Whole profile	Negative	3.55E-05	0.63

*The variable introduced at the end of the list of independent variables used in the regression analysis, such that the effect of the principal variable is tested after all other variables are accounted for.

^ Is the relationship between the principal explanatory variable and the response variable.

Appendix I Regression analyses output data for chemical variables of the fine earth with significant effects.

Response variable	Principal explanatory variable*	Volume	Relationship^	P-value	R^2
VWC of the whole soil	Proportion of RFs	Whole profile	Negative	< 2e-16	0.97
Total porosity	Proportion 2-20 mm RFs	20-30 cm	Positive	0.0029	0.48
Total porosity	Proportion 2-20 mm RFs	30-40 cm	Positive	0.031	0.43
Total porosity	Proportion 20-60 mm RFs	20-30 cm	Positive	0.025	0.40
Fine earth bulk density	Proportion 2-20 mm RFs	Whole profile	Negative	0.045	0.40
Fine earth bulk density	Proportion 2-20 mm RFs	20-30 cm	Negative	0.010	0.60
Fine earth bulk density	Proportion 20-60 mm RFs	20-30 cm	Negative	0.011	0.60
Fine earth VWC	Proportion of RFs	Whole profile	Negative	< 2e-16	0.92
Fine earth VWC	Proportion of RFs	0-10 cm	Negative	0.0015	0.79
Fine earth VWC	Proportion of RFs	10-20 cm	Negative	0.015	0.82
Fine earth VWC	Proportion of RFs	20-30 cm	Negative	0.0042	0.89
Fine earth VWC	Proportion of RFs	30-40 cm	Negative	1.61E-05	0.87
Fine earth VWC	Proportion of RFs	40-50 cm	Negative	0.00032	0.92
Fine earth VWC	Proportion of RFs	50-60 cm	Negative	0.0052	0.85
Fine earth VWC	Proportion 2-20 mm RFs	Whole profile	Negative	6.65E-09	0.89
Fine earth VWC	Proportion 2-20 mm RFs	30-40 cm	Negative	0.0089	0.76
Fine earth VWC	Proportion 20-60 mm RFs	Whole profile	Negative	0.019	0.87
Fine earth VWC	Proportion >60 mm RFs	0-10 cm	Negative	0.010	0.76
Fine earth VWC	Proportion >60 mm RFs	10-20 cm	Negative	0.025	0.82

*The variable introduced at the end of the list of independent variables used in the regression analysis, such that the effect of the principal variable is tested after all other variables are accounted for.

^Is the relationship between the principal explanatory variable and the response variable.

Appendix J Regression analyses output data for chemical variables of the fine earth with significant effects.

Response variable	Principal explanatory variable*	Volume	Relationship^	P-value	R^2
Carbon	Proportion 2-20 mm RFs	0-10 cm	Positive	0.049	0.98
Carbon	Proportion 6-20 mm RFs	40-50 cm	Negative	0.027	0.98
Carbon	Proportion 6-20 mm RFs	50-60 cm	Negative	0.021	0.99
P-retention	Proportion of RFs	Whole profile	Positive	0.0017	0.87
Nitrogen	Proportion 2-6 mm RFs	Whole profile	Negative	0.014	0.99
Nitrogen	Proportion 2-6 mm RFs	0-10 cm	Negative	0.049	0.98
Nitrogen	Proportion 2-6 mm RFs	20-30 cm	Negative	0.0052	0.96

*The variable introduced at the end of the list of independent variables used in the regression analysis, such that the effect of the principal variable is tested after all other variables are accounted for.

^Is the relationship between the principal explanatory variable and the response variable.

Appendix K Output data for the treatment regression analyses with significant effects.

Response variable	Principal explanatory variable*	Volume	Relationship^	P-value	R^2
Fine earth VWC	Treatment	Whole profile	Positive	1.46E-05	0.93
Fine earth VWC	Treatment	10-20 cm	Positive	0.033	0.86
P-retention	Treatment	10-20 cm	Positive	0.012	0.83
Carbon	Treatment	Whole profile	Negative	0.035	0.99

*The variable introduced at the end of the list of independent variables used in the regression analysis, such that the effect of the principal variable is tested after all other variables are accounted for.

^Is the relationship between the principal explanatory variable and the response variable.

References

Al-Yahyai, R., Schaffer, B., Davies, F.S., Munoz-Carpena, R., 2006. Characterization of soil-water retention of a very gravelly loam soil varied with determination method. Soil Sci. 171(2), 85-93. https://doi.org/10.1097/01.ss.0000187372.53896.9d.

Artigao, A., Ortega, J.F., Tarjuelo, J.M., Juan, J.A.d., 2002. The impact of irrigation application upon soil physical degradation in Castilla-La Mancha (Spain). Adv. Geoecol. (35), 83-90.

Baetens, J.M., Verbist, K., Cornelis, W.M., Gabriels, D., Soto, G., 2009. On the influence of coarse fragments on soil water retention. Water Resour. Res. 45. https://doi.org/10.1029/2008wr007402.

Baruck, J., Nestroy, O., Sartori, G., Baize, D., Traidl, R., Vrščaj, B., Bräm, E., Gruber, F.E., Heinrich, K., Geitner, C., 2016. Soil classification and mapping in the Alps: the current state and future challenges. Geoderma 264, 312-331. https://doi.org/10.1016/j.geoderma.2015.08.005.

Batjes, N.H., 2009. Harmonized soil profile data for applications at global and continental scales: updates to the WISE database. Soil Use Manag. 25(2), 124-127. https://doi.org/10.1111/j.1475-2743.2009.00202.x.

Carrick, S., Fraser, P., Dennis, S., Knight, T., Tabley, F., 2013a. Challenges for leachate monitoring from alluvial sedimentary soils. In: L.D. Currie, C.L. Christensen (Eds.), Accurate and Efficient Use of Nutrients on Farms, Occasional Report No. 26. Fertiliser and Lime Research Centre, Massey University, Palmerston North, New Zealand.

Carrick, S., Palmer, D., Webb, T., Scott, J., Lilburne, L., 2013b. Stony soils are a major challenge for nutrient management under irrigation development. In: L.D. Currie, C.L. Christensen (Eds.), Accurate and Efficient Use of Nutrients on Farms, Occasional Report No. 26. Fertiliser and Lime Research Centre, Massey University, Palmerston North, New Zealand.

Carrick, S., Rogers, G., Cameron, K., Malcolm, B., Payne, J., 2017. Testing large area lysimeter designs to measure leaching under multiple urine patches. N. Z. J. Agric. Res. 60(2), 205-215. https://doi.org/10.1080/00288233.2017.1291527.

Claydon, J.J., 1989. Determination of particle size in fine grained soils – pipette method. Division of Land and Soil Sciences Technical Record (LH5), DSIR Division of Land & Soil Sciences.

Cornell, J.A., 1981. Experiments with Mixtures. John Wiley and Sons, New York.

Cuniglio, R., Corti, G., Agnelli, A., 2009. Rock fragments evolution and nutrients release in vineyard soils developed on a thinly layered limestone (Tuscany, Italy). Geoderma 148(3), 375-383. https://doi.org/10.1016/j.geoderma.2008.11.005.

da Silva, L.P., van Lier, Q.D., Correa, M.M., de Miranda, J.H., de Oliveira, L.A., 2016. Retention and solute transport properties in disturbed and undisturbed soil samples. Rev. Bras. Ciênc. Solo 40. http://dx.doi.org/10.1590/18069657rbcs20151045.

Dai, Y.J., Wei, S.G., Nan, W., Xin, Q.C., Hua, Y., Zhang, S.P., Liu, S.F., Lu, X.J., Wang, D.G., Yan, F.P., 2019. A review of the global soil property maps for Earth system models. Soil 5(2), 137-158. https://doi.org/10.5194/soil-5-137-2019.

Dann, R., Close, M., Flintoft, M., Hector, R., Barlow, H., Thomas, S., Francis, G., 2009. Characterization and estimation of hydraulic properties in an alluvial gravel vadose zone. Vadose Zone J. 8(3), 651-663. https://doi.org/10.2136/vzj2008.0174.

Du, Z., Cai, Y., Yan, Y., Wang, X., 2017. Embedded rock fragments affect alpine steppe plant growth, soil carbon and nitrogen in the northern Tibetan Plateau. Plant and Soil 420(1), 79-92. https://doi.org/10.1007/s11104-017-3376-9.

Fiès, J.C., Louvigny, N.D.E., Chanzy, A., 2002. The role of stones in soil water retention. Eur. J. Soil Sci. 53(1), 95-104. https://doi.org/10.1046/j.1365-2389.2002.00431.x.

Forsyth, P.J., Jongens, R., Barrell (Compilers), D.J.A., 2008. Geology of the Christchurch Area. Institute of Geological & Nuclear Sciences 1:250 000 geologial map 16. GNS Science, Lower Hutt, New Zealand.

Gargiulo, L., Mele, G., Terribile, F., 2016. Effect of rock fragments on soil porosity: a laboratory experiment with two physically degraded soils. Eur. J. Soil Sci. 67(5), 597-604. https://doi.org/10.1111/ejss.12370.

Gradwell, M., Birrell, K., 1972. Soil Bureau laboratory methods. C. Methods for physical analysis of soils. New Zealand Soil Bureau Scientific Report 10C.

Graham, S., Srinivasan, M.S., Faulkner, N., Carrick, S., 2018. Soil hydraulic modeling outcomes with four parameterization methods: comparing soil description and inverse estimation approaches. Vadose Zone J. 17. https://doi.org/10.2136/vzj2017.01.0002.

Hallett, S.H., Sakrabani, R., Keay, C.A., Hannam, J.A., 2017. Developments in land information systems: examples demonstrating land resource management capabilities and options. Soil Use Manag. 33(4), 514-529. https://doi.org/10.1111/sum.12380.

Hanson, C.T., Blevins, R.L., 1979. Soil water in coarse fragments. Soil Sci. Soc. Am. J. 43(4), 819-820. https://doi.org/10.2136/sssaj1979.03615995004300040044x.

Hedley, C.B., Payton, I.J., Lynn, I.H., Carrick, S.T., Webb, T.H., McNeill, S., 2012. Random sampling of stony and non-stony soils for testing a national soil carbon monitoring system. Soil Res. 50(1), 18-29. https://doi.org/10.1071/SR11171.

Hewitt, A.E., 2010. New Zealand Soil Classification. Landcare Research Science Series no. 1. 3rd ed. Manaaki Whenua Press, Lincoln, New Zealand.

Hlavacikova, H., Novak, V., Holko, L., 2015. On the role of rock fragments and initial soil water content in the potential subsurface runoff formation. J. Hydrol. Hydromech. 63(1), 71-81. https://doi.org/10.1515/johh-2015-0002.

Houlbrooke, D.J., Laurenson, S., 2013. Effect of sheep and cattle treading damage on soil microporosity and soil water holding capacity. Agric. Water Manage. 121, 81-84. https://doi.org/10.1016/j.agwat.2013.01.010.

Houlbrooke, D.J., Littlejohn, R.P., Morton, J.D., Paton, R.J., 2008. Effect of irrigation and grazing animals on soil quality measurements in the North Otago Rolling Downlands of New Zealand. Soil Use Manag. 24(4), 416-423. https://doi.org/10.1111/j.1475-2743.2008.00183.x.

Ives, D., 1973. Nature and distribution of loess in Canterbury, New Zealand. N. Z. J. Geol. Geophys. 16(3), 587-610. https://doi.org/10.1080/00288306.1973.10431382.

Jones, T.P.C., 2016. Physical and mechanical controls of matrix permeability on rocks from Rotokawa Geothermal Field, Taupo Volcanic Zone, New Zealand, University of Canterbury.

Korboulewsky, N., Tétégan, M., Samouelian, A., Cousin, I., 2020. Plants use water in the pores of rock fragments during drought. Plant and Soil. https://doi.org/10.1007/s11104-020-04425-3.

Lachat Instruments, 1998g. Quik Chem Method 12-115-01-1-J, Milwaukee, WI, USA.

Leco, 2003. Total/Organic Carbon and Nitrogen in Soils. Organic Application Note 203-821-165, LECO Corporation, St. Joseph, MO.

Lee, M., 2019. Prescriptions for optimal management of stony soils at Te Whenua Hou in Canterbury, New Zealand, Lincoln University.

Lunt, I.A., Bridge, J.S., 2007. Formation and preservation of open-framework gravel strata in unidirectional flows. Sedimentology 54(1), 71-87. https://doi.org/10.1111/j.1365-3091.2006.00829.x.

Manaaki Whenua - Landcare Research, 2019. S-map - New Zealand's National Digital Soil Map. 10.7931/L1WC7.

McNamara, D., Faulkner, D., McCarney, E., 2014. Rock properties of greywacke basement hosting geothermal reservoirs, New Zealand: preliminary results, Thirty-Ninth Workshop on Geothermal Reservoir Engineering, Stanford University, Stanford, California.

McNeill, S.J., Lilburne, L.R., Carrick, S., Webb, T.H., Cuthill, T., 2018. Pedotransfer functions for the soil water characteristics of New Zealand soils using S-map information. Geoderma 326, 96-110. https://doi.org/10.1016/j.geoderma.2018.04.011.

Meersmans, J., Martin, M.P., De Ridder, F., Lacarce, E., Wetterlind, J., De Baets, S., Le Bas, C., Louis, B.P., Orton, T.G., Bispo, A., Arrouays, D., 2012. A novel soil organic C model using climate, soil type and management data at the national scale in France. Agron. Sustainable Dev. 32(4), 873-888. https://doi.org/10.1007/s13593-012-0085-x.

Milne, J., Clayden, B., L., S.P., Wilson, A.D., 1995. Soil Description Handbook. Manaaki Whenua Press, Lincoln, New Zealand.

Mudge, P.L., Kelliher, F.M., Knight, T.L., O'Connell, D., Fraser, S., Schipper, L.A., 2017. Irrigating grazed pasture decreases soil carbon and nitrogen stocks. Global Change Biol. 23(2), 945-954. https://doi.org/10.1111/gcb.13448.

Parajuli, K., Sadeghi, M., Jones, S.B., 2017. A binary mixing model for characterizing stony-soil water retention. Agric. For. Meteorol. 244-245, 1-8. https://doi.org/10.1016/j.agrformet.2017.05.013.

Pineda, M.C., Viloria, J., Martínez-Casasnovas, J.A., Valera, A., Lobo, D., Timm, L.C., Pires, L.F., Gabriels, D., 2018. Predicting soil water content at − 33 kPa by pedotransfer functions in stoniness 1 soils in northeast Venezuela. Environ. Monit. Assess. 190(3), 161. https://doi.org/10.1007/s10661-018-6528-3.

Poesen, J., Lavee, H., 1994. Rock fragments in top soils: significance and processes. Catena 23(1), 1-28. https://doi.org/10.1016/0341-8162(94)90050-7.

Pollacco, J., 2017. Literature review of hydrological processes of soils with rock fragments. LC2688, Landcare Research.

Presley, D.R., Ransom, M.D., Kluitenberg, G.J., Finnell, P.R., 2004. Effects of thirty years of irrigation on the genesis and morphology of two semiarid soils in Kansas. Soil Sci. Soc. Am. J. 68(6), 1916-1926. https://doi.org/10.2136/sssaj2004.1916.

Román Dobarco, M., Bourennane, H., Arrouays, D., Saby, N.P.A., Cousin, I., Martin, M.P., 2019. Uncertainty assessment of GlobalSoilMap soil available water capacity products: a French case study. Geoderma 344, 14-30. https://doi.org/10.1016/j.geoderma.2019.02.036.

Saunders, W.M.H., 1965. Phosphate retention by New Zealand soils and its relationship to free sesquioxides, organic matter, and other soil properties. N. Z. J. Agric. Res. 8(1), 30-57. https://doi.org/10.1080/00288233.1965.10420021.

Scheinost, A.C., Sinowski, W., Auerswald, K., 1997. Regionalization of soil water retention curves in a highly variable soilscape, I. Developing a new pedotransfer function. Geoderma 78(3), 129-143. https://doi.org/10.1016/S0016-7061(97)00046-3.

Schiedung, H., Tilly, N., Hütt, C., Welp, G., Brüggemann, N., Amelung, W., 2017. Spatial controls of topsoil and subsoil organic carbon turnover under C3–C4 vegetation change. Geoderma 303, 44-51. https://doi.org/10.1016/j.geoderma.2017.05.006.

Schoeman, J.L., Kruger, M.M., Loock, A.H., 1997. Water-holding capacity of rock fragments in rehabilitated opencast mine soils. S. Afr. J. Plant Soil 14(3), 98-102. https://doi.org/10.1080/02571862.1997.10635089.

Shangguan, W., Dai, Y., Duan, Q., Liu, B., Yuan, H., 2014. A global soil data set for earth system modeling. J. Adv. Model. Earth Syst. 6(1), 249-263. https://doi.org/10.1002/2013ms000293.

Shi, Z.J., Xu, L.H., Wang, Y.H., Yang, X., Jia, Z., Guo, H., Xiong, W., Yu, P., 2012. Effect of rock fragments on macropores and water effluent in a forest soil in the stony mountains of the Loess Plateau, China. Afr. J. Biotechnol. 11(39), 9350-9361. https://doi.org/10.5897/AJB12.145.

Tetegan, M., Nicoullaud, B., Baize, D., Bouthier, A., Cousin, I., 2011. The contribution of rock fragments to the available water content of stony soils: proposition of new pedotransfer functions. Geoderma 165(1), 40-49. https://doi.org/10.1016/j.geoderma.2011.07.001.

Twarakavi, N.K.C., Sakai, M., Simunek, J., 2009. An objective analysis of the dynamic nature of field capacity. Water Resour. Res. 45. https://doi.org/10.1029/2009wr007944.

UMS, 2009. User manual: T5/T5x pressure transducer tensiometer. UMS GmbH München.

van Wesemael, B., Poesen, J., de Figueiredo, T., 1995. Effects of rock fragments on physical degradation of cultivated soils by rainfall. Soil Tillage Res. 33(3), 229-250. https://doi.org/10.1016/0167-1987(94)00439-L.

Webb, T.H., Lilburne, L.R., 2011. Criteria for Defining the Soil Family and Soil Sibling: the Fourth and Fifth Categories of the New Zealand Soil Classification. Landcare Research Science Series No. 3. Manaaki Whenua Press, Lincoln, New Zealand.

Zhou, B.B., Shao, M.A., Wang, Q.J., Yang, T., 2011. Effects of different rock fragment contents and sizes on solute transport in soil columns. Vadose Zone J. 10(1), 386-393. https://doi.org/10.2136/vzj2009.0195.

Chapter 5

Predicting field capacity in undisturbed stony soils

The manuscript has been accepted by *Geoderma*:

Robertson B.B., Carrick S.T., Almond P.C., McNeill S., Penny V., Chau H.W. and Smith C.M.S., 2021. Predicting field capacity in undisturbed stony soils. *Geoderma*.
https://doi.org/10.1016/j.geoderma.2021.115346

Abstract

An increasing number of studies around the world are showing that a long-held assumption that rock fragments (RFs) are inert with respect to water retention is incorrect. Yet very few pedotransfer functions (PtFs) account for water held by RFs or the effect RFs have on the water retention of the fine earth. The few PtFs that incorporate the water content (WC) of RFs have relied upon measurement methods that may not be representative of field conditions. This indicates a gap in research regarding the characterisation of the water holding behaviour of stony soils *in situ* using soil volumes that adequately represent the soil. We address this gap in research by developing PtFs that predict the field capacity WC of stony soils using soil water storage measurements from 52 pits excavated into stony soils on the Canterbury Plains, New Zealand. These soils comprise sediment derived from a indurated sandstone. The soils at each site were watered to saturation, and then after two days of drainage (a proxy for field capacity), a 30 x 30 cm pit was excavated in 10 cm increments to a depth of 60 cm. Matric potential was measured *in situ* for each increment, and soil WC was calculated from samples taken back to the laboratory. Our results showed it was possible to accurately predict the field capacity WC of stony soils using only explanatory variables that could be easily measured or estimated from a minimalistic field survey. An existing PtF calibrated on NZ soils (logit PtF), which was constructed on the assumption that RFs had no effect on WC at FC other than reducing the volume of the fine earth, performed worse than our models. By modifying the logit PtF, we conclude that its poorer performance stems from its inability to account for deviations from 1) the matric potential it assumes for field capacity (-10 kPa), 2) water held by RFs, and 3) the effect of RFs on the water retention characteristics of the fine earth. Our results demonstrate that even the low porosity RFs measured in this study can significantly affect model performance, but by including two variables (depth and volumetric proportion of RFs) that are routinely measured or estimated in most soil sampling projects, it is possible to improve prediction accuracy in established models.

5.1 Introduction

Worldwide, there are concerns about rising nutrient concentrations in surface and groundwater systems (McDowell et al., 2020). A leading source of leached nutrients is agricultural land, which has expanded significantly with global demand for food (McDowell et al., 2020; Wu et al., 2014). To mitigate nutrient leaching, more effective land management practices operating within an appropriate regulatory environment are necessary, making knowledge of soil water and nutrient retention properties indispensable. However, soil hydraulic properties are costly and time-consuming to measure, making it difficult or impossible to provide representative soil hydraulic properties at the farm scale, let alone regional and national scales. Therefore, models have been developed to provide estimates of soil retention properties like field capacity (FC) using more readily available field data (Vereecken et al., 1990). When applied to soil mapping units, these models (known as pedotransfer functions or PtFs) can be utilised for management and regulation purposes at the national scale when appropriate uncertainty analysis is included (Johnston et al., 2003; Lilburne et al., 2012). But PtFs for water retention properties often rely on the assumption that rock fragments (RFs) in the soil are inert, such that all retention estimates are based solely on fine earth (<2 mm fraction) properties and its volumetric proportion.

Several studies have demonstrated that RFs can account for a significant proportion of the water held in soil (Hanson and Blevins, 1979; Poesen and Lavee, 1994; Schoeman et al., 1997). For instance, Tetegan et al. (2011) found the soil available water content of a horizon containing 30% RFs could be underestimated by 5-33% depending on the lithology of the RFs. Similarly, Jones and Graham (1993) found large volumes of low porosity granite could hold more plant available water than the surrounding fine earth in soils under forest. As a result, a potentially significant error could exist for predictions of FC water content (WC) in stony soils (soils with over 30-35% RFs by volume), which represent large areas of land in many countries, including ~30% of Western Europe (Tetegan et al., 2011) and >60% of land in the Mediterranean area (Poesen, 1990). This is especially important considering PtFs that do not account for RF WC are used in national soil information systems (Lilburne et al., 2012; McNeill et al., 2018) and are used in the Global Soil Map project (Román Dobarco et al., 2019a; Román Dobarco et al., 2019b). For instance, S-map (the national soil information system of New Zealand; Lilburne et al., 2012) do not incorporate the WC of RFs in FC predictions, even though two-thirds of the irrigated land area in one of New Zealand's most important agricultural region (Canterbury) is on stony soil. The few PtFs that incorporate the WC of RFs (Cousin et al., 2014; Parajuli et al., 2017; Scheinost et al., 1997; Wang et al., 2013) have relied upon measurement methods that may not be representative of field conditions: they used small sample sizes, relied upon repacked soil, or neglected to include the effect RFs may have on fine earth

in situ. This indicates a gap in research regarding the characterisation of the water holding behaviour of stony soils *in situ* using soil volumes that adequately represent the soil.

This paper aims to develop PtFs that incorporate characteristics of the skeletal material in soils, and thus implicitly account for water held by RFs. The PtFs are calibrated on data derived from representative elementary volumes of stony soils *in situ* on alluvial fans in Canterbury, New Zealand. To develop better PtFs for FC in stony soils worldwide, we identify variables that have predictive value and are easy to measure. We then use them to augment the logit model of McNeill et al. (2018) to demonstrate how they may improve model performance in stony soils.

5.2 Materials and methods

5.2.1 Soil data

The soil data used to develop the FC PtFs was sourced from Chapter 3 and Chapter 4. Data from these studies are derived from 52 soil pits located throughout the Canterbury Plains of New Zealand. The Plains are approximately 180 km long and 70 km at their widest and consists of geomorphic surfaces of latest Pleistocene and Holocene age. The Plains have been built of coalescing aggrading Pleistocene glacial outwash fans constructed by large rivers sourced in the Southern Alps. The large rivers are now entrenched within the Pleistocene fans to form inset fans of Holocene age. Most of the soils on the Canterbury Plains are shallow stony soils (Carrick et al., 2013) comprising RFs of indurated muddy fine sandstone (greywacke) of the Rakaia terrane (Coates and Cox, 2002; Forsyth et al., 2008). On the late Pleistocene surfaces, Pallic and Brown soils dominate, while Holocene surfaces are dominated by Recent soils in the NZ Soil Classification (Hewitt, 2010). The stony soils of the Canterbury Plains include Firm Brown Soils (Dystrudepts and Dystrustepts) and Fluvial Recent Soils (Fluvents and Ustepts).

We adopt Webb and Lilburne's (2011) definition of stony soils as applied at the family level (level 4) of the NZ Soil Classification; specifically, soils with >35% RFs by volume within 45 cm of the soil surface. This definition is comparable to soil families of the USDA *Soil Taxonomy* system with the skeletal or fragmental particle sizes classes; or taxa having the skeletic soil qualifier for the second-level units of the WRB (IUSS Working Group WRB, 2015).

The 52 soil pits spanned 24 sites on land under pasture for at least three years and which were predominately grazed by dairy cattle. At each site, a minimum of two pits were sampled. One pit was under a spray irrigator for at least two years, while the other pit was in the same paddock but in soil that had never been irrigated (e.g. in the corner of a paddock outside the arc of a centre pivot irrigator). For each sampling location, the soil was first wet-up by applying >100 mm from a bespoke trickle irrigation system designed to wet a local area. The soil was allowed to drain for two days,

which was used as a proxy for FC. A 30 cm by 30 cm pit was then excavated in 10 cm increments to a depth of 60 cm. Each increment was equal to ~9000 cm^3, a volume that Novák and Hlaváčiková (2019) suggest is a representative elementary volume for measuring hydraulic properties in stony soils with gravels (2-75 mm RFs). After each increment was excavated, matric potential was measured by inserting a UMS T5 pressure transducer tensiometer horizontally into the pit wall, with readings taken with an Infield 7C handheld read-out device (UMS, 2009). The volume of each increment was determined using the pit and bead method (Hedley et al., 2012). Excavated material from each increment was passed through a 20 mm sieve. All the largest (>20 mm) RFs were collected and weighed in the field to avoid any biases introduced by sub-sampling. This sample was taken back to the lab to determine the size distribution and FC WC of >20 mm RFs. The <20 mm material was then mixed and quartered. One quarter was collected and weighed for the purpose of estimating the whole soil bulk density, the fine earth bulk density, the 2 – 20 mm RF size distribution, the whole soil WC and the WC of the 2-20 mm RFs. One scoopful (with a trowel) was collected and weighed for estimating the WC of the fine earth and the specific surface area (SSA) of the fine earth (for methods see below). A second quarter of the <20 mm material was sieved at 10 mm; the <10 mm material was used for particle size analysis (Claydon, 1989), particle density (Gradwell and Birrell, 1972), WC of the fine earth at -1500 kPa (Gradwell and Birrell, 1972), phosphate retention (Saunders, 1965), total nitrogen (Leco, 2003) and organic carbon (Leco, 2003). Soils were then described according to the terminology of Milne et al. (1995) and classified to the subgroup level of the New Zealand Soil Classification, according to Hewitt (2010). The remaining <20 mm material (~50%) was not analysed any further.

SSA was estimated using the methods of Kirschbaum et al. (2020),

$$SSA = \frac{2000(M_{<2,30} - M_{<2,od})}{M_{<2,od}} \quad (33)$$

where the factor, 2000 m^2 gH_2O^{-1} converts from water adsorption to SSA of soils, $M_{<2,30}$ is the mass of a fine earth sample dried at 30°C and 30% relative humidity, and $M_{<2,od}$ is the mass of the same sample after being oven-dried at 105°C.

Some manipulation of raw data was required before statistical analyses. As the proportion of sand (p_{sand}), silt (p_{silt}), and clay (p_{clay}) in the fine earth form a ternary simplex; a structural correlation exists (McNeill et al., 2018). As a result, conditions that may only affect clay, for instance, will have an apparent statistical effect on sand and silt even though no functional relationship is present, as changes to one fraction alter the other two. For computational convenience, texture proportions were transformed to a Cartesian system as this generally reduces the apparent correlation between texture fractions by removing the structural correlation component. As per the method used by

McNeill et al. (2018) and Cornell (1981), the texture proportions were transformed to a Cartesian system by generating two auxiliary variables as follows,

$$\omega_1 = 2p_{sand} - p_{silt} - p_{clay} \quad (34)$$

$$\omega_2 = p_{silt} - p_{clay} \quad (35)$$

The data set was also censored according to relative errors in data values. Many of the variables used for model development are derived from calculations on primary variables, with inherent uncertainty. Those uncertainties compound and grow in relative magnitude, especially where subtractions and divisions are involved. We quantified the magnitude of errors, both absolute and relative, by applying Gaussian error propagation (refer to Chapter 4 Appendix F). Increments were removed if the relative error for an increment's fine earth (VWC), fine earth bulk density or total porosity was >25%. As the New Zealand Soil Classification Order (top level of the NZSC, Hewitt, 2010) was used as an explanatory variable, increments from soils belonging to rare soil orders (Pallic (2 pits) and Gley (2 pits)) were excluded. The texture group of a soil was also an explanatory variable, making it necessary to remove increments from the rare clayey texture group (4 increments). The resulting dataset had 230 measured increments.

5.2.2 Statistical modelling

For modelling purposes, the dataset was randomly split 70:30 into training and validation datasets, respectively. Two multiple linear regression models to predict total FC WC (matrix plus RFs) were constructed in R version 4.0.2 (R Core Team, 2016) using different combinations of independent variables (Table 6). These models constituted PtFs referred to as an optimal and a practical PtF. The optimal PtF included all the explanatory variables measured in the experiment and was developed as a standard to compare the relative accuracy of the other models. The practical model used explanatory variables that could be easily measured or estimated from a minimalistic field survey. The explanatory set of variables for each model (PtF) was refined by selecting only significant variables according to a backwards selection process based on finding the model with the lowest Akaike information criterion value (AIC). This method of development is commonly found in modelling literature (Burnham and Anderson, 2002).

Table 6 Variables used in initial models for PtF development.

Optimal PtF	Practical PtF
Soil order	Soil order
Irrigation treatment (irrigated, dryland)	Irrigation treatment (irrigated, dryland)
Geomorphic surface age*	Geomorphic surface age*
Depth	Depth
Measured FC matric potential	Texture class^
Phosphate retention	Texture group~
Total nitrogen	SSA
Organic carbon	Proportion of vol. that is RFs
Total porosity	Proportion of vol. that is 2-6 mm RFs
Particle density	Proportion of vol. that is 6-20 mm RFs
-1500 kPa WC	Proportion of vol. that is 20-60 mm RFs
Texture class^	Proportion of vol. that is >60 mm RFs
Texture group~	
ω_1	
ω_2	
SSA	
Proportion of vol. that is RFs	
Proportion of vol. that is 2-6 mm RFs	
Proportion of vol. that is 6-20 mm RFs	
Proportion of vol. that is 20-60 mm RFs	
Proportion of vol. that is >60 mm RFs	
ρ_b	
$\rho_{<2}$	

*Pleistocene, Holocene and Pleistocene to Holocene.
^ Such as sand, silt loam and loamy clay.
~ Namely, sandy, loamy, silty and clayey texture groups.

5.2.3 An existing New Zealand PtF

To quantify the value of implicitly accounting for the effects of RFs on soil water retention, we sought a model we could apply to our data to compare predictions against. McNeill et al. (2018) developed PtFs calibrated on NZ soil data to predict soil water retention when evaluating modelling methods for NZ's S-map spatial soil information system. They concluded a logit-transformation model (logit PtF) performed best, and we compare our results directly with output from that PtF (McNeill et al., 2018). In the logit PtF, the WC of a stony soil is estimated as the predicted WC of the fine earth scaled on a volumetric basis by the concentration of RFs (McNeill et al., 2018). Thus, it does not take account of water held in RFs or the effect of RFs on the water retention of the fine earth. For example, when estimating FC WC, the logit PtF predicts the VWC of the fine earth only, assuming a FC matric potential of -10 kPa (θ_{10kPa}). The FC VWC of stony soils ($\theta_{FCstony}$) is then estimated by adjusting θ_{10kPa} by the volume proportion of RFs in an increment (χ), which are considered inert;

$$\theta_{FCstony} = \theta_{10kPa}(1 - \chi). \quad (36)$$

The explanatory variables of the logit PtF include the soil order (top level of the NZSC, Hewitt, 2010), natural soil drainage (poorly-drained, imperfectly-drained, well-drained), rock class of the fine earth, mean texture values (proportions of sand, silt and clay) and parsed information derived from a codified functional horizon description (Webb and Lilburne, 2011). A functional horizon is a class of horizon defined by properties of significance to soil hydraulic behaviour (Webb, 2003), namely ped size, texture, stoniness, a topsoil identifier, tephra descriptor and consistence (Webb and Lilburne, 2011). We applied the functional horizon classification to our soil descriptions to provide the necessary data for the logit PtF. The water retention curve of the fine earth is predicted by first fitting the logit transformed WC at -1500 kPa, $logit(\theta_{1500kPa})$, using a linear model,

$$logit(\theta_{1500kPa}) = f(\cdots) + \varepsilon \quad (37)$$

where $f(\cdots)$ is the linear function of the explanatory variables and ε is the uncertainty, which is assumed to be Gaussian distributed. The explanatory set of variables was optimised using the AIC. The response difference between different matric potentials (e.g. $\theta_{100\,kPa} - \theta_{1500kPa}$ and $\theta_{40\,kPa} - \theta_{100kPa}$) was then fit using the difference between logit-transformed responses as the response variable and the other variables as explanatory variables. The same procedure was repeated to span the water retention curve (0 to -1500 kPa) in seven matric potential increments; i.e. seven models were developed (Appendix L), the explanatory variables for each having been refined using the AIC selection process.

To explore the limitations and avenues for improvement of the logit PtF, we generated two variants, logit2 and logit3. Logit2 was essentially the same statistical model as the logit PtF but evaluated at the matric potential observed in the field at the time of sampling (θ_{FC}) instead of -10 kPa. This model could never be used in practice because matric potential at FC is rarely going to be available. Logit3 was a new linear regression model, which incorporated the logit-predicted WC plus two variables that were identified as significant to FC predictions in our practical model, namely increment depth (z) and the volume proportion of RFs. The significance of the two variables was determined by a variable scaling procedure, which is explained in more detail in Section 5.2.4. The model was calibrated using 70% of the measured data like the optimal and practical PtFs.

$$\theta_{FCstony} = b_1\theta_{10kPa} + b_2 z + b_3\chi + \alpha + \varepsilon \quad (38)$$

where b_1, b_2, b_3 are regression coefficients and α is the intercept parameter.

5.2.4 Comparing models

The five models were compared by using the validation dataset. Each of the models was used to predict the whole soil FC VWC of the validation dataset and were then ranked using the mean bias, mean absolute error (MAE) and the root mean square error (RMSE) of predictions,

$$bias = \frac{\sum_{i=1}^{N}(y_i - \hat{y})}{N} \quad (39)$$

$$MAE = \frac{\sum_{i=1}^{N}|y_i - \hat{y}|}{N} \quad (40)$$

$$RMSE = \sqrt{\frac{\sum_{i=1}^{N}(y_i - \hat{y})^2}{N}} \quad (41)$$

where y_i is the measured FC VWC, while $\hat{y}$ is the estimate derived from one of the PtFs. As per McNeill et al. (2018), a distribution of the three error measures above was made by bootstrap sampling the training data. An error estimate (e.g. RMSE) was derived using the validation dataset for each bootstrap, resulting in a distribution of each error measure. This analysis was used as the distributions give an indication of the likely range of error as a result of all possible training data, as opposed to the more limited information derived from the more commonly used single-value estimates of error.

To understand variation in model performance and to identify the influential variables (which were incorporated in the logit3 model), the "standardised" function in R was also used to centre all the model variables and scale by the standard deviation. Following this scaling procedure, the size of the coefficients can be used as a direct measure of relative importance – large coefficients indicate strong influence, and small coefficients indicate weak influence.

5.3 Results and Discussion

5.3.1 Descriptive statistics

Descriptive statistics of soil properties were similar between the training and validation datasets (Figure 17, Table 7). Soil textures fell within 6 of the 11 soil texture classes used by the NZSC (Milne et al., 1995). There were no samples in the clay, loamy clay, silt, sandy clay loam or silty clay textures. Textural distribution was biased toward the sand and silt-dominated textures with silt loam representing ~50% of the dataset (Table 7).

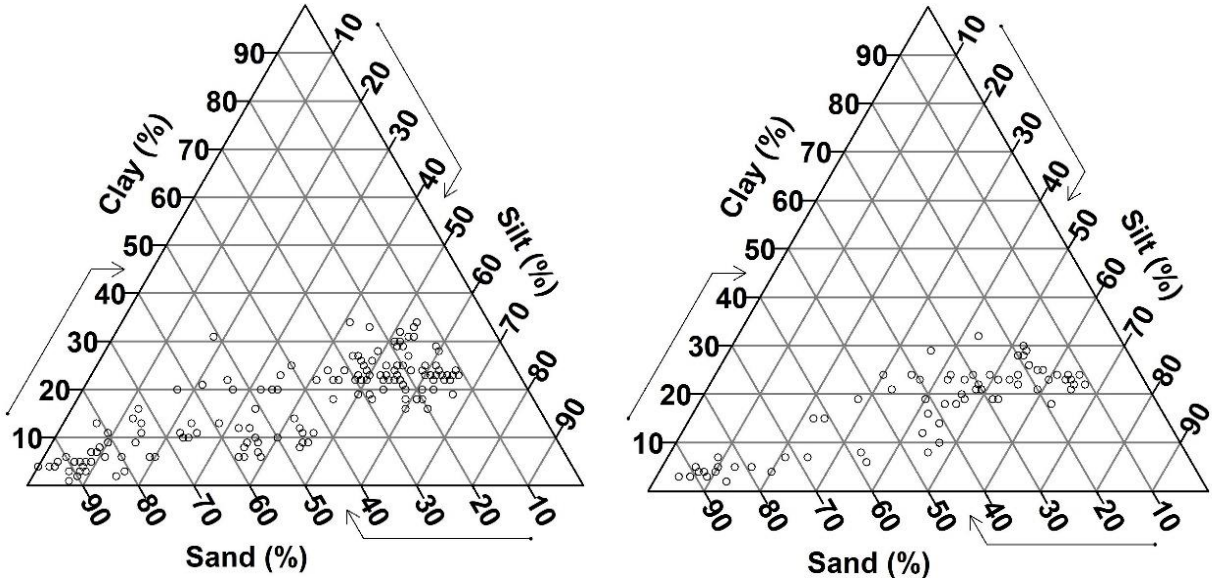

Figure 17 Soil texture diagram displaying textures for each increment in the training dataset (left) compared to those of the validation dataset (right).

The proportion of RFs to an increment's volume varied from 0% to 78.8% for the training dataset and 0% to 83.2% for the validation dataset (Table 7). On average, the volume of RFs accounted for <15% of the total soil volume in the 0-10 cm increment, but >60% for the 40-50 cm and 50-60 cm increments. Whole soil bulk density was very similar between training and validation datasets, increasing from an average of 1.37 g cm^{-3} in the 0-10 cm increment to 2.04 g cm^{-3} in the 50-60 cm increment. The organic carbon content of soils was 2.11% on average in the training dataset and 1.97% in the validation dataset (Table 7). In the topsoil (0-20 cm depth increments), the average organic carbon was 3.68% in the training dataset and 3.52% in the validation dataset, while in the subsoil (20-60 cm depth increments), the average carbon content decreased to 1.20% for the training dataset and 1.26% for the validation dataset. The FC VWC of the whole soil varied widely with texture and depth, ranging from 0.02-0.44 and 0.04-0.47 for the training and validation datasets, respectively. Brown Soils were the dominant soil order, accounting for 57% and 67% of the training and validation datasets, respectively, while Recent Soils accounted for 43% and 33% of the training and validation datasets, respectively. Pits were distributed over two geomorphic surfaces: ~79% were on Late Pleistocene glacial outwash in both datasets, 18 and 14% (training dataset-validation dataset, respectively) were on Holocene alluvial deposits and 4 and 6% (training dataset-validation dataset, respectively) were on Late Pleistocene to Holocene alluvial deposits.

Table 7 Descriptive statistics for training and validation databases.

		Training data set					Validation data set				
		Min	Median	Mean	SE	Max	Min	Median	Mean	SE	Max
Clay	%	1.00	20.0	17.9	0.68	34.0	2.00	21.0	17.5	1.02	32.0
Silt	%	0.00	46.0	40.5	1.52	67.0	4.00	46.0	40.6	2.20	67.0
Sand	%	11.0	29.0	41.7	2.07	96.0	11.0	34.0	41.9	3.07	93.0
Prop. RF	%	0.00	33.0	35.5	0.02	78.8	0.00	43.1	39.5	0.03	83.2
Carbon	%	0.21	1.88	2.11	0.10	5.15	0.26	1.58	1.97	0.14	4.98
-Topsoil~		1.97	3.90	3.68	0.18	5.15	1.62	3.57	3.52	0.32	4.98
-Subsoil>		0.21	1.17	1.20	0.08	3.30	0.26	1.24	1.26	0.10	2.95
Bulk	*	1.13	1.74	1.77	0.03	2.41	1.16	1.89	1.82	0.04	2.43
FC VWC	^	0.02	0.25	0.24	0.01	0.44	0.04	0.21	0.22	0.01	0.47

[+] whole soil bulk density (RFs and fine earth);
* g cm^{-3}; ^ m^3 m^{-3};
~ Average carbon (%) in 0-20 cm increments; > Average carbon (%) in 20-60 cm increments

5.3.2 Model structures and performance

The optimal PtF had an R^2=0.98 and included 12 of 23 variables once those that did not minimise the AIC were removed (Table 8).

Table 8 Multiple linear regression results for optimal PtF.

Coefficients		Estimate	Std Error	t-value	Pr(>|t|)	
(Intercept)		1.15	7.29E-01	1.58	0.116	
Depth	10-20 cm	-2.12E-02	6.07E-03	-3.50	6.29E-04	***
	20-30 cm	-2.49E-02	8.25E-03	-3.02	3.01E-03	**
	30-40 cm	-2.62E-02	1.01E-02	-2.59	0.0107	*
	40-50 cm	-2.34E-02	1.11E-02	-2.11	0.0363	*
	50-60 cm	-2.13E-02	1.19E-02	-1.79	0.0750	.
Particle.density		5.61E-01	2.37E-01	2.37	0.0194	*
Total.N		3.26E-01	4.46E-02	7.30	1.84E-11	***
Total.porosity		-2.55	1.293528	-1.97	0.0504	.
Phosphate.retention		9.32E-04	1.53E-04	6.10	9.3E-09	***
Fine.earth.bulk.density		-0.958	4.86E-01	-1.97	0.0509	.
Whole.soil.bulk.density		1.44E-01	3.30E-02	4.35	2.54E-05	***
Vol.proportion.RFs		-4.74E-01	4.31E-02	-11.0	8.87E-21	***
15.bar.WC		1.23E-03	3.42E-04	3.60	4.42E-04	***
Treatment.irrigated		1.13E-02	3.33E-03	3.39	9.12E-04	***
ω_1		-3.28E-04	4.33E-05	-7.58	3.87E-12	***
Geomorphic surface	Pleistocene	-2.41E-02	5.31E-03	-4.54	1.18E-05	***
	Pleistocene to Holocene	-1.55E-02	9.34E-03	-1.66	0.0987	.

Residual standard error: 0.01918 on 143 degrees of freedom
Multiple R-squared: 0.9783, Adjusted R-squared: 0.9757
F-statistic: 379.4 on 17 and 143 DF, p-value: < 2.2e-16
Significance codes: '***' 0.001 '**' 0.01 '*' 0.05 '.' 0.1 ' ' 1

The practical PtF, generated from 12 pre-selected, easily measured soil variables, had an R^2 of 0.95 and retained 6 of 12 variables after the AIC was applied (Table 9).

Table 9 Multiple linear regression results for practical PtF.

Coefficients		Estimate	Std Error	t-value	Pr(>|t|)	
(Intercept)		0.320	1.37E-02	23.3	1.78E-51	***
Depth	10-20 cm	-0.0120	6.80E-03	-1.76	0.0798	.
	20-30 cm	-0.0321	7.70E-03	-4.17	5.26E-05	***
	30-40 cm	-0.0344	8.74E-03	-3.93	1.30E-04	***
	40-50 cm	-0.0451	1.03E-02	-4.37	2.34E-05	***
	50-60 cm	-0.0530	1.09E-02	-4.88	2.74E-06	***
Vol.proportion.RFs		-0.307	1.34E-02	-23.0	1.29E-50	***
Treatment.irrigated		0.0124	4.41E-03	2.82	5.44E-03	**
SSA		0.00141	2.12E-04	6.64	5.6E-10	***
Geomorphic surface	Pleistocene	-0.0132	6.10E-03	-2.16	3.24E-02	*
	Pleistocene to Holocene	-0.00688	1.29E-02	-0.533	0.595	
Texture.group	Sandy	-0.0363	7.83E-03	-4.64	7.61E-06	***
	Silty	0.0164	8.20E-03	2.00	0.0470	*
Residual standard error: 0.02672 on 148 degrees of freedom						
Multiple R-squared: 0.9564, Adjusted R-squared: 0.9529						
F-statistic: 270.8 on 12 and 148 DF, p-value: < 2.2e-16						
Significance codes: '***' 0.001 '**' 0.01 '*' 0.05 '.' 0.1 ' ' 1						

The logit and logit2 PtFs are established models that did not require model formulation and thus no regression results are presented. The logit3 PtF, generated from three variables, had an R^2 of 0.95 and retained all three variables after the AIC was applied (Table 10).

Table 10 Multiple linear regression results for logit3.

Coefficients		Estimate	Std Error	t-value	Pr(>|t|)	
(Intercept)		0.193	2.04E-02	9.49	4.4E-17	***
logit.prediction		0.520	4.97E-02	10.5	1.21E-19	***
Depth	10-20 cm	-0.0179	7.14E-03	-2.51	0.0132	*
	20-30 cm	-0.0281	8.08E-03	-3.48	6.57E-04	***
	30-40 cm	-0.0292	9.47E-03	-3.08	2.45E-03	**
	40-50 cm	-0.0420	1.10E-02	-3.82	1.93E-04	***
	50-60 cm	-0.0432	1.21E-02	-3.56	4.98E-04	***
Vol.proportion.RFs		-0.244	1.44E-02	-16.9	6.17E-37	***
Residual standard error: 0.02889 on 153 degrees of freedom						
Multiple R-squared: 0.9474, Adjusted R-squared: 0.945						
F-statistic: 393.5 on 7 and 153 DF, p-value: < 2.2e-16						
Significance codes: '***' 0.001 '**' 0.01 '*' 0.05 '.' 0.1 ' ' 1						

The five PtFs produced distinct distributions of RMSE (Figure 18), bias and MAE (Table 11) when applied to the validation dataset.

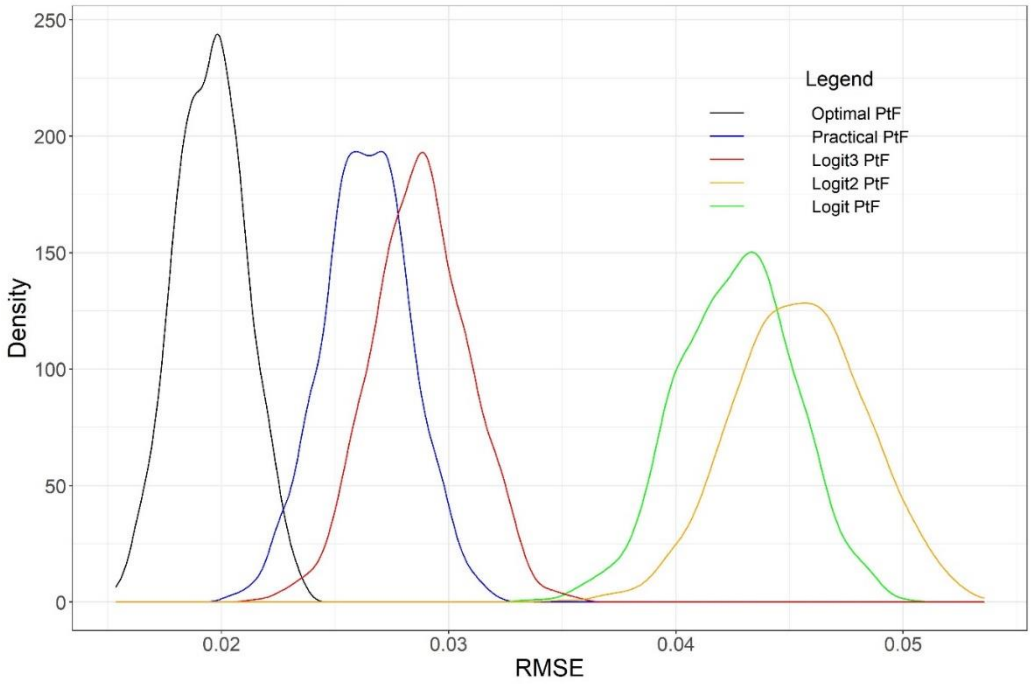

Figure 18 Density plots of the root mean square error for the five regression models for FC WC.

Ranked in order of lowest to highest bias, the PtFs follow the sequence: optimal, practical, logit3, logit2, and logit. The mean bias for all but the logit PtF were within ±0.01 m^3 m^{-3} of 0, showing the PtFs had no substantial positive or negative biases overall. The 0.027 bias of the logit PtF indicates a pattern of underestimation.

Table 11 Model performance based on the means of error measure distributions obtained from bootstrap sampling.

	Order	Bias	RMSE	MAE
Optimal PtF	1	0.0001	0.020	0.016
Practical PtF	2	0.001	0.026	0.021
logit3 PtF	3	0.0016	0.029	0.023
logit2 PtF	4	0.006	0.045	0.038
logit PtF	5	0.027	0.043	0.036

Despite displaying the best performance, the relative improvement of the optimal model in comparison to the practical model is only modest considering the increase in explanatory variables. We expected the optimal model would perform much better considering the practical model does not include a number of variables commonly associated with predicting soil VWC, such as carbon,

bulk density (whole soil or fine earth) or even continuous measures of texture (i.e. proportion sand, silt or clay) (Mohamed and Ali, 2006; Ostovari et al., 2015; Pollacco, 2008; Román Dobarco et al., 2019b; Santra et al., 2018). Regardless of the absence of these 'standard' variables, the RMSE of the practical PtF (0.026 m^3 m^{-3}) is still low when compared to the logit PtF or the performance of other PtFs in the literature, which commonly predict FC with RMSE >0.04 m^3 m^{-3} (Ostovari et al., 2015; Pollacco, 2008; Román Dobarco et al., 2019b).

Using the "standardised" scaling procedure in R, it was found that the proportion of RFs, geomorphic surface and nitrogen content were the most influential variables in the optimal PtF (Appendix M), while the practical model was mostly influenced by the proportion of RFs and depth (Appendix N). The depth variable in the practical model was correlated with several variables found in the optimal PtF (such as nitrogen and particle density) as seen in Figure 19. As such, depth may act as a proxy for several other variables, allowing the practical model to predict accurately even with a limited number of variables. These results are consistent with international literature that have also found depth to be a significant explanatory variable for many soil properties including soil carbon, texture, soil development and solute transport (Fontaine et al., 2007; Minasny et al., 2016; Vasques et al., 2010).

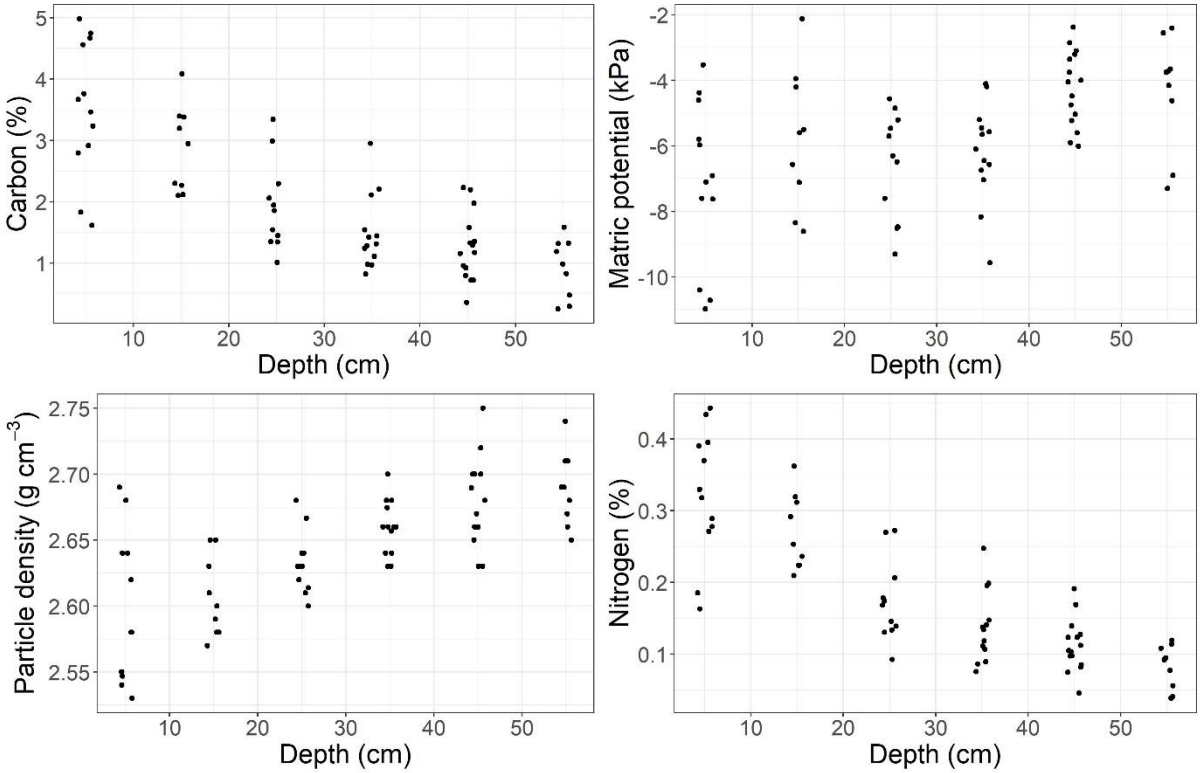

Figure 19 Correlations between soil variables (carbon, matric potential, particle density and total nitrogen) and depth. Note, data points within each increment have had slight adjustments to their depth to aid readability.

In contrast, the logit and logit2 PtFs did not include several of the variables used in both the optimal and practical models, which most likely caused the lower model performances. As the logit and logit2 PtFs are pre-existing models, which did not require a training dataset for calibration (like the other PtFs), they could be tested against the entire dataset. The average error for whole soil VWC showed logit predictions were less than the measured VWC at all depths, while the logit2 predictions were more evenly distributed around a mean error of 0 (Figure 20A and 20B). To understand the cause of this bias, the logit and logit2 predicted fine earth WCs were compared to the measured fine earth WC. The measured fine earth WC was greater than the logit predictions in all but the 50-60 cm increment (Figure 20C). Alternatively, logit2 predictions of fine earth WC generally exceeded measured fine earth WC at all depths except the 20-40 cm increments (Figure 20D).

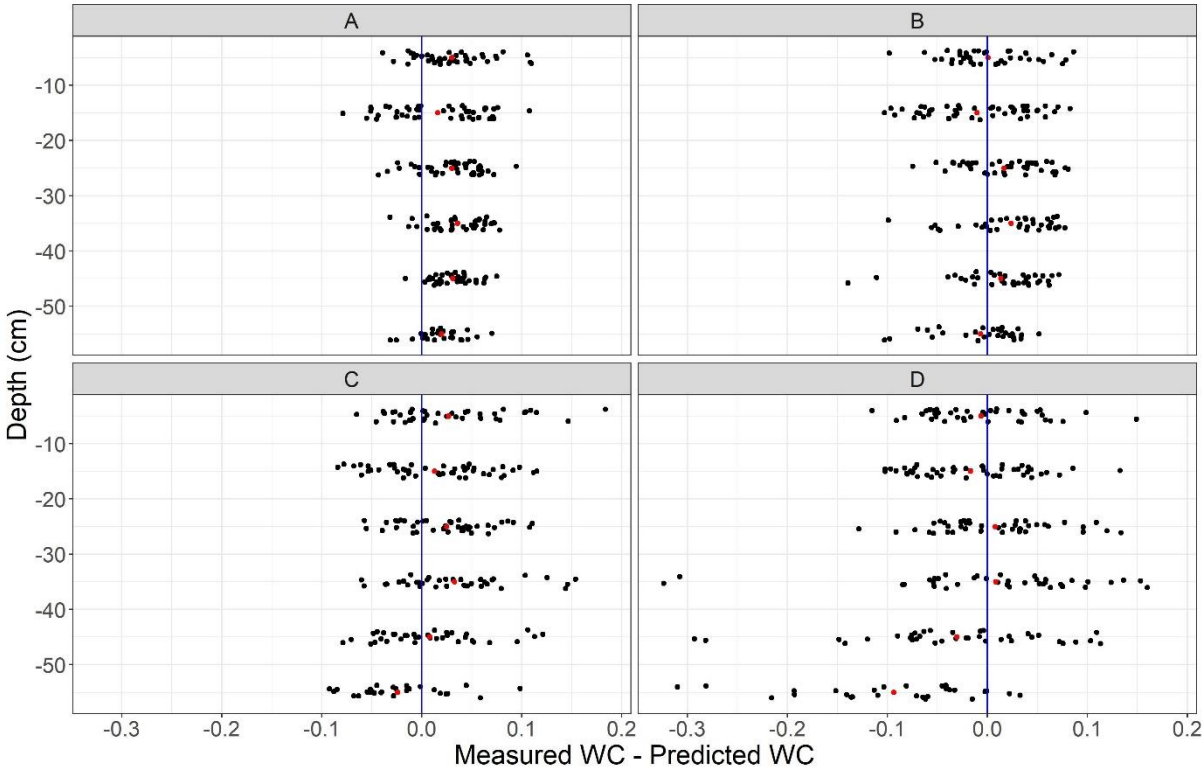

Figure 20 A: Measured total VWC – logit total VWC prediction, B: Measured total VWC – logit2 total VWC prediction, C: Measured fine earth VWC – logit fine earth VWC prediction, D: Measured fine earth VWC – logit2 fine earth VWC prediction. Blue line depicts zero error, red dots are the average error for an increment. Note, data points within each increment have had slight adjustments to their depth to aid readability.

These results demonstrate that on average, logit underestimates the WC of the fine earth, while logit2 maintains a near zero bias in the 0-40 cm increments with substantial overestimation in the 40-60 cm increments. However, as logit2 considers RFs to be inert (when they in fact hold water; Chapter 4), bias in total WC predictions tends towards zero or underestimation. For instance, in the 50-60 cm increment, logit2 (which takes into account actual matric potential) overestimates fine earth WC by 0.09 m^3 m^{-3} on average, but total WC is overestimated by only 0.007 m^3 m^{-3}. By chance,

the greater overestimation of fine earth WC by logit2 better compensates for the neglected WC of RFs in the 40-60 cm increments, resulting in logit2 having a lower average error compared to the logit PtF when predicting the whole soil WC.

The inclusion of depth and RF proportion variables in logit3 substantially improved model performance in comparison to logit, with logit3 demonstrating a similar accuracy to the practical model (Figure 21). Model performance may have improved because depth acts as a proxy for several variables, as discussed previously (Figure 19). Furthermore, including RF proportion as a predictor variable may capture the influence of the WC of the RFs, as well as the indirect effects RFs have on water retention of the fine earth, by way of changes to soil properties such as fine earth bulk density (Gargiulo et al., 2016; Shi et al., 2012) or carbon content (Bornemann et al., 2011; Schiedung et al., 2017).

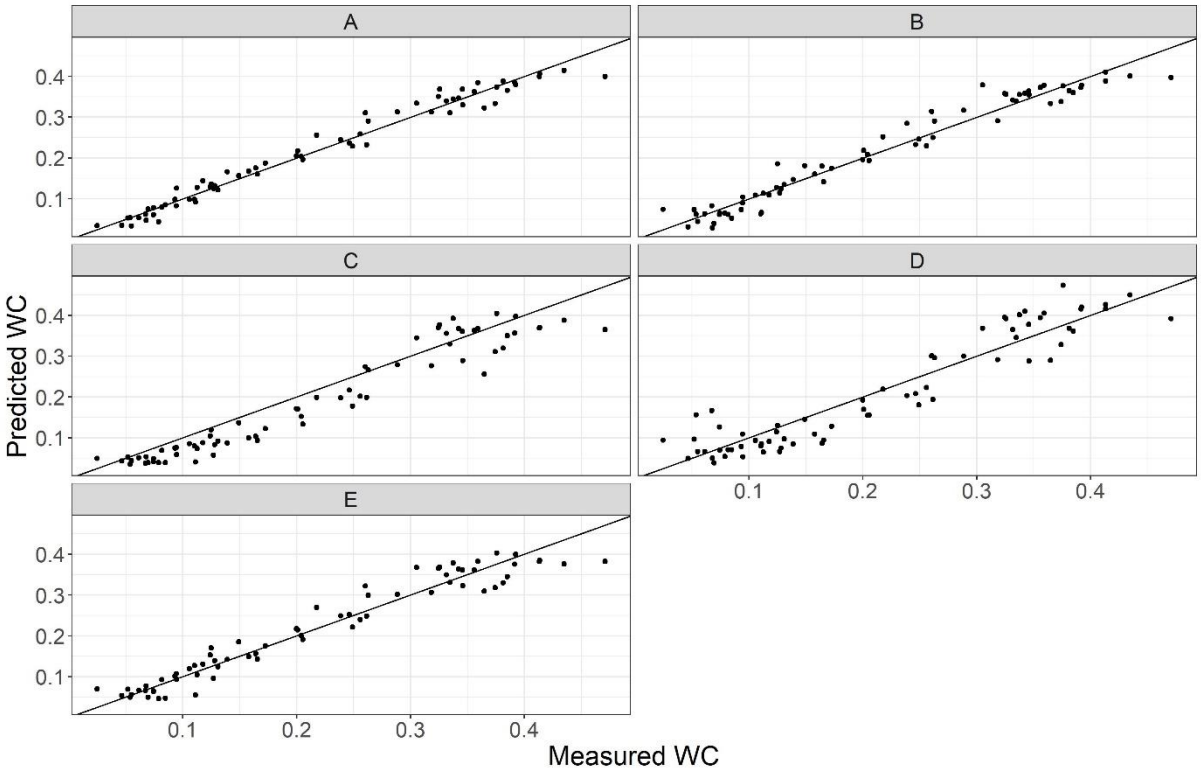

Figure 21 Predicted total FC WC as a function of measured total FC WC. A: optimal PtF, B: practical PtF, C: logit PtF, D: logit2 PtF and E: logit3 PtF.

There remain only three variables in the practical model (SSA, irrigation treatment and age of geomorphic surface) that are absent in logit3, which could explain the model's lower performance when compared to the practical PtF. When SSA was added to the logit3 PtF, the performance of the model was not notably different from the practical PtF. The SSA is a metric that may relate grain-scale properties to macro-scale physical and chemical properties of a porous medium (Petersen et al., 1996). Accordingly, Hillel (1980) suggested that SSA may become a more pertinent index for

characterising soil than the proportions of sand, silt and clay. Currently, SSA is more commonly used for determining soil WC at low matric potentials (Arthur et al., 2013; Chang and Cheng, 2018; Resurreccion et al., 2011), although our results suggest it could be relevant to FC estimates as well. In contrast, Petersen et al. (1996) found that SSA did not relate well with the WC at -10 kPa; however, they used different methods to estimate SSA, which can cause widely different results (de Jong, 1999; Petersen et al., 1996).

5.3.3 Implications and future work

Results of this study demonstrate that current assumptions for modelling stony soil FC could be significantly affecting accuracy of predictions. Assuming RFs do not hold water or have no effect on water retention of the fine earth leads to non-negligible, systematic error in soil water storage estimates, as demonstrated by the performance of the logit PtF. This model underestimated total soil VWC at FC because it underestimated fine earth WC and assumed no water in RFs. The fine earth under-estimate is partly attributable to evaluating the PtF at -10 kPa instead of the higher *in situ* matric potentials, as demonstrated by the improvement in the mean bias shown by the logit2 Ptf. The latter essentially applies the logit PtF at the extant matric potentials, which reduced the fine earth under-estimation, although the whole soil FC VWC remained an under-estimate, at least in part because water in RFs was still disregarded. When RF abundance was incorporated (logit3 PtF), the water those RFs contained was captured indirectly and estimates further improved.

We have identified depth and the volume proportion of RFs as important variables for reducing error when predicting FC WC of stony soils. Our results have potentially significant implications for developing better stony soil PtFs worldwide, as these variables are easy to measure (or estimate) and are generally already included in minimum datasets for soil survey and soil classification. However, further research is required to determine the importance of these variables in stony soils formed in depositional settings contrasting to those of our study. For instance, the significant influence of depth we found may disappear where stony soils are formed in diamicts such as debris flows or till. Similarly, the influence of the volumetric proportion of RFs is likely to vary with RF lithology and weathering (Poesen and Lavee, 1994; Tetegan et al., 2011), requiring different calibrations for each. Importantly, our results show even low porosity greywacke can have a significant effect on soil moisture storage at FC, demonstrating the need for PtFs that implicitly account for water held by RFs of varying lithologies. Results also indicate the potential for SSA as a useful predictor, especially as it is both cheap and quick to determine. Finally, our practical model offers an accurate method for predicting FC using information derived from a minimalistic field survey; however, to be used routinely in an operational way, the model needs to be tested using field-based assessments of soil texture and RF abundance instead of the lab measured values used in this study.

5.4 Conclusions

Results of this study demonstrate that hard sandstone RFs in Canterbury stony soils are not inert and can in fact cause significant error in FC WC predictions when the water held by RFs is not implicitly accounted for. However, the practical PtF we derived demonstrates that it is possible to accurately predict FC WC in stony soils, while only using explanatory variables that could be easily measured or estimated from a minimalistic field survey. This model also indicated the potential of SSA as an explanatory variable that is quick and cheap to determine. The logit model did not account for RF WC and tended to underestimate fine earth WC, resulting in a substantial bias in predictions for increments with high and low RF content. Alternatively, logit2 tended to overestimate fine earth WC in the lower increments, which by chance compensated for the neglected WC of RFs in the 40-60 cm increments, resulting in logit2 having a near-zero bias on average. However, incorporating depth and volumetric proportion of RFs as explanatory variables substantially improved prediction accuracy as demonstrated by the logit3 PtF. Our findings could have significant implications for the modelling of FC WC worldwide, as the effect of RFs (even those with much greater porosity than those measured in this study) are not currently accounted for in most PtFs. But, by including two variables (depth and volume proportion of RFs) that are already measured or estimated in most soil sampling projects, WC predictions may be significantly improved in stony soils. However, research must be repeated in soils that are not of alluvial origin and with RFs of varying weathering and lithology, to determine if depth and the proportion of RFs remain important predictor variables.

5.5 Appendix

Appendix L Explanatory variables selected in the logit models with the lowest AICc (corrected Akaike information criterion value) by backward selection. Retrieved from McNeill et al. (2018).

Response	Pedsize	ω2	ω1	Tephra	Strength	Topsoil	Rock class fines	Soil order	Topsoil & tephra	Topsoil rock class fines	ω2 & soil order	ω1 & soil order	ω2 & topsoil	ω1 & topsoil	ω1 & ω2	Topsoil & pedsize	Soil order & topsoil
Logit (θ1500 kPa)	✓	✓	✓		✓	✓	✓	✓					✓	✓	✓	✓	✓
Δ100, 1500 kPa	✓	✓	✓		✓	✓	✓	✓			✓	✓		✓	✓		
Δ40,100 kPa		✓	✓	✓	✓	✓	✓	✓				✓		✓	✓		
Δ20, 40 kPa	✓	✓	✓	✓		✓	✓	✓	✓	✓	✓	✓		✓	✓		
Δ10, 20 kPa	✓	✓	✓	✓	✓	✓	✓	✓	✓	✓		✓			✓		✓
Δ5, 10 kPa	✓	✓	✓	✓		✓	✓	✓	✓	✓		✓		✓		✓	✓
Δ0, 5 kPa	✓	✓	✓	✓		✓	✓	✓		✓		✓				✓	✓

Appendix M Standardised variables of optimal model.

Coefficients		Estimate	Std Error	t-value	Pr(>|t|)	
(Intercept)		0.157	0.0583	2.69	9.57E-03	**
Depth	0-10 cm	0.0239	0.135	0.178	0.860	
	10-20 cm	-0.117	0.0937	-1.25	0.218	
	20-30 cm	-0.0698	0.0615	-1.14	0.262	
	30-40 cm	4.36E-03	0.0654	0.0666	0.947	
	40-50 cm	0.0627	0.106	0.590	0.558	
Particle.density		0.0698	0.186	0.375	0.710	
Total.N		0.206	0.0723	2.85	6.37E-03	**
Total.porosity		-1.24	2.14	-0.578	0.566	
Phosphate.retention		0.132	0.0339	3.90	2.79E-04	***
Fine.earth.bulk.density		-1.14	2.16	-0.526	0.601	
Whole.soil.bulk.density		0.112	0.197	0.568	0.573	
Vol.proportion.RFs		-0.827	0.197	-4.19	1.11E-04	***
15.bar.WC		0.0489	0.0287	1.71	0.0940	.
Treatment.dryland		-0.0550	0.0233	-2.36	0.0222	*
ω_1		-0.161	0.0486	-3.32	1.69E-03	**
Geomorphic surface	Holocene	0.0607	0.0617	0.984	0.330	
	Pleistocene	-0.215	0.0699	-3.08	0.00333	**
Residual standard error: 0.1728 on 51 degrees of freedom						
Multiple R-squared: 0.9776, Adjusted R-squared: 0.9701						
F-statistic: 131 on 17 and 51 DF, p-value: < 2.2e-16						
Significance codes: '***' 0.001 '**' 0.01 '*' 0.05 '.' 0.1 ' ' 1						

Appendix N Standardised variables of practical model.

Coefficients		Estimate	Std Error	t-value	Pr(>|t|)	
(Intercept)		-0.0644	0.0565	-1.14	0.259	
Depth	0-10 cm	0.343	0.0737	4.66	2.00E-05	***
	10-20 cm	0.122	0.0792	1.54	0.129	
	20-30 cm	-0.0556	0.0653	-0.852	0.398	
	30-40 cm	-0.00656	0.0711	-0.092	0.927	
	40-50 cm	-0.129	0.0651	-1.98	0.0521	.
Vol.proportion.RFs		-0.747	0.0433	-17.2	4.65E-24	***
Treatment.dryland		-0.0804	0.0305	-2.64	0.0108	*
SSA		0.181	0.0396	4.57	2.78E-05	***
Geomorphic surface	Holocene	0.0337	0.0645	0.523	0.603	
	Pleistocene	0.0342	0.0608	0.563	0.576	
Texture.group	Loamy	-0.0004	0.0696	-0.00513	1.00	
	Sandy	-0.0607	0.0719	-0.843	0.403	
Residual standard error: 0.2266 on 56 degrees of freedom						
Multiple R-squared: 0.9577, Adjusted R-squared: 0.9487						
F-statistic: 105.7 on 12 and 56 DF, p-value: < 2.2e-16						
Significance codes: '***' 0.001 '**' 0.01 '*' 0.05 '.' 0.1 ' ' 1						

References

Arthur, E., Tuller, M., Moldrup, P., Resurreccion, A.C., Meding, M.S., Kawamoto, K., Komatsu, T., de Jonge, L.W., 2013. Soil specific surface area and non-singularity of soil-water retention at low saturations. Soil Sci. Soc. Am. J. 77(1), 43-53. https://doi.org/10.2136/sssaj2012.0262.

Bornemann, L., Herbst, M., Welp, G., Vereecken, H., Amelung, W., 2011. Rock fragments control size and saturation of organic carbon pools in agricultural topsoil. Soil Sci. Soc. Am. J. 75(5), 1898-1907. https://doi.org/10.2136/sssaj2010.0454.

Burnham, K., Anderson, D., 2002. Model Selection and Multi-Model Inference: A Practical Information-Theoretic Approach. 2nd ed. Springer-Verlag, New York.

Carrick, S., Fraser, P., Dennis, S., Knight, T., Tabley, F., 2013. Challenges for leachate monitoring from alluvial sedimentary soils. In: L.D. Currie, C.L. Christensen (Eds.), Accurate and Efficient Use of Nutrients on Farms, Occasional Report No. 26. Fertiliser and Lime Research Centre, Massey University, Palmerston North, New Zealand.

Chang, C.C., Cheng, D.H., 2018. Predicting the soil water retention curve from the particle size distribution based on a pore space geometry containing slit-shaped spaces. Hydrol. Earth Syst. Sci. 22(9), 4621-4632. https://doi.org/10.5194/hess-22-4621-2018.

Claydon, J.J., 1989. Determination of particle size in fine grained soils – pipette method. Division of Land and Soil Sciences Technical Record (LH5), DSIR Division of Land & Soil Sciences.

Coates, G., Cox, G.J., 2002. The Rise and Fall of the Southern Alps. Canterbury University Press Christchurch.

Cornell, J.A., 1981. Experiments with Mixtures. John Wiley and Sons, New York.

Cousin, I., Nicoullaud, B., Tetegan, M., de Forges, A.C.R., Arrouays, D., Bouthier, A., 2014. Estimating the available water content of highly heterogeneous soils including stony soils at the regional scale. Globalsoilmap: Basis of the Global Spatial Soil Information System. Taylor and Francis Group, London.

de Jong, E., 1999. Comparison of three methods of measuring surface area of soils. Can. J. Soil Sci. 79(2), 345-351. https://doi.org/10.4141/s98-069.

Fontaine, S., Barot, S., Barré, P., Bdioui, N., Mary, B., Rumpel, C., 2007. Stability of organic carbon in deep soil layers controlled by fresh carbon supply. Nature 450(7167), 277-280. https://doi.org/10.1038/nature06275.

Forsyth, P.J., Jongens, R., Barrell (Compilers), D.J.A., 2008. Geology of the Christchurch Area. Institute of Geological & Nuclear Sciences 1:250 000 geologial map 16. GNS Science, Lower Hutt, New Zealand.

Gargiulo, L., Mele, G., Terribile, F., 2016. Effect of rock fragments on soil porosity: a laboratory experiment with two physically degraded soils. Eur. J. Soil Sci. 67(5), 597-604. https://doi.org/10.1111/ejss.12370.

Gradwell, M., Birrell, K., 1972. Soil Bureau laboratory methods. C. Methods for physical analysis of soils. New Zealand Soil Bureau Scientific Report 10C.

Hanson, C.T., Blevins, R.L., 1979. Soil water in coarse fragments. Soil Sci. Soc. Am. J. 43(4), 819-820. https://doi.org/10.2136/sssaj1979.03615995004300040044x.

Hedley, C.B., Payton, I.J., Lynn, I.H., Carrick, S.T., Webb, T.H., McNeill, S., 2012. Random sampling of stony and non-stony soils for testing a national soil carbon monitoring system. Soil Res. 50(1), 18-29. https://doi.org/10.1071/SR11171.

Hewitt, A.E., 2010. New Zealand Soil Classification. Landcare Research Science Series no. 1. 3rd ed. Manaaki Whenua Press, Lincoln, New Zealand.

Hillel, D., 1980. Fundamentals of Soil Physics. Academic Press, New York.

Johnston, R., Barry, S., Bleys, E., Bui, E.N., Moran, C., Simon, D., Carlile, P., McKenzie, N., Henderson, B., Chapman, G., 2003. ASRIS: the database. Soil Res. 41(6), 1021-1036. https://doi.org/10.1071/SR02033.

Jones, D.P., Graham, R.C., 1993. Water-holding characteristics of weathered granitic rock in chaparral and forest ecosystems. Soil Sci. Soc. Am. J. 57(1), 256-261. https://doi.org/10.2136/sssaj1993.03615995005700010044x.

Kirschbaum, M.U.F., Giltrap, D.L., McNally, S.R., Liáng, L.L., Hedley, C.B., Moinet, G.Y.K., Blaschek, M., Beare, M.H., Theng, B.K.G., Hunt, J.E., Whitehead, D., 2020. Estimating the mineral surface area of soils by measured water adsorption. Adjusting for the confounding effect of water adsorption by soil organic carbon. Eur. J. Soil Sci. 71(3), 382-391. https://doi.org/10.1111/ejss.12892.

Leco, 2003. Total/Organic Carbon and Nitrogen in Soils. Organic Application Note 203-821-165, LECO Corporation, St. Joseph, MO.

Lilburne, L.R., Hewitt, A.E., Webb, T.W., 2012. Soil and informatics science combine to develop S-map: a new generation soil information system for New Zealand. Geoderma 170, 232-238. https://doi.org/10.1016/j.geoderma.2011.11.012.

McDowell, R.W., Noble, A., Pletnyakov, P., Haggard, B.E., Mosley, L.M., 2020. Global mapping of freshwater nutrient enrichment and periphyton growth potential. Sci. Rep. 10(1), 3568. https://doi.org/10.1038/s41598-020-60279-w.

McNeill, S.J., Lilburne, L.R., Carrick, S., Webb, T.H., Cuthill, T., 2018. Pedotransfer functions for the soil water characteristics of New Zealand soils using S-map information. Geoderma 326, 96-110. https://doi.org/10.1016/j.geoderma.2018.04.011.

Milne, J., Clayden, B., L., S.P., Wilson, A.D., 1995. Soil Description Handbook. Manaaki Whenua Press, Lincoln, New Zealand.

Minasny, B., Stockmann, U., Hartemink, A.E., McBratney, A.B., 2016. Measuring and modelling soil depth functions. In: A.E. Hartemink, B. Minasny (Eds.), Digital Soil Morphometrics. Progress in Soil Science. Springer International, Switzerland, pp. 225-240.

Mohamed, J., Ali, S., 2006. Development and comparative analysis of pedotransfer functions for predicting soil water characteristic content for Tunisian soils. Proceedings of the 7th Edition of TJASSST, 170-178.

Novák, V., Hlaváčiková, H., 2019. Applied Soil Hydrology. Springer, Cham, Switzerland.

Ostovari, Y., Asgari, K., Cornelis, W., 2015. Performance evaluation of pedotransfer functions to predict field capacity and permanent wilting point using UNSODA and HYPRES datasets. Arid Land Res. Manag. 29(4), 383-398. https://doi.org/10.1080/15324982.2015.1029649.

Parajuli, K., Sadeghi, M., Jones, S.B., 2017. A binary mixing model for characterizing stony-soil water retention. Agric. For. Meteorol. 244-245, 1-8. https://doi.org/10.1016/j.agrformet.2017.05.013.

Petersen, L.W., Moldrup, P., Jacobsen, O.H., Rolston, D.E., 1996. Relations between specific surface area and soil physical and chemical properties. Soil Sci. 161(1), 9-21. https://doi.org/10.1097/00010694-199601000-00003.

Poesen, J., 1990. Erosion process research in relation to soil erodibility and some implications for improving soil quality. In: J. Albaladejo, M. Stocking, I. Diaz (Eds.), Soil Degradation and Rehabilitation in Mediterranean Environmental Conditions. Consejo Superior de Investigaciones Cientificas, Spain, pp. 159-170.

Poesen, J., Lavee, H., 1994. Rock fragments in top soils: significance and processes. Catena 23(1), 1-28. https://doi.org/10.1016/0341-8162(94)90050-7.

Pollacco, J.A.P., 2008. A generally applicable pedotransfer function that estimates field capacity and permanent wilting point from soil texture and bulk density. Can. J. Soil Sci. 88(5), 761-774. https://doi.org/10.4141/CJSS07120.

R Core Team, 2016. R: A Language and Environment for Statistical Computing. R Foundation for Statistical Computing, Vienna, Austria.

Resurreccion, A.C., Moldrup, P., Tuller, M., Ferré, T.P.A., Kawamoto, K., Komatsu, T., de Jonge, L.W., 2011. Relationship between specific surface area and the dry end of the water retention curve for soils with varying clay and organic carbon contents. Water Resour. Res. 47(6). https://doi.org/10.1029/2010wr010229.

Román Dobarco, M., Bourennane, H., Arrouays, D., Saby, N.P.A., Cousin, I., Martin, M.P., 2019a. Uncertainty assessment of GlobalSoilMap soil available water capacity products: a French case study. Geoderma 344, 14-30. https://doi.org/10.1016/j.geoderma.2019.02.036.

Román Dobarco, M., Cousin, I., Le Bas, C., Martin, M.P., 2019b. Pedotransfer functions for predicting available water capacity in French soils, their applicability domain and associated uncertainty. Geoderma 336, 81-95. https://doi.org/10.1016/j.geoderma.2018.08.022.

Santra, P., Kumar, M., Kumawat, R., Painuli, D., Hati, K., Heuvelink, G., Batjes, N., 2018. Pedotransfer functions to estimate soil water content at field capacity and permanent wilting point in hot Arid Western India. J. Earth Syst. Sci. 127. https://doi.org/10.1007/s12040-018-0937-0.

Saunders, W.M.H., 1965. Phosphate retention by New Zealand soils and its relationship to free sesquioxides, organic matter, and other soil properties. N. Z. J. Agric. Res. 8(1), 30-57. https://doi.org/10.1080/00288233.1965.10420021.

Scheinost, A.C., Sinowski, W., Auerswald, K., 1997. Regionalization of soil water retention curves in a highly variable soilscape, I. Developing a new pedotransfer function. Geoderma 78(3), 129-143. https://doi.org/10.1016/S0016-7061(97)00046-3.

Schiedung, H., Tilly, N., Hütt, C., Welp, G., Brüggemann, N., Amelung, W., 2017. Spatial controls of topsoil and subsoil organic carbon turnover under C3–C4 vegetation change. Geoderma 303, 44-51. https://doi.org/10.1016/j.geoderma.2017.05.006.

Schoeman, J.L., Kruger, M.M., Loock, A.H., 1997. Water-holding capacity of rock fragments in rehabilitated opencast mine soils. S. Afr. J. Plant Soil 14(3), 98-102. https://doi.org/10.1080/02571862.1997.10635089.

Shi, Z.J., Xu, L.H., Wang, Y.H., Yang, X., Jia, Z., Guo, H., Xiong, W., Yu, P., 2012. Effect of rock fragments on macropores and water effluent in a forest soil in the stony mountains of the Loess Plateau, China. Afr. J. Biotechnol. 11(39), 9350-9361. https://doi.org/10.5897/AJB12.145.

Tetegan, M., Nicoullaud, B., Baize, D., Bouthier, A., Cousin, I., 2011. The contribution of rock fragments to the available water content of stony soils: proposition of new pedotransfer functions. Geoderma 165(1), 40-49. https://doi.org/10.1016/j.geoderma.2011.07.001.

UMS, 2009. User manual: T5/T5x pressure transducer tensiometer. UMS GmbH München.

Vasques, G.M., Grunwald, S., Comerford, N.B., Sickman, J.O., 2010. Regional modelling of soil carbon at multiple depths within a subtropical watershed. Geoderma 156(3), 326-336. https://doi.org/10.1016/j.geoderma.2010.03.002.

Vereecken, H., Maes, J., Feyen, J., 1990. Estimating unsaturated hydraulic conductivity from easily measured soil properties. Soil Sci. 149(1), 1-12.

Wang, H.F., Xiao, B., Wang, M.Y., Shao, M.A., 2013. Modeling the soil water retention curves of soil-gravel mixtures with regression method on the loess plateau of China. Plos One 8(3). https://doi.org/10.1371/journal.pone.0059475.

Webb, T.H., 2003. Identification of functional horizons to predict physical properties for soils from alluvium in Canterbury, New Zealand. Soil Res. 41(5), 1005-1019. https://doi.org/10.1071/SR01077.

Webb, T.H., Lilburne, L.R., 2011. Criteria for Defining the Soil Family and Soil Sibling: the Fourth and Fifth Categories of the New Zealand Soil Classification. Landcare Research Science Series No. 3. Manaaki Whenua Press, Lincoln, New Zealand.

Wu, W.-b., Yu, Q.-y., Peter, V.H., You, L.-z., Yang, P., Tang, H.-j., 2014. How could agricultural land systems contribute to raise food production under global change? J. Integr. Agric. 13(7), 1432-1442. https://doi.org/10.1016/S2095-3119(14)60819-4.

Chapter 6

Measuring the water retention curve of low porosity rock fragments: a novel suction plate methodology

The manuscript has been accepted by *European Journal of Soil Science*:

Robertson B.B., Gillespie J.D., Carrick S.T., Almond P.C., Payne J., Chau H.W. and Smith C.M.S., 2021. Measuring the water retention curve of rock fragments: A novel repacked core methodology. European Journal of Soil Science, 1-7. https://doi.org/10.1111/ejss.13181

6.1 Introduction

Hydraulic characteristics of unsaturated soils, namely the water retention curve (WRC), serve as key input data in the quantitative assessment of water storage and drainage in agricultural soils. Over the past decade, when the WRCs of soils including rock fragments (RFs) have been investigated, it has been found that RFs can store appreciable quantities of water (Parajuli et al., 2017; Poesen and Lavee, 1994; Tetegan et al., 2011). However, existing research has concentrated on porous RFs, while few studies that have targeted low porosity RFs. Though this focus is to be expected, there are areas such as the Canterbury Plains of New Zealand, on which two thirds of irrigated land includes stony soils formed in hard sandstone alluvium (Carrick et al., 2013). In New Zealand, stony soils are classified as soils with ≥35% RFs by volume, extending from a depth within 45 cm of the soil surface to a depth >100 cm (Webb and Lilburne, 2011). Due to the large volume of RFs in stony soils, even RFs with a low porosity could account for a substantial quantity of a soil's available water (Jones and Graham, 1993).

The low porosity of Canterbury RFs could mean current methods of measuring WRCs in stony soils are not accurate enough to elucidate the water retention of Canterbury's fine sandstone RFs. Typically, RF WRCs are measured using single RFs (Cousin et al., 2003; Novak and Surda, 2010) or in cores with volumes <200 cm^3 (Schoeman et al., 1997; Wang et al., 2013). Considering the field capacity (FC) volumetric water content (VWC) of Canterbury RFs is 0.07 or less (refer to Chapter 4), a single RF or a small repacked core (30% RFs and 200 cm^3 core) has little water (<4.2 g), and consequently, determinations of RF WRCs at these characteristic volumes are prone to error. In addition, methods using repacked cores have assumed that the porosity of fine earth (FE) remains the same between cores with varying RF volumes (Schoeman et al., 1997). This assumption permits the WRC of RFs to be determined by regression analysis of data from cores with varying RF proportion, or by subtracting the WRC of stony cores by the WRC of cores containing FE only.

However, numerous studies have found that the FE bulk density and porosity of a soil is significantly affected by variation in RF volume (Fiès et al., 2002; Gargiulo et al., 2016; Poesen and Lavee, 1994; Torri et al., 1994; van Wesemael et al., 1995), which indicates the above assumption is likely to be invalid.

The aim of this chapter is to test a method of determining the WRC of low porosity RFs that overcomes the limitations described above. The method uses 1) suction plates, which permits a larger repacked core to be used, mitigating the small water volume effect; and 2) includes glass fragments (GFs) as an ostensibly inert component to minimise variations in FE characteristics induced by varying clast volume.

6.1.1 Experimental design

The simplest solution for increasing the volume of RFs and the water they hold (and thereby reducing relative errors) would be to increase the volumetric proportion of RFs in the repacked cores, for instance from 30% to >60%. However, a 30% volumetric proportion usually corresponds to the transition between a matrix-supported and a clast-supported state, where RFs are in contact (Milne et al., 1995). These contact points can store water (Poesen and Lavee, 1994; Schoeman et al., 1997) and as such, artificially increase the observed water retention of the RFs. Also, contact between RFs inhibits the ability to pack soils to specific bulk densities, making repacked cores with high RF proportions impractical (Naseri et al., 2019).

The second option would be to increase the volume of the repacked cores and in so doing, increase the absolute volume of RFs for the same 30% volumetric proportion. However, increases in the dimensions of a core can compromise the accuracy of measurements. Repacked cores are commonly constrained to a height and diameter of ~5 cm to limit the total volume so that equilibration times are not excessive. Moreover, large-diameter cores present problems for handling when weighing, as the weight of the material in the core can cause fissures and cracks without adequate support, especially in coarse-textured soils. A limited core height is preferable because it restricts the range of matric potential that occurs down a core (due to hydrostatic equilibrium) when it equilibrates with the underlying vacuum plate.

We develop a method to exploit the benefits of a large diameter core by constructing a suction plate-core containment system that can be weighed as a unit, whereby the plate and core are never separated once the experiment begins. As a result, the diameter of the core is only restricted by the size of the vacuum plate, allowing us to use cores with an internal diameter (ID) of 19.4 cm. The experimental system was comprised of ten 23 cm-square polyethylene suction plates (ecoTech Umwelt-Meßsysteme GmbH, Bonn, Germany). The suction plates had a mean pore width of 0.45 µm,

and an air entry value of -100 kPa. Each plate was placed in a container with self-adhesive sealer around the lid to limit water loss from evaporation, with a vacuum tube from the plate base connected to a vacuum pump via a manifold to provide basal suction to the cores.

The container and plate were connected to the rest of the vacuum system (manifold, drainage containers and vacuum pump; Figure 22) via a shut-off valve. The valve is directional, allowing the vacuum to be released from the plate, while still maintaining the vacuum in the rest of the system. When the vacuum was released, the container, plate and core (which will be collectively classified as a core setup) could be disconnected from the system and weighed. This was repeated for each core setup. After all the core setups were weighed, the vacuum system was returned to atmospheric pressure so that the core setups could be reconnected. When the system was open to atmospheric pressure, it was prone to air pockets which can cause variation in the vacuum that is applied to each of the plates. To account for this, the system was air-filled (as opposed to the conventional water-filled systems) except for any water that may be draining at the time. The air-filled system was prone to drainage tubes developing water plugs, so all drainage tubing had an ID of 8 mm (bar the 4 mm ID tube connecting the drainage plate to the valves), to reduce capillarity so that water plugs could not form.

The system (Figure 22) incorporated manifolds (100 mm outer diameter PVC pipe) to prevent any vacuum gradient that may arise for plates located further from the vacuum pump. T5 pressure transducer tensiometers (UMS, 2009) were used to ensure the applied vacuum was consistent across the plates in the system. The manifolds were fixed at a slight angle to facilitate water flow into a drainage vessel. The drainage vessel was connected in turn to a vessel containing silica gel, which dehumidified the air before it reached the vacuum pump.

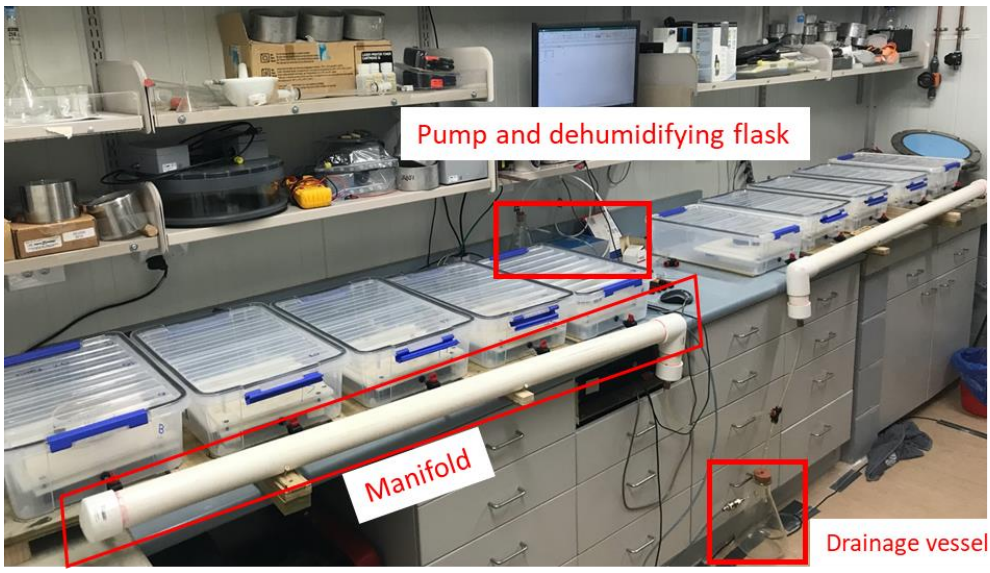

Figure 22 Vacuum system.

The VWC of RFs in repacked cores at a given matric potential can be determined from the relationship between core water content (WC) and the proportion of RFs. This approach exploits the different water-holding characteristics of each component. To overcome the effect of varying RF proportion on FE characteristics we varied RF volumetric proportion from 3-30% but added GFs when necessary to maintain the total clast content at 30% (Table 12). The WC of the core can be described by the following,

$$\theta_T = \mathrm{X}_{RF}(\theta_{RF} - \theta_{GF}) + \theta_{FE}(1 - C) + \mathrm{C}\theta_{GF} \quad (42)$$

The full derivation of Equation 42 is given in Appendix O. From this equation, it can be seen that a plot of core WC vs RF volumetric proportion should be linear, with a slope that is given by the RF WC and the GF WC. By assuming GFs are inert, the WC of RFs may be derived by the slope coefficient of a linear regression with core WC as the response variable and volumetric proportion of RFs as an explanatory variable.

Table 12 The volumetric proportion of each fraction that make-up the repacked core treatments.

Core	Proportion of core volume (%)		
	RF	GF	FE
1	3	27	70
2	6	24	70
3	9	21	70
4	12	18	70
5	15	15	70
6	18	12	70
7	21	9	70
8	24	6	70
9	27	3	70
10	30	0	70

6.2 Materials and methods

RFs were sourced from the B-horizon (30-60 cm depth) of a Balmoral stony soil located at the Ashley Dene Research Farm, Canterbury (Webb and Bennett, 1986). Samples were wet sieved into RF size classes (2-6 mm, 6-12 mm and >12 mm), RFs between 2-6 mm (to be used later for measuring -1500 kPa) and 6-12 mm were collected, while the larger RFs and FE were discarded. The collected RFs were cleaned of adhered FE by agitation in a bottle of water and coarse sand, before being submerged in water for a minimum of four weeks. Every couple of days, saturating RFs were agitated to dislodge air bubbles that may have formed on or within the RFs.

After the saturation period, an ~500 g sub-sample of 6-12 mm RFs were placed on a damp cloth and agitated to remove excess water (surface water and water held at RF-RF contact points) before the

saturated mass of the RFs was measured. The volume of the 6-12 mm RFs were then measured using the volume displacement method, and then the bulk density of the RFs (ρ_{RF}) and saturated gravimetric WC of the RFs ($w_{RF,S}$) were determined from the 105°C oven-dried mass.

The GFs were prepared by hitting 17-20 mm Nouveau garden glass gemstones with a centre punch and hammer (Figure 23). The GFs were then wet sieved; fragments with diameters between 6-12 mm were collected. The density of the GFs (ρ_{GF}) was determined using the same method as for the RFs.

Figure 23 Glass fragments.

The FE used for the repacked cores was silica sand. To increase uniformity, the FE was sieved to between 63 and 250 microns; 25% by weight was material between 63 and 125 microns, 75% was material between 125 and 250 microns. Sieved FE was mixed thoroughly before a subsample of ~400 g was used to determine its gravimetric WC (w_{FE}). The target FE dry bulk density (ρ_{FE}) for cores was 1.1 g cm^{-3}.

The materials (FE, RFs and GFs) were packed into cores of PVC, which were 4.9 cm in height with an inner diameter of 19.4 cm, with a layer of fine mesh secured to the base. The total core volume (V_{core}) was 1441 cm^3. Each core was packed in two equal increments, with the material for each increment weighed and bagged separately to ensure uniformity between the increments. Using the volumetric proportions of the RFs (χ_{RF}), GFs (χ_{GF}) and FE (χ_{FE}) outlined in Table 12, the mass of saturated 6-12 mm RFs ($M_{RF,trt}$), oven dried GFs ($M_{GF,trt}$) and sieved FE ($M_{FE,trt}$) required for each of the two packing increments was determined by:

$$M_{RF,trt} = 0.5 * V_{core} * \chi_{RF} * \rho_{RF} * (1 + w_{RF,s}) \quad (43),$$

$$M_{GF,trt} = 0.5 * V_{core} * \chi_{GF} * \rho_{GF} \quad (44),$$

and

$$M_{FE,trt} = 0.5 * V_{core} * \chi_{FE} * \rho_{FE} * (1 + w_{FE}) \quad (45).$$

For each core increment, the FE was first to be weighed and sealed in a watertight bag. As the FE had such a low WC (0.001 g g^{-1}), a mass of water (M_{water}) was added to the bagged FE to increase the gravimetric WC to 0.05, which is a suitable WC for packing sand as per the methods of Dane and Hopmans (2002). The mass of water was determined by:

$$M_{water} = 0.5 * V_{core} * \chi_{FE} * \rho_{FE} * 1.05 - M_{FE,trt} \quad (46).$$

For two hours, the FE and M_{water} for each increment were intermittently mixed within the watertight bags to homogenise FE WC. The 6-12 mm RFs were then added to each bag of moist FE. Like the RFs weighed for the RF bulk density measurement, saturated RFs were first agitated in a moist cloth before being weighed. The GFs were then weighed before being agitated in a moist cloth so that the surface moisture of the GFs was similar to the saturated RFs. The material (FE, RFs and GFs) for each of the increments were then thoroughly mixed within the watertight bags. A core was then placed on a thin aluminium baseplate before the material from the first increment was added and lightly levelled out by hand (Figure 24). The baseplate was used to keep the soil mixture supported following the packing process. The increment material was evenly compacted to a height of 2.45 cm (half the height of the core) using a plastic tamper propelled by a hydraulic jack. The plastic tamper had a diameter that was ~2 mm less than the internal diameter of the cores.

Figure 24 Photoplate of the compaction process.

A second core was then taped on top of the half-filled core before the material for the second increment was added, levelled and compacted (Figure 24). The second core was used to ensure no

material from the second increment was lost during the compaction procedure, which ended when the material from the second increment was flush with the top of the core. Repacked cores (with the base plates) were then saturated with degassed water by partial immersion for four days.

Once saturated, cores (still supported by the baseplate) were removed from the water, one at a time, and allowed to drain for ~10 seconds. One edge of the core was then placed on a suction plate, before slowly removing the baseplate, allowing the core to be supported until it was in full contact with the plate, minimising disturbance to the soil. A 1 mm thick layer of silica flour, formed to the same diameter as the core, ensured connectivity between the base of the core and the suction plate. Water retention was measured at seven matric potentials: -3 kPa, -6 kPa, -10 kPa, -20 kPa, -40 kPa, -60 kPa and -80 kPa. After equilibrating at each matric potential (which took 7-12 days), water in the drainage vessel was emptied before the next matric potential was set. Over the course of the experiment, condensation built up on container lids. When cores equilibrated, condensation was removed with paper towels, and then core setups were weighed, thus treating condensation like water drained from the core.

Once equilibrium was reached at -80 kPa, the soil core setups (container, vacuum plate and core) were weighed for a final time ($M_{core,80kPa}$). As the applied suction increased, some soil shrinkage occurred during the experiment. To quantify shrinkage, a layer of plastic wrap was laid over each core (following their final weight measurement) and pressed down until the surface of the soil in the core was covered. Water was then added until it was flush with the top of the core and the volume of water used was recorded (V_{H2O}). The soil/RF/GF material was then removed from the core, weighed ($M_{whole,80kPa}$), oven-dried at 105°C and weighed again ($M_{whole,OD}$). The whole soil bulk density at matric potential h ($\rho_{whole,h}$) was calculated assuming linear shrinkage between saturation and the final matric potential (h_{final}),

$$\rho_{whole,h} = \frac{M_{whole,OD}}{V_{core} - V_{H2O} * \frac{h}{h_{final}}} \quad (47)$$

The gravimetric WC of the whole soil at matric potential h ($W_{whole,h}$) was calculated by,

$$W_{whole,h} = \frac{(M_{whole,80kPa} - M_{whole,OD}) + (M_{core,h} - M_{core,80kPa})}{M_{whole,OD}} \quad (48)$$

where $M_{core,h}$ represents the mass of the soil core setup when equilibrated at matric potential h. These whole soil gravimetric WCs were then converted to volumetric WC ($\theta_{whole,h}$) by

$$\theta_{whole,h} = W_{whole,h}\left(\frac{\rho_{whole,h}}{\rho_w}\right) \quad (49)$$

in which ρ_w is the density of water which was assumed to be 1.00 g cm^{-3}. Using the linear regression (Equation 42) described in Section 6.1.1, the VWC of the RFs can be estimated using the whole soil volumetric WC and the volumetric proportion of the RFs. As an indication of regression stability, the standard error of the slope at each matric potential was calculated in sequence while decreasing the number of cores used in the regression from 9 to 3. This test calculates the standard error for all possible combinations of cores that can occur within the regression, for instance, when all nine cores are used, only one combination of cores can be used; however, when eight cores are used, nine combinations are possible and so on. Mean standard errors of the slope were then calculated for regression combinations with the same number of cores used in the analysis, i.e. a mean standard error for all the regressions that used eight cores in the analysis. If the mean standard error of the slope changes drastically for regressions using fewer cores, this indicates the results are sensitive to the layout of the experiment, while if the mean standard error of the slope does not change, this indicates the estimation process is stable.

To complete the WRC, the RF WC at thirteen matric potentials between -100 and -1700 kPa were measured. The range of matric potentials was achieved by air drying thirteen samples of saturated 2-6 mm RFs for varying lengths of time (between 50 and 75 minutes) at a constant temperature (25°C) and humidity (60%). To ensure uniform drying of all surfaces, the 2-6 mm RFs were stirred every 10 minutes. A WP4C Dewpoint Potentiometer was used to determine the matric potential of the RFs. After weighing, the air-dried 2-6 mm RFs ($M_{2.6,h}$) were then oven-dried at 105°C ($M_{2.6,OD}$) and the volumetric WC ($\theta_{2.6,h}$) at matric potential h was determined,

$$\theta_{2.6,h} = \frac{M_{2.6,h} - M_{2.6,OD}}{M_{2.6,OD}} \left(\frac{\rho_{RF}}{\rho_w}\right) \quad (50)$$

The WRC (a combination of vacuum plate and dewpoint potentiometer readings) was fit to the van Genuchten model (van Genuchten, 1980) using the SWRC Fit Version 3.0 software (Seki, 2007), according to

$$\theta = \theta_r + (\theta_s - \theta_r) * \left[\frac{1}{1+(\alpha h)^n}\right]^m \quad (51),$$

where θ_r is the residual WC, θ_s is the saturated WC, α relates to the inverse of the air entry value, h is matric potential, and m and n are empirical shape defining parameters. Core 3 (RF volumetric proportion = 0.09; Table 12) had a systematically high VWC at all matric potentials and was thus removed from the analysis. The fitted model was used to predict VWC of RFs at specific matric potentials, such as wilting point (-1500 kPa). The uncertainty of these WC predictions was estimated by generating 1000 realisations of the model parameters using the nominal values and their standard errors generated by the SWRC Fit software. The WC at the specified matric potential was then

predicted using the 1000 realisations of the model parameters. The standard deviation of the output was taken as the uncertainty of the predicted WC. This approach assumes that the parameters are independent (when they are jointly dependent), but this is a reasonable simplification, which only results in the variability being slightly higher than is the case.

6.3 Results and discussion

Results show that the measurement method was accurate enough to elucidate the WRC of low porosity greywacke RFs (Figure 26). When compared to other research and the different methods of measuring RF WRCs, we found the standard errors of our calculated WCs (Table 13) was relatively small. Brouwer and Anderson (2000) measured the VWC of nonmagnetic ironstone gravel at -20 kPa using small repacked cores and a suction table. The average standard error calculated on the ironstone gravels (0.027) was over three times greater than what was measured in this study at -20 kPa (0.007). Still, the relative standard error between studies was almost the same (11% and 15%, respectively). Cousin et al. (2003) measured individual RFs of calcareous origin with a pressure plate apparatus and had a standard error of 0.12 and relative error of >100% at -1 kPa. Though not direct comparisons of method performance, the above results indicate that the method developed in this study performed well. High numerical precision notwithstanding, our assumption that GFs do not retain water is a potential source of error, especially as Fiès et al. (2002) found <6 mm GFs had VWCs of 0.02 and 0.04 at -3 and -5 kPa, respectively. However, Fiès et al. (2002) used cores with 100% GFs, which optimises the number of GF contact points and hence the amount of water retained by the GFs (as discussed in Section 6.2). As clast proportion was maintained at 30% for this study (which minimises clast contact points), the water retention of GFs in this study is likely to be much lower than was measured by Fiès et al. (2002).

Table 13 Regression of whole soil WC at selected matric potentials, where the slope is equal to the VWC of RFs.

Dependant variable	Regression equation	R^2	Slope (RF VWC)	SE* of the slope	SE*%
3 kPa VWC	$\theta_{whole,h} = 0.092\chi_{RF} + 0.175$	0.58	0.09	0.030	33%
6 kPa VWC	$\theta_{whole,h} = 0.037\chi_{RF} + 0.072$	0.44	0.04	0.016	43%
10 kPa VWC	$\theta_{whole,h} = 0.052\chi_{RF} + 0.042$	0.72	0.05	0.012	23%
20 kPa VWC	$\theta_{whole,h} = 0.047\chi_{RF} + 0.034$	0.88	0.05	0.007	15%
40 kPa VWC	$\theta_{whole,h} = 0.044\chi_{RF} + 0.029$	0.90	0.04	0.006	14%
60 kPa VWC	$\theta_{whole,h} = 0.042\chi_{RF} + 0.017$	0.75	0.04	0.009	21%
80 kPa VWC	$\theta_{whole,h} = 0.046\chi_{RF} + 0.010$	0.68	0.05	0.012	26%

*SE means standard error.

It was noted during the experiment that the number of cores used for the regression might hinder the method's ability to be used routinely in an operational way. By calculating the standard error of

the slope as cores were removed from the analysis, we could get an indication of method accuracy when fewer cores were used. The mean standard error of the slope varied little with the number of cores used in the regression, indicating that the estimation process is reasonably stable (Figure 25). As such, the process of estimation does not seem to critically depend on having nine cores, with fewer cores capable of producing satisfactory results.

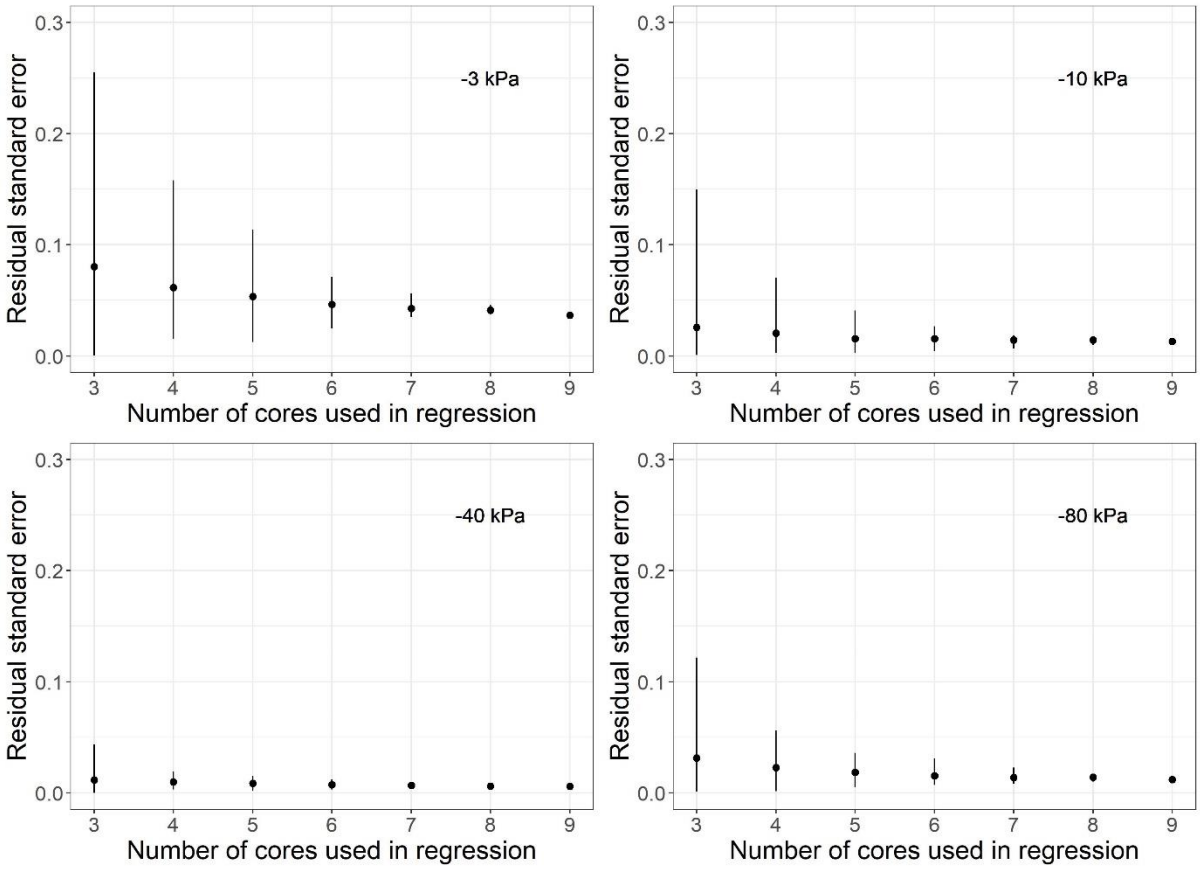

Figure 25 Range of standard error when varying numbers of soil cores are used in the analysis. The standard error is applicable to the slope and thus the VWC of the RFs.

The van Genuchten model was fit using all data points except -6 kPa, which deviated from the results of the other matric potentials (Figure 26). This deviation is likely due to the covid-19 lockdown requirements, which made it necessary for the experiment to be relocated while cores were equilibrating at -6 kPa. Water held by RFs was released at relatively high matric potentials, with VWC proportionally decreasing by 44% between -3 kPa (0.09 ± 0.03) and -10 kPa (0.05 ± 0.01). The available water holding capacity (AWC), defined as the difference between the WC determined at -10 kPa and the predicted -1500 kPa WC (0.02 ± 0.01) was equivalent to 0.03 ± 0.02 on a volumetric basis, of which, about half was released by -80 kPa. Schoeman et al. (1997), studying fine-grained micaceous sandstone RFs (4-10 mm), found the VWC released between -33 kPa and -1500 kPa was over double (9%) that of the greywacke used in this study. Alternatively, Tetegan et al. (2011)

measured a variety of lithologies (namely flint, chert, chalk, gaize and limestone) and found the AWC of flint (~0.03) and chert (~0.02) was similar to greywacke (0.03 ± 0.02).

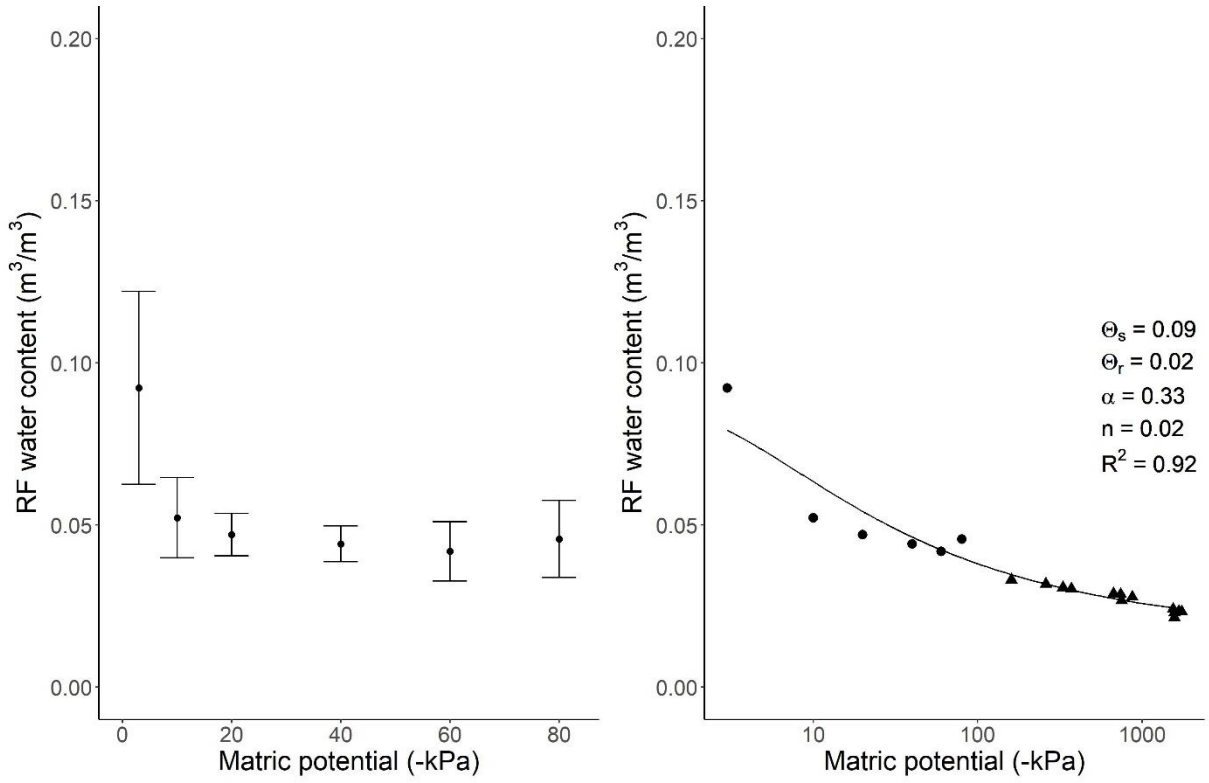

Figure 26 Water retention curve of greywacke RFs. Dots represent regression averages from soil core experiment with standard error bars (on the left) whereas triangles represent point measurements using the dew point potentiometer (on the right). The curve represents the fitted van Genuchten model using all data points except for -6 kPa and is displayed with associated model parameters and R^2.

Chapter 4 is the only other study that has measured the VWC of Canterbury greywacke RFs. In the study, the VWC of the RFs at FC was measured from *in situ* soils, with FC defined as the soil moisture condition after two days of drainage following irrigation. The average VWC of 2-20 mm RFs was equal to 0.07 ± 0.01 at an average FC matric potential of -4.8 kPa. Using the fitted van Genuchten equation, the greywacke measured in this study also had a VWC of 0.07 at -4.8 kPa, justifying our inert GF assumption and demonstrating our results apply to field soils.

Although the AWC of greywacke is low, the volumetric abundance of RFs in stony soils can mean even greywacke releases a non-negligible quantity of water. For instance, the 52 pits in Chapter 4 that were excavated in stony soils of the Canterbury region had a mean RF volumetric abundance of 39% over the 0-60 cm depth interval. At these volumes, greywacke RFs would supply 6.4 ± 4.7 mm of water on average between -10 kPa and -1500 kPa. As a majority of New Zealand stony soils (58%) have low available-water storage capacity (30-90 mm, Carrick et al., 2013), the water supplied by even low porosity RFs is substantial.

6.4 Conclusions

Results of this study demonstrate that the RF WRC of low porosity RFs can be determined precisely using large repacked cores with RF and GF mixtures. When compared to the results of other measurement methods, the error of the large cores was either similar or lower, indicating that the method performed well. Results were also validated by comparing the FC WC values measured *in situ* in Chapter 4 with WRC predictions from this study, which showed no significant difference between WC values, indicating the method is likely to be accurate. Also, we found that although greywacke has low porosity and AWC (0.03 ± 0.02), in an average Canterbury stony soil, RFs could release 6.4 ± 4.7 mm of water between -10 kPa and -1500 kPa. As a majority of New Zealand stony soils have low AWC, our findings could have significant implications for management practices, such as irrigation scheduling, as the effect of RFs on AWC is not currently accounted for. The focus of future work will be to determine the minimum number of cores necessary in the regression analysis to produce precise WC estimates.

6.5 Appendix

Appendix O Mathematic derivation of volumetric water content.

$$\theta_T = \frac{V_{wFE}+V_{wRF}+V_{wGF}}{V_T} \quad (52)$$

$$\theta_T = \frac{\theta_{FE}\,V_{FE}+\theta_{RF}\,V_{RF}+\theta_{GF}\,V_{GF}}{V_T} \quad (53)$$

$$\mathrm{X}_{GF} = \frac{V_{GF}}{V_T} \quad (54)$$

$$\mathrm{X}_{RF} = \frac{V_{RF}}{V_T} \quad (55)$$

$$V_{FE} = (1 - \mathrm{X}_{GF} - \mathrm{X}_{RF})V_T \quad (56)$$

$$\theta_T = \frac{\theta_{FE}(1-\mathrm{X}_{GF}-\mathrm{X}_{RF})V_T+\theta_{RF}\,\mathrm{X}_{RF}V_T+\theta_{GF}\,\mathrm{X}_{GF}V_T}{V_T} \quad (57)$$

$$\theta_T = \theta_{FE} - \theta_{FE}\mathrm{X}_{GF} - \theta_{FE}\mathrm{X}_{RF} + \theta_{RF}\,\mathrm{X}_{RF} + \theta_{GF}\,\mathrm{X}_{GF} \quad (58)$$

$$\theta_T = \mathrm{X}_{RF}(\theta_{RF} - \theta_{FE}) + \mathrm{X}_{GF}(\theta_{GF} - \theta_{FE}) + \theta_{FE} \quad (59)$$

As X_{RF}+X_{GF} is a constant which = 0.3 = C,

$$\theta_T = \mathrm{X}_{RF}(\theta_{RF} - \theta_{FE}) + (C - \mathrm{X}_{RF})(\theta_{GF} - \theta_{FE}) + \theta_{FE} \quad (60)$$

By rearranging we get,

$$\theta_T = \mathrm{X}_{RF}(\theta_{RF} - \theta_{GF}) + \theta_{FE}(1 - C) + \mathrm{C}\theta_{GF} \quad (61)$$

References

Brouwer, J., Anderson, H., 2000. Water holding capacity of ironstone gravel in a typic plinthoxeralf in southeast Australia. Soil Sci. Soc. Am. J. 64(5), 1603-1608. https://doi.org/10.2136/sssaj2000.6451603x.

Carrick, S., Palmer, D., Webb, T., Scott, J., Lilburne, L., 2013. Stony soils are a major challenge for nutrient management under irrigation development. In: L.D. Currie, C.L. Christensen (Eds.), Accurate and Efficient Use of Nutrients on Farms, Occasional Report No. 26. Fertiliser and Lime Research Centre, Massey University, Palmerston North, New Zealand.

Cousin, I., Nicoullaud, B., Coutadeur, C., 2003. Influence of rock fragments on the water retention and water percolation in a calcareous soil. Catena 53(2), 97-114. https://doi.org/10.1016/S0341-8162(03)00037-7.

Dane, J.H., Hopmans, J.W., 2002. 3.3.2 Laboratory. In: J.H. Dane, G.C. Topp (Eds.), Methods of Soil Analysis: Part 4 Physical Methods. Soil Science Society of America, Madison, Wisconsin, pp. 675-720.

Fiès, J.C., Louvigny, N.D.E., Chanzy, A., 2002. The role of stones in soil water retention. Eur. J. Soil Sci. 53(1), 95-104. https://doi.org/10.1046/j.1365-2389.2002.00431.x.

Gargiulo, L., Mele, G., Terribile, F., 2016. Effect of rock fragments on soil porosity: a laboratory experiment with two physically degraded soils. Eur. J. Soil Sci. 67(5), 597-604. https://doi.org/10.1111/ejss.12370.

Jones, D.P., Graham, R.C., 1993. Water-holding characteristics of weathered granitic rock in chaparral and forest ecosystems. Soil Sci. Soc. Am. J. 57(1), 256-261. https://doi.org/10.2136/sssaj1993.03615995005700010044x.

Milne, J., Clayden, B., L., S.P., Wilson, A.D., 1995. Soil Description Handbook. Manaaki Whenua Press, Lincoln, New Zealand.

Naseri, M., Iden, S., Richter, N., Durner, W., 2019. Influence of stone content on soil hydraulic properties: experimental investigation and test of existing model concepts. Vadose Zone J. 18. https://doi.org/10.2136/vzj2018.08.0163.

Novak, V., Surda, P., 2010. The water retention of a granite rock fragments in high tatras stony soils. J. Hydrol. Hydromech. 58(3), 181-187. https://doi.org/10.2478/v10098-010-0017-x.

Parajuli, K., Sadeghi, M., Jones, S.B., 2017. A binary mixing model for characterizing stony-soil water retention. Agric. For. Meteorol. 244-245, 1-8. https://doi.org/10.1016/j.agrformet.2017.05.013.

Poesen, J., Lavee, H., 1994. Rock fragments in top soils: significance and processes. Catena 23(1), 1-28. https://doi.org/10.1016/0341-8162(94)90050-7.

Schoeman, J.L., Kruger, M.M., Loock, A.H., 1997. Water-holding capacity of rock fragments in rehabilitated opencast mine soils. S. Afr. J. Plant Soil 14(3), 98-102. https://doi.org/10.1080/02571862.1997.10635089.

Seki, K., 2007. SWRC fit – a nonlinear fitting program with a water retention curve for soils having unimodal and bimodal pore structure. Hydrol. Earth Syst. Sci. Discuss. 4(1), 407-437. http://dx.doi.org/10.5194/hessd-4-407-2007.

Tetegan, M., Nicoullaud, B., Baize, D., Bouthier, A., Cousin, I., 2011. The contribution of rock fragments to the available water content of stony soils: proposition of new pedotransfer functions. Geoderma 165(1), 40-49. https://doi.org/10.1016/j.geoderma.2011.07.001.

Torri, D., Poesen, J., Monaci, F., Busoni, E., 1994. Rock fragment content and fine soil bulk density. Catena 23(1), 65-71. https://doi.org/10.1016/0341-8162(94)90053-1.

UMS, 2009. User manual: T5/T5x pressure transducer tensiometer. UMS GmbH München.

van Genuchten, M.T., 1980. A closed-form equation for predicting the hydraulic conductivity of unsaturated soils. Soil Sci. Soc. Am. J. 44(5), 892-898. https://doi.org/10.2136/sssaj1980.03615995004400050002x.

van Wesemael, B., Poesen, J., de Figueiredo, T., 1995. Effects of rock fragments on physical degradation of cultivated soils by rainfall. Soil Tillage Res. 33(3), 229-250. https://doi.org/10.1016/0167-1987(94)00439-L.

Wang, H.F., Xiao, B., Wang, M.Y., Shao, M.A., 2013. Modeling the soil water retention curves of soil-gravel mixtures with regression method on the loess plateau of China. Plos One 8(3). https://doi.org/10.1371/journal.pone.0059475.

Webb, T.H., Bennett, C.M., 1986. Soils of Ashley Dene, Department of Scientific and Industrial Research.

Webb, T.H., Lilburne, L.R., 2011. Criteria for Defining the Soil Family and Soil Sibling: the Fourth and Fifth Categories of the New Zealand Soil Classification. Landcare Research Science Series No. 3. Manaaki Whenua Press, Lincoln, New Zealand.

Chapter 7

Effects of rock fragment water retention on simulated dairy farm nutrient losses

7.1 Introduction

The implementation of the National Policy Statement for Freshwater Management in 2014 made it necessary for regional councils to develop regional plans for planning and managing freshwater resources (Hughes and Snelder, 2018). These plans had to contain freshwater objectives, policies and limits, which enforce rules on land and water use as directed by national bottom lines and compulsory water values (Hughes and Snelder, 2018). In Canterbury, this is seen in the form of the Land and Water Regional Plan (Environment Canterbury, 2018), which makes it necessary for the majority of farmers to produce a farm environment plan and determine a nitrogen (N) baseline for their farm. The farm environment plan is unique to each property and outlines areas of environmental risk and how these risks may be managed by implementing industry agreed good management practices. The N baseline is the N loss from a property as modelled by OVERSEER® (or equivalent approved model), averaged over a 48 month consecutive period between January 2009 and December 2013. For the Selwyn-Waihora sub-region, a N loss threshold exists (15 kg N ha^{-1} yr^{-1}) for farms larger than 10 ha (Environment Canterbury, 2018). Those dairy farms with a N loss that exceeds the threshold are required by 2022 to reduce losses of N from the property by 30% (which is also determined through OVERSEER® predictions). Farming activities in the Hinds/Hekeao Plains sub-region are also regulated by a 15 kg N ha^{-1} yr^{-1} threshold modelled by OVERSEER®. Farm properties in this sub-region that exceed the threshold are required to reduce N loss by 36%, or until an N loss of <20 kg N ha^{-1} yr^{-1} is reached. As such, OVERSEER® predictions could lead to substantial land use management changes for some farmers in the Canterbury region. However, the accuracy of any model depends on the representativeness of the data used for model development and validation. As has been highlighted in the previous thesis chapters, stony soil research in New Zealand commonly assumes rock fragments (RFs) are inert with respect to soil water retention. The S-map pedotransfer functions which supply the soil hydraulic values used by the OVERSEER® model utilise this assumption (McNeill et al., 2018). Results from Chapter 4 show that RFs can account for an additional ~10% of soil water above that held by the fine earth in a Canterbury stony soil at field capacity (FC) to a depth of 60 cm. For Canterbury stony soils, this means ~13 mm of soil water is not being included in water budgets or nutrient discharge predictions, potentially leading to unnecessarily strict limits on land management practices. As a result, it is important that the current

nutrient discharge values predicted by OVERSEER® for stony soils are validated using WC data from Chapter 4.

This chapter aims to develop farm simulations for a dairy farm located on a Canterbury stony soil using the OVERSEER® model, to determine the potential error in current predictions that consider RFs inert.

7.2 OVERSEER® simulations

Data describing the dairy farm simulation (Appendix P) was entered into OverseerEd (2018 | 3.2.0.3). Six scenarios were then generated by varying soil properties to create three soil types (an average stony Brown soil, an average stony Recent soil and a very stony Brown soil) with RF water retention included and excluded. The soil properties of the average stony Brown soil (now referred to as the Brown soil) was generated by taking the average soil properties of all the pits described as a stony Brown soil in Chapter 4 and Chapter 5 (Appendix Q). The average stony Recent soil (now referred to as the Recent soil) was generated using the same method, but for pits identified as stony Recent soils in Chapter 4 and Chapter 5 (Appendix R). Both the Recent and the Brown soil had an average profile RF volumetric proportion of 39%. The way the data were censored (see the error propagation method described in Chapter 4 and Chapter 5), meant the stony soil properties were skewed by increments with fewer RFs. Increments with high RF abundances had smaller volumes of fine earth and were thus more likely to propagate large relative errors for fine earth bulk density, volumetric water content (VWC) and total porosity, causing these increments to be removed from the analysis. To amplify the potential effect of including water storage of RFs, a very stony brown soil (RF proportion 54%) was selected from the dataset used in Chapter 4 and Chapter 5 (Appendix S).

The WC at wilting point (WP) and FC in the 'fines only' scenarios in Appendices B-D excluded the WC of the RFs ($\theta_{-RF\_H_2O}$), and was calculated by scaling the fine earth WC at WP or FC (θ_{Fines}) by its volumetric proportion ($1 - \mathrm{X}_{RF}$),

$$\theta_{-RF\_H_2O} = \theta_{Fines}(1 - \mathrm{X}_{RF}) \quad (62)$$

Alternatively, the scenarios in Appendices B-D where RF water storage was included, the WC at WP or FC ($\theta_{+RF\_H_2O}$) was calculated by summing the fine earth WC with the WC of the 2-20 mm and >20 mm RFs, all scaled by their respective volumes,

$$\theta_{+RF\_H_2O} = \theta_{-RF\_H_2O} + \mathrm{X}_{2-20} * \theta_{2.20} + \mathrm{X}_{>20} * \theta_{>20} \quad (63)$$

where X_{2-20} and $\mathrm{X}_{>20}$ are the volumetric proportions of the 2-20 mm and >20 mm RFs, respectively, with $\theta_{2.20}$ and $\theta_{>20}$ the volumetric WC (at WP or FC) of the 2-20 mm and >20 mm RFs, respectively.

The RF WC at FC was set equal to the average 2-20 mm (0.07 m^3 m^{-3}) and >20 mm (0.03 m^3 m^{-3}) RF WCs in Chapter 4. The RF WC at WP (0.02 ± 0.01 m^3 m^{-3}) was equivalent to the -1500 kPa WC predicted in Chapter 6 and was used for both 2-20 mm and >20 mm RFs. The WC at saturation of the whole soil was also calculated according to Equation 63; however, $\theta_{-RF\_H_2O}$ at saturation was calculated as the total porosity of the fine earth, while $\theta_{2.20}$ and $\theta_{>20}$ at saturation (0.15 cm^{-3} cm^{-3}) were estimated from the van Genuchten model presented in Chapter 6. The RF WC estimates for WP and saturation apply to 2-12 mm RFs. However, >20 mm RFs represent ~50% of the total RF volume in the Recent, Brown and very stony Brown soils, which means estimates of WC at WP and saturation are likely overestimated, as smaller RFs have higher water retention than larger RFs. Consequently, estimates of RF available water holding capacity (AWC) may be an underestimate, as WP WC could be too high.

7.3 Results and discussion

The losses of phosphorus (P) and greenhouse gases (GHGs) were relatively insensitive to the inclusion of RF water storage (Table 14). P losses had no observable change, as the input variables that OVERSEER® uses to predict losses of P (such as irrigation management, fertiliser management, soil chemistry and soil drainage class) are not affected by changes in water storage (Watkins and Selbie, 2015).

Slight variation in GHG losses between different scenarios and soil types show that changes in water storage had a minor effect on GHG losses, but predictions appear to be more influenced by farm management practices (fertiliser application, effluent application), farm facilities (feed pads and animal shelters) and animal production (Wheeler et al., 2008), which do not vary between scenarios.

The inclusion of RF water storage in OVERSEER® simulations caused a reduction in N losses of 1-6 kg N per ha (Table 14). Though the absolute difference in nutrient losses was small, they equated to a relative difference of 4-19% depending on the soil type used. The very stony Brown soil had a substantially greater N loss between scenarios (RF water storage included and RF water storage excluded) when compared to the other two soil types. Pollaco et al. (2014) found OVERSEER® predictions are sensitive to changes in AWC, particularly at the low AWC end. The very stony Brown soil had only 63 mm of available water to a soil depth of 1 m when RF water storage was not included (Table 14). As a result, including RF water storage produced a large relative increase (27%), and hence a substantial effect on the predicted N loss. This large relative increase in available water is also shown in the irrigation demand, which is the amount of irrigation required per year to keep the soil above a threshold percentage of profile available water. The irrigation demand varied by 17 mm between the scenarios of the very stony Brown soil, but has no change for the Brown or Recent soil simulations (Table 14). This will likely influence the large difference in N loss for the very stony brown

soil scenarios, as the fines only simulation requires more irrigation, which means the soil is closer to FC for a greater period and thus more susceptible to N leaching from rainfall.

Table 14 Variation in OVERSEER® output between stony soil simulations.

Soil type	AWC to 1 m depth	Irrigation demand*	P loss	GHG loss	N loss	Relative difference in N loss
	mm	mm yr^{-1}	kg ha^{-1} yr^{-1}	kg CO_2 ha^{-1} yr^{-1}	kg ha^{-1} yr^{-1}	
Brown soil (fines)	90	425	0.6	14404	24	
Brown soil (fines+RFs)	104	425	0.6	14400	22	9%
Recent soil (fines)	81	418	0.7	14397	27	
Recent soil (fines+RFs)	88	418	0.7	14404	26	4%
Very stony Brown soil (fines)	63	435	0.6	14439	37	
Very stony Brown soil (fines+RFs)	80	418	0.6	14426	31	19%

*For pastoral block.
#Greenhouse gas losses are in kg CO_2 equivalents

An uncertainty of 25-30% is commonly quoted for OVERSEER® N loss predictions (Ledgard et al., 2001). This uncertainty applies to estimates for farms that have characteristics similar to those from which field data has been gathered and used to calibrate the OVERSEER® N loss model (Parlimentary Commissioner for the Environment, 2018). When farms with characteristics outside the model calibration are used, prediction uncertainty on dairy farms could be anywhere between 32 and 62% (Etheridge et al., 2018). Our results indicate that an additional 4-19% error could exist for OVERSEER® predictions of N-leaching for Canterbury dairy farms located on stony soils. Considering the current regulatory framework for the Selwyn-Waihora and Hinds/Hekeao Plains sub-regions, the results indicate that farmers on stony soils in these areas may be subject to N-leaching overestimates using the current modelling set-up of assuming RFs do not contribute to soil water storage. However, the soils most affected by these overestimates (very stony soils) are likely susceptible to elevated N loss from preferential flow (Cichota et al., 2016; Robertson, 2016), which is not taken into account in the above predictions.

7.4 Conclusions

The inclusion of RF water storage had little to no effect on P and GHG losses but could reduce N losses by 1-6 kg N ha^{-1} yr^{-1} depending on soil type. Variation in N losses was equivalent to a relative change of 4-19% for the simulated soils, which indicates that farmers on stony soils may be subject to N-leaching overestimates. However, the soils most likely to be affected by including RF WC (soils with

high RF content and low AWC) are likely susceptible to rapid N leaching from preferential flow, which is not taken into account in the above simulations. The focus of future work will be on determining if the degree of impact on nutrient losses from incorporating RF water storage remains the same in varying farm scenarios with a greater variety of soil types and management practices.

7.5 Appendix

Appendix P Variables entered into OVERSEER® for dairy farm simulation.

Climate	11.8°C (average temperature) 589 mm yr^{-1} (average rainfall) 908 mm (annual PET)
Pasture/Crops	
- Ryegrass/white clover	Hectares sown: 120 Pasture grown: 2,366 T DM^{-1} yr^{-1} Pasture Intake: 2,008 T DM^{-1} yr^{-1}
- Kale	Hectares sown: 5.5 Yield: 83 T DM^{-1}
Animals	Breed: Ayrshire Peak # cows milked: 350 Milk solids: 165,000 kg yr^{-1}
Dairy effluent system	Holding pond: solids are separated Solids management: Spread on blocks Pond solids management: Spread on blocks Liquid management: Spray regularly
Supplement imported	60 T DM^{-1} soya bean meal distributed in milking
Irrigation	
- Season (pasture)	October - March
- Season (kale)	November - March
- Irrigation system type	Linear and centre pivot
- Strategy	Trigger point; fixed depth applied
- Based on	Soil moisture sensors: probes/tapes
Fertiliser inputs	
- Pasture	Superphosphate (270 kg ha^{-1}; September) Urea (50 kg ha^{-1}; October) Urea (50 kg ha^{-1}; December) Urea (50 kg ha^{-1}; February) Lime (375 kg ha^{-1}; March) Urea (40 kg ha^{-1}; April)
- Fodder crop	Cropmaster 15 (150 kg ha^{-1}; November)

Appendix Q Soil properties of the Brown soil scenarios (fines only and fines+RFs WC).

Depth increment	Variable	Fines only	Fines+RFs
Topsoil (0-10 cm)	Texture	Silt loam	-
	Bulk density (g cm^{-3})	1.103	-
	Carbon (%)	4.1	-
	Clay (%)	23	-
	Sand (%)	21.7	-
Subsoil (10-60 cm)	Clay (%)	19	-
Top (0-30 cm)	Wilting point (mm/10 cm)	0.09	0.09
	Field capacity(mm/10 cm)	0.29	0.3
	Saturation (mm/10 cm)	0.4	0.44
Middle (30-60 cm)	Wilting point (mm/10 cm)	0.04	0.06
	Field capacity (mm/10 cm)	0.1	0.13
	Saturation (mm/10 cm)	0.23	0.32
Bottom (>60 cm)*	Wilting point (mm/10 cm)	0.02	0.04
	Field capacity (mm/10 cm)	0.05	0.09
	Saturation (mm/10 cm)	0.23	0.32

*Assumed to be equivalent to the properties of the 50-60 cm increment.

Appendix R Soil properties of the Recent soil scenarios (fines only and fines+RFs WC).

Depth increment	Variable	Fines only	Fines+RFs
Topsoil (0-10 cm)	Texture	Silty sand	-
	Bulk density (g cm^{-3})	1.242	-
	Carbon (%)	3.2	-
	Clay (%)	17	-
	Sand (%)	34.6	-
Subsoil (10-60 cm)	Clay (%)	14	-
Top (0-30 cm)	Wilting point (mm/10 cm)	0.09	0.1
	Field capacity(mm/10 cm)	0.28	0.29
	Saturation (mm/10 cm)	0.4	0.43
Middle (30-60 cm)	Wilting point (mm/10 cm)	0.03	0.05
	Field capacity (mm/10 cm)	0.07	0.1
	Saturation (mm/10 cm)	0.18	0.28
Bottom (>60 cm)*	Wilting point (mm/10 cm)	0.02	0.04
	Field capacity (mm/10 cm)	0.05	0.08
	Saturation (mm/10 cm)	0.018	0.28

*Assumed to be equivalent to the properties of the 50-60 cm increment.

Appendix S Soil properties of the very stony Brown soil scenarios (fines only and fines+RFs WC).

Depth increment	Variable	Fines only	Fines+RFs
Topsoil (0-10 cm)	Texture	Silt loam	-
	Bulk density (g cm^{-3})	1.025	-
	Carbon (%)	4.3	-
	Clay (%)	23	-
	Sand (%)	25	-
Subsoil (10-50 cm)	Clay (%)	18	-
Top (0-30 cm)	Wilting point (mm/10 cm)	0.08	0.09
	Field capacity(mm/10 cm)	0.21	0.23
	Saturation (mm/10 cm)	0.33	0.4
Middle (30-50 cm)	Wilting point (mm/10 cm)	0.04	0.06
	Field capacity (mm/10 cm)	0.08	0.12
	Saturation (mm/10 cm)	0.14	0.25
Bottom (>50 cm)*	Wilting point (mm/10 cm)	0.04	0.06
	Field capacity (mm/10 cm)	0.07	0.11
	Saturation (mm/10 cm)	0.12	0.23

*Assumed to be equivalent to the properties of the 40-50 cm increment.

References

Cichota, R., Kelliher, F.M., Thomas, S.M., Clemens, G., Fraser, P.M., Carrick, S., 2016. Effects of irrigation intensity on preferential solute transport in a stony soil. N. Z. J. Agric. Res. 59(2), 141-155. https://doi.org/10.1080/00288233.2016.1155631.

Environment Canterbury, 2018. Canterbury Land and Water Regional Plan: Plan change 5. Author, Canterbury.

Etheridge, Z., Fietje, L., Metherell, A., Lilburne, L., Mojsilovich, O., Robson, M., Steel, K., Hanson, M., 2018. Collaborative expert judgement analysis of uncertainty associated with catchment-scale nitrogen load modelling with OVERSEER®, Fertilizer and Lime Research Centre, Massey University, New Zealand.

Hughes, B., Snelder, T., 2018. Freshwater management units for the Canterbury region: review of existing water management spatial frameworks (LWP Client Report 2018-11), Land Water People Ltd.

Ledgard, S., Thorrold, B., Petch, R., Young, J., 2001. Use of OVERSEER as a tool to identify management strategies for reducing nitrate leaching from farms around Lake Taupo. Palmerston North, Fertilizer and Lime Research Centre, Massey University.

McNeill, S.J., Lilburne, L.R., Carrick, S., Webb, T.H., Cuthill, T., 2018. Pedotransfer functions for the soil water characteristics of New Zealand soils using S-map information. Geoderma 326, 96-110. https://doi.org/10.1016/j.geoderma.2018.04.011.

Parlimentary Commissioner for the Environment, 2018. Overseer and regulatory oversight: models, uncertainty and cleaning up our waterways. Wellington, New Zealand, Author, Wellington, New Zealand.

Pollaco, A.P., Lilburne, L.R., Webb, T.H., Wheeler, D.M., 2014. Preliminary assessment and review of soil parameters in Overseer® 6.1. Landcare Research Contract Report LC2002. Landcare Research, Lincoln, New Zealand.

Robertson, B.B., 2016. The effect of irrigation practice on drainage and solute leaching under spray irrigation on a stony soil, Lincoln University.

Watkins, N., Selbie, D., 2015. Technical description of OVERSEER for regional councils (RE500/2015/084), Bay of Plenty Regional Council, New Zealand.

Wheeler, D.M., Ledgard, S.F., DeKlein, C.A.M., 2008. Using the OVERSEER nutrient budget model to estimate on-farm greenhouse gas emissions. Aust. J. Exp. Agr. 48(2), 99-103. https://doi.org/10.1071/EA07250.

Chapter 8

Conclusions and recommendations

8.1 Introduction

The main aims of this study were to:

- Study the soil properties affecting the water retention behaviour of undisturbed stony soils at field capacity (FC).
- Investigate the validity of assumptions that are commonly used when measuring and modelling stony soil water holding behaviour.

To achieve these aims, the following hypotheses were tested:

1. Because of the peculiar conductivity characteristics of stony soil horizons, a single matric potential of -10 kPa as adopted in NZ for defining FC is not appropriate.
2. FC at shallow depths in stony soils is best characterised by a state of hydrostatic equilibrium, which can establish because a shallow stony layer's drainage characteristics establish a finite but near-zero matric potential close to the soil surface.
3. The water held at FC can be partitioned between fine earth and rock fragments (RFs) at pedon scale.
4. RFs have significant effects on soil hydraulic, physical and chemical properties
5. Statistical models used to predict soil water content (WC) at FC (pedotransfer functions) perform better when the characteristics of RFs are implicit.
6. Greywacke RFs hold sufficient water and release it in a sufficiently systematic way that a water retention curve (WRC) can be determined.
7. Greywacke RFs in stony soils substantially influence the accuracy of water retention and nutrient loss predictions from OVERSEER®.

To test the hypotheses, four research experiments were conducted (as summarised in Chapter 1 Section 1.2):

1. Experiment 1 involved the field measurement of the matric potential and soil WC in stony soils of Canterbury at FC using an operational definition of two days of drainage after a saturation event.

2. Experiment 2 involved field measurement of matric potential after four to five days following a saturation event to a depth of 1.5 m in stony soils of Canterbury.

3. Experiment 3 was a novel repacked soil core experiment designed to measure the plant available water of low porosity, greywacke RFs.

4. Experiment 4 involved a simulation exercise using the OVERSEER® model and an irrigated, intensive dairy farm scenario, parameterised with results from Experiments 1 and 3 to determine the effect of RFs on water retention and nutrient loss predictions in stony soils.

8.2 Main conclusions

In relation to the seven hypotheses, the main conclusions are:

Hypothesis 1: Because of the peculiar conductivity characteristics of stony soil horizons, a single matric potential of -10 kPa as adopted in NZ for defining FC is not appropriate.

- Results showed that the matric potential at FC was generally higher than -10 kPa and could vary from -1 kPa to -13 kPa. The variability in matric potential showed that a single static matric potential could not adequately describe FC.

- Matric potential was found to vary with depth, with results indicating a relatively linear increase in the average matric potential with increasing depth. When each pit was considered individually, matric potential depth-profiles could be assigned into five modes of drainage behaviour (hydrostatic equilibrium, wet-top, gap, wet-profile and shallow break), with hydrostatic equilibrium being the most common mode. The four other modes tend towards hydrostatic equilibrium, but some form of drainage impediment meant that hydrostatic equilibrium was not reached after only two days of drainage.

Hypothesis 2: FC at shallow depths in stony soils is best characterised by a state of hydrostatic equilibrium, which can establish because a shallow stony layer's drainage characteristics establish a finite but near-zero matric potential close to the soil surface.

- Though FC normally only approximates hydrostatic equilibrium in soils with shallow groundwater systems, results from Chapter 3 showed that a near-surface layer (called a capillary break) with low conductivity at negative but near-zero matric potentials is an alternative condition. The capillary break may correspond to either: 1) a layer of open framework gravels or 2) fine earth with <15 $m^2 g^{-1}$ specific surface area (SSA).

- Though hydrostatic equilibrium did not represent FC for all of the measured soils, it is a more informed strategy for describing FC than a static matric potential value. In conclusion,

hydrostatic equilibrium may represent a conservative approach with regard to refill point, as the soils we studied were always wetter at FC than hydrostatic equilibrium would dictate when hydrostatic equilibrium was not achieved.

Hypothesis 3: The water held at FC can be partitioned between fine earth and RFs at pedon scale.

- Error analysis showed that error associated with the pit and bead method for estimating volume can be propagated and amplified in variables derived from calculations on primary variables. Variables particularly sensitive to volume error were fine earth bulk density, volumetric water content (VWC), total porosity and macroporosity, with the latter so prone to error that it could not be used in the analysis. Data censored in accordance with a relative error of no more than 25% resulted in 20-57% (60-168 data points) being removed.

- RFs accounted for a substantial quantity of the water retained at FC in undisturbed stony soils. Though the measured greywacke RFs had relatively low water storage in comparison to other lithologies, the volumetric abundance of RFs in stony soils means the greywacke RFs still account for ~13 mm of water at FC (or ~10% of the total water held at FC) in Canterbury stony soils.

- The water retention of the RFs was found to be strongly influenced by size, whereby the VWC of 2-20 mm RFs (0.07 m^3 m^{-3}) was found to be twice that of >20 mm RFs (0.03 m^3 m^{-3}). This is likely because smaller RFs have a greater SSA, which results in a greater proportion of the clast's volume having undergone weathering, resulting in greater water retention.

- The abundance of RFs had both a positive and a negative influence on FC VWC. Possible explanations include:

    - Positive - with greater RF abundance RFs may store water at contact points between neighbouring RFs or as puddles on the rock surface for larger RFs.

    - Negative - This may be an expression of how soil age affects the water retention of the RFs. On the Canterbury Plains, older soils have a larger contribution of loess, which dilutes the coarse fraction (RFs). Older soils are more likely also to have more weathered RFs, which have higher porosity and store more water.

Hypothesis 4: RFs have significant effects on soil hydraulic, physical and chemical properties.

- RFs had a significant negative relationship with fine earth WC. The cause for this is potentially from a strong positive correlation between the total volume of RFs and coarse sand, as coarse sand has low water retention and would negatively affect fine earth WC. It is also speculated

that the >20 mm RFs may allow water to run freely on the surface of the RFs with little interaction with the adjacent fine earth, causing a negative relationship with fine earth WC.

- Total nitrogen in the fine earth was negatively affected while P-retention was positively affected by the volume of RFs. Soil carbon had a positive relationship with RFs in the 0-10 cm increment. This correlation was attributed to a concentration of carbon inputs into a smaller volume of fines as the proportion of RFs increases. Conversely, in the subsoil (40-60 cm depth) the proportion of 6-20 mm RFs had a negative relationship with carbon. This may be due to limitations to plant growth caused by RF proportion (such as reduced water holding capacity or nutrient supply), which could result in reduced carbon inputs at depth.

- RFs influenced the fine earth bulk density and total porosity of undisturbed stony soils. Fine earth bulk density was negatively affected, and total porosity was positively affected by RFs. The relationship was mostly linked to the 2-20 mm RFs in the 20-40 cm depth increments. It is proposed that the generally high clay content (20-21%) in these increments imbues sufficient contrast between matrix and RFs in their propensity to shrink and swell on drying and wetting that lacunar pores develop in the matrix, resulting in a lower fine earth bulk density and higher total porosity. The significance of the results made it necessary to develop a new method of repacking stony soils to reduce error when determining the WRC of greywacke RFs.

Hypothesis 5: Statistical models used to predict soil WC at FC (pedotransfer functions) perform better when characteristics of RFs are implicit.

- PtFs that included the abundance of RFs could accurately and precisely predict the FC WC in stony soils.

- The PtF developed in this study performed better than an existing PtF, calibrated on NZ soils (Logit PtF), which treated RFs as an inert volume.

- The error in the Logit PtF stems from its inability to account for deviations from 1) the matric potential it assumes for FC (-10 kPa), 2) water held by RFs, and 3) the effect of RFs on the water retention characteristics of the fine earth.

- By using depth and volume proportion of RFs to augment the logit model, model accuracy was improved substantially.

Hypothesis 6: Greywacke RFs hold sufficient water and release it in a sufficiently systematic way that a WRC can be determined.

- By using a novel repacked core experiment, it was possible to precisely measure the available water holding capacity (AWC) of low porosity RFs (greywacke). When compared to the results

of other measurement methods, the error of the developed method was either similar or lower, indicating that the method performed well. Results were also validated by comparing the FC WC values measured *in situ* in Chapter 4 with WRC predictions from this study, which showed no significant difference between WC values, indicating the method is likely to be accurate.

- Results showed that although greywacke has low porosity and AWC (0.03 ± 0.02), in an average Canterbury stony soil, RFs could release 6.4 ± 4.7 mm of water between -10 kPa and -1500 kPa.

Hypothesis 7: Greywacke RFs in stony soils substantially influence the accuracy of water retention and nutrient loss predictions from OVERSEER®*.*

- The inclusion of RF WC could substantially affect the nutrient loss predictions of OVERSEER® simulations. Though phosphorus and greenhouse gas losses were affected negligibly, the inclusion of RF WC could reduce nitrogen (N) losses by 1-6 kg N ha^{-1} yr^{-1} depending on soil type.
- Variation in OVERSEER® N losses was equivalent to a relative change of 4-19% for the simulated soils, which indicates that farmers on stony soils may be subject to N-leaching overestimates. A caveat to this conclusion is that the OVERSEER® model does not account for bypass flow, which is a common phenomenon in stony soils. Any N-leaching overestimates indicated by the present research should be treated as a desirable buffer for potential underestimates generated by N-loss processes unaccounted for in the current version of OVERSEER®.

8.3 Practical implications

- Currently, the management and regulation of farming practices on stony soils in New Zealand (and most other countries) are based on the properties of the fine earth only, such that RFs are considered inert. However, the results of this study show that RFs affect many soil properties including water dynamics and retention, soil structure and soil chemistry, which puts into question long-held assumptions on how stony soils should be characterised, modelled and managed.
- This research highlights the practical importance of understanding how RFs influence soil properties, as it could have significant implications for management practices (such as irrigation scheduling) and modelling (such as nutrient leaching). Considering stony soils are commonly characterised by a low AWC, not taking into account the water RFs retain, or the tendency for stony soils to reach FC at a matric potential higher than -10 kPa, can equate to large relative errors in water retention and nutrient leaching estimates. However, for the

greywacke RFs of Canterbury, we have shown it is possible to account for these effects in existing models by including depth and RF proportion variables.

- The identification of capillary breaks and hydrostatic equilibrium matric potential-depth profiles in the stony soils of Canterbury indicate an opportunity to improve the management of water flow and solute losses in these soils. Our finding could have significant implications for management practices, such as irrigation scheduling, which should aim to not wet the subsoil to the point that causes the capillary break to become conductive. If kept at non-conductive matric potentials, the capillary break should allow the water (and nutrients) in the soil above to be retained for longer periods. Also, by incorporating the depth to the capillary break, the matric potential at which the capillary break becomes conductive, and the vertical matric potential gradient at hydrostatic equilibrium (0.098 kPa cm^{-1}), more informed approximations of FC matric potential can be determined than the standard use of a depth invariant -10 kPa.

8.4 Research needs

- Further work is required to develop methods of efficiently identifying the depth of open framework gravels at the paddock and farm scale. It is also necessary to fully characterise the capillary break, including what conditions and matric potentials it occurs. Geophysical remote sensing such as ground-penetrating radar offer potential.

- Results showed that including two variables (depth and volume proportion of RFs) could significantly improve WC predictions in stony soils. However, research must be repeated in soils that are not of alluvial origin and with RFs of varying weathering and lithology, to determine if the depth and the proportion of RFs remain important predictor variables.

- The novel repacked core method that was developed for measuring the plant available water of greywacke RFs requires additional research into determining the minimum number of cores necessary in the regression analysis to produce accurate WC estimates. The method may then be used to measure the plant available water of RFs of varying lithologies and weathering.

- OVERSEER® simulations were a good demonstration of how not incorporating RF WC may affect nutrient loss predictions. However, results were limited to one simulated farm. The focus of future work will be on determining if the degree of impact on nutrient losses from incorporating RF WC remains the same in varying farm scenarios with a greater variety of soil types and management practices.